Synthesis of Site-Specific Artificial Ribonucleases

Dissertation
zur Erlangung des Doktorgrades der
Naturwissenschaften

vorgelegt beim Fachbereich Biochemie, Chemie und Pharmazie
der Johann Wolfgang Goethe-Universität
in Frankfurt am Main

von
Claudio Gnaccarini
aus Verona (Italia)

Frankfurt am Main
2007
(D30)

Vom Fachbereich Biochemie, Chemie und Pharmazie der
Johann Wolfgang Goethe-Universität als Dissertation angenommen.

Dekan: Prof. Dr. H. Schwalbe
1. Gutachter: Prof. Dr. M. W. Göbel
2. Gutachter:
Datum der Disputation:

Acknowledgements

First of all, I want to thank Professor Dr. Michael Göbel for the opportunity he gave me of working in his group and for supporting me during my studies.

I thank Dr. Ute Scheffer and Elisabeth Kalden for the tests of RNA cleavage and the help during my biological experiments and I also thank Sascha Peter and Kathrin Beier for the collaboration in my projects. I am obliged to: Dr. Nelly Piton and Professor Dr. Joachim Engels for the deoxyuridine derivative, Dr. Jörg Bäumler and Dr. Manuel Grez for the Bcr-Abl peptide, Jérôme Désiré and Professor Dr. Jean-Luc Décaut from the University of Grenoble for the neamine conjugate and to Flavio Manea and Professor Dr. Paolo Scrimin from the University of Padova for the collaboration on gold nanoparticles.

I am thankful for the teaching of Dr. Marcus Hey with the DNA synthesiser. A sincere thank goes to Dr. Christo Roussev for the time we spent together in the laboratory. I thank in particular Marcel Suhartono for the company in the laboratory and the careful lecture of my thesis.

Among my colleagues, I am indebted to Dr. Ute Scheffer, Sven Breitung, Deniz Akalay, Stefan Ullrich, and Marko Weimar for the company, the scientific discussions and the critical lecture of my thesis. I appreciated Gunther Seifert, Christoph Timm, Cristiano Pinto Gomes, and Mirco Zeiger for keeping company.

Further special thanks go to Theodora Ruppenthal for the help with the administrative matters.

My work was financially supported by the ENDEVAN:"European Network on the Development of Artificial Nucleases'', and the SFB 579-A3 "Zufall und Design: komplementäre Wege zu neuen RNA-Liganden''.

I am also grateful to Ilona Prieß and Hannelore Brill for the mass spectrums, to Dr. Gottfried Zimmerman and Reinhard Olbrich for the assistance with the NMR. I show my appreciations to Marianne Christof for the elementary analysis, to Dr. Gerd Dürner, and to Gabriele Stracke from the HPLC department for the purifications.

To conclude I dedicate the last and most important part of my acknowledgements to people who did not contribute to my thesis directly, but who have helped me a lot while working on this thesis: my family, my parents, and all those people I met in my life who trusted in me and supported me with their affections.

Thanks to all of you.

Claudio Gnaccarini

Zusammenfassung

Seit gezeigt wurde, dass die genetischen Informationen in Form von DNA gespeichert wird, ist das Geheimnis der DNA-Struktur gelöst, der Mechanismus der Gen-Expression und die Rolle der RNA verstanden worden. Das Interesse für die Chemie und die Biologie der Nukleinsäuren ist somit kontinuierlich gewachsen. Besonders interessant ist die RNA, die eine Rolle als ein Vermittler der genetischen Informationen (mRNA) spielt, aber auch als Bote von Aminosäuren (tRNA). Sie ist im Ribosom (rRNA) anwesend, arbeitet als Templat in Telomerasen für DNA-Synthese und hat außerdem wichtige Funktionen in der RNA-Spaltung, z.B. bei Ribozymen wie RNAse P inne. Betreffend bestimmter Spaltstellen in RNA hat auch das Phänomen der siRNA beträchtliche Aufmerksamkeit in diesem Prozess erregt. Der sogenannte RISC-Komplex wird programmiert, einzelsträngige RNA mit hoher Sequenz-Spezifität zu schneiden. Die für die RNA-Interferenz verantwortliche zelluläre Maschinerie ist auch an der Bilbung von MikroRNAs beteiligt. RNA-Interferenz ist heute eines der nützlichsten Werkzeuge in *functional genomics* geworden. Die große Hoffnung ist, dass es auch vielleicht in der Therapie angewandt werden könnte.

Das Thema meiner Doktorarbeit trägt den Titel „*Synthesis of Site-Specific Artificial Ribonucleases*“. Es beschäftigt sich mit der Entwicklung künstlicher bindungsspezifischer Ribonucleasen. Diese künstlichen Katalysatoren sind im Wesentlichen aus drei Gründen bedeutsam:

Zum einen liegt eine mögliche Anwendung in der *Affinity-Cleavage* (Affinitätsspaltung), eine Technik, die Bindungsstellen von RNA-Liganden durch das kovalente Anbringen eines Reagenzes lokalisiert, das zwischen den Nukleinsäuren schneidet.

Zum anderen entsteht die Möglichkeit, neue Werkzeuge für eine gezielte Manipulation großer RNA-Moleküle zu schaffen.

Die Vorteile des Ansatzes sind, dass man damit beliebige Zielsequenzen anwählen kann. Das Problem dieser Strategie ist die Notwendigkeit, hohe Genauigkeit im Spaltungsschritt zu erreichen, wie zum Beispiel mit natürlichen Ribozymen. Wichtige Ergebnisse wurden auch während meiner Arbeit erhalten, mit einem Fall

von genauer Spaltung zwischen zwei Basen. Der dritte Grund ist die potentielle Anwendung als katalytische *antisense*-Oligonucleotide in der Chemotherapie.

Gegenwärtig existieren zwei Ansätze, unspezifische künstliche RNasen relativ kleiner Größe zu schaffen. Der erste basiert auf Metallkomplexen und führt im Allgemeinen zu höheren Raten. Die Idee ist, ein Metall als elektrophiles Zentrum zur Unterstützung der Transesterfikation zu nutzen. Unter diesen Katalysatoren enthalten die effizientesten Lanthanid-Ionen, Cu^{2+} und Zn^{2+}.

Der zweite Ansatz zielt darauf ab, metallfreie künstliche Ribonucleasen zu entwickeln. Die Vorteile dieser Strategie sind, den Katalysator von der Stabilität der Metallkomplexe, die *in vivo* problematisch sein könnten, unabhängig zu machen. In diesem Ansatz wird die natürliche Katalyse durch Enzyme simuliert. Zweckmäßige Gruppen mit beschränkter katalytischer Aktivität z.B. als Nucleophile, Säuren oder Basen, werden in einer Weise zusammengesetzt, um Kooperation zu ermöglichen. Potente Katalysatoren können so ohne die Notwendigkeit von Metallen als Cofaktoren erzeugt werden.

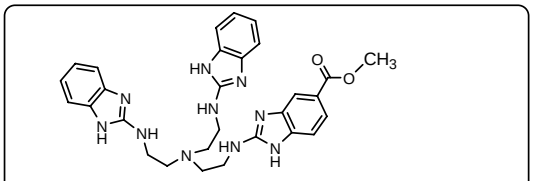

Tris{2-[(benzimidazol-2-yl)amino]ethyl}amine

Abb 1: RNA-Spaltungsagens in dieser Arbeit.

Unsere Gruppe hat einen der potentesten metallfreien Katalysatoren, das Tris{2-[(benzimidazol-2-yl)amino]ethyl}amin (Abb. 1), erfolgreich entwickelt. Dieses Molekül katalysiert die Umesterung der Phosphodiesterbindung von RNA. Allerdings wurde die mechanistische Charakterisierung z.B. durch die pH-Wert-abhängige Tendenz zur Aggregation mit der Zunahme des pH-Wertes kompliziert. Um dieses Problem zu lösen und um regiospezifische Spaltung zu erreichen, wurden während meiner Arbeit vier verschiedene 5'- DNA-Konjugate hergestellt, die über Disulfid-Bindungen verknüpft waren (Abb. 2: **1000**, **1001**, **1002 1006**).

Die RNA-Spaltungstests dieser Konjugate bewiesen ohne jeden Zweifel die Aktivität von Aminobenzimidazol-Katalysatoren. Weiterhin wurde eine pH-Abhängigkeit der Aktivität festgestellt, welche ein Optimum bei einem pH-Wert von 8 zeigte. Ein hohes Niveau regiospezifischer Spaltung wurde durch die Verwendung von Helfer-Oligonucleotiden erreicht. Ein analoges PNA-Konjugat wurde ebenfalls synthetisiert (Abb. 2: **1011**), welches sich aber interessanterweise als inaktiv erwies. Die Gründe dieses Misserfolges müssen noch geklärt werden. Auch wenn Anwendungen *in vivo* immer noch schwerer erreichbar scheinen, könnten diese Konjugate *in vitro* als sequenzspezifische künstlichen RNasen eingesetzt werden. Einige Fragen über den Mechanismus des Katalysators sind noch offen, doch könnten weitere wichtige Hinweise von einem Kristall des Katalysator-Substrat-Komplexes kommen. Weitere Studien, die die Wirkungsweise dieser Aminobenzimidazol-Katalysatoren aufklären, sind wichtig, um neue Spaltagentien zu entwerfen, die es erlauben, vielversprechende Ergebnisse für *in vivo*-Anwendungen zu erhalten.

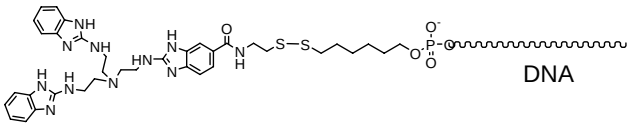

catalyst-linker-5'TCGGCAGTCGGCTAG3' **1000**
catalyst-linker-5'GATCGGCAGTCGGCTAG3' **1001**
catalyst-linker-5'CGAGATCGGCAGTCGGCTAG3' **1002**
catalyst-linker-5'CTCCTGACAAGGTAT3' **1006**

catalyst-linker-5'tcggcagtcg3' **PNA-Oligo1011**

Abb 2: 5'-Oligonucleotid-Konjugate.

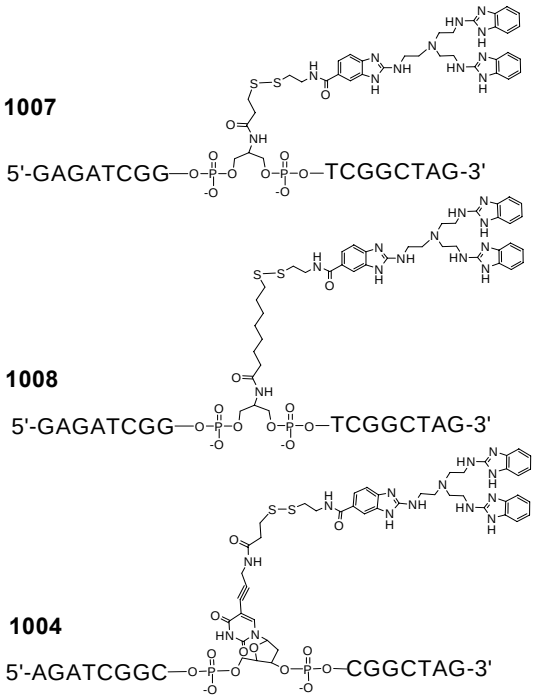

Abb. 3: Oligonucleotid- Konjugate, die turnover zeigen.

Diese 5'-Konjugate zeigten wie erwartet keinen turnover. Infolgedessen wurde eine neue Klasse von Konjugaten entworfen, die den Katalysator in der Mitte der DNA-Stränge tragen, um mehrfachen turnover zu erlauben (Abb. 3). Von diesem neuen Konjugat basierten zwei auf Serinol,

1007, **1008** und eins auf einem modifizierten Nukleotid (**1004**). Das Konjugat **1007,** basierend auf Serinol mit einem kurzen Linker erwies sich als das Aktivste. Diese Moleküle erreichten eine erfolgreiche regiospezifische Spaltung und außerdem mehrfachen turnover. Für **1007** wurde ein ungefährer k_{cat} von 0.03 h^{-1} erhalten. Betreffend dieses Projektes bleibt es immer noch, die Spezifität und die Effizienz zu erforschen, die von der *bulge*-Größe abhängen. Dieses Problem konnte ohne besonderen Aufwand einer speziellen Synthese von einem neuem Substrat gelöst werden, welches *bulges* der gewünschten Größe ausbilden kann.

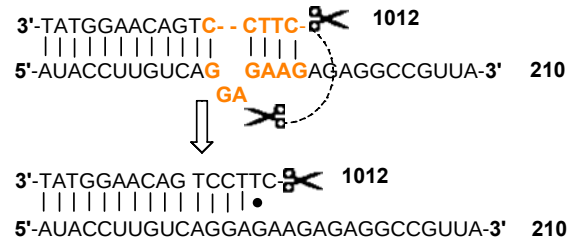

Abb. 4: 5'-Oligonucleotid Konjugat, um turnover zu erreichen.

Auf einer Arbeit von Häner basierend wurde eine alternative Strategie, die turnover erlaubt, angewendet, und zwar durch die Synthese von **1012** (Abb. 4). Dieses neue DNA-Konjugat wurde hergestellt, um am 5' -Ende durch eine Amid-Bindung den Katalysator zu tragen. In Analogie zur Arbeit von Häner wurde erwartet, dass Konjugat **1012** einen *bulge* mit Substrat **210** bildet. Dieser *bulge* ist die primäre Spaltungsstelle in der Arbeit von Häner gewesen (Abb. 4). Leider scheint in unserem Fall die Formation des *bulges* nicht energetisch begünstigt zu sein, während eine alternative *bulgeless* doppelsträngige Struktur mehr bevorzugt zu sein scheint. Deshalb kam die Spaltung ausschließlich im einzelsträngigem Bereich vor (ohne turnover). Hier wird deutlich, dass der Schlüssel zum Verständnis dieses Projektes das Wissen über die Stabilisierung der *bulge*-Formation ist.

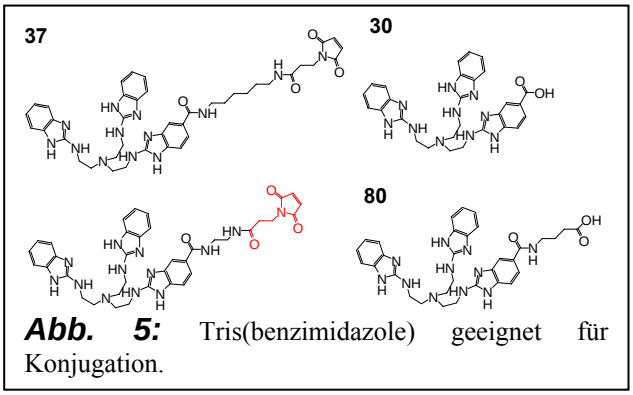

Abb. 5: Tris(benzimidazole) geeignet für Konjugation.

Nach diesen Konjugationsstudien mit der DNA erschien der Tris(2-aminobenzimidazol)- Katalysator für Anwendungen wie Affinitätsspaltung geeignet. Um diese Anwendung zu prüfen wurden andere Derivate hergestellt, die geeignet waren für Konjugation über Amid-Bindungen und über Maleimid-Chemie (Abb. 5). **37** benutzend wurden vier verschiedene Peptidkonjugate synthetisiert (Abb. 6). **2001**

und **2003** basierten auf der kurzen Sequenz 49-57 von Tat, die für die Erkennung des TAR wesentlich ist. **2004** und **2005** wurden aus einem Peptid, welches von Jörg Bäumler aus der Gruppe von Dr. Manuel Grez aus dem Georg- Speyer- Haus in Frankfurt ausgewählt wurde, das Affinität zu mRNA von Bcr-Abl hat. Wieder auf TAR zielend wurde noch ein Konjugat mit Neamin hergestellt, was in Zusammenarbeit mit der Universität von Grenoble (Professor Jean-Luc-Décout) geschah. Die Prüfungen dieser 5 Konjugate, um die Affinitätsspaltung unseres Katalysators zu bestätigen, wiesen darauf hin, dass die Spaltungsaktivität immer erhalten wurde, aber in einem Fall die Spezifität für das Target fehlte. Dadurch wurde in diesem Projekt ein optimales System für die Konjugation über Maleinimid- und Peptidbindungen etabliert, aber um diese Methode schließlich in der Affinitätsspaltung zu prüfen, müssen einige weitere Tests mit zuverlässigeren spezifischen RNA-Liganden durchgeführt werden.

2001 NH_2**-YRKKR RQRRR C-Linker- Catalyst**

2003 NH_2**-AAARKKRRQRRRAAAC-Linker-Catalyst**

2004 NH_2**-KHLHLHKGGGC -Linker-Catalyst (L)**

2005 NH_2**-KHLHLHKGGGC -Linker-Catalyst (D)**

Neamine-Linker- Catalyst

Abb. 6: Peptid- Konjugate, Neamin Koniugat.

In Zusammenarbeit mit Professor Paolo Scrimin und Flavio Manea wurde ein Goldnanopartikel, mit 2-Aminobenzimidazol funktionalisiert, hergestellt (Abb. 7). Dieses Projekt versuchte die Frage zu beantworten, ob mehrere Kopien von 2-Aminobenzimidazol in der Phosphoryl-Transfer-Katalyse kooperieren könnten, wenn sie in einer geometrisch weniger definierten Ansammlung bestehen. Aus Gründen schlechter Löslichkeit trugen nur 30% der Liganden auf dem metallischen Kern 2-Aminobenzimidazol. Der Spaltungstest konnte keine signifikante katalytische Aktivität zeigen. Um ein positives Ergebnis zu erreichen, scheint es notwendig, den Prozentsatz funktioneller Gruppen auf der metallischen Oberfläche zu erhöhen. Eine alternative Strategie, um diese funktionellen Gruppen zu koordinieren, könnte die Verwendung von Dendrimeren sein.

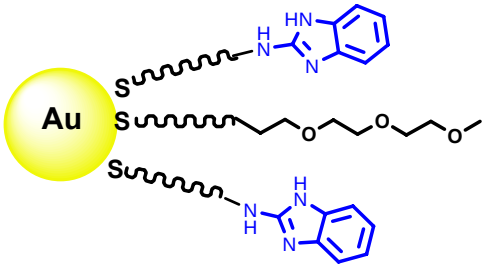

Abb. 7: Gold Nanopartikel funktionalisiert mit 2-Aminobenzimidazolen.

Ein letztes Projekt dieser Arbeit war die Synthese einer palindromischen Sequenz von 2',5'-Guanosin/Isoguanosin um die Stabilität dieses Duplexes zu verifizieren, die erwartet wurde, wenn sich Watson-Crick-artige Purin-Purin Basenpaare bilden. Dieses Projekt sollte die Grundlage für neue Experimente von nicht-enzymatischem Oligomerisierungen von Ribonucleotiden sein. Infolgedessen wurde die Synthese eines Phosphoramidits von Isoguanosin begonnen. Die Beendigung dieses Projektes ist noch zu erwarten. Trotzdem wurde an einer Syntheseroute zu diesem Molekül durch die Verwendung neuer Schutzgruppen weiter gearbeitet, um die synthetischen Herausforderungen in Zukunft lösen zu können, wie Abb. 8 illustriert.

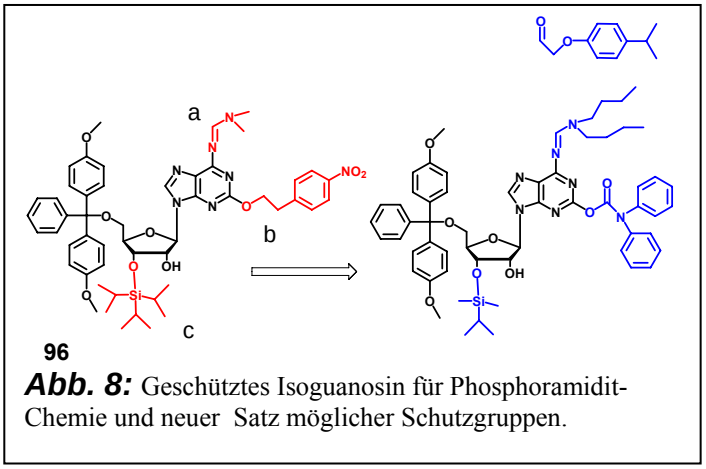

Abb. 8: Geschütztes Isoguanosin für Phosphoramidit-Chemie und neuer Satz möglicher Schutzgruppen.

Index

1. Introduction

Since it was demonstrated that the genetic information is stored in DNA,[1][2][3] the puzzle of DNA structure was solved,[4] the mechanism of gene expression and the role of RNA was understood.[5][6][7] The interest for the chemistry and the biology of the nucleic acids has continued to grow. Particularly interesting is RNA, which plays a role as a mediator of the genetic information (mRNA), but also as a carrier of the amino acids (tRNA). It is present in the ribosome (rRNA), works as template for DNA synthesis in telomerases, and can play important functions in RNA cleavage, e.g. in ribozymes such as RNAse P. Concerning site specific cleavage of RNA, also the phenomenon of siRNAs has attracted considerable attention.[8] In this process the so called RISC complex is programmed to cut single–stranded RNA with high sequence specificity. The cellular machinery responsible for RNA interference is also involved in the formation of micro-RNAs. RNA interference today has become one of the most useful tools in functional genomics. The big hope is that it may also be applied in therapy.

In this context my thesis was focused on the development of artificial site-specific ribonucleases. These artificial catalysts have received attention for three reasons.

The first aspect coming closest to possible applications is in affinity cleavage,[9] which is a technique to localize the binding sites of RNA ligands by attaching covalently a reagent that cuts the nucleic acids. The second reason is the possibility of creating new tools for the sequence selective manipulation of large RNA molecules. The advantages of this approach are that one could have such tools for any sequence. The problem of this strategy is the necessity to achieve high precision in the cutting step, like for instance with the natural ribozymes. Important results were achieved also during my work.[10] With a case of exact cleavage between two bases. Further improvements are still possible, as it will be described later. The third reason, but not in order of importance, is the potential application as catalytic antisense oligonucleotides in chemotherapy.[11] Briefly, when the oligodeoxyribonucleotides (ODN), or their phosphorothioate analogues enter the cells, a RNA/ODN duplex is formed. The RNA/DNA duplexes activate an intracellular enzyme, the RNase H,[12] which degrades the RNA component releasing

the ODN antisense. However, the stability of DNA and their phosphorothioate derivative in cells against enzymatic degradation is not exceptional. Efforts to improve the derivatives gave satisfactory results with respect to affinity and stability against non-specific nucleases, like in the case of PNA.[13] Unfortunately not all of these structurally modified nucleic acids are substrates for RNAse H.[14][15] Therefore the attachment of a catalyst able to destroy the target could become important.

Currently two approaches exist for creating unspecific artificial RNases of relatively small size. The first one is based on metal complexes and has generally resulted in higher rates.[15] The idea is to use a metal as an electrophilic centre, for promoting the transesterification. Among these catalysts the most efficient ones are made with lanthanide ions, Cu^{2+} and Zn^{2+}.

The second approach aims at developing metal-free artificial ribonucleases. The advantages of this strategy are to render the catalyst independent from the stability of metal complexes that could be problematic *in vivo*. In this approach the natural catalysis of the enzymes is simulated. Functional groups with limited catalytic activity e.g. as nucleophiles, acids or bases, are put together in a way to enable cooperativity. Potent catalyst can thus be generated, without the requirement of metals as cofactors.

Our group has successfully developed one of the most powerful metal-free catalysts, the tris{2-[(benzimidazol-2-yl)amino]ethyl}amine.[16] This molecule acts catalysing the transesterification of the phosphodiester bond of RNA however, the mechanistic characterization e.g. the pH-dependent activity was complicated by the tendency to aggregate with the increase of the pH. To solve this problem and to achieve site specific cleavage, a series of 5' DNA conjugates, different in length and sequence, were synthesized during my work.[10] The resulting compounds behaved as true artificial ribonucleases, and allowed to complete mechanistic studies on tris{2-[(benzimidazol-2-yl)amino]ethyl}amine. However, this kind of site-specific ribonucleases, as expected did not show turnover. To generate site-specific ribonucleases exhibiting turnover, a series of oligonucleotides inducing a bulge in the RNA substrate were synthesized. These conjugates carry the benzimidazole catalyst unit in an intrachain position of DNA. To complete the synthetic part, a PNA conjugate was also investigated. In long terms the artificial nucleases might offer new opportunities for chemotherapy *in vivo*. In short terms, however, a more realistic

application of such catalysts could be in affinity cleavage. Towards this purpose and for the conjugation with RNA ligands carrying thiols (e.g. peptides and proteins), a maleimide derivative of the tris{2-[(benzimidazol-2-yl)amino]ethyl}amine was synthesised. Conjugates of different peptidic RNA ligands ending with cysteine were obtained. For the conjugation with RNA ligands with free amino groups via amide bonds, another derivative with a GABA linker was made. A further project, relevant in the context of affinity cleavage, was the conjugation of trisbenzimidazole catalysts with neamine,[17] which was achieved in collaboration with the group of Professor Jean-Luc Décout (Université Joseph Fourier in Grenoble). The objectives of this first part of my thesis are summarized in Fig. 1.

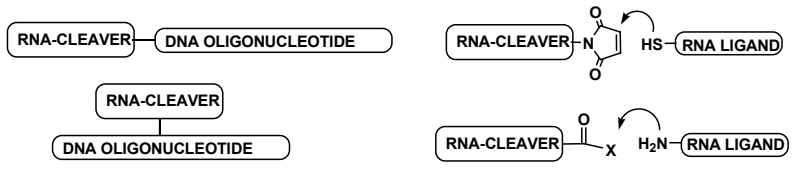

Figure 1: representation of the principal objectives of this thesis.

Starting from the observation that in the trisbenzimidazole catalyst three subunits interact cooperatively, raised almost spontaneously the idea to benefit more broadly of this effect. The concept was to prepare gold nanoparticles functionalised with 2-amino-benzimidazole residues that may act cooperatively. Once an unspecific RNase is obtained, gold nanoparticles have the ability to exchange thiols on their surface.[18][19] Therefore, by a partial exchange with thiols carrying a specific ligand they could become specific nucleases (this project is done in collaboration with the group of Professor Paolo Scrimin at the university of Padova).

A second project has been the synthesis of isoguanosine nucleotides for studies of the *"non-enzymatic oligomerization of ribonucleotides"*. The discovery that RNA by itself exhibits catalytic activity[20][21][22] led to the hypothesis that life could have its origin from a prebiotic *''RNA world''*. To support this hypothesis it is necessary to explain, how RNA could spontaneously polymerise and self-replicate. Orgel and co-workers have tried to develop a system of ''*non-enzymatic oligomerization of ribonucleotides*''[23][24] based on imidazole activated nucleotides. This system has been studied also in our group. However, a series of obstacles hampering

oligomerization became visible: the tendency of G-rich templates to form quadruplexes, the weakness of the A-U base pair, less efficient stacking of pyrimidines compared to purines, inhibition by enantiomeric monomers, inhibition by single 2',5' connections, inhibition by purine-pyrimidine alternation and by-products due to hydrolysis or erroneous chain extension that cause irreversible "poisoning". An alternative mechanism for non-enzymatic oligomerization could start from ribonucleotides 2',3'-cyclic phosphates as activated monomers. It was experimentally observed that the template controlled polymerisation of ribonucleotides 2',3'-cyclic-phosphates leads mainly to chains with the 2'-5'connection.[25] This connection, although less stable,[26] could be desirable, because it allows a reversible process of elongation and cleavage by formation of ribonucleotides 2',3'-cyclic-phosphates. A possible correction of errors during chain elongation could thus be achieved under thermodynamic control. The problem is that with the normal bases and the normal Watson-Crick base pairings, because of the vicinity of the negatively charged phosphates the duplex of 2'-5' connected RNA are unstable.[27] Furthermore, it remains to explain the origin of the natural RNA, which has a connection 3'-5'. How is it possible to find a solution that solves all these problems? A hypothesis could be that before the development of an RNA world there might have been another kind of nucleic acid that somehow transmitted by selection and evolution its information to the RNA.

One approach to form stable duplexes of 2'-5' RNA and to solve the rest of the obstacles for the non-enzymatic polymerisation could be to consider RNA analogues composed of purine-purine base pairs. Expanding the base pairs should diminish charge-charge repulsion thus leading to stable duplexes. To support this hypothesis a duplex consisting only of purines should be prepared and tested for stability. In this context my project was to synthesise the isoguanosine phosphoramidite to assemble a palindromic sequence of guanosine and isoguanosine and to test the duplex stability. Considering that the tris{2-[(benzimidazol-2-yl)amino]ethyl}amine is a catalyst for cleavage which produces 2',3'-cyclic phosphates ribonucleotides, by the principle of microscopic reversibility, it must also work in the inverse process becoming a candidate catalyst for polymerisation of nucleosides 2',3'-cyclic phosphates, and for ligation.

2 Catalysis and Catalysts for RNA Cleavage

2.1 Phosphodiester Bond

In general the cleavage–transesterification of a phosphodiester bond can be schematised as it is shown in Fig. 2.1, with a S_N2 type mechanism, where the nucleophile and the leaving group are in apical positions.[28] We speak about transesterification when an alcohol or an alkoxide is the nucleophile, while we speak about hydrolysis when a molecule of water or hydroxide is the nucleophile.

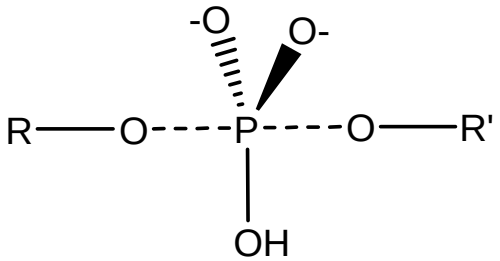

Figure 2.1: Trigonal-bipyramidal dianionic phosphorane.

Under physiological conditions the cleavage of RNA involves the formation of a marginally stable trigonal-bipyramidal dianionic phosphorane.[28c] If it is more correct to speak about an intermediated or transition state is still object of dispute.

Early studies gave evidence that RNA has an higher instability compared to DNA.[28a] The reason of this difference is commonly attributed to the presence of an intramolecular nucleophile, the OH in 2' position. To realize how resistant a phosphodiester bond can be, we can consider that the half life of the diphenyl phosphate. It is 180 years under neutral conditions at 100 °C and in absence of catalysis.[29] To have an idea of what can be the effect of the 2'-OH, other studies have estimated the effective molarity of the 2'-OH group of RNA as 3×10^7 M for the hydroxide-catalysed reaction of a phenyl ester.[30]

Although the presence of the OH in 2' position increase tremendously the rate of the cleavage, the half-life of a model for RNA like cytidylylcytidine is still quite long

(1000 to 10000 days at 60 °C and pH 7).[31] Hence the interest for possible catalysts of RNA cleavage is understandable.

2.2 Cleavage of RNA

In the mechanism of RNA-cleavage (Fig. 2.2), there is an attack of the 2'-oxyanion on the phosphorus (V), formation of the dianionic trigonal-bipyramidal phosphorane "intermediate", and departure of the 5' oxyanion. Contemporarily the reactive 2',3'-cyclic monophoshate is formed, which generates by hydrolysis a mixture of 2' and 3' nucleoside monophosphates.[28a]

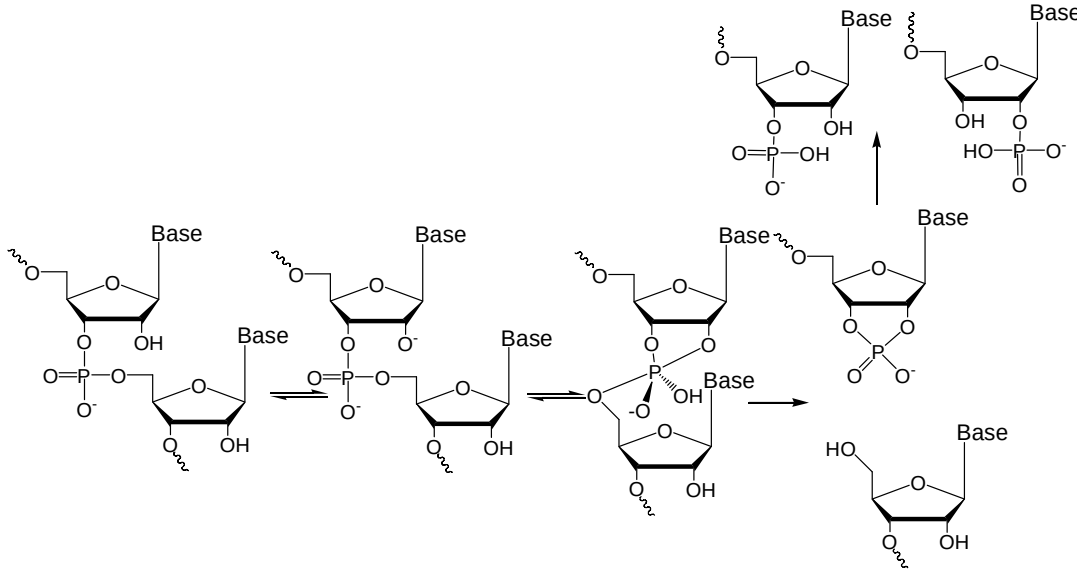

Figure 2.2: Cleavage of RNA.

2.3 Catalysis of RNA Cleavage

In accord with what has been said so far, how should a catalyst act to accelerate this reaction? In a recent publication Lönnberg[32] says that viable candidates for cleaving agents are molecules or ions that:

(i) Enhance deprotonation of the 2'-OH.

(ii) Reduce the electron density at the phosphorus atom upon formation of the phosphorane "intermediate", but allow it to be increased upon cleavage of the P–O5-bond.

(iii) Reduce the electron density at the departing 5-oxygen atom upon cleavage of the P–O5 bond.

There is still another factor to be considered, in accord with the rules of Westheimer[33] nucleophiles are expected to enter and leave the phosphorane only through apical positions. To let the cleavage to occur, the 2'OH and the leaving 5'O must be in line (Fig. 2.3a). Collinearity is required because the phosphorane is too short-unstable to allow an interchange of apical and equatorial positions by pseudo rotation (Fig. 2.3b). What said is particular important in helical structures as of RNA duplexes where the geometry prevents a collinear arrangement of the 2'-OH and the 5'O, thus stabilizing the phosphodiester bonds. This is also the reason why the target for artificial RNases should not be a RNA duplex or a region rich in purines that by stacking tends to assume a helical form.[32][34] On the other hand some sequence combinations of nucleotides seem to be particular reactive.[34b]

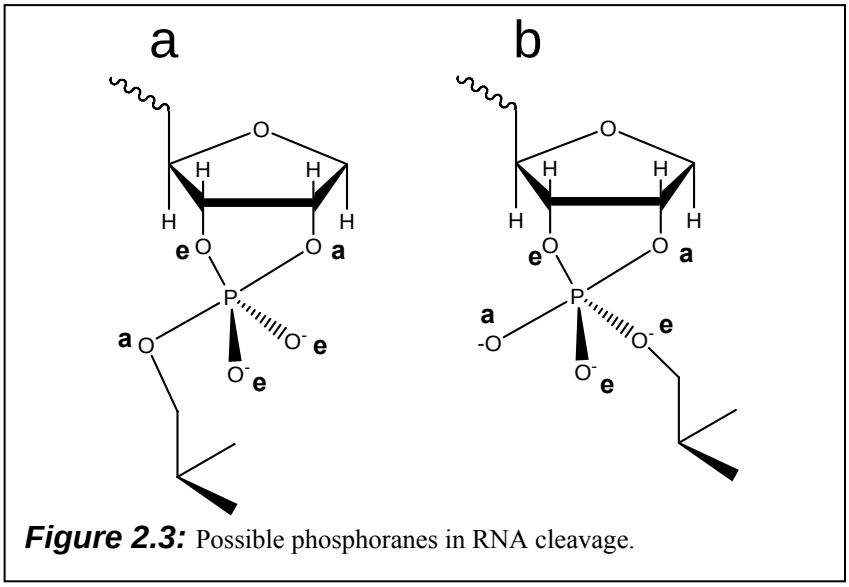

Figure 2.3: Possible phosphoranes in RNA cleavage.

2.4 Enzymatic Catalysis

The problem of the catalysis was first solved by nature through enzymes. The variety of natural enzymes that catalyse phosphoryl transfer reactions is really enormous. There are not only nucleases or ribonucleases, but also phosphatases, DNA topoisomerases. DNA polymerases have a mechanism of correction therefore, they can also work as nucleases. We have then reverse transcriptases, integrases, without consider the ribozymes. Not all these enzymes are well characterized, but their use in biotechnology is increasing tremendously. Of all these enzymes, RNase A and the staphylococcal nuclease are particularly well known and studied. Therefore, they can be taken as classical examples to elucidate how nature arrived to optimise these reactions fundamental for life. A short description of these two enzymes will be done in the next two subchapters.

2.4.1 Ribonuclease A

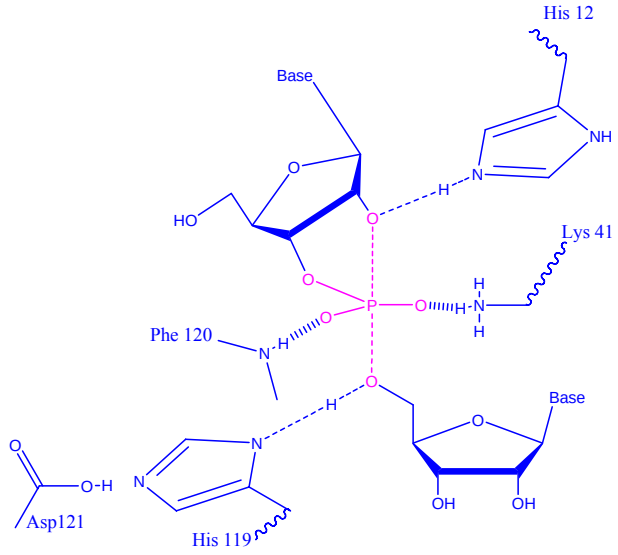

Figure 2.4: Active site of ribonuclease A.[38]

The bovine pancreatic ribonuclease A (Fig. 2.4) is one of the most studied enzymes, probably because even in the past it was easily available from the ruminants' pancreas. It was crystallized already in 1939[35], and in 1941[36] it was possible to

have a resolution of 2 Å in X-ray structural analysis. What is really fascinating and probably also the reason why this enzyme has inspired the design of several artificial ribonucleases is its "Ping-Pong" mechanism.[37][38] In this enzyme metal cofactors are not directly involved, but we have two imidazoles of two histidines that work in concert. His-12 deprotonates the 2'-OH, which becomes a better nucleophile to attack the phosphorus (V). On the other site the His-119 donates a proton to 5'O, neutralising the negative charge of the leaving group, which departure in this way is accelerated. Then other elements like Lys-41, are involved in the stabilization of the phosphorane. The role attributed to this amino acid is to reduce by electrostatic interaction the excess of negative charge that accumulates on the non-bridging phosphoryl oxygens in the "transition state".[39][40] It has also been proposed that the stabilization could occur by a short strong hydrogen bond, involving the partial transfer of a proton.[41] No real detailed studies exist on the role in the catalysis of the main-chain nitrogen of Phe-120, but the closeness to the active site suggests an involvement by donating a proton in an hydrogen bond to a non-bridging oxygen.[38]

2.4.2 Staphylococcal Nuclease

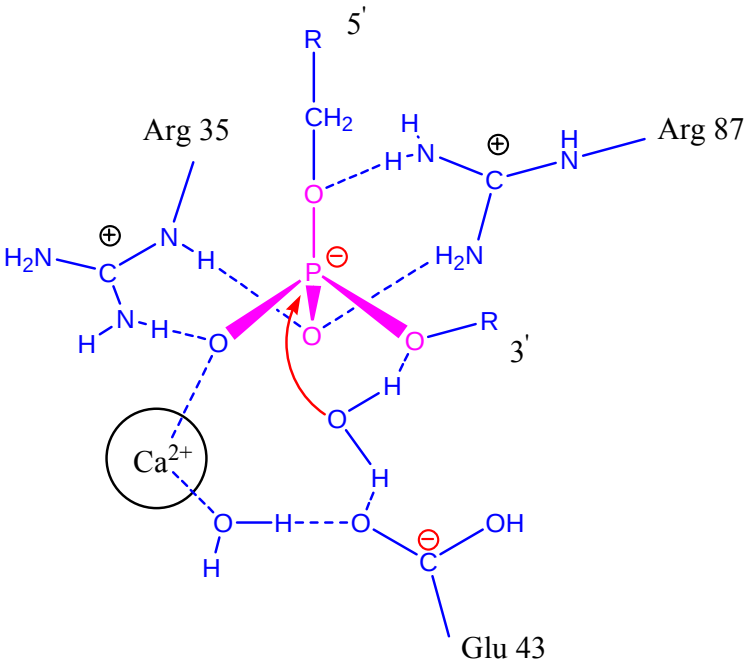

Figure 2.5: Active site of Staphylococcal nuclease.[43]

The second widely studied enzyme and source of inspiration for the design of artificial nucleases is staphylococcal nuclease. In a publication of 1979 Cotton et al. proposed a mechanism of action for this enzyme (Fig. 2.5).[42] In the active site Ca^{2+} is involved with its inner-sphere in the activation of a molecule of H_2O, which is close enough to the Glu-43 to donate a hydrogen bond to this residue. In this way H_2O is sufficiently nucleophilic to attack the phosphorus (V). Therefore, the carboxylate of Glu-43 acts as general base. Regarding the role of Arg-35 and Arg-87, both are involved in the catalysis by stabilising the dianionic phosphorane as strong donors of a bifunctional hydrogen bond, but their role seems to be different.[43] In fact by mutation of Arg-87 with a Gly, the catalysis is profoundly reduced, but not the affinity. This suggests that Arg-87 interacts with the trigonal-bipyramidal phosphorane rather than with the tetrahedral ground state of the substrate. In the other hand the mutation of Arg-35 corresponds to a large reduction in activity and affinity, suggesting also a role in the recognition of the tetrahedral phosphodiester group of the substrate.

2.5 Artificial Ribonucleases

The development of articial ribonucleases has followed mainly two directions, one based on metal complex, and the other based on metal free catalysts. With this preface a short presentation of the metal based catalyst will begin here, followed by a more deep description of the metal free catalysts.

2.5.1 Metal Based Catalysis

The modes in which metal ions can catalyse the RNA cleavage are basically 3, and they are summarized in Fig. 2.6.[44][45][46][47] In the first mode the metal can promote the nucleophilic attack of the 2'-OH by interacting with it and deprotonating it. This interaction can occur directly (Fig. 2.6a) or by an hydroxide ion ligand of the outer sphere (Fig 2.6b). In the second mode the metal can interact with the negative charge of the phosphate (Fig. 2.6c), making the phosphodiester more electrophilic and more

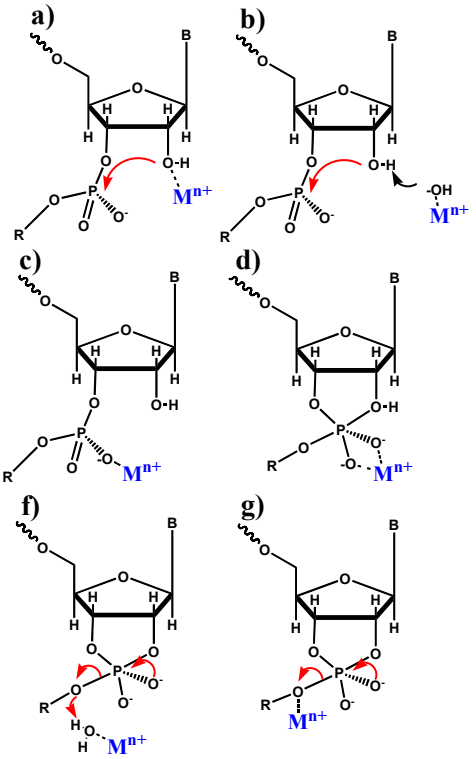

Figure 2.6: Modes by which the metal iones can catalyse the RNA cleavage.[44]

prone towards nucleophilic attack. After the attack the formation of the dianionic phosphorane can be stabilized by the positive charge of the cationic metals (Fig. 2.6d). In the third mode the metal can assist the departure of the leaving group protonating the oxygen by a water molecule of his outer sphere, or directly by interaction of the metal ion with the partial negative charge on the leaving oxygen. Therefore, metals combine intrinsic properties to catalyse the RNA cleavage.[48][49] To illustrate these catalytic properties we can take a recent publication, where with the simple incorporation of a modified nucleotide in the middle of a DNA sequence, a conformational change in the complementary RNA strand was induced, and 10 mM $MgCl_2$ (pH 8) was sufficient to cleave specifically this site (Fig. 2.7).[50]

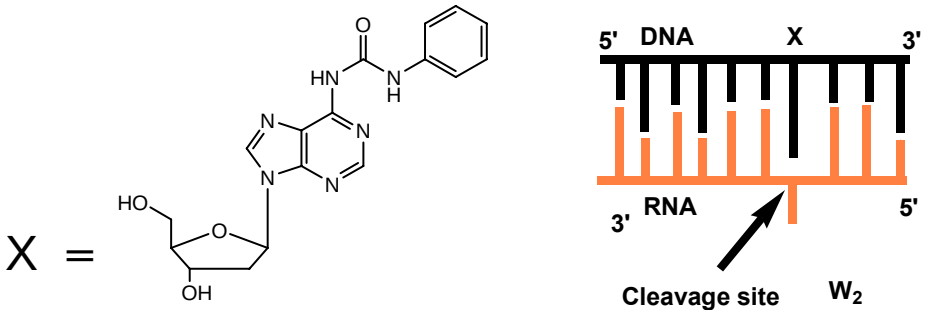

Figure 2.7: Modified nucleotide induced a conformational change, with a concentration of 10 mM of $MgCl_2$ (pH 8) a site specific cleavage was achieved.[50]

2.5.2 Metal-Based Catalysts

Already in 1938 it was observed that certain metals like lanthanide ions were able to catalyse the cleavage of phosphoric acid esters.[51] Knowing the properties of these

metals, one strategy towards artificial nucleases was to attach related metal complexes to DNA oligonucleotides in order to get site specific cleavage by formation of antisense conjugates. With this strategy the best results were achieved by complexes of lanthanide ions, Cu^{2+} and Zn^{2+}.[32][15]

The most promising complexes of lanthanides are macrocyclic complexes,[52] which were conjugated with different modalities to antisense oligonucleotides (Fig. 2.8).[53][54][55]

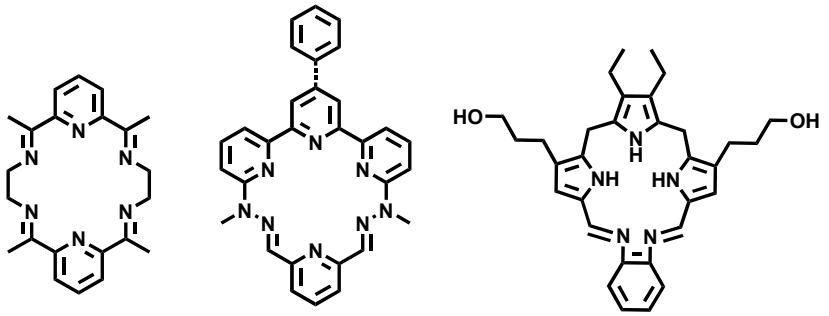

***Figure 2.8*:** Macrocycles complexing lanthanides as catalysts for RNA cleavage.

The catalysts based on Cu^{2+} ions are usually complexes of terpyridines and dimethylphenanthroline (Fig. 2.9), then conjugated to have specificity.[32][15] The first conjugate was obtained by Bashkin et al. using terpyridine as agent to complex Cu^{2+}.[56] Improvements to optimize the cleavage continued by the conjugation of these complexing agent in different positions.[32][15]

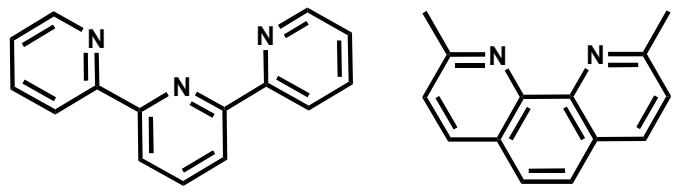

Figure 2.9: Terpyridine and dimethylphenanthroline as Cu2+ complexing agent for RNA cleavage catalysts.

Another ion metal often used in metal based ribonucleases is Zn^{2+}. The catalysts that form complexes with this metal in different constructs, are usually a combination of the following chelating agents: dimethylphenantroline, 1,4,7-triazacyclononane,

1,5,9-triazacyclododecane and 1,4,7,10-tetraazacyclododecane (Fig. 2.10).[15][32][44][45][47][57]

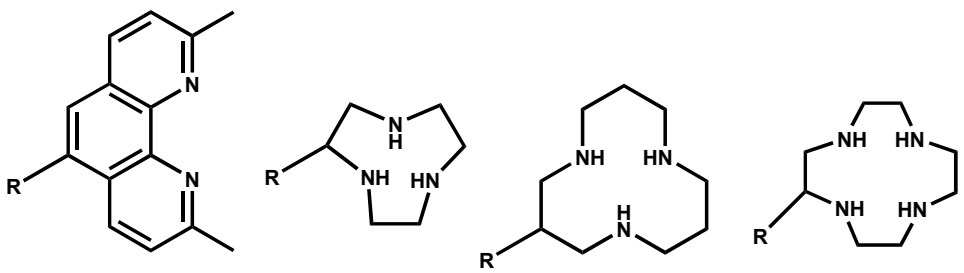

dimethylphenanthroline 1,4,7-triazacyclononane 1,5,9-triazacyclododecane 1,4,7,10-tetraazacyclododecane

Figure 2.10: Zn^{2+} and its chelating agents as elements to build artificial RNases.

2.5.3 Metal Free Artificial RNases

In the development of artificial RNases the second strategy is based on metal free catalysts, agents able to cleave independently of metallic cofactors, however, without excluding a possible participation of physiological metals *in vivo*. The aim of such strategies is clear, to make the catalyst independent from complexes, whose stability can be challenged *in vivo* by other natural metal-binding sites. Even for uses *in vitro*, the structures of RNA could form metal-binding sites that could compete for the metal of the cleaving agent.

In some cases these catalysts have been inspirited by RNase A, where an important role is played by two residues of histidine. Also staphylococcal nuclease has been source of inspiration. Here an important role is played by two residues of arginine. Another category of these catalysts are the polyamines.

In these catalysts are combined elements that represent single chemical functions, like acid-basic properties or the ability to form pairs by hydrogen bonds. Such elements by themselves are not powerful catalysts. However, when combined in more complicated molecules to work cooperatively, they are able to generate large catalytic effects. An analysis of the elements that can catalyse RNA cleavage will follow in the next subchapters.

2.5.3.1 Imidazole Based Catalysis

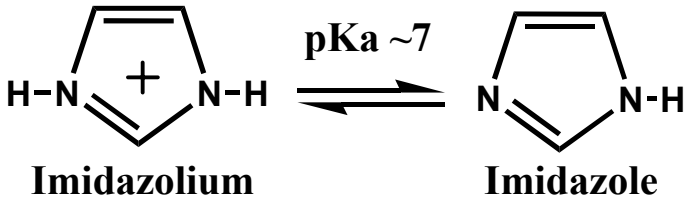

Figure 2.11: Imidazolium imidizole equilibrium.

The imidazole in form of histidine with its pKa close to 7 has important functions in several enzymatic reactions, because it can exist at neutral pH as imidazolium or as imidizole. Under physiological conditions the imidazole residues are the strongest bases that can exist at least partially deprotonated, while the imidazolium is the strongest acid that can exist at least partially protonated. These properties allow the imidazolium to act as general acid, and the imidazole as general base, or like in RNase A as combined acid and base catalysis.[58][59][60]

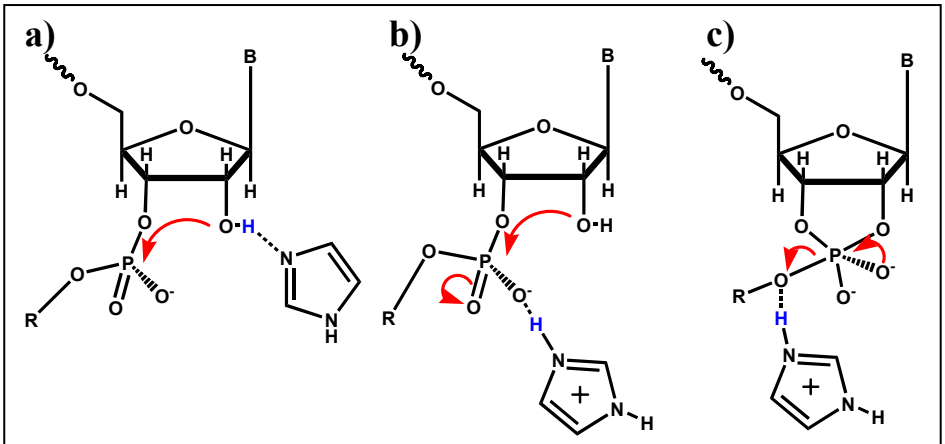

***Figure 2.12*:** Modes with which the imidazole can catalyse the RNA cleavage.

The options of imidazole to catalyse the transesterification of RNA are shown in Fig. 2.12, where we have three modes.[28a][28c][60] The first modality a) is by general base catalysis, the free base in proximity to the 2'-OH can support the deprotonation and therefore, the subsequent nucleophilic attack. The second modality b) is by general acid catalysis. We can have a protonation of the phosphodiester anionic oxygen (pKa ≈ 1)[28a] prior to nucleophilic attack, making the phosphodiester more electrophilic. This event can also occur simultaneously with the formation of the dianionic

phosphorane, thus stabilizing this intermediate/transitionstate. The oxygen of the dianionic phosphorane by theoretical calculations can assume a pKa in the range of 6.5-11.[28c] The last modality c) is also by acid catalysis, the imidazolium in proximity to the leaving 5'O can protonate it, and make the departure of the leaving group easier.

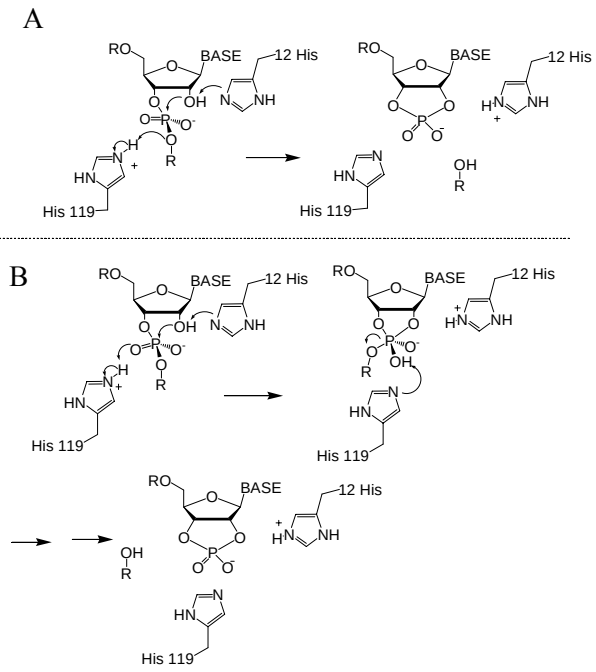

Figure 2.13: Mechanism for imidazole catalysis and RNase A: A) Classical mechanism. B) Triester mechanism.[28c]

On the base of these three modalities and numerous studies, two mechanisms for imidazole catalysis and in RNase A are proposed (Fig. 2.13).[28a][28c][60] In the classical mechanism (Fig. 2.13a) an imidazole acts as base deprotonating the 2'-OH and in a second step or simultaneously an imidazolium group protonates the leaving 5'O. While in the second mechanism called "Triester Mechanism" (Fig. 2.13b), an imidazole deprotonates the 2'-OH. The other imidazolium first protonates the phosphorane and then removes the proton to place it on the leaving group. With this mechanism of ''push-pull'' the second imidazolium in first step lowers the barrier for the nucleophilic attack and then by transferring the proton to the leaving group reduces the barrier for its departure. Note that the protonated phosphorane, in contrast to its dianion, is thought to be a stable intermediate.

2.5.3.2 Guanidium Based Catalysis

The guanidinium group is the residue of the arginines present in the active site of SNase (staphylococcal nuclease) as well in other enzymes. It is particularly versatile because it can make 5 hydrogen bonds, due to its high pKa (in arginine 12.48)[61] it

can carry a positive charge, and is planar. The general modalities of guanidinium-phosphate interactions are described in (Fig. 2.14).[62]

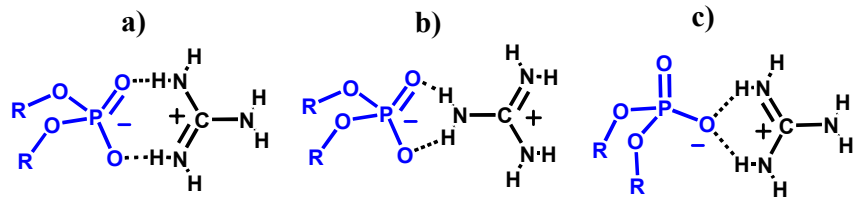

***Figure 2.14*:** Interaction patterns between guanidinium and phosphate.[62]

Two other patterns of interaction between guanidinium and phosphate are described in Fig. 2.15. In Fig. 2.15a two guanidiniums form strong hydrogen bonds with a monohydrogenphosphate.[63] While in Fig. 2.15b one guanidinium is able to coordinate two phosphates forming four hydrogens bonds. This last pattern is also called ‘‘Arginine fork’’.[64]

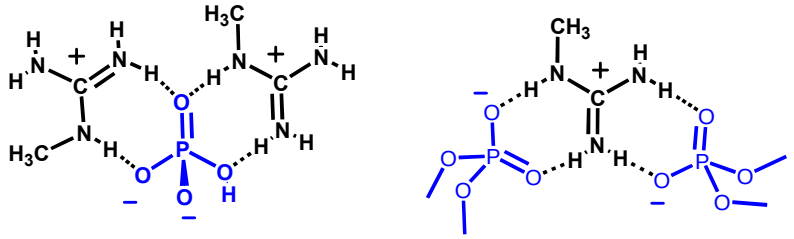

Figure 2.15: a) Two guanidiniums form strong hydrogen bonds with a monohydrogenphosphate.[63] b) A guanidinium coordinates two phosphates ‘‘Arginine fork’’.[64]

These modes of interactions are more interesting for the recognition of phosphates by guanidinium, nevertheless our goal is catalysis. Anslyn[62] has postulated that for the guanidinium group at least three roles can be played in the nuclease-mediated hydrolysis:

1. **The ditopic nature of the hydrogen-bonding pattern can bind and orient a phosphoester substrate.**
2. **The positive charge allows for electrostatic stabilization of anionic phosphorane-like transition states.**

3. **Proton transfer to the leaving groups (whose pKa comes close to 14.8)**[65] **may occur.**[66] **Given our phosphorane pKa, guanidinium groups (with pKa near 13) should also act as general acids and therefore protonate the phosphoranes (Fig. 2.16).**

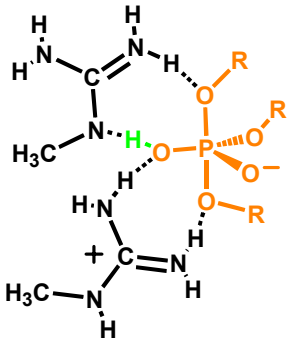

Figure 2.16: Guanidinium mediates RNA hydrolysis.

According to these roles a guanidinium group can act as acid and base to shuttle protons on and off the phosphorane intermediates formed along the hydrolysis pathway.

2.5.3.3 Catalysis Based on Oligomeric Amines

The first studies about activity of oligoamines in RNA cleavage, were reported by Komiyama and co-workers.[67] On the base of these studies it was shown that the simple ethylenediamine or its oligomerers diethylenetriamine, triethylenetetraamine at pH 8 and pH 7, give an acceleration of RNA hydrolysis, however this effect was negligible for ethylamine (Fig. 2.17a). Therefore it was deduced that this catalysis

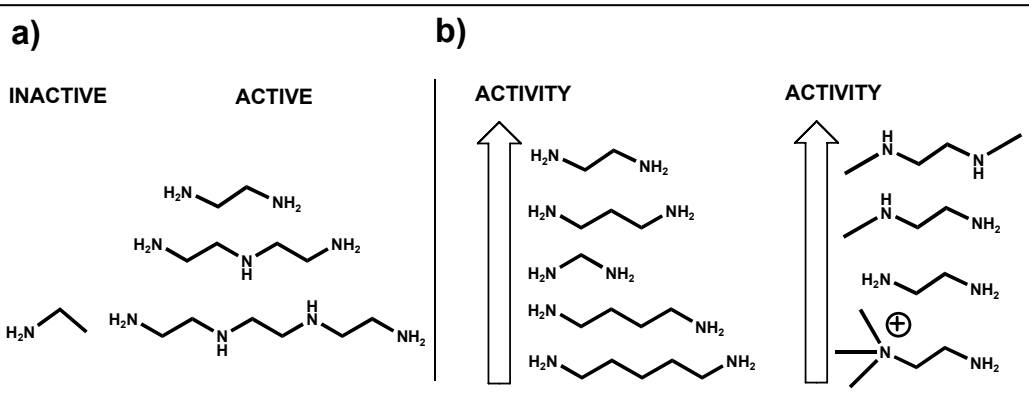

Figure 2.17: Different orders of activity for oligoamines in RNA cleavage.

was due to a cooperativity of two amino groups. Accurate analysis of RNA cleavage for different amines at pH 7 showed the order of activity reported in Fig. 2.17b left.[68] The explanation was that of the possible forms of these diamines; neutral, mono cationic, and fully protonated, only the first two are active. At pH 7 the 1,4-diaminobutane and the 1,5-diaminopentane are almost completely protonated and thus show only a small activity. On the contrary the ethylenediamine and the 1,3-diaminopropane preferentially form the monocation. This is caused by the electrostatic suppression of the second protonation. If at pH 7 the active diamines adopt the monocationic form, the mechanism may occur with two modalities (Fig. 2.18). In the first hypothesis the free amino group acts as general base and the protonated one can be a general acid. In the second hypothesis the free amino group again acts as genereral base, while the protonated amino group assists by electrostatic stabilisation. To clarify which of these two hypothetic mechanisms are real, the activity of (2-aminoethyl)trimethylammonium ion [$H_2N(CH_2)_2N(CH_3)_3^+$] were checked (Fig. 2.18).

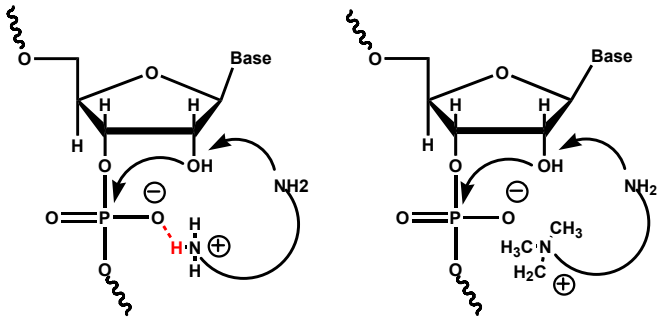

Active **4.4 Times less Active**

Figure 2.18: Mechanism for oligoamines in RNA cleavage

This ion has a positive charge as does the monocation of ethylenediamine, but at pH 7 it has no acidic proton, and is 4.4 fold less active. The conclusion was that the ammonium cation acts as general acid. Another test was done in D_2O to see the "Solvent Isotope Effect". For the ApA hydrolysis by the monocation of ethylenediamine and by its neutral species: k_c(in H_2O)/k_c(in D_2O) = 2.0 and 1.4 respectively.[68] This was another argument for a proton transfer from the ammonium group. The conclusions of these studies were that for the monocation of

ethylenediamine the mechanism proceeds by acid–basic catalysis, with the amino group that acts as base taking away the proton of the 2'-OH and the protonated amino group donating a proton during phosphorane formation. The diamines with longer chains, are less active in catalysis, because at neutral pH exist predominantly in form of dications. The increased distance of the nitrogens renders the electrostatic suppression of the second protonation less effective. At more basic pH the neutral amines should then react mainly by general base catalysis.

2.5.3.4 Metal Free Cleaving Agents

In the last years various metal-free catalysts have been developed.[28a] After the description of the elements that generally are used in the design of artificial metal free RNases, some examples of catalysts will be now taken in consideration.
The compound in Fig. 2.19a was synthesized with the aim to take advantage of the properties of the oligomeric amines and trying to improve the cleavage by conjugation with an intercalator.[69] The cleavage induced by this compound (1 mM) was 40 % of rRNA (0.1 unit A_{260}) in 1 h at 37 °C and pH 7.4.

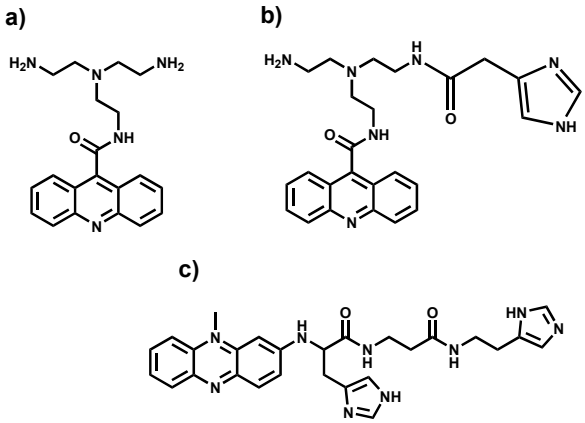

Figure 2.19: Some metal free cleaving agent.

The compound shown in Fig. 2.19b[69] (1 mM) was reported to cleave 60 % of rRNA (0.1 unit A_{260}) in 1h at 37 °C and pH 7.4. While for the compound in Fig: 2.19c[70] showed to be able to cleave the 50 % of the substrate in 12 h at pH 7.5 and 37 °C. With the aim to reproduce the active site of RNase A, different cleaving agents were produced. One of the first catalysts is shown in Fig. 2.20b,[71] where is also proposed a possible mechanism. Such catalyst showed to cleave 30 % of the

RNA target in 4 days at pH 7.5 and 50°C. A catalyst inspired by staphylococcal nuclease and based on the guanidinium groups, is given in Fig. 2.20a.[72] This molecule was able to cleave RNA in the presence of imidazole, which should work as base deprotonating the 2'-OH.

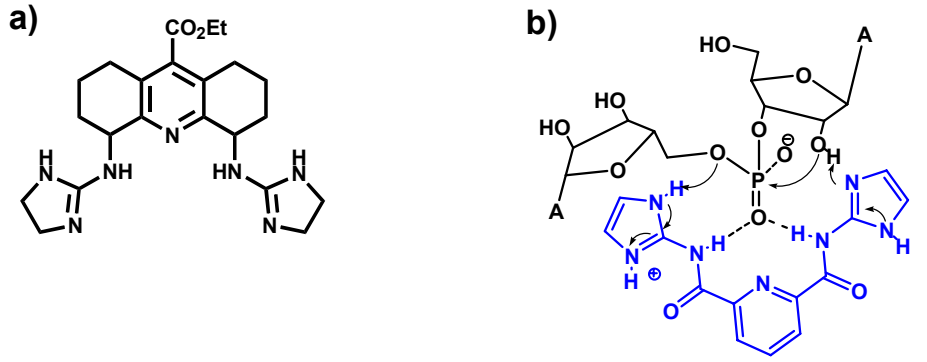

Figure 2.20: Some metal free cleaving agent.

2.6 The Tris(2-aminobenzimidazole)

In the last years tris{2-[(benzimidazol-2-yl)amino]ethyl}amine (**29**) (Fig. 2.22) was developed in our group as a catalyst for RNA cleavage.[16] During my work this catalyst was used to obtain site specific RNA cleavage.

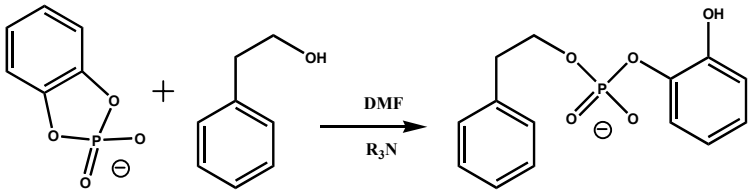

***Figure 2.21*:** Reaction of catechol cyclic phosphate and phenylethanol.[16]

This compound was the result of studies on the catalytic influence of guanidinium ions on the phosphodiester transesterification. An important observation was made by analysing the reaction of catechol cyclic phosphate and phenylethanol in DMF in presence of different guanidinium derivatives (Fig. 2.21).[16][73] The connection of two guanidinium groups by a proper spacer (Fig. 2.22**a**) could show an interesting catalytic cooperativity.

The substitution of the guanidinium groups by heterocycles (Fig. 2.22**b**) led to a further rate increase by a factor of 10. This effect was attributed to the increased acidity of the heterocyclic guanidinium analogue.[74] In fact the increased acidity reinforces hydrogen bonds with the substrate and improves the transition state stabilization. In addition, it enables the cation to participate in general acid/base catalysis.[66] However, in water this effect was not visible anymore. The explanation can be found in the electrophilicity and polarity of water that allows it to stabilize the phosphorane transition state by solvation. The guanidinium ions in aqueous solutions are mostly protonated and not sufficiently acidic to compete with water as general acid. Therefore, the remaining activity of the compounds in Fig. 2.22**a** and **b** was too weak to induce major rate effects in aqueous solution. As a consequence of these observations it was decided to decrease the pKa of the guanidinium group by incorporating them into aromatic heterocycles.

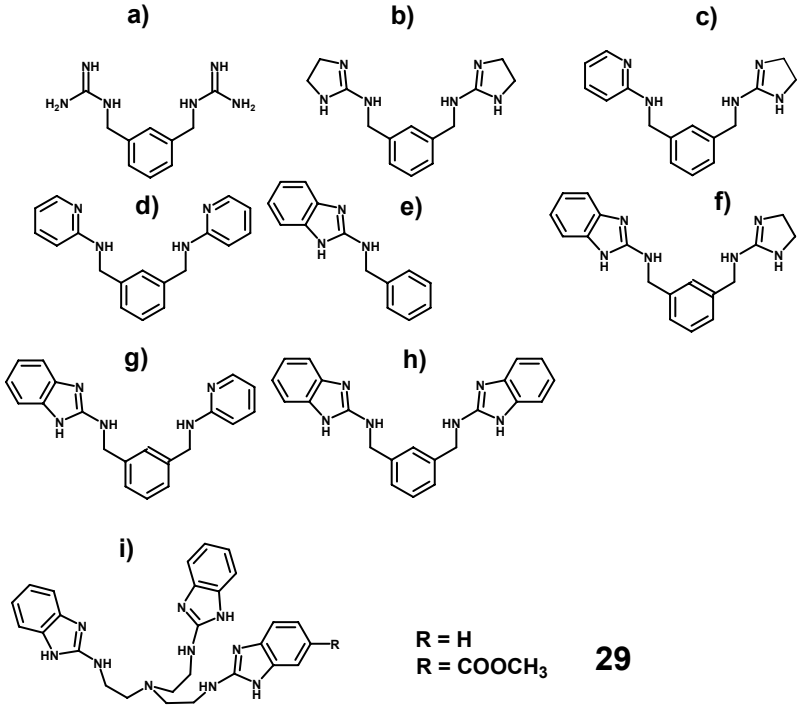

Figure 2.22: Structure of the compounds that preceded **29**.

Table 2.1: RNA degradation for the compounds in Fig. 2.22. at 10 mM Catalyst, 50 mM Tris HCl, pH 7, 0.01 % SDS, 37 °C, 20 h, RNA 120-140 nM.

		% degradation	
compound	pKa	RNA 1*	RNA 2*
c	6.2	6	4
d	6.5	2	<1
e	6.9	15	13
f	6.6	15	13
g	7.1	31	31
h	7.0	n.d.	86
i	n.d	n.d.	n.d

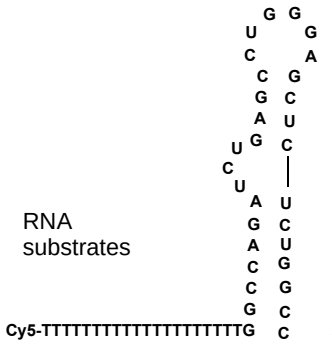

Figure 2.23: RNA structures used to test the compounds in Fig. 2.22.

Table 2.2: RNA cleavage for the compounds in Fig. 2.22. at 1 mM Catalyst, 50 mM Tris-HCl, pH 6, 0.01 % SDS, 37 °C, 20 h, RNA 120-140 nM.

		% degradation	
compound	pKa	RNA 124	RNA 2*
c	6.2		
d	6.5		
e	6.9	4.8	2.4
f	6.6	4.6	3.0
g	7.1	4.5	3.2
h	7.0	23.1	15.3
i	n.d	92.9	87.6

To really prove a relation between the activity and the acidity, different guanidinium analogues were synthesized. The pKa values were determinated and are reported in Tab. 2.1. For the tris(benzimidazole) Fig. 2.22**i** it was not possible to measure reproducible values. The absorption versus concentration curves around pH 7 did not fulfil Lambert-Beer's law, indicating some form of aggregation. In the first tests to evaluate these different guanidinium and amidinium derivatives, the monomeric 2-aminobenzimidazole derivative in Fig. 2.22**e** (10 mM) already cleaved 13–15 % of the RNA substrate (120-140 nM) at 37 °C, 20 h and pH 7. For the bisbenzimidazole in Fig. 2.22**h** the cleavage could reach 31 % in the same conditions. The problem was that under such conditions excessive RNA precipitation was observed in several experiments. For the same reason, no data could be obtained for the tris(benzimidazole). To minimize such effects 0.01 % of *n*-dodecyl sulfate (SDS) was added to the cleavage buffer. To exclude precipitation effects new sets of experiments were run at pH 6 (Tab. 2.2). From these experiments it was possible to see that the tris(benzimidazole) was the best catalyst, inducing cleavage yields of 87-92 % in 20 h, at 37 °C and pH 6. The resulting half-lives are 120 min for the linear substrate **124** (Fig. 2.23) and

200 min for the TAR analogue sequence **2*** (Fig. 2.23). This corresponds to a formal first-order rate constant of 3.3×10^{-6} s^1 for a mean phosphodiester linkage in substrate **124**. After these first series of experiments the most promising compound was the tris(benzimidazole). Therefore, more detailed investigations were done studying the cleavage as a function of catalyst concentration. From these studies a non-linear dependency was found, with a sudden decrease of activity around 100 μM (Tab. 2.3). The phenomenon was again investigated with the suspect that the formation of aggregates could be the reason. To verify aggregation the Fluorescence Correlation Spectroscopy (FCS) was used. With this method the diffusion time is measured in relation to the size of a molecule. Bigger molecules will have a longer diffusion times. This parameter was measured using a dye labelled DNA sequence, incubated with different concentrations of the tris(2-aminobenzimidazole) and with different detergents. A clear correlation between aggregation and catalytic activity was found. With the formation of the aggregates the activity was much higher.

Table 2.3: RNA degradation for **29** at different concentrations. Conditions: 50 mM Tris-HCl, pH 6, 0.01 % SDS, 37 °C, 20 h, RNA 120-140 nM.

	% degradation	
Concentration **29** [μM]	RNA 1	RNA 2
250	87.4	48.7
200	85.6	44.8
150	63.3	27.1
120	60.3	26.7
100	16.6	8.5
80	6.2	6.4
60	3.9	6.5
40	5.2	5.2
20	6.3	7.7
10	4.1	1.1

Therefore, a non-aggregated form of catalyst **29** suitable for pH dependency correlation was desirable. A task of my thesis was to solve this problem of solubility. At the same time a method for site specific RNA cleavage had to be developed. To reach this objective, during my thesis different DNA conjugates were synthesised to generate a soluble and specific derivative of the tris(2-aminobenzimidazole).

2.7 Assays for RNA Cleavage

2.7.1 Models for RNA Cleavage

In recent years different assays have been developed to measure the reaction rates of RNA cleavage. Some of the most successful systems are reported here. One method is to use reactive models of RNA.

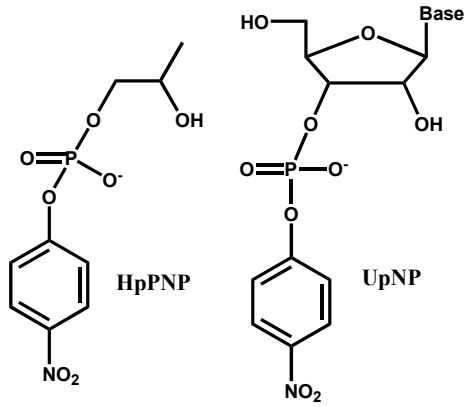

Figure 2.24: Activated models for RNA cleavage assays **HpPNP** and **UpNP.**

Among the models of RNA the two mostly used are shown in Fig. 2.24.[31][75][76] The names are **HpPNP** and **UpNP** when the base is uracile. These compounds are designed to mimic the dialkyl phosphate esters that form the backbone of RNA. The leaving group is 4-nitrophenolate, which is a better leaving group compared with an alkoxylate. Consequently, these compounds are more prone to base catalyzed cleavage. The advantage of these models is the possibility to monitor by UV absorbance the release of 4-nitrophenolate, which gives an increase of absorbance at 400 nm. These models are then particularly useful for studying the mechanism of phosphate ester hydrolysis. Furthermore, the cleavage can be followed by HPLC and ^{31}P NMR. Caution should be taken, however, to predict reactivity of real RNA, which can largely differ from the rates observed with RNA models.

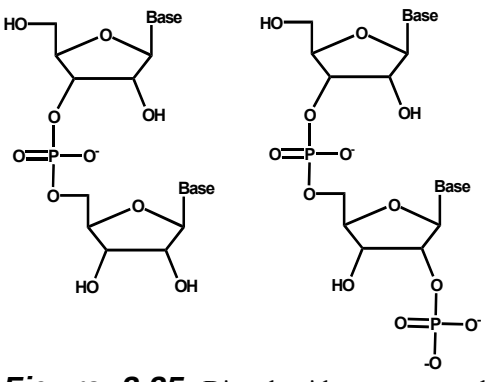

Figure 2.25 Dinucleotides mono and diphosphates as models for RNA cleavage assays.

Other substrates for mechanistic and kinetic studies of RNA cleavage are dinucleotide mono and diphosphates[15] such as **ApA**, and **ApUp** (Fig 2.25). The reactivity of these dinucleotides comes closer to the properties of the polymeric RNA, and they have the advantage of a single cleavage site. The cleavage can be then monitored by HPLC, or by NMR

exploiting the different δ of C1' protons in the starting dinucleotide and the cleavage products. As disadvantage they have not the polymeric and polyanionic character of the biological RNA. Significant differences have been observed between dinucleotides and the polymeric RNA, and even between ApA and ApAp.[15]

2.7.2 Fluorescently Labelled RNA Probes Analysed by Alfexpress™

Although RNA models can be useful tools to probe the activity of artificial nucleases, the final test should be done with real RNA. Site specificity was among the objectives of this work. Therefore, the cleavage assays were performed with defined RNA sequences. The methods to analyse RNA cleavage are usually based on gel electrophoresis. Traditional procedures with standard electrophoresis chambers and radioactively labelled sequences have some inconveniencies, like the cost of the waste disposal, radiation protection, and the short half-life of the radioisotopes (usually ^{32}P, ^{35}S).

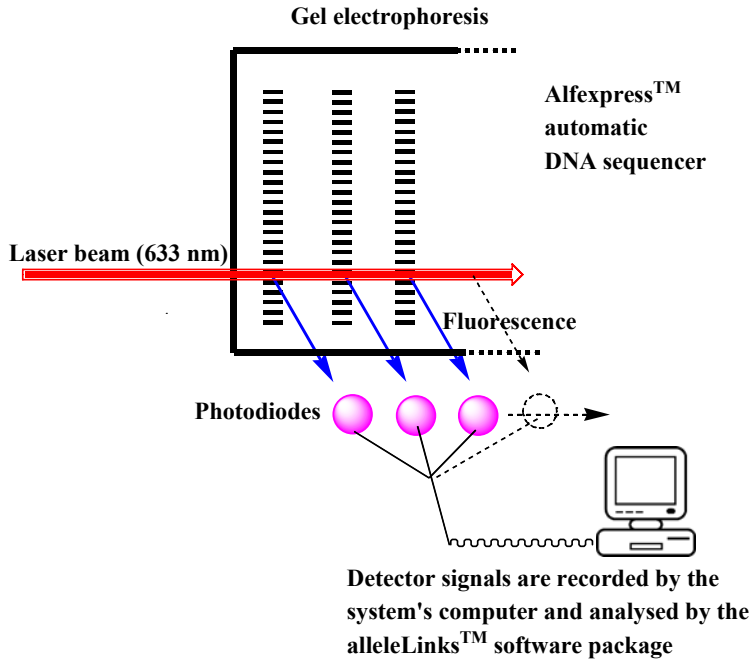

Figure 2.26: Alfexpress™ automatic sequencer for RNA cleavage assays.

To avoid these inconveniencies a method based on fluorescently labelled RNA probes and automatic deoxyribonucleic (DNA) sequencers was developed in our group (Fig. 2.26).[77][78] During the electrophoresis, Cy5-labeled RNA products are detected as they pass through a laser beam (633 nm) at the bottom of the gel. Cy5 is a

carbocyanine dye with an absorption maximum at 643 nm and λ_{em}= 667 nm. It withstands a wide variety of solvents and incubation conditions. Laser excitation of the dye takes place simultaneously in the 40 lanes of the gel. Thus a great number of probes can be analysed in parallel. The emitted fluorescence is measured by a linear array of photodiodes with a detection limit similar to that of modern laser fluorescence scanners. Detector signals are recorded by the system's computer and analysed by the AlleleLinks™ software package. Compared to a simple electrophoresis chamber, the sequencer offers superior band resolution owing a long migration distance (26 cm), and the machine controls the temperature of the gel, normally 55 °C. A typical result of cleavage experiments analysed with the Alfexpress™ automatic deoxyribonucleic (DNA) sequencer, is reported in Fig. 2.27, where an example of the electropherograms is shown. Lane B shows the result of a partial alkaline hydrolysis of RNA, used to prepare base ladders to analyse cleavage patterns and to identify cleavage sites. In lane A the result of one site-specific cleavage experiment is reported. In the right of both the lanes is present a big peake corresponding to the non-degraded substrate. The electropherograms are integrated using the AlleleLinks™ software. The percentage of degraded RNA is then calculated from the ratio of integrals for product and product + substrate.

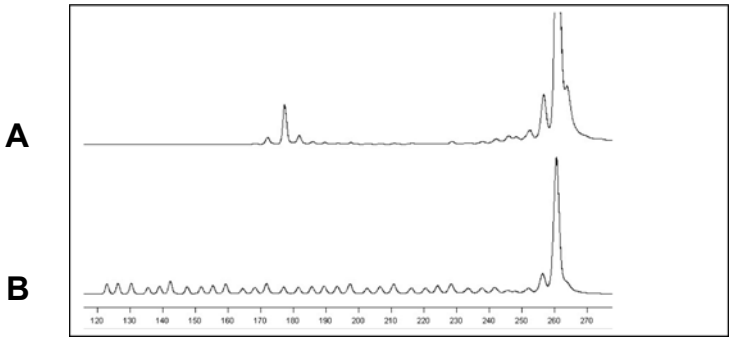

Figure 2.27: An electropherograms integrated using the AlleleLinks™ software.

The RNA substrates used in these experiments have in common the general structure shown in Fig. 2.38. The oligonucleotides are dye labelled with a fluorescent cyanine. This allows the detection of the RNA and of all degradation products with high sensitivity on the DNA sequencer. A short spacer of DNA (T_{10}) was placed between the dye and the RNA sequence to prevent the formation of very short fragments that

would complicate the electrophoretic separation. The DNA lacking the 2'-OH group is stable under the conditions of RNA cleavage. A T_4 fragment is also attached to the 3'-end. A second type of RNA substrate, constructed in a similar way, contains a stem-loop element from HIV-1 TAR (Fig. 2.30).

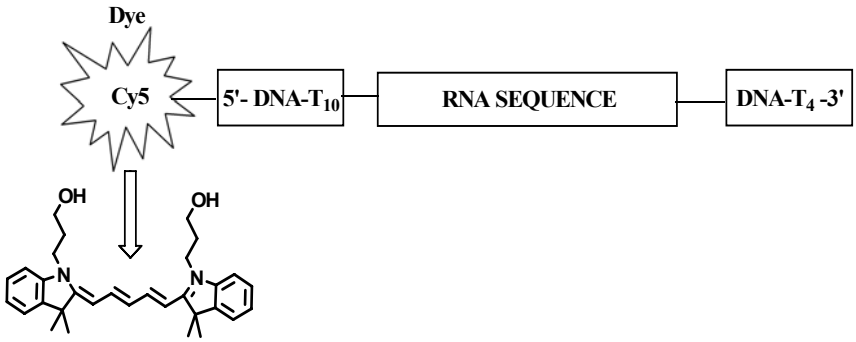

Figure 2.28: Oligonucleotides dye labelled with a fluorescent cyanine as probe for RNA cleavage.

A problem that often arises during RNA cleavage experiments is the contamination by natural RNases, which can falsify the results. Our group has developed an incorruptible assay[79] that makes use of enantiomeric RNA. In fact the natural enzymes are chiral entities, capable to cleave natural RNA with high enatioselectivity while the mirror image RNA is completely resistant to the natural RNases. Achiral catalysts however, are expected to cleave both enantiomeric substrates with the same pattern. For this reason enantiomeric RNA oligonucleotides were also studied (Fig. 2.30, substrate **158** and **190**).

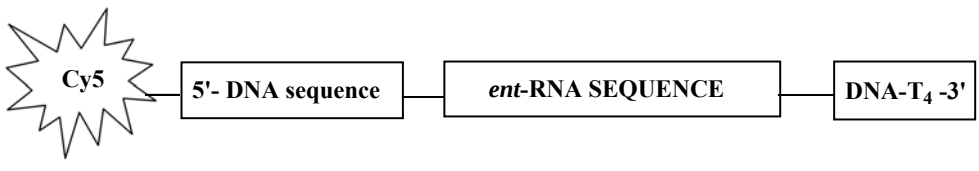

Figure 2.29: Enantiomeric oligonucleotides dye labelled with a fluorescent cyanine as probe for RNA cleavage.

Another construct with the schematic structure reported in Fig. 2.29 (Fig. 2.30 substrate **202**) was used to test the activity of antisense DNA conjugates. In this substrate a sequence of DNA in 3' is complementary to the antisense DNA, while the catalyst is held close to the enantiomeric RNA sequence. Therefore, the binding is

guaranteed by the DNA sequence and the cleavage should occur in the enantiomeric RNA, excluding in this way the effect of possible contaminations. At the end of this chapter a survey of all substrates used in this thesis is given (Fig. 2.30). The numeration of Fig. 2.30 will be used later for describing the experiments of RNA cleavage.

RNA substrates :

Cy5-T_{10}-ribo($^{5'}$CUAGCCGACUGCCGAUCUCGCUGACUGAC)-$T_4{}^{3'}$ 124

Cy5-$^{5'}$CTAGCCGACTGCCGA-*ent*-ribo(UCUCGCUGACUGAC)-$T_4{}^{3'}$ 202

Cy5-T_{10}-ribo($^{5'}$AUACCUUGUCAGGAGAAGAGAGGCCGUUA)-$T_4{}^{3'}$ 210

RNA

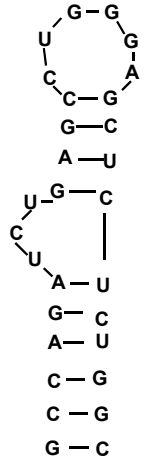

Cy5-T_{10}-ribo($^{5'}$G — C)-T $_4{}^{3'}$ 153

Enantio-RNA

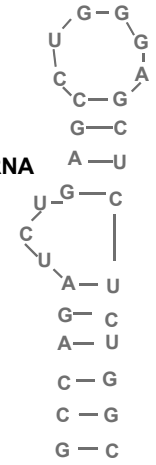

Cy5-T_{10}-ribo($^{5'}$G — C)-T $_4{}^{3'}$ 158

Cy5-T_{10}-ribo($^{5'}$GGCUGACCAUCAAUAAGGAAGAAGCCCUUCAGCGGCCAGUA)-$T_4{}^{3'}$ 176

Cy5-T_{10}-*ent*-ribo($^{5'}$GGCUGACCAUCAAUAAGGAAGAAGCCCUUCAGCGGCCAGUA)-$T_4{}^{3'}$ 190

accessory DNA oligonucleotides:

Cy5-TTTTTTTTTTTTTTTTTTTTU 3' **108**

TGTGGAATTGTGAGCGGATA 3' **109**

$^{5'}$TAACGGCCTCTC$^{3'}$ **246**

$^{5'}$TAACGGCCTCTCT$^{3'}$ **245**

$^{5'}$TAACGGCCTCTCTT$^{3'}$ **244**

Figure 2.30: Oligonucleotides used during this work.

3 Site-Specific Cleavage of RNA by 5' Antisense Conjugates

We have already seen in the precedent chapter how the tris(2-aminobenzimidazole) was identified as a powerful cleaver of ribonucleic acids. Unfortunately this molecule shows a tendency to aggregate in a pH-dependent way. This feature prevented deeper mechanistic studies such as pH-rate correlations and similar experiments. To solve this problem and to achieve a site-specific cleavage, a conjugation with DNA was planned. The investigations of the mechanism of the tris(2-aminobenzimidazole) was the first objective of these conjugates. Furthermore, this thesis also hopes to contribute to future practical applications.

Useful synthetic ribonucleases should be characterized by two properties:

1) **High site specificity**

   For this purpose different antisense oligonucleotides were synthesized of which one presented a single cleavage site. In collaboration with Kathrin Beier it was furthermore tested if helper antisense oligonucleotides placed after the cleavage site might improve the site specificity.

2) **Turnover**

   This problem is generally solved by placing the catalyst in an intrachain position of the antisense oligonucleotide. With this approach the RNA fragments after cleavage are bound less strongly to the catalyst. Thus they can be released for a new catalytic cycle.

A conjugate of this catalyst with a sequence of PNA was also synthesized.

3.1 DNA Conjugates

In artificial ribonucleases the probe for sequence recognition is usually an oligonucleotide, which can be made of DNA or its modified analogues. Due to its relatively low cost and its standard automated synthesis, in these preliminary experiments of site specific cleavage the conjugation was done with DNA. Some general characteristics of DNA are summarized in Fig. 3.1. The typical Waston-

Crick base pairings permit a specific recognition of a complementary DNA or RNA sequence.

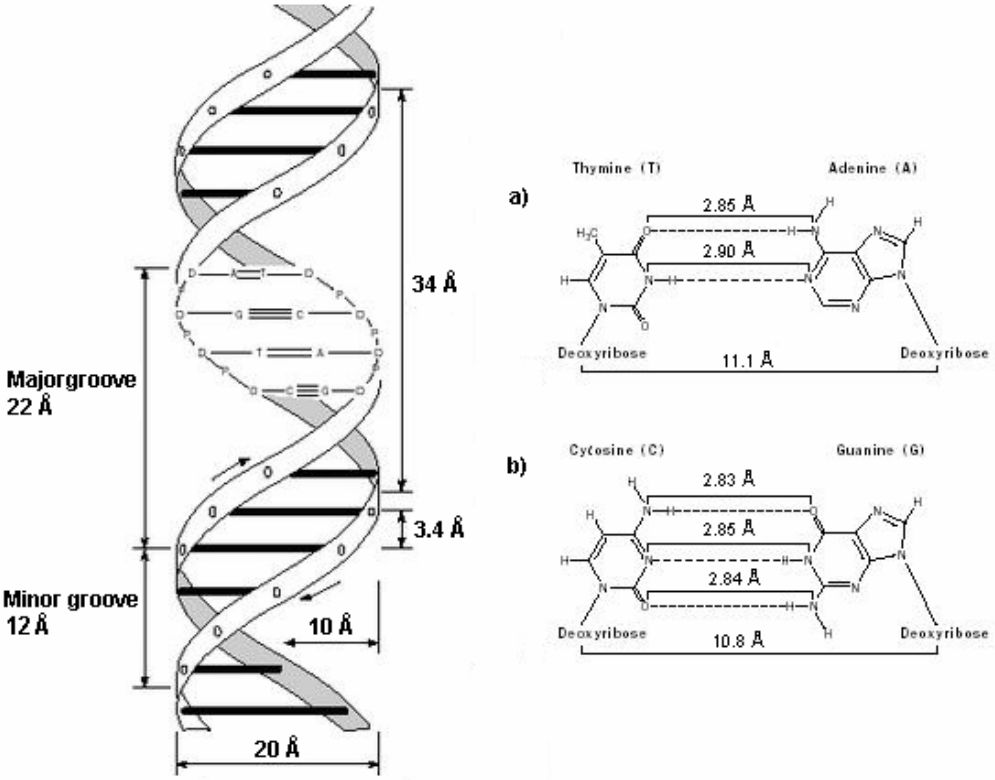

Figure 3.1: Parameters of the duplex helix in B form.[80]

From a structural point of view, the possibility to form these fixed pairings allows to the single polynucleotides to form a duplex helix, which structures are mostly of three types: B for DNA, A for RNA and in certain conditions Z for DNA. The duplex RNA-DNA assumes indeed the A structure.

In the last 20-30 years the automated synthesis of nucleic acids has become standard. This chemistry is based on the phosphoramidite method, because of the inherently high coupling efficiency and the stability of the starting material.[81] The building blocks are the phosphoramidites of the 4 bases, which are commercially available as well as the other reagents. The cycle of oligonucleotide synthesis by phosphoramidite chemistry (Fig. 3.2) can be dissected in 5 steps: 1) Detritylation. The dimethoxy trityl group that protects the 5'-OH is removed by treatment with trichloroacetic acid (TCA). This liberates the 5'-OH for the coupling step. 2) Coupling. The tetrazole and the phosphoramidites are mixed as they enter the reaction chamber. These form a highly reactive species, which rapidly reacts with the

5'-OH. 3) Capping. Acetic anhydride and dimethyl amino pyridine are mixed and form a powerful acetylating species, which terminates any chain that did not react during the coupling step. 4) Oxidation. The labile phosphorous linkage formed in the coupling step is converted to the stable, pentavalent phosphorous linkage of biologically active DNA. 5) Deprotection. After chain assembly is completed, the phosphate protecting groups are removed, the chains are separated from the solid support, and the base protecting groups are removed. Alternatively the newly inserted nucleotide can enter another elongation cycle.

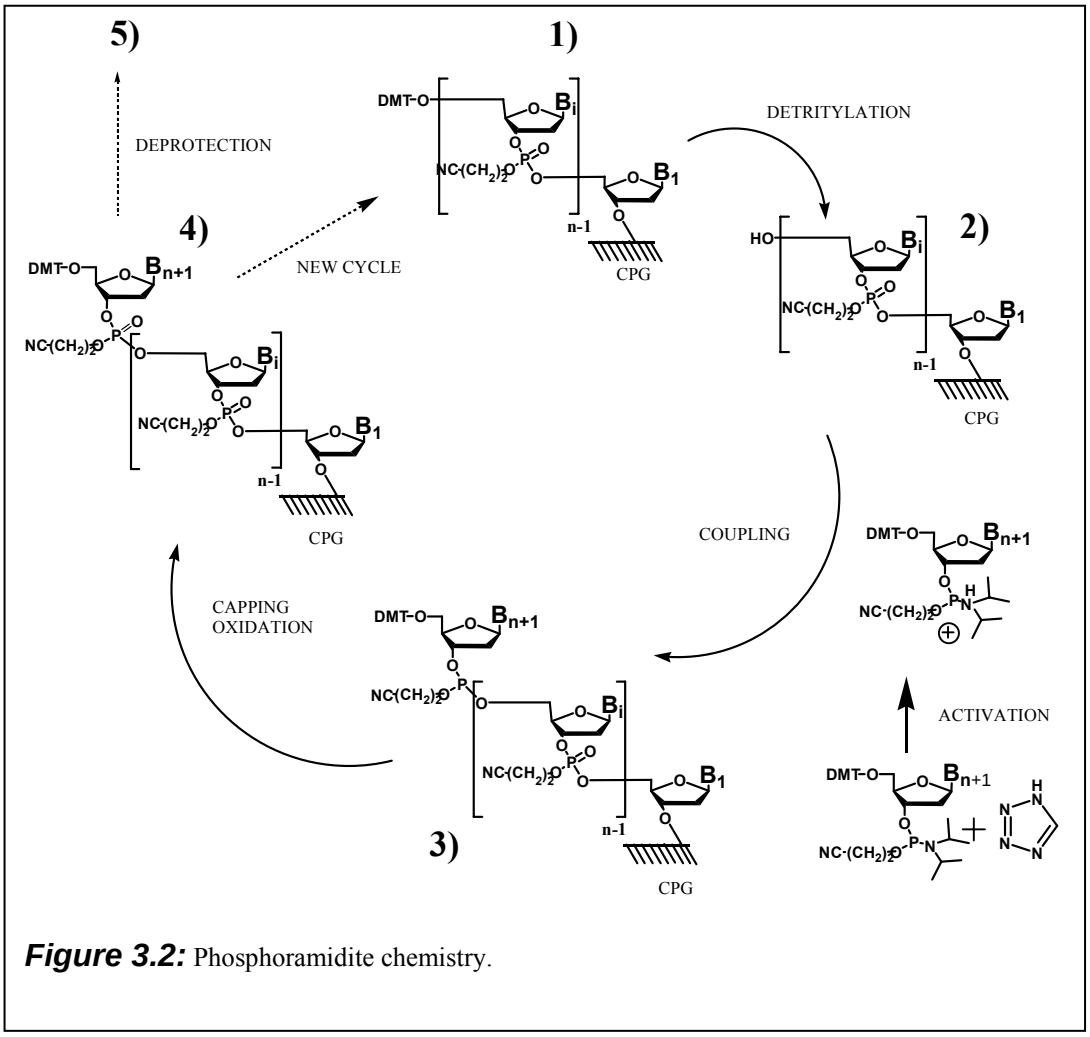

Figure 3.2: Phosphoramidite chemistry.

3.2 Conjugation at the 5' Terminus

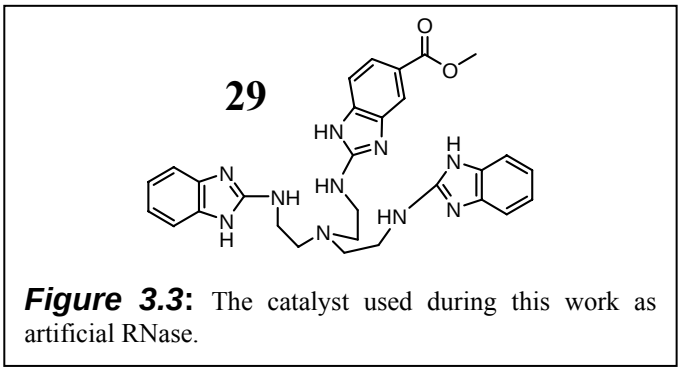

***Figure 3.3*:** The catalyst used during this work as artificial RNase.

The conjugation of **29** (Fig. 3.3) was attempted first with the standard procedure to synthesize DNA conjugates involving acylation of amino linkers by active esters in aqueous buffer. When it was applied to the charged benzimidazole **29** however, complete precipitation of the oligonucleotides occurred and therefore, the coupling was prevented. At this point it was decided to proceed with the conjugation by solid phase synthesis. Two possible methods for the conjugation were taken in consideration, by peptidic linkage and by disulfide linkage.[82][83] The disulfide linkage was used in this work. The choice of the disulfide chemistry was also suggested by a recent work of Lönnberg where a 1,5,9-triazacyclododecane conjugated to 2'-O-methyl oligoribonucleotides by a disulfide linkage showed to be 8 times faster than the amide bond conjugate although the length of the linker was almost equal.[83] The disulfide bond was preferred for a first investigation also because it should be more flexible and more capable of possible conformational adjustments to reach the phosphodiester bond.

3.2.1 Synthesis of the Building Blocks for the Conjugation

The thio linker phosphoramidite **62** was synthesized in two steps following the scheme 3.1. 6-Bromo-1-hexanol was converted into **61** by substitution with triphenylmethyl mercaptan using a published procedure.[82d-e] The corresponding phosphoramidite was obtained in the classical way by phosphitylating the hydroxyl group with 2-cyanoethoxy-*N,N*-diisopropylchloro-phosphoramidite in the presence of *N,N*-diisopropylethylamine.

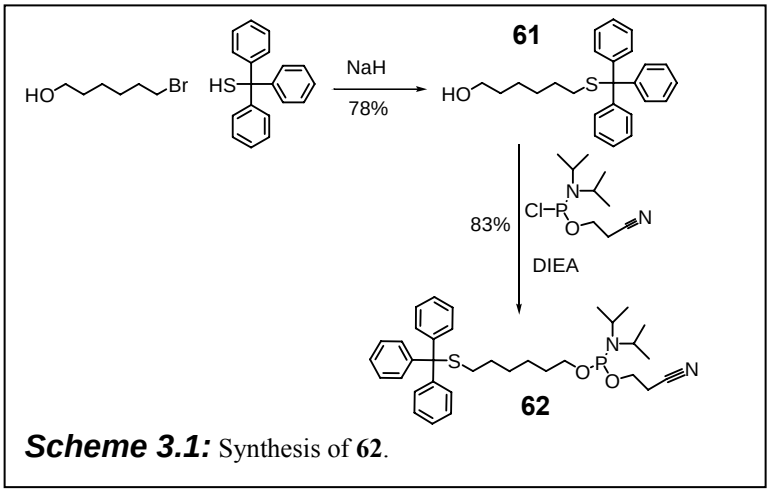

Scheme 3.1: Synthesis of **62**.

According to the procedure published by our group, the compound **29** was synthesized as shown in the scheme 3.2.[16]

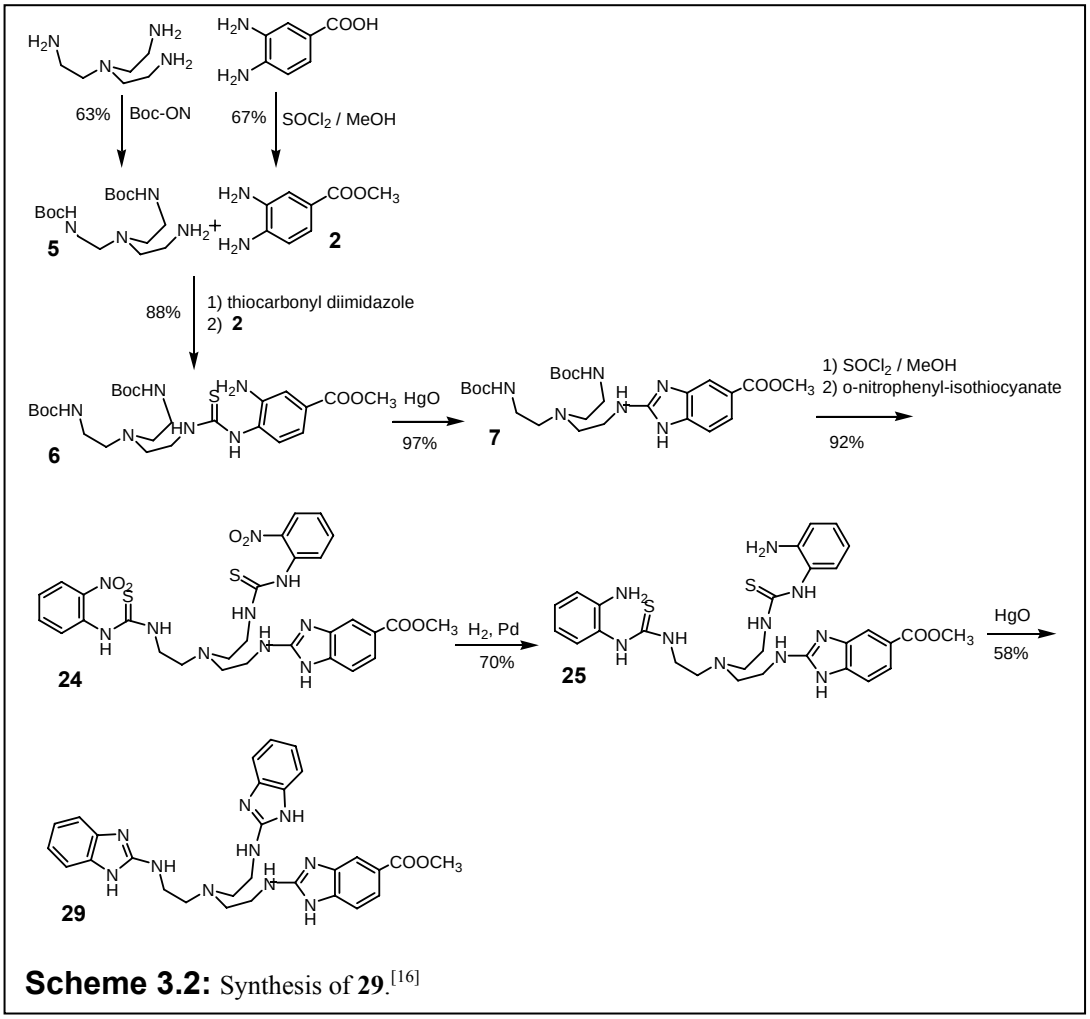

Scheme 3.2: Synthesis of **29**.[16]

Using Boc-ON, tris (2-aminoethyl) amine (TREN) was doubly Boc protected. In parallel the carboxyl group of the diaminobenzoic acid dissolved in methanol was protected by methyl esterification using thionylchloride. The stepwise reaction of **5** with thiocarbonyl diimidazole and the compound **2** gave the thiourea **6**. The compound **6** was cyclized forming the monobenzimidazole **7** using HgO as condensing agent. The Boc protecting groups of **7** were removed by adding $SOCl_2$ to a solution in MeOH giving the compound **23**, which was converted in the thiourea **24** adding o-nitrophenylisothiocyanate. The nitro groups of **24** were reduced by Pd catalysed hydrogenation and the final compound **29** was achieved using HgO for the ring closure of intermediate **25**.

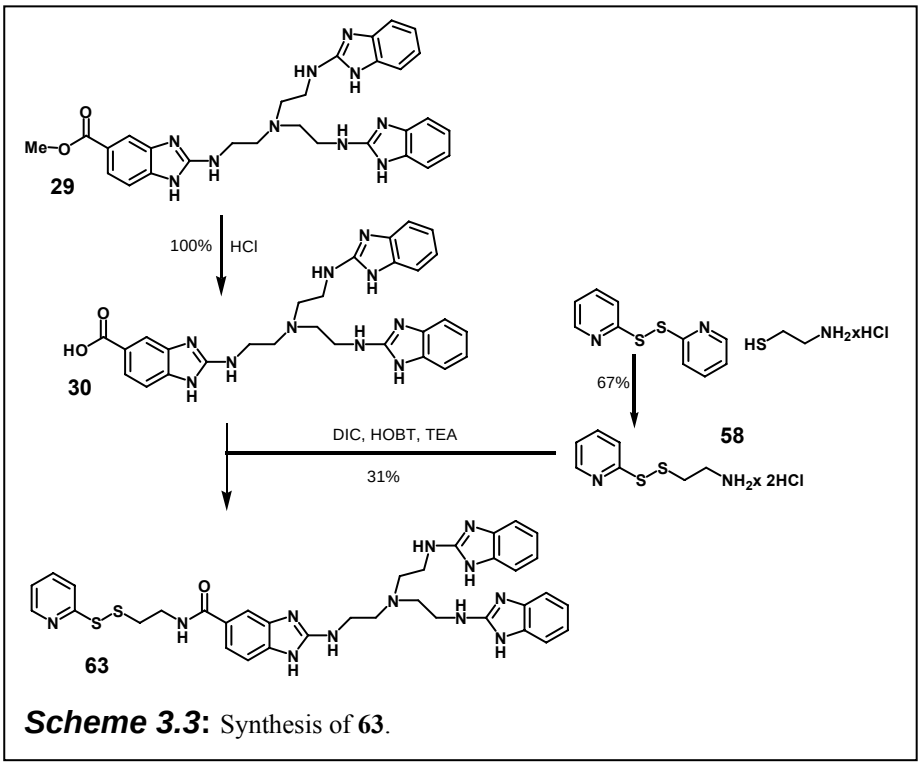

***Scheme 3.3*:** Synthesis of **63**.

The 2-thiopyridine activated compound **63** was obtained following the scheme 3.3. In accordance with the published procedure[82b] Aldrithiol-2™ was mixed with 2-aminoethanethiol hydrochloride giving the desired compound **58**.

The compound **29** was then converted into **63** in two steps. The methyl ester was refluxed in 6 M aqueous HCl giving the carboxylic acid **30**, which was coupled with **58** using DIC and HOBT.

3.2.2 Conjugation at 5' via Disulfide Linkage

In the procedure used for the conjugation of compound **29** with DNA (Sch. 3.4), the thio linker **62** was introduced in position 5' of a DNA strand by a synthesizer cycle. The trityl group was selectively removed by treating the modified oligonucleotide on solid phase with a 0.1 M solution of $AgNO_3$. To reduce possible disulfide bonds followed a treatment with a 0.1 M solution of TCEP.[84] Compound **63** that is the 2-thiopyridine activated compound **29**, was dissolved in DMF to form a 0.1 M solution, and was incubated for 12 h with the mercaptooligonucleotide on solid phase.

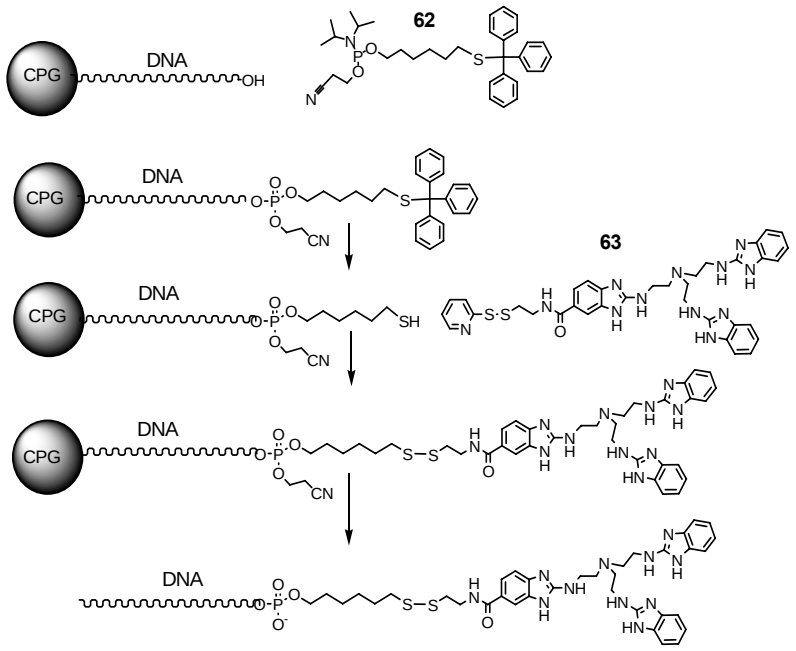

conjugates

3'GATCGGCTGACGGCT5'-linker-catalyst	**Oligo1000**
3'GATCGGCTGACGGCTAG5'-linker-catalyst	**Oligo1001**
3'GATCGGCTGACGGCTAGAGC5'-linker-catalyst	**Oligo1002**
3' TATGGAACAGTCCTC5'-linker(1)-catalyst	**Oligo1006**

accessory oligonucleotides:

Cy5-TTTTTTTTTTTTTTTTTTTU 3'	**108**
TGTGGAATTGTGAGCGGATA 3'	**109**

RNA substrates :

Cy5-T_{10}-ribo(5'CUAGCCGACUGCCGAUCUCGCUGACUGAC)-$T_4$3' **124**

Cy5-5'CTAGCCGACTGCCGA-*ent*-ribo(UCUCGCUGACUGAC)-$T_4$3' **202**

Cy5-T_{10}-ribo(5'AUACCUUGUCAGGAGAAGAGAGGCCGUUA)-$T_4$3' **210**

Scheme 3.4: Conjugation at the 5' via disulfide linkage.

To remove possible impurities, the solid phase was then washed with DMF and CH_3CN. Afterwards a treatment with ammonia 25 % for 24 h was done in order to cleave off the conjugate from the solid support and to remove the protecting groups. The crude conjugates were purified by denaturing PAGE, and characterized by MALDI mass spectrometry. In some cases it was possible to detect a mass peak with 70 units above the calculated mass, which corresponds to an isobutyryl protecting group still attached to the oligonucleotide. For this reason in the future it is recommended to use fast deprotecting phosphoramidites, which make use of the 4-isopropyl phenoxy acetyl protecting group instead of isobutyryl. In this way it should be possible to reduce the time of the deprotecting step to have a major guarantee to preserve the disulfide bond and at the same time be sure of a total deprotection of the nucleotide. Following this protocol the pure conjugates **1000**, **1001**, **1002** and **1006** were finally isolated and fractions of 60-70 % of conjugated versus non-conjugated strands were typically obtained.

3.3 Experiments towards Site Specific RNA Cleavage

Dr. Ute Scheffer carried out the experiments of RNA cleavage. One of the objectives of these first conjugates was to analyse the activity of the tris(2-aminobenzimidazole) in a non-aggregated state. For this reason preliminary studies to exclude the existence of molecular aggregates were performed. The dye-labelled DNA **108** (25 nM), diluted with 175 nM unlabeled DNA **109** was studied by fluorescence correlation spectroscopy (for FCS see 2.6 and Sch. 3.1 for **108** and **109**).[10][16] The diffusion time around 150 μs at 24 °C is consistent with the size of **108**. Upon addition of conjugates **1000, 1001, 1002** (1.5 μM), no change in diffusion times and no signs of aggregation could be observed. Substrate **124** (200 nM) was then mixed with complementary conjugates **1000, 1001, 1002,** (1.5 μM), again without producing significant effects. The gain in molecular mass by hybridization was not expected to be sufficient to influence the diffusion time of **124**. Further experiments with substrate **210** and conjugate **1006** confirmed the general view that higher aggregates

of oligonucleotides beyond the stage of hybridisation did not occur in the experiments shown below.

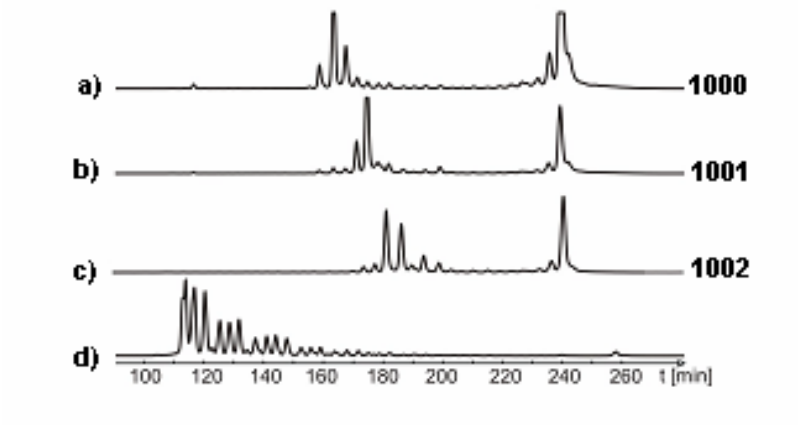

Figure 3.4: Cleavage of RNA **124** (150 nM) induced by conjugates **1000** – **1002** (1.5 μM). Conditions: 50 mM Tris-HCl pH 8.0, 37 °C, 20 h. Lane **d**: base ladder of substrate **124** (Na_2CO_3).

The results of the first cleavage tests are illustrated in Fig. 3.4. When the substrate **124** was incubated with the catalysts **1000**, **1001** and **1002** at pH 8, strong cleavage occurred. To locate the cleavage positions, lane **d** can be taken as a reference**,** which corresponds to alkaline hydrolysis of RNA substrate **124**. The cleavage site was related to the position of the catalyst. In particular for 15mer **1000** the cleavage occurred mainly in position 13, 14 and 15. For 17mer **1001** the cleavage occurred mainly in position 17, while for the 20mer **1002** the main cleavage sites were in position 19 and 20. Under these conditions no turnover was observed.

The influence of the pH was another important aspect determining the amount of aggregation of trisbenzimidazole **29**. The complete water solubility of these conjugates on the other hand allowed to determine pH/rate correlations. In Tab. 3.1 are summarized the results of the experiments of pH dependency, done in 50 mM Tris-HCl buffer ranging from pH 6 to 9. The pH dependent rates showed an increase of activity till pH 8. Keeping in mind that the pKa of the amino-benzimidazole is close to 7,[16] at pH 8 the catalyst should be mostly deprotonated. Therefore, general base catalysis should be an important mechanistic aspect of benzimidazole mediated RNA hydrolysis.

Table 3.1: Substrate degradation (%) as a function of pH. Cleavage of RNA **124** (150 nM) by conjugates **1000, 1001, 1002** (1500 nM), and cleavage of RNA **210** (150 nM) by conjugate **1006** (1500 nM)**.** Conditions: 50 mM Tris-HCl pH 8.0, 37 °C, 20 h.

pH	1000	1001	1002	1006
6.0	25.3	18.8	29.3	18.8
7.0	46.9	41.1	54.4	41.1
8.0	68.8	54.8	69.1	60.4
9.0	-	-	66.9	66.9

Subsequently saturation experiments were carried out with constant concentration of the substrate and an increasing concentration of the conjugates (Fig 3.5). Saturation could be observed above 200-300 nM. Consequently, running the experiments at a concentration of 1.5 μM, the substrate was completely saturated and the results should therefore not be affected by minor pH-dependent changes of duplex stability. In addition these experiments were done at constant ionic strength (100 mM NaCl).[10]

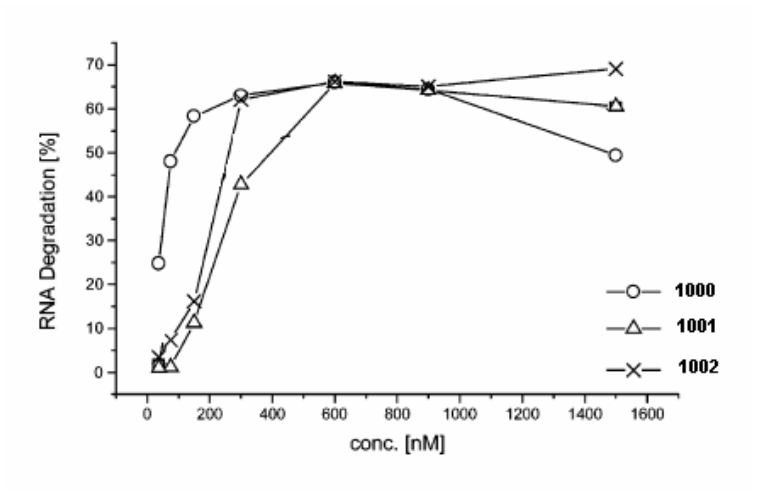

Figure 3.5: Cleavage of RNA substrates **124** as function of conjugate concentration 150 nM **124**, 20-1500 nM of conjugates **1000**, **1001** and **1002**. Conditions: 50 mM Tris-HCl, pH 8.0, 37 °C, 20 h.

An important requirement for an artificial nuclease is the specificity for the substrate. In Fig. 3.6 an experiment of cross reactivity is shown. The substrates **124** and **210**

were incubated separately with the complementary and with the non-complementary conjugate. As we can see the cleavage was dependent on the hybridization of substrate and conjugate.

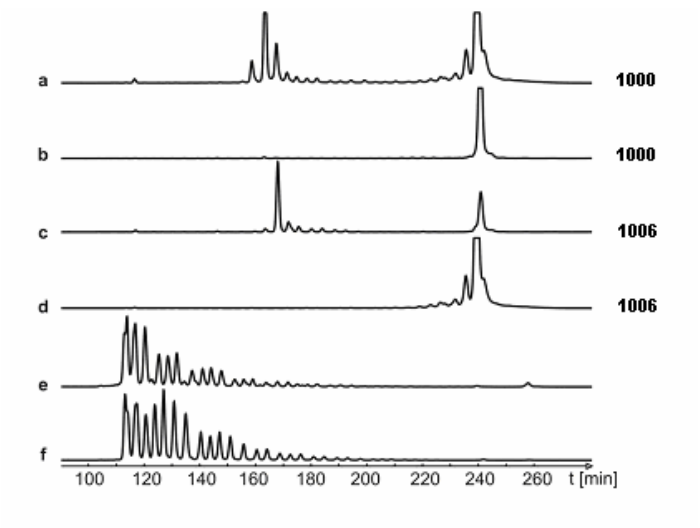

Figure 3.6: Substrate specificity of conjugates **1000** and **1006**. Lane a: Conjugate **1000** and substrate **124**. b: Conjugate **1000** and substrate **210**. c: Conjugate **1006** and substrate **210**. d: Conjugate **1006** and substrate **124**. e and f: Base ladder of **124** and **210** (Na_2CO_3).

Cleavage kinetics were studied in detail for the reaction of conjugate **1006**, with the substrate **210** (pH 8, with 150 mM NaCl). Without catalyst, the substrate was practically stable for several days (Fig. 3.8 lane **b**). In contrast, conjugate **1006** cleaved significantly within a few hours and the substrate was almost completely degraded after 56 hours (Fig. 3.7). A small percentage however, did not react even after 1 week (Fig. 3.7, lane **o**). This may result from structural damages in chemically synthesized RNA preventing hybridisation with conjugate **1006** (e.g., 2′,5′ linkages, residual protective groups, etc.). Interestingly, a more defined cleavage pattern arises after longer incubation times (Fig. 3.7). In fact upon standing, secondary cleavage events may cut off all conformationally mobile ribonucleotides protruding out of the duplex with conjugate **1006**.

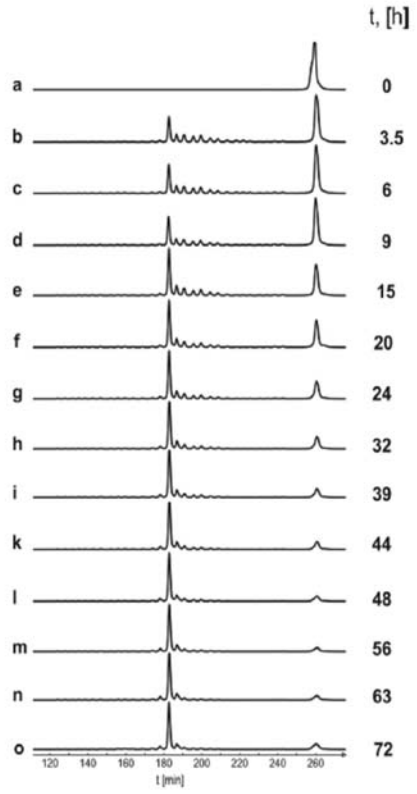

Figure 3.7: Time dependent cleavage of RNA **210** by conjugate **1006**. Conditions: 150 nM substrate, 1.5 µM conjugate, 50 mM Tris-HCl pH 8.0, 100 mM NaCl, 37 ° C.

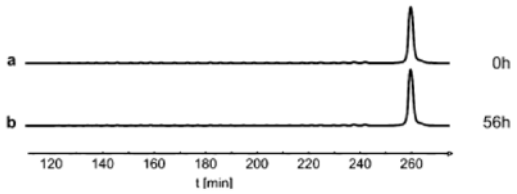

Figure 3.8: Controlls of time-dependent cleavage of RNA. Conditions: 150 nM substrate, 50 mM Tris-HCl, pH 8.0, 100 mM NaCl, 37 °C. a) Control without incubation. b) Control after 56h.

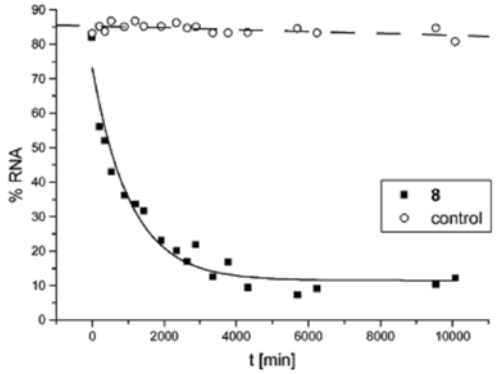

Figure 3.9: Cleavage kinetics of **210** in the presence and absence of conjugate **1006**. Conditions: 150 nM substrate, 0 or 1.5 µM conjugate, 50 mM Tris- HCl, pH 8.0, 100 mM NaCl, 37 °C. The solid curve is calculated by assuming first-order kinetics.

Fig. 3.9 shows the decay of RNA **210** as a function of time. The regression line demonstrates the high substrate stability in the control reaction (Fig. 3.8) with $t_{1/2}$ ~ 3500 h. For the cleavage induced by conjugate **1006**, a proper fit of experimental and calculated data (Fig. 3.9 solid curve) was obtained by assuming a first order rate law with $k_1 = 0.056\ h^{-1}$ and $t_{1/2} = 12.4$ h.

A general problem in studies of artificial ribonucleases are contaminations of natural ribonucleases that can give false positive results.[79] To exclude these possible effects the chimeric substrate **202** (Fig. 2.29 - 2.30) was used. In this substrate a DNA sequence of 15 bases complementary to the sequence of the conjugate **1000**, is followed by a sequence of enantiomeric RNA that is resistant to natural ribonucleases, but not to achiral catalysts. The cleavage with this substrate is illustrated in Fig. 3.10. As expected the cleavage occurred with the complementary conjugate **1000** selectively after nucleotide 16, the first ribonucleotide placed in close proximity to the benzimidazole moiety (Fig. 3.10 lane **a**). Note that the DNA part of

substrate **202** cannot be degraded. The preferred cleavage sites of the duplex **1000•124** (nucleotides 13, 14, and 15), were thus inert in duplex **1000•202**. As counterproof the substrate **202** proved resistant to degradation when incubated with the non-complementary conjugate **1006** (Fig. 3.10 lane **b**).

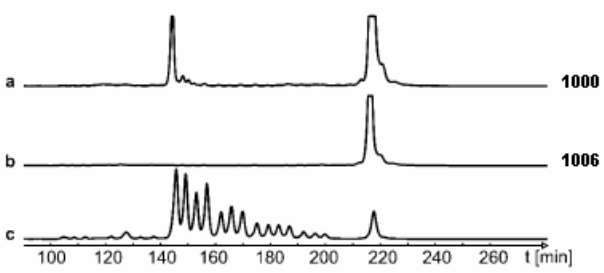

Figure 3.10: Lane a: conjugate **1000** cleaves the *enantio* RNA insert of substrate **202**. Lane b: no cleavage occurs with the non-complementary conjugate **1006**. Conditions: 150 nM substrate, 1.5 μM conjugate, 50 mM Tris-HCl, pH 8.0, 37 °C, 20 h. Lane c: base ladder of substrate **202** (Na_2CO_3).

3.3.1 Effect of Sulfate on Cleavage

Further cleavage studies were made to explore the effects of SO_4^{2-}, which should interact with guanidinium groups thus inhibiting the cleavage, by competition with the substrate phosphate.[85] Moreover the guanidinium should change the pKa when in complex with the sulfate.[86] To evaluate the effect of SO_4^{2-} at different pH and to exclude possible effects due to the increased ionic strength, NaCl was used as inert salt. Consequently two sets of samples were prepared in Tris-HCl buffer at different pH, one with Na_2SO_4 and one with a concentration of NaCl such to have the same ionic strength **μ** (Fig. 3.11).

$$\mu = \frac{1}{2}\sum_{i=1}^{N} c_i z_i^2$$

μ = ionic strength
c = concentration of a ion ***i***
z = charge of the ion ***i***

Figure 3.11: Ionic strength **μ**.

Table 3.2: Conditions: 150 nM substrate, 1.5 μM conjugate, 50 mM Tris-HCl, pH 6, 7, 8, 9, 100 mM for NaCl, and 67 mM for Na_2SO_4, 37 °C, 20 h..

pH	% Cleavage	
	Na_2SO_4	NaCl
6	11.1	11.1
7	34.4	31.7
8	52.3	42.0
9	43.7	39.3

The results are reported in Tab. 3.2 and in Fig. 3.12, where a weak increase of cleavage was observed with Na_2SO_4. This was in contrast with the expected inhibition. Interestingly it seems to appear a bell shape with a maximun around pH 8. (Conditions: 150 nM substrate, 1.5 μM conjugate, 50 mM Tris-HCl, pH 6, 7, 8, 9, 100 mM for NaCl, and 67 mM for Na_2SO_4, 37 °C, 20 h.).

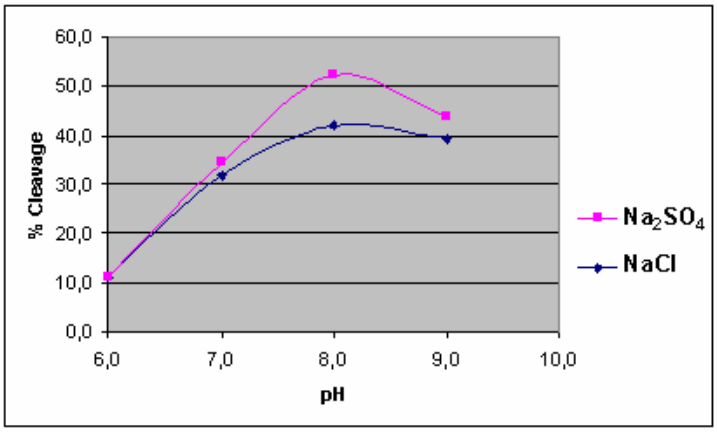

Figure 3.12: Cleavage in relation of pH and NaCl or Na_2SO_4.

3.3.2 Effect of Imidazole on Cleavage

Imidazole as described in the precedent chapter can play an important role in RNA cleavage.[72] To test the effect of imdazole, **1000** at 4 different concentrations (10, 5, 1, 0.5 µM) was incubated with RNA **124** (150 nM), in one series with Tris-HCl buffer (50 mM, 0.01 % SDS, pH 7) at 37 °C for 20 h, and in the other series with an imidazole buffer (50 mM, 0.2 M KCl, 1 mM EDTA, pH 7) at same temperature and for the same time. In Tab. 3.3 are reported the results of these experiments. Interestingly from these data resulted that when the concentration of **1000** was 1 µM in imidazole buffer, the cleavage was of 48.3 % compared with 35.9 % in TRIS buffer showing an increase of 34 % as possible catalytic enhancement due to imidazole.

Table 3.3: Cleavage in presence of imidazole. Conditions: see text.

Cg1000	% Cleavage	
	Imidazole	TRIS
10 µM	48.1	41.1
5 µM	46.6	41.5
1 µM	48.3	35.9
0.5 µM	45.3	36.5

3.4 Highly Site Specific Cleavage

Once the general concept of trisbenzimidazole DNA conjugates was proven successful, the focus of my work was shifted to find the conditions for increasing specificity and multiple turnover. This task was solved by conjugating **29** in the middle of a DNA sequence. The turnover problem is discussed in the next chapter. Furthermore, the attention was focused on the objective of cleavage precision. At this stage an collaboration with Kathrin Beier in my group was started.

Using the conjugate **1006** synthesized during my work, Kathrin Beier improved the specificity of the construct, applying a method reported by Komiyama.[87] The strategy is illustrated Fig. 3.13a. It consists in placing a helper oligonucleotide after the cleavage site. In RNA duplexes the attack of the 2'-OH at phosphorus is a stereoelectronically forbidden process. If just a single base of RNA is not involved in duplexes, the cleavage should be restricted to this position. In contrast simple conjugates may cleave in all the positions that are single stranded and accessible to the catalyst (Fig. 3.13b). The final result of this strategy therefore, should be a single base cleavage.

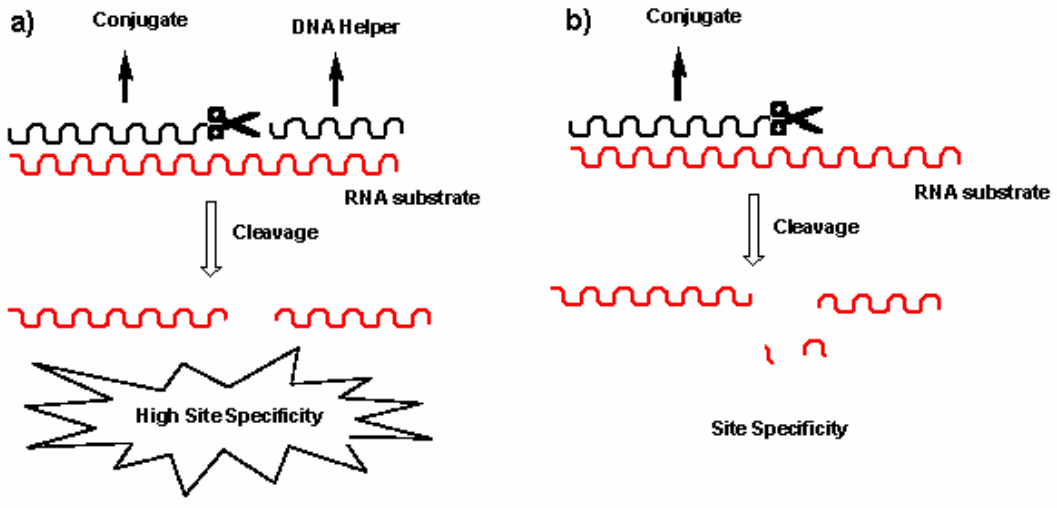

Figure 3.13: Strategy to have high specificity by helper oligonucleotides.

The helper DNA oligomers **246**, **245** and **244** used in this experiment are reported in Fig. 3.14. They let a space for the cleavage of 2, 1 and 0 bases respectively. This strategy proved particularly successful as reported in Fig. 3.15. We can see that

incubating **210**, with **1006** and **246**, the cleavage occurred in two positions lane **c**, using then **245** instead the cleavage occurred in only one position, and using **244** the cleavage was almost suppressed. To better figure out the improvement Fig. 3.15 lane **b** and Fig. 3.7 lane **b** should be compared.

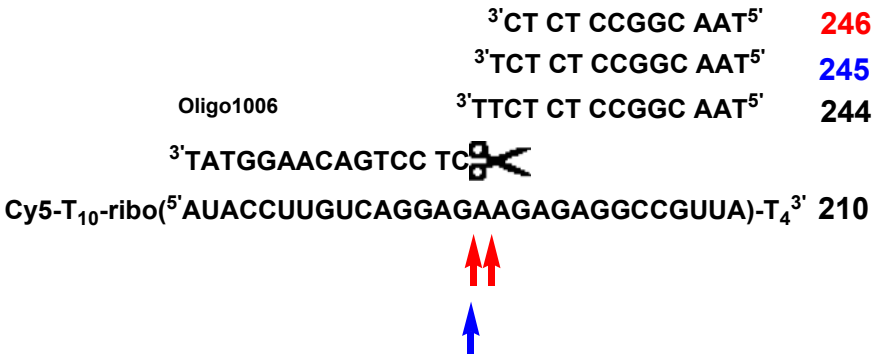

Figure 3.14: The helper oligonucleotides and the cleavage sites.

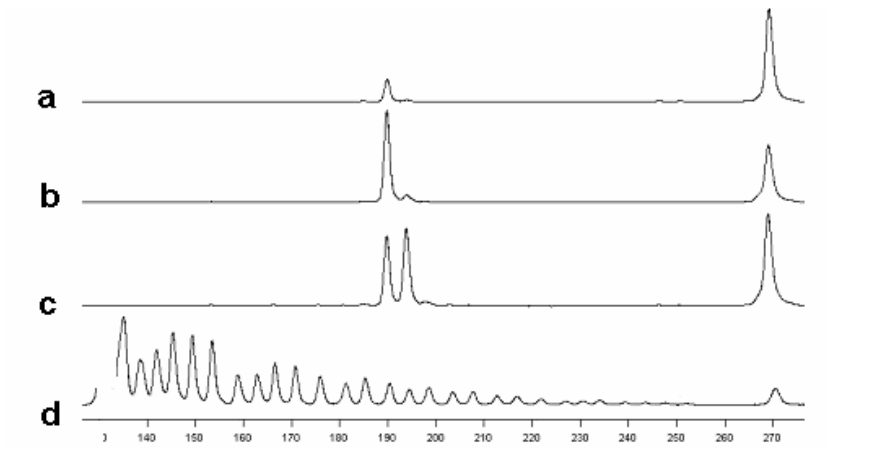

Figure 3.15: Lane **a**: **1006**, **244**, **210**. Lane **b**: **1006**, **245**, **210**. Lane **c**: **1006**, **246**, **210**. 150 nM substrate, 1.5 μM conjugate, helper 1.5 µM. Conditions: 50 mM Tris-HCl, pH 8, 100 mM NaCl. Lane **d**: base ladder of substrate **210** (Na_2CO_3).

3.5 PNA Conjugation

A buffer even if particularly complex can only mimic a cellular environment. The presence of proteins or enzymes could inhibit the activity of **29** and by recruitment of some cellular machinery even an improvement could be observed. With no possibility to be excluded, some preliminary cellular experiment could clarify how such catalyst could behave *in vivo*. DNA conjugates such as **1006** however, suffer

from cellular instability. For this reason an analogous PNA conjugate was synthesized. The synthetic methodology is simple. Sequences of PNA still on solid phase are commercially available. Hence a sequence of PNA corresponding to the decamer shown in Fig. 3.16 was purchased, and coupled on solid phase to **30** using DIC and HOBT (see 9.3.25). The conjugate was then deprotected and cleaved off from the solid phase with the standard procedure for PNA.

1011

gctgacggct✂

Cy5-T_{10}-ribo($^{5'}$CUAGCCGACUGCCGAUCUCGCUGACUGAC)-$T_4{}^{3'}$ **124**

Figure 3.16: The PNA conjugate.

When **1011** (1500 and 150 nM) was incubated with **124** (150 nM) or as control with **210** (150nM) in Tris-HCl buffer 50 mM, pH 8, 37 °C, for 20 h, unexpectedly no sign of cleavage was detectable (Fig 3.17). The cause of this inactivity could be due to a collapse of the cleaver in the hydrophobic structure of PNA or to an insufficient duplex stability between **1011** and **124** that could prevent an efficient cleavage, although this should be in contrast with the higher stability of RNA-PNA duplexes. This problem might be solved by future experiments: trying the cleavage in presence of ethanol to prevent a hydrophobic collapse, by conjugation to a longer sequence of PNA or by using some other nucleic acid analogues.

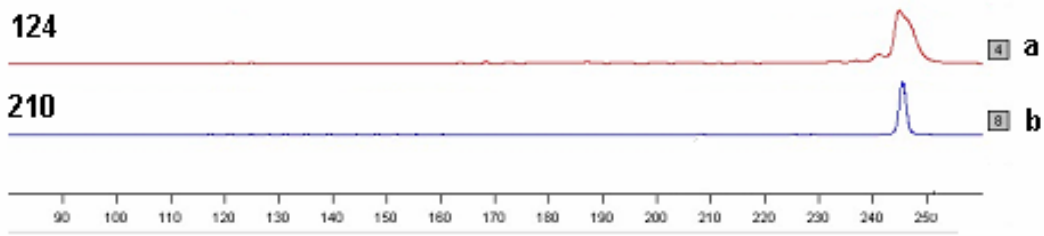

Figure 3.17: RNA cleavage test for the PNA conjugate. Lane a: **1011** and **124**, lane b: **1011** and **210**. Conditions: 150 nM substrate, 1500 nM conjugate, 50 mM Tris-HCl, pH 8, 37 °C, for 20 h.

3.6 Comparison with other Conjugates

For a comparison of the conjugates obtained in this work with others, it is here reported a small list of the best conjugates with RNase activity (a deeper overview about these conjugates is present in a recent publication of Lönnberg).[32]

The best results until now were achieved with artificial nucleases based on lanthanide ions. The texaphyrin-Dy^{3+} conjugate in Fig. 3.18b was reported to cleave its substrate with a half life of 2.1 h at pH 7.5 and 37 °C, showing also turnover.[55] The Eu^{3+} pyridine cyclophanes conjugate in Fig. 3.18a also showed to cleave the RNA with similar efficiency. In this case the half life of the substrate was 4 h at pH 7.5 and 37 °C.[54a] Continuing with conjugates bound to the 5' or 3' ends of an ODN sequence, the artificial ribonucleases based on Cu^{2+} ions are less active. The Cu^{2+} conjugate in Fig. 3.18d cleaved its substrate with a half life of 70 h at pH 7.4 and 45 °C, while the conjugate at the 5' Fig. 3.18c was inactive. Nevertheless, when these two conjugates were incubated together with the same cleavage-site the half life of the substrate was reduced to 5 h (Fig. 3.18e).[32][88]

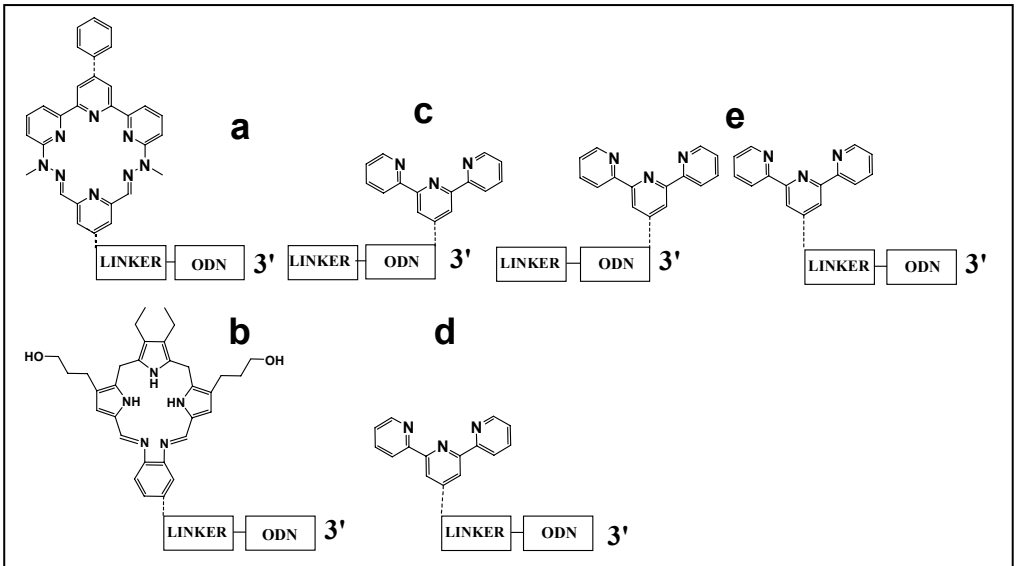

Figure 3.18: Some site-specific artificial RNases based on metal complexes.

A more interesting comparison could be done with conjugates based on metal free artificial ribonucleases. Two examples are reported in Fig. 3.19. The PNA conjugate in Fig. 3.19a induced a half life for its RNA substrate of 8 h at pH 7.0 and 40 °C.[89]

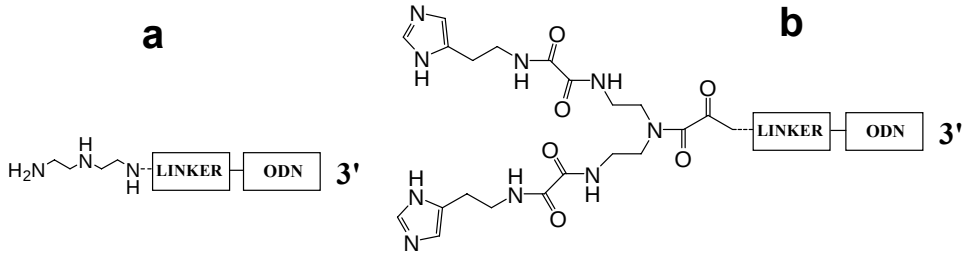

Figure 3.19: Some site specific artificial RNases based on metal free catalysts.

When the conjugate in Fig. 3.19b was addressed to a particular instable site of t-RNA^{phe} (C63-A64A) the half life of the substrate was reported to be 1.5 h in 50 mM imidazole at pH 7.0, and 37 °C.[90]

3.7 Conclusions

With the 5' conjugates **1000**, **1001**, **1002** and **1006** it was possible to prove the activity of the tris(2-aminobenzimidazoles) as real catalyst for RNA cleavage. The activity of aminobenzimidazoles seems to be among the best reported for metal-free constructs.

An important improvement of specificity was obtained with helper oligonucleotides.

Concerning the mechanistic aspects, it was possible to establish the pH dependency of cleavage rates, which shows an optimum at pH 8, suggesting a maximal activity for the deprotonated form. This is somewhat in contrast with the initial idea, considering to combine general base and general acid catalysis with electrostatic stabilization of the pentacoordinated transition state. However, it is premature to give a final interpretation of the mechanism. In fact the conjugation of the catalyst to the polymeric DNA, could shift the pKa.

4 Site-Specific Artificial RNases Exhibiting Turnover

After the successful conjugation of **29** to the 5'-end of DNA sequences the RNase activity of this catalyst was proven without any doubt. Site-specific cleavage was also obtained, but an enzyme mimic should exhibit turnover as well. The new objective of this work became therefore, the development of a new class of conjugates showing specificity and turnover.

The approach to this new objective is similar to the conjugates already presented. The synthetic RNase consists of two domains: the first domain can be a strand of DNA or its analogues and ensures substrate recognition. The second domain consists of our tris(2-aminobenzimidazole) moiety which provides the RNA-cleaving feature.

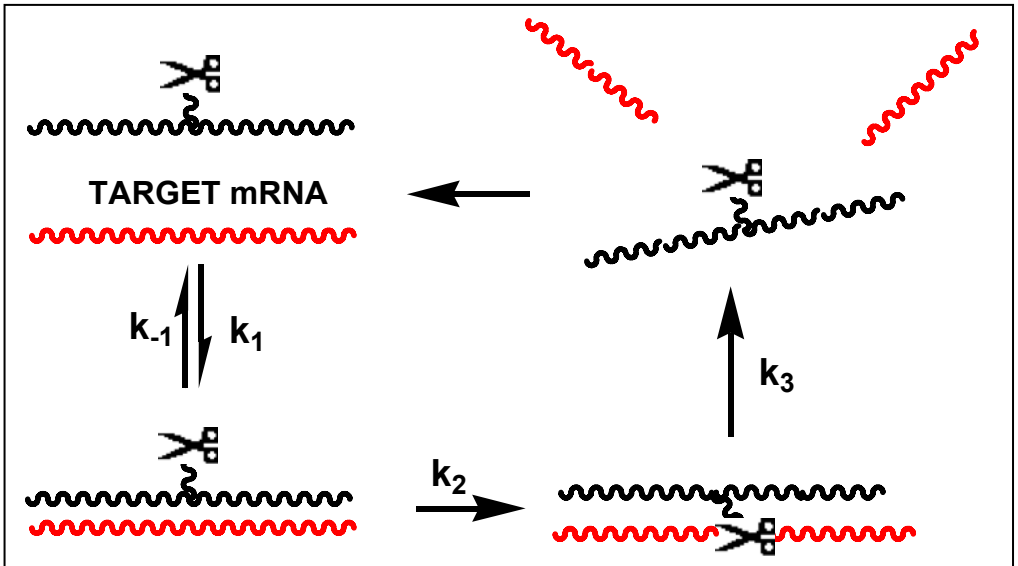

Figure 4.1: Possible catalytic cycle of a ribozyme mimic**.**

A possible catalytic cycle of this class of RNases is described in Fig. 4.1: at first the conjugate binds to the RNA substrate with k_1 and then cleaves the substrate with k_2 within the duplex region. The stability of RNA-DNA helices is strongly length dependent. Thus the generated RNA-fragments are released with k_3 allowing a new catalytic cycle. This makes the major difference between the precedent conjugates and this new class. In contrast, when the cleavage by conjugates occurs at one extremity of the duplex, the helix stability is not reduced. Therefore, the conjugate

stays tightly bound to the RNA strand without being released for a new catalytic cycle. Clearly the constants of these new constructs must be properly balanced to achieve a optimally operating catalyst.[15]

4.1 Resistance of RNA-Duplexes to Cleavage

A fundamental aspect of this project is the enhanced resistance of RNA-duplexes to cleavage.[91] In fact the topology of the helix prevents even enzymatic degradation.[92] The reason of this resistance is illustrated in Fig. 4.2. Generally, for small catalyst the cleavage of RNA occurs via attack of the 2'-OH at phosphorus in a pentacoordinated transition state with the 5'oxygen in line with the 2'-OH (Fig. 4.2a).

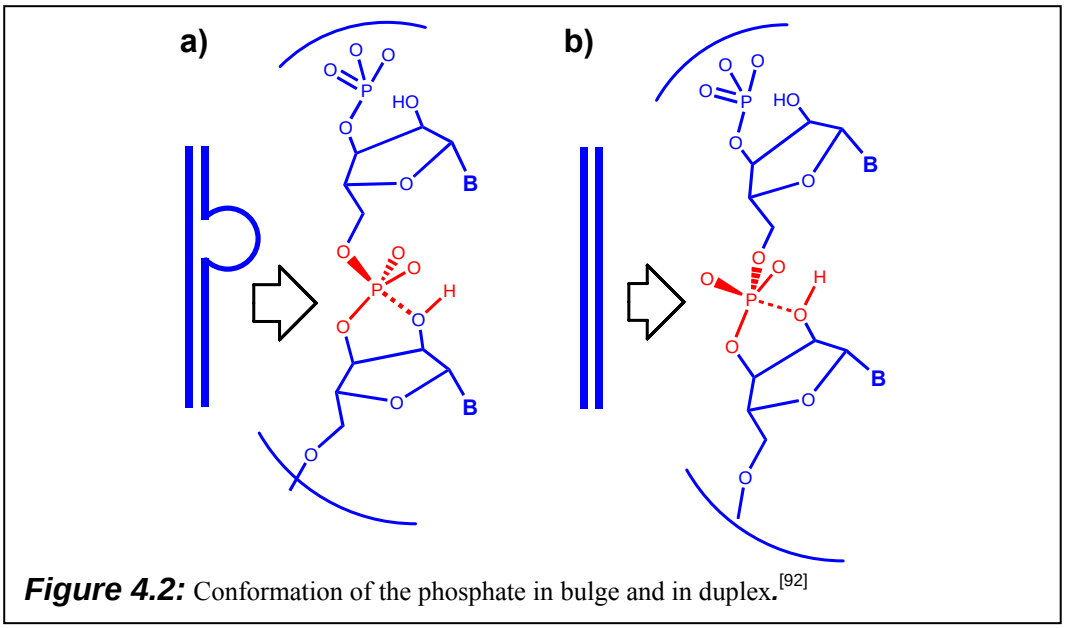

Figure 4.2: Conformation of the phosphate in bulge and in duplex.[92]

This trigonal-bipyramidal arrangement is only possible in flexible, single stranded parts of RNA. In a more rigid structure like in a helix after the initial attack of the 2'-OH at phosphorus, the oxygen in 5'-position is in equatorial position and has to pseudorotate to the apical position before the cleavage can occur (Fig. 4.2b). Nevertheless, in an RNA-DNA duplex the phosphodiester backbone of the RNA can be forced to assume a favourable conformation for a catalysed transesterification reaction. For instance, this can be obtained by forming secondary structures like mismatches and bulges in the RNA strand. In these structures the conformation of

the phosphate is favourable to the cleavage and can be induced even by Mg^{2+} (2.5 mM, pH 8).[50][92] Therefore, a fundamental feature for these intra-chain conjugates is the induction of a bulge where the cleaving agent should be addressed.

4.2 Key Design Features for Site Specific RNases with Turnover

In creating these constructs some key design features should be taken in consideration. Fig. 4.3 summarizes the most important variants of these systems.
The first characteristic is the presence of a bulge in the cleavage site. Häner et al.[54b] reported that fully complementary conjugates cleave only 7 % of the substrate. In contrast 92 % are cleaved under the same conditions by addressing the catalyst into a bulge of the substrate.

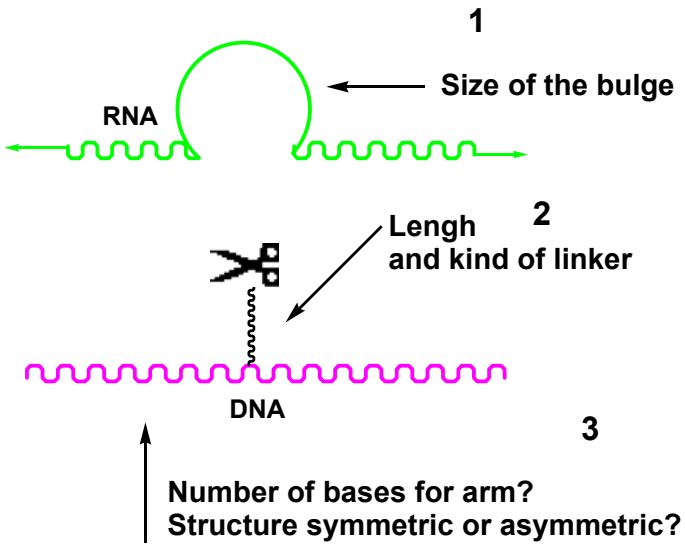

Figure 4.3: Key structure elements of RNases with turnover.

Similar observations were also reported by Strömberg et al.[93] Furthermore, this author reported a strong cleavage-rate dependency on the size of the bulge, observing optimal rates when the bulge has a size of 3-4 bases.
Another structural aspect is the type of linker that carries the catalyst. When nucleotides are used to attach the catalyst, it can be located in different helix grooves depending on the position of the conjugation as illustrated in Fig. 4.4.[15]

Again Häner reported for his system a cleavage of 61-92 % when the catalyst was delivered through the minor groove, in contrast to 21 % when the same catalyst was delivered through the major groove.[54b]

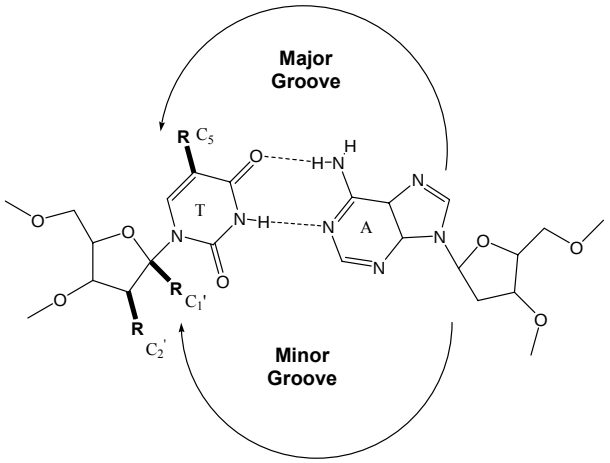

Figure 4.4: Orientation of possible sites for catalyst attachment.

Concerning the length of the linker a longer and more flexible linker should assure more possibilities to reach phosphodiester moieties. On the other hand a short linker should allow a more precise cleavage.[94]

A last parameter to analyze is the size of the duplexes surrounding the bulge. Clearly longer helices permit a higher specificity. Nevertheless this means also retarding the release of cleavage products. Experiments with ribozymes suggest that the optimal helix length depends on the substrate. However, my work was based on a model of Joyce and Santoro, who developed a RNA-cleaving DNA enzyme, which showed an optimum when the arms were between 7+7 or 8+8 nucleobases.[94][95]

4.3 Design of the Conjugates

During my work not all of the possible combinations of these parameters have been tested. It was rather decided an initial conjugation, to which could follow future improvements. The chosen sequence for these conjugates is complementary to the sequence of **124**: Two first conjugates **1007-1008** (Fig. 4.5) were made with a structure 8+8 bases inducing a bulge of 3 bases. The problem of the optimisation of the binding constant has been solved modulating the ionic strength.

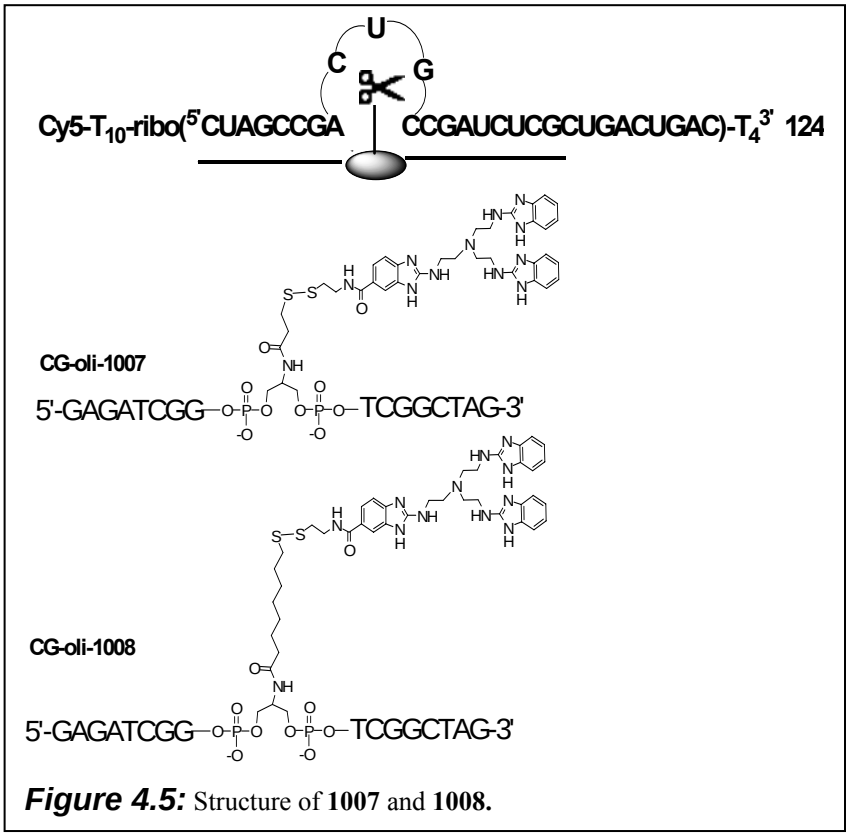

Figure 4.5: Structure of **1007** and **1008.**

The linkers used are based on serinol, the reduced form of serine. As shown in Fig. 4.6, serinol can be accounted as a minimal nucleotide replacement. This kind of linker without any complementary base should introduce a local flexibility into the duplex, thereby rendering the phosphodiester bond of the opposing base more prone to cleavage.[96][15] An amino group is then suitable for the anchorage of the catalyst and the length of the linker is easily adjustable. This very flexible serinol might be a good choice for an initial exploration of conjugation in intra-chain position, because it does not force the catalyst into a certain position. A disadvantage of this approach could be the formation of two stereoisomers, but since in the serinol backbone free rotation can occur it should not be a problem.[96b]

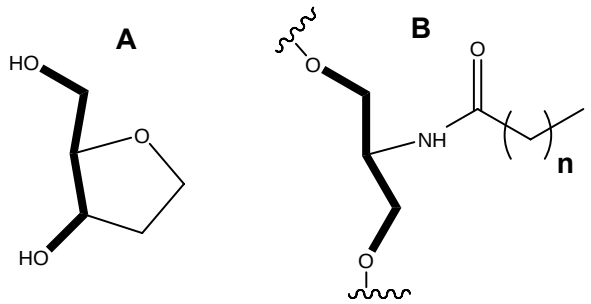

Figure 4.6: Comparison of deoxynucleoside and serinol structures.

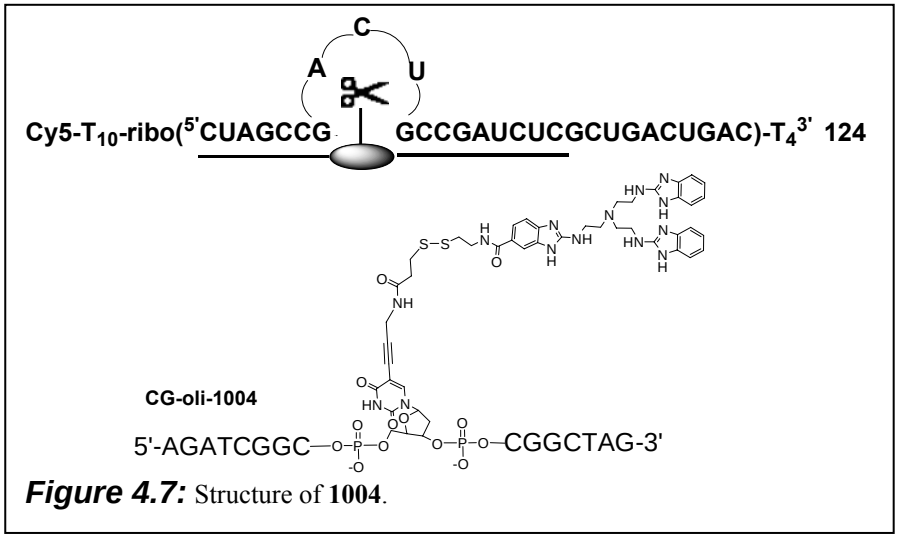

Figure 4.7: Structure of **1004**.

The conjugate **1004** (Fig. 4.7) was prepared using the modified desoxy uridine furnished by Nelly Piton of the group of Professor Engels. In this case the conjugate structure was 8+7 bases inducing a bulge of 3 bases.

4.4 Synthetic Strategy

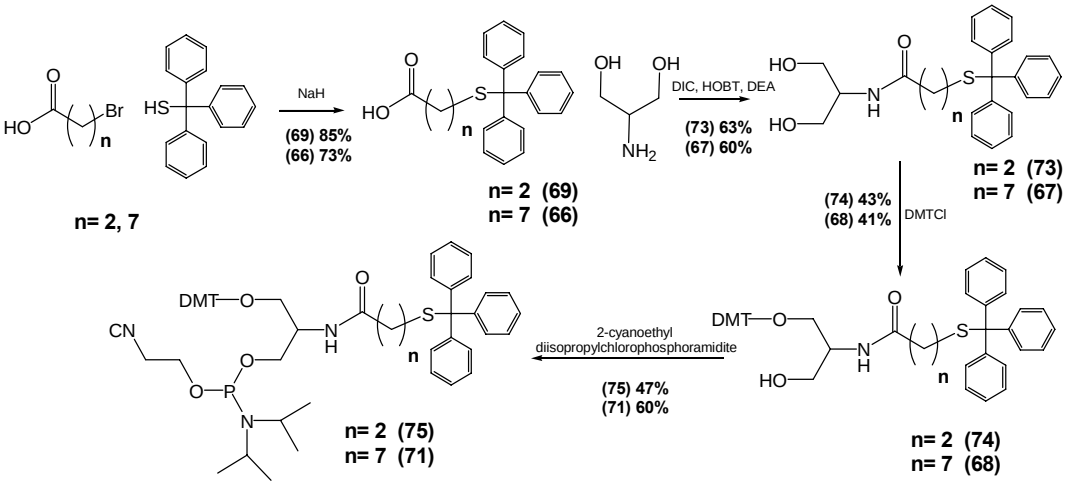

Scheme 4.1: Synthesis of the serinol-linker.

With the aim to test the effect of the linker length, two phosphoramidites based on serinol, one with 3-mercaptopropionic acid and one with 8-mercaptootanoic acid have been synthesised (Sch. 4.1). The synthesis started with 8-bromooctanoic acid or 3-bromopropionic acid, which by nucleophilic substitution with the triphenylmethyl mercaptan was converted into **66** or **69**. The subsequent coupling with serinol, using

DIC and HOBT, led to **67** or **73**. A following partial DMT protection using DMTCl in Pyridine gave *rac*-**68** or *rac*-**74**. (At this point a mixture of two enantiomers was generated) The remaining OH group was then converted into the phosphoramidites **71** or **75** as mixture of the diastereoisomers, using 2-cyanoethoxy diisopropylchlorophosphoramidite.

A different nucleotide phosphoramidite was prepared in collaboration with Nelly Piton who furnished the starting desoxy uridine derivative, which was converted into **70** by coupling with **69**. With the following phosphitylation using 2-cyanoethoxy diisopropylchlorophosphoramidite the phosphoramidite **72** was produced.

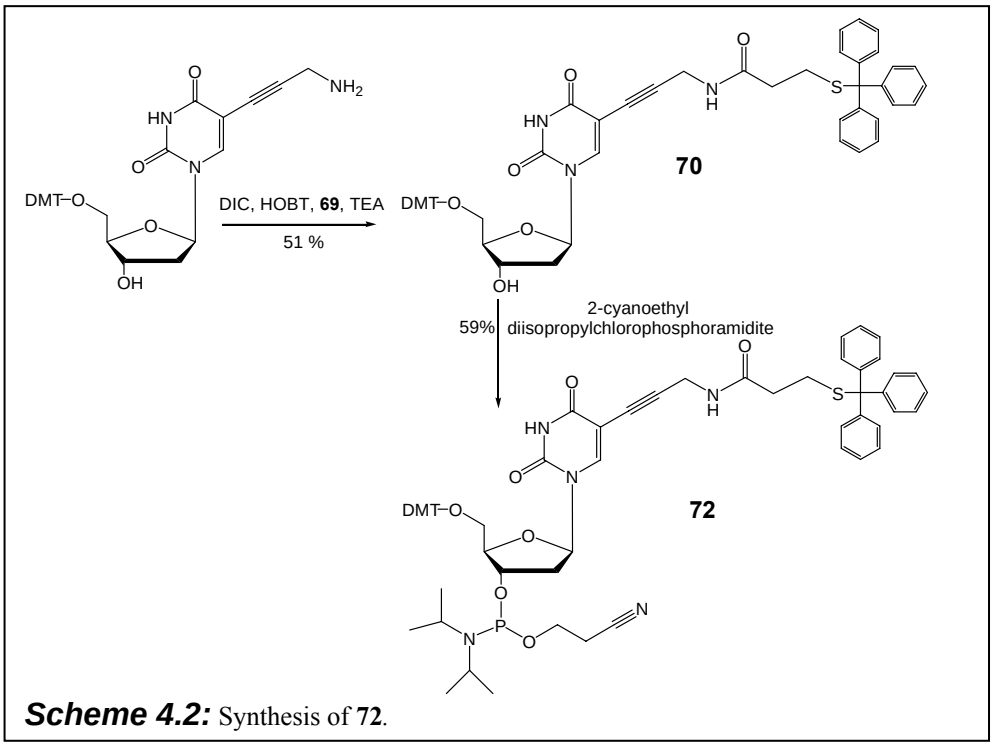

Scheme 4.2: Synthesis of **72**.

The phosphoramidites **71**, **72**, and **75** were used in solid phase nucleic acid synthesis. With this methodology the linkers could be introduced at any position along the sequence. After finishing the solid–phase synthesis the trityl group was still on the mercaptan. Therefore, it was removed on solid phase by treatment with $AgNO_3$. Subsequently followed a treatment with TECP to reduce the possible disulfides. After which the oligonucleotides with the free mercaptans were coupled with **63**. The corresponding conjugates were deprotected and cleaved off the solid phase using

aqueous NH_3 (25 %). With this procedure were synthesised the conjugates **1004**, **1007** and **1008**.

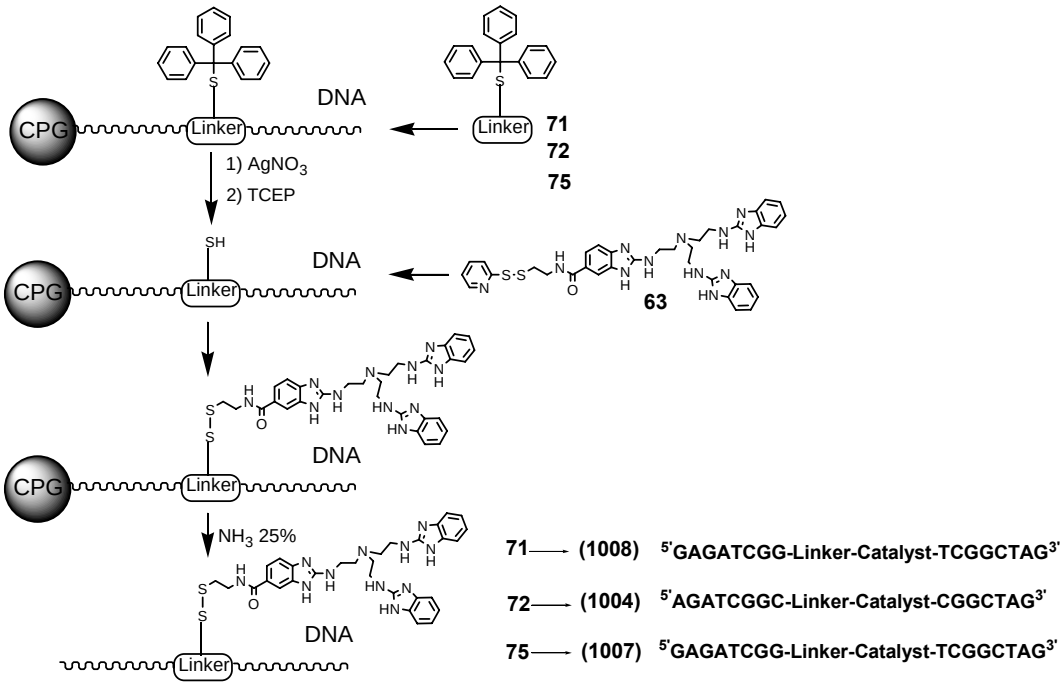

Scheme 4.3: Conjugation scheme.

4.5 Test of Cleavage

Dr. Ute Scheffer performed the experiments of RNA cleavage. Having completed the synthesis of the conjugates, a first screening was done to select the best candidate for kinetic studies. In Fig. 4.8 the electropherograms of a first experiment are shown. The conjugate **1004**, **1007** and **1008** at two different concentrations 150 and 1500 nM, were incubated with the corresponding substrate **124** (150 nM) in 50 mM Tris-HCl at pH 8.0, 37 °C for 20 h. These preliminary results proved that **1007** with the short linker was the best catalyst and **1004** was the worst. It was consequently decided to continue only with **1007** and **1008**, because **1004** did not show a significant cleavage.

In general this first experiment was disappointing when compared with the cleavage of the 5' conjugates. As already illustrated in Fig. 4.1 for obtaining an optimal cleavage all the constants involved in this system must be well balanced. The RNAase activity can be modulated with the pH, but pH 8 represents already the optimum. Therefore, the binding constant could be still modulated. This was done by changing the ionic strength. Increasing the ionic strength is known to stabilize oligonucleotide duplexes.

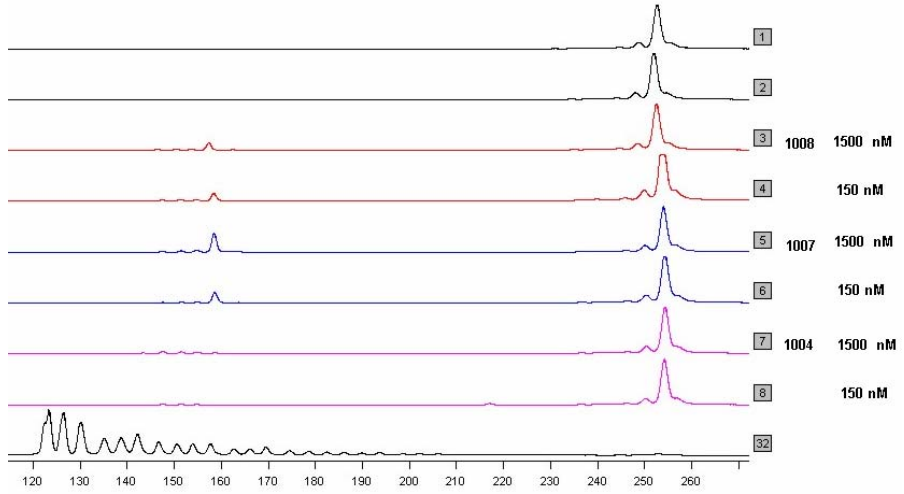

Figure 4.8: Preliminary test of clevage of **1008**, **1007** and **1004** at pH 8.

A first test of saturation was run to assure that the system was working under saturation conditions. In Tab. 4.1 are reported the rates of RNA-cleavage keeping the concentration of **124** constant (150 nM) and varying the concentration of **1007** and **1008** from 1500 to 37.5 nM.

Table 4.1: Results of saturation experiments. Conditions: 150 nM substrate, 50 mM Tris-HCl, pH 8.0, 37 °C, 20 h.

	290_041		291_041		290_041		291_041	
Conc., nM	total % degr CG1007	main site % degr CG1007	total % degr CG1007	main site % degr CG1007	total % degr. CG1008	main site % degr. CG1008	total % degr. CG1008	main site % degr. CG1008
0	n.d.	n.d.	0,1	0,1	n.d.	n.d.	0,1	0,1
1500	33,9	25,8	18,8	14,6	8,9	4,6	12,1	8,0
1200	29,9	23,0	23,4	18,1	18,6	11,8	3,3	1,3
900	-	-	24,3	18,7	23,4	14,7	11,2	7,0
600	25,4	19,5	27,0	20,6	20,9	13,2	9,4	5,6
300	31,6	24,3	19,9	15,3	15,6	9,8	14,5	9,2
150	22,9	17,5	12,1	9,1	17,4	10,8	12,5	7,9
75	15,3	11,4	6,7	5,0	11,2	7,2	7,4	4,6
37,5	11,2	8,1	2,8	2,0	7,9	5,0	3,6	2,2

The experiment was repeated twice (290_041 and 291_041) in 50 mM Tris-HCl, pH 8.0, 37 °C, 20 h. The analysis of the data showed complete saturation of the substrate with conjugates concentration between 150 and 300 nM and further increase of the concentration did not lead to an increase of cleavage. To prove the real site-specific cleavage, an experiment of cross reactivity was also made. **1008** and **1007** (1500 nM) were incubated with **124** (150 nM) in lane **b** and **c** and with **210** (150 nM) lane **d** and **e** respectively (50 mM Tris-HCl at pH 8.0, 37 °C for 20 h). The specificity was therefore proved, because the cleavage occurred only in presence of the complementary RNA substrate (Fig. 4.9).

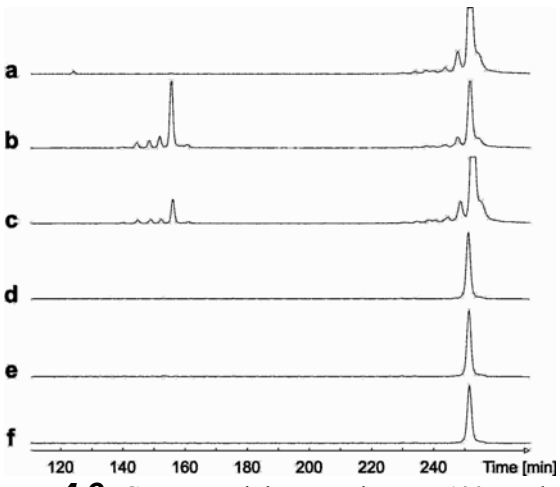

Figure 4.9: Cross reactivity experiments, **1007** and **1008** with **124** lane **b** and **c**, **1007** and **1008** with **210** lane **d** and **e**.

Further experiments were conducted to test the influence of Mg^{2+} on cleavage. The incubations were done at different ionic strength, with $MgCl_2$ or without $MgCl_2$. The results are reported in Tab. 4.2.

Table 4.2: RNA cleavage of **124** (150 nM) with **1007** (1500 nM) and **1008** (1500 nM) in presence of NaCl and $MgCl_2$. Conditions: 50 mM Tris-HCl pH 8.0, 37 °C, 20 h.

		total	**total**	**total**	**main site**	**main site**	**main site**
mM NaCl	mM MgCl2	% degr control	% degr CG**1007**	% degr. CG**1008**	% degr control	% degr CG**1007**	% degr. CG**1008**
0	0	1,26	27,35	15,20	0	25,09	14,14
0	10	9,73	14,80	18,42	0,83	9,66	10,00
0	5	10,98	25,74	19,61	0,76	20,26	11,75
0	1	6,04	29,83	12,23	0,47	26,56	6,41
100	0	0,00		12,46	0,00	43,30	11,81
100	10	6,14		9,52	0,42	16,77	8,53
100	5	3,48		11,89	0,30	28,72	11,24
100	1	2,93		15,19	0,25	28,02	14,17

From these results it appears clear that the $MgCl_2$ has more an effect of inhibition then to enhance the cleavage, but at high ionic strength (100 mM NaCl) without $MgCl_2$ the cleavage increased. Following these results the next subject of the tests became the study of cleavage rates in dependency on different concentrations of NaCl. In fact, the ionic strength can influence the binding constant helping to find a proper balance of the system constants.

Table 4.3: RNA cleavage of **124** (150 nM) with **1007** (1500 nM) and **1008** (1500 nM) in presence of NaCl at different concentrations. Conditions: 50 mM Tris-HCl pH 8.0, 37 °C, 20 h.

	290_041		291_041		290_041		291_041	
NaCl Conc., mM	total % degr CG**1007**	main site % degr CG**1007**	total % degr CG**1007**	main site % degr CG**1007**	total % degr. CG**1008**	main site % degr. CG**1008**	total % degr. CG**1008**	main site % degr. CG**1008**
0	n.d.	n.d.	0,1	0,1	n.d.	n.d.	0,1	0,1
1000	36,8	23,7	46,0	29,0	19,5	11,0	14,8	8,2
800	35,4	23,5	41,6	27,0	22,3	12,8	15,1	8,7
400	45,5	32,1	43,2	30,2	15,6	9,4	15,3	9,2
200	32,9	24,3	38,0	27,8	24,9	15,4	14,6	9,1

Table 4.4: Turnover experiment 1 with 50 nM **1007** against 300 nM **124**. Conditions: 50 mM Tris-HCl, 100 mM NaCl, at pH 8.0, 37 °C.

294_041	control		CG1007	
Time, h	total % degr	main site % degr	total % degr	main site % degr
0	n.a.	n.a.	n.d.	n.d.
24	0,2	0,1	12,3	9,1
48	0,3	0,1	26,4	19,5
72	0,5	0,2	45,7	34,2
96	0,5	0,2	56,2	41,4
168	0,8	0,3	75,9	55,3
192	0,8	0,3	74,0	56,2
216	0,9	0,3	80,4	57,7
264	1,0	0,4	84,7	58,4
337	1,0	0,4	82,0	58,2

Table 4.5: Turnover experiment 2 with 50 nM **1007** against 300 nM **124**. Conditions: 50 mM Tris-HCl, 100 mM NaCl, at pH 8.0, 37 °C.

295_041	control		**CG1007**	
Time, h	total % degr	main site % degr	total % degr	main site % degr
0	n.d.	n.d.	n.a.	n.a.
19	0,1	0,0	8,9	6,7
50	0,3	0,1	23,1	17,2
72	0,4	0,2	41,8	31,4
75	0,3	0,1	38,0	28,3
93	0,4	0,1	44,5	33,9
101	0,4	0,2	55,6	41,2
120	0,5	0,2	66,2	47,9
141	0,8	0,3	68,7	50,8
151	0,6	0,3	77,4	57,0
175	0,8	0,3	82,2	60,0
194	0,8	0,3	83,1	60,6
242	1,0	0,5	85,5	61,3

In Tab. 4.3 is reported the percentage of cleavage of two experiments at the following conditions: 50 mM Tris-HCl at pH 8.0, 37 °C for 20 h and at different ionic strengths. The results shown indicate an improvement of cleavage increasing the ionic strength. The physiological concentration of NaCl corresponds at 100 mM consequently this ionic strength was used for the next experiments. The final observation of this table is that **1007** is the best construct. Cleaving under the reported conditions 43-46 % of the substrate. Therefore, this conjugate became the candidate for running turnover-experiments.

To have turnover a catalyst must be able to carry out more catalytic cycles when incubated with an excess of substrate.

Therefore, **1007** (50 nM) was incubated with excess of **124** (300 nM in 50 mM Tris-HCl buffer, NaCl 150 mM, pH 8.0, 37 °C). In Tab. 4.4, and 4.5 are reported the results of two turnover experiments, one for 337 h, and the other for 242 h. The experiment was stopped after 337 h because it is known that part of the substrate is not cleaved.[10]

Fig. 4.10 illustrates the electropherograms of the sequencer at different times.

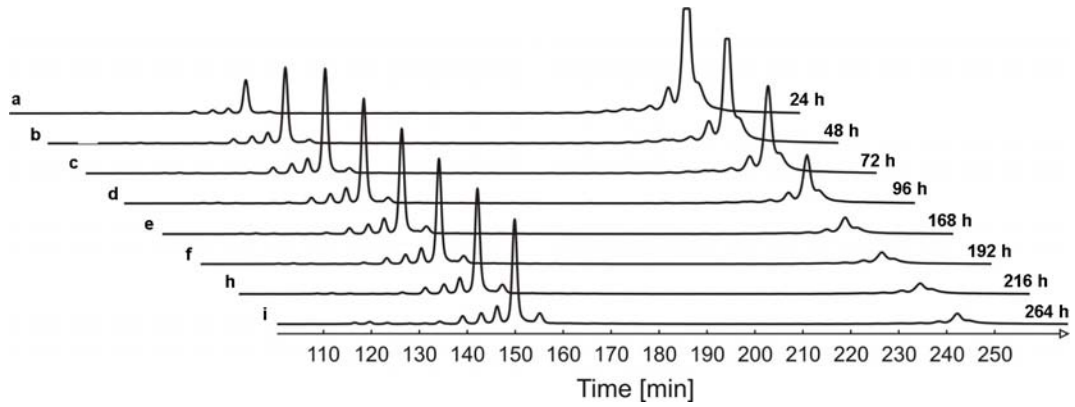

Figure 4.10: Electropherograms of the sequencer show the increase of the cleavage and the reduction of the substrate.

The ability to exhibit turnover for **1007** was therefore proved, because the excess of substrate was site specifically cleaved. The values of Tab. 4.4 and 4.5 are represented in a graphic percentage of substrate in dependency on time in Fig. 4.11. In the next section are analysed the kinetic data.

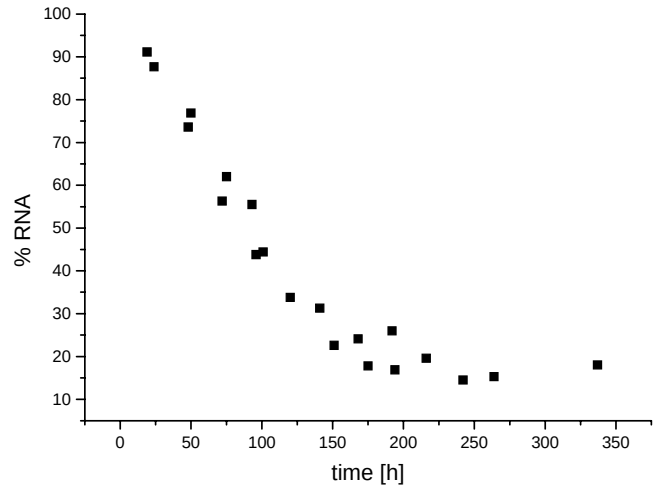

Figure 4.11: Degradation of the substrate in dependency on time.

4.6 Turnover Kinetic Analysis

A minimal kinetic scheme for these types of artificial RNases is shown in Fig. 4.12. In this assumption also the reverse reactions k_{-3} and k_{-5} are taken in consideration. In fact if the products of the reaction are the 2'-3'-cyclic phosphates also the ligation can be catalysed by the same catalyst.[94]

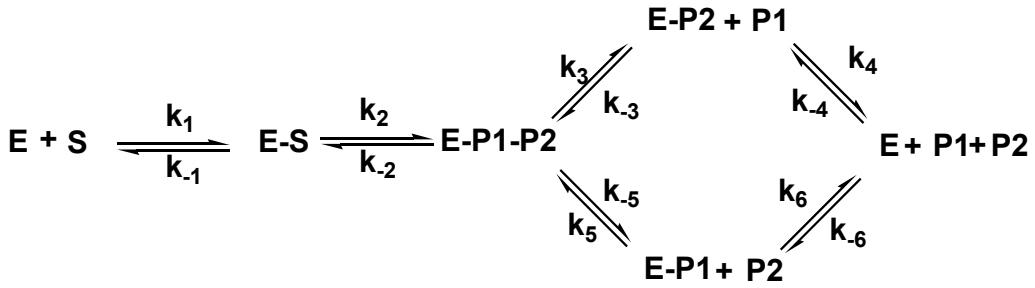

Figure 4.12: Minimal kinetic mechanism for intermolecular catalysis.

A complete analysis of each event is complicated and goes beyond the scope of this work. However, the analysis can be simplified in accord with the theory of Henry, Michaelis, Menten and the following modifications of Briggs and Haldane.[97] Therefore, it could be interesting to extract the values of K_m and k_{cat}. This would help to evaluate the efficiency of our system and to allow a possible comparison with other systems for site-specific cleavage.

In accord with these theories, the kinetic experiments should be made in *steady state* conditions where the [ES] is constant with an excess of substrate, and in the initial part of the reaction where the slope of the plot of the products formation versus time is linear. Under these conditions the substrate is in great excess compared with the products. Consequently, the inhibition by the products and the reverse reaction are negligible. Taking these assumptions as a basis it should be possible to monitor the first part of the complicated scheme shown in Fig. 4.12 and to extract the values of K_m and k_{cat}.

These problems have already been encountered by other authors.[88b][94b][95][98] Classically this analysis is done by a modified Eadie-Hofstee linear plot of k_{obs} vs. k_{obs}/[S] where the slope is $-K_m$, the y intercept is equal to $Vmax$ and $k_{cat}=Vmax$/[E]. The reaction rates (k_{obs}) should be calculated from the linear slope of plots

concentration of the product vs. time over the first 5-10 % of the reaction, in a set of kinetics where the concentration of the substrate span a range ≥10-fold excess over [E]. An illustrative example is given in Fig. 4.13.

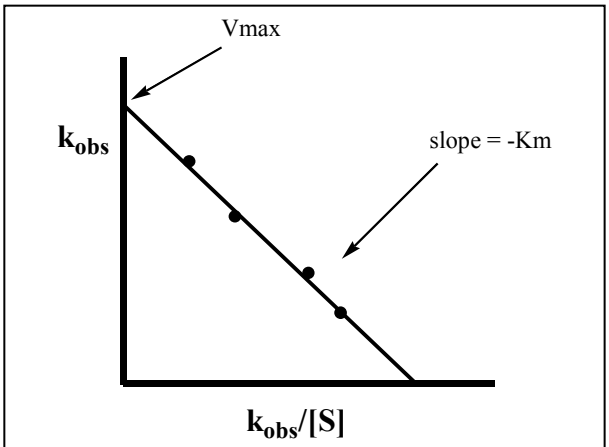

Figure 4.13: A typical modified Eadie-Hofstee linear plot.

An analysis like in Fig. 4.13 should be desirable. However, at the moment there are not enough data available. The experiments done are nevertheless sufficient for an approximate analysis. In fact assuming that when [S] is in 6-fold excess compared to [E], the catalyst should operate under conditions of saturation. Hence, the velocity over the first 10% of the reaction corresponds to *Vmax* and it becomes easy to calculate an approximate k_{cat}.

$\Delta[P] = C_0 \times$ % Cleavage, $V = \Delta[P] / \Delta[t]$ that in our case correspond to *Vmax*. Considering Tab. 4.4 and 4.5, a cleavage of 12.3 % occurs in 24 h and of 8.9 % in 19 h. The *Vmax* is therefore 1.54 nM h^{-1} and 1.41 nM h^{-1}. Now, if the concentration of the catalyst was 50 nM, k_{cat} is 0.031-0.028 h^{-1}.

4.7 Alternative Strategy to Have Turnover with 5' Oligonucleotide Conjugates

Until now we have illustrated the classical procedure to design conjugates with turnover capacity. An alternative strategy with indisputable synthetic advantages was proposed by Häner et al.[54b][54c] According to this author, if a bulge is induced closely to the 5'-end of the conjugate, the catalyst should be able to reach the bulge and to cleave the RNA in the single stranded region as well as in the double strand (Fig 4.14B). The consequence is obvious, the two fragments of RNA will bind more weakly to the conjugate and they will be released for another cleavage cycle. Following this strategy, Häner reported two conjugates, which were able to cleave in the bulge.[54b][54c] One of these antisense constructs, 12 base long and built from 2'methoxyethoxy modified RNA, exhibited also turnover. Since the last 7 bases at the 3' terminus of our RNA substrate **210** are identical with the corresponding bases in Häner's substrate (Fig. 4.14a), it was thought to design a similar DNA conjugate applying the same strategy. This new project was started in collaboration with Kathrin Beier (Fig. 4.14).

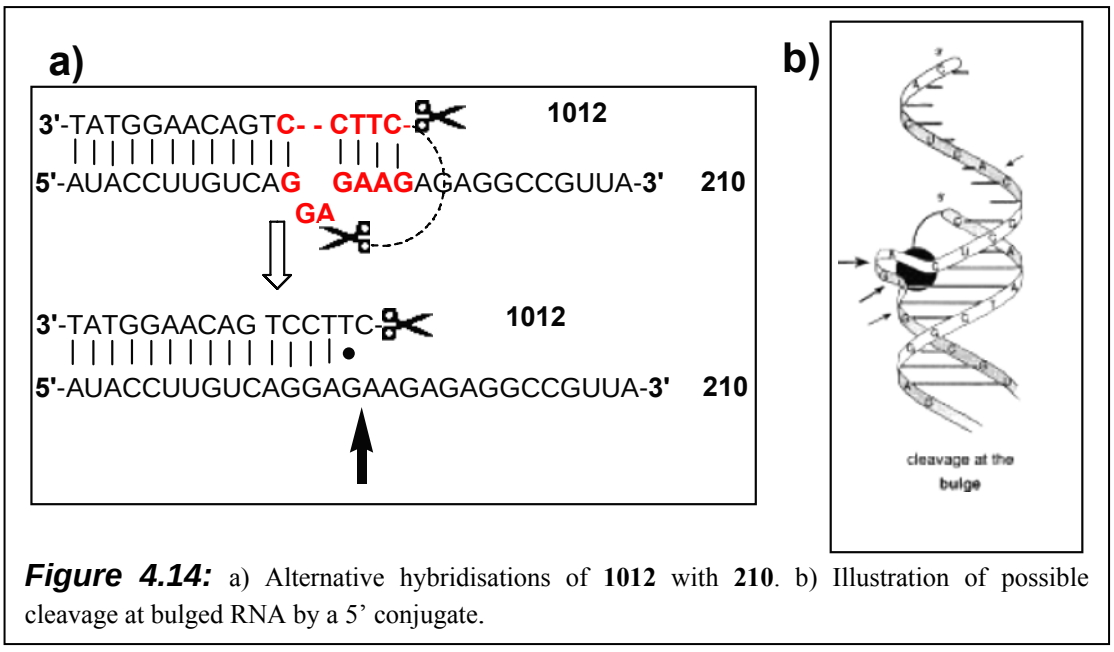

Figure 4.14: a) Alternative hybridisations of **1012** with **210**. b) Illustration of possible cleavage at bulged RNA by a 5' conjugate.

The conjugate **1012** was synthesized applying the classical automated synthesis on solid phase, following the synthetic strategy illustrated in Fig. 4.15. The

monomethoxytrityl protected C_6 amino linker was coupled to the 5'-end of the DNA sequence and detritylated by the synthesizer. **30** was conjugated on solid phase manually using DIC and HOBT as condensing agents. Finally, the conjugate was cleaved off from the solid phase and deprotected by aqueous ammonia (25 %).

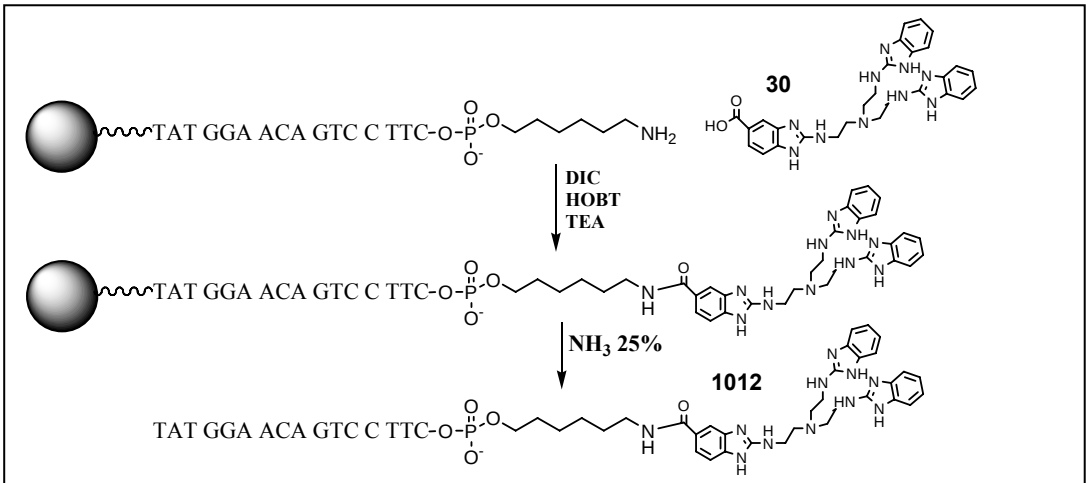

Figure 4.15: Conjugation strategy for **1012**.

As preliminary experiment **1012** (1500 nM) was incubated with **210** (150 nM) under the usual conditions (50 mM Tris-HCl, NaCl 150 mM, pH 8.0, 37 °C), but the cleavage occurred mostly at position 15, as illustrated in Fig. 4.14a and 4.16a. This led to the conclusion that in this construct the structure without a bulge is preferred over the one with a bulge.

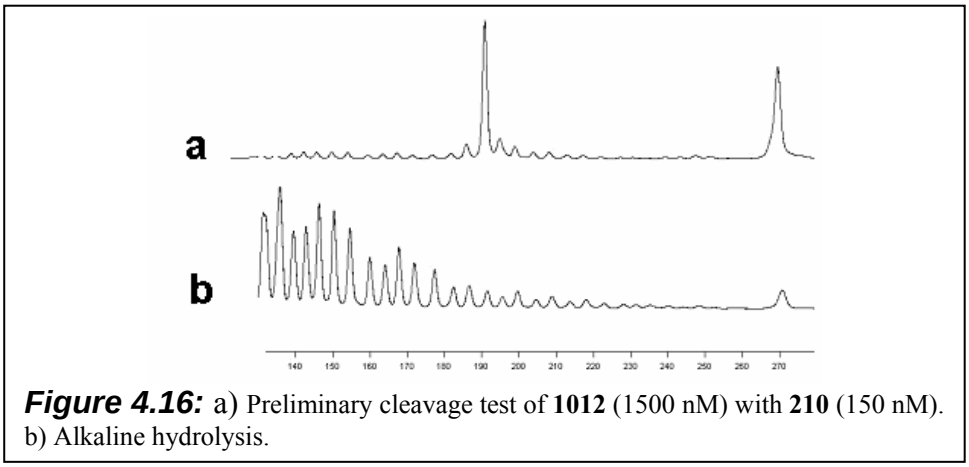

Figure 4.16: a) Preliminary cleavage test of **1012** (1500 nM) with **210** (150 nM). b) Alkaline hydrolysis.

However, Häner used 2'methoxyethoxy modified RNA for the synthesis of his conjugate. This probably is of fundamental importance for the stabilization of the

bulge. The same author obtained similar results also with DNA,[54b] but with a different sequence. Therefore, a sequence dependency in the stabilization of these constructs must exist. A new oligonucleotide was made by Kathrin Beier using the compound **30** for conjugation. These experiments are still in progress and they will be reported in her dissertation.

4.8 Comparison with other Systems Exhibiting Turnover

To evaluate the efficiency of the system created in my PhD thesis, a short comparison with other systems is done here (an overview on these conjugates is also presented in a recent publication of Lönnberg).[32]

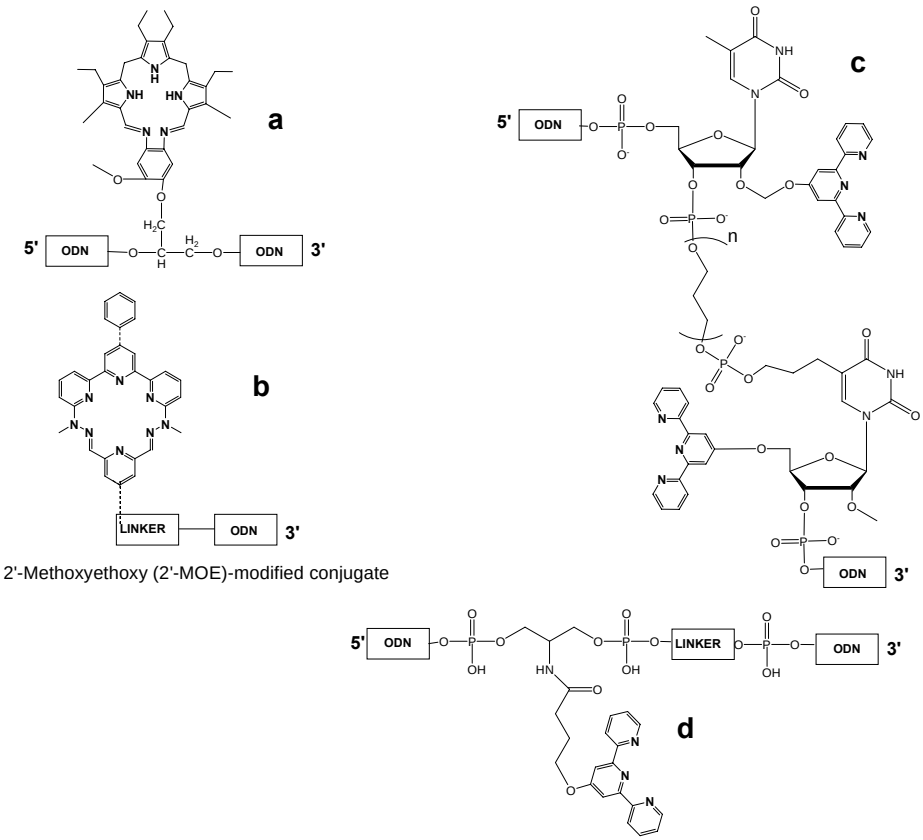

Figure 4.17: Structures of some of the best site specific artificial RNases based on metals and exhibiting turnover.

Starting with the metal dependent catalysts, the dysprosium texaphyrin conjugate in Fig. 4.17a showed to cleave 67 % of the 10 fold excess substrate in 50 mM HEPES, pH 7.5, 100 mM NaCl in 24 h at 37 °C, with k_{cat} of 0.286 h^{-1}.[55c]

The macrocyclic lanthanide complex artificial RNase in Fig. 4.17b inducing a bulge in the substrate 4 bases before the 5' end of the conjugate, showed turnover cleaving 90.3 % of the 5 fold excess substrate, at pH 7.2, 37 °C in 64 h. The bis-Cu^{2+}-terpyridine-2'-O-methyl oligoribonucleotide conjugate in Fig. 4.14c with n = 1 (n = 0-3), showed a k_{cat} of 0.647 h^{-1} at pH 7.5, 37 °C, and 100 nM $NaClO_4$.[88b] Bashkin et al. reported that the Cu^{2+}-terpyridine conjugate in Fig. 4.17d was able to cleave 6.7 equivalents of 10 equivalents of RNA, at pH 7.4, 45 °C in 40 h with 0.1 mM $NaClO_4$.[100]

Concerning the metal free constructs the results are not so brilliant. For instance the triethylenetetramine conjugate in Fig. 4.18a cleaved 3 % of the RNA substrate in 16 h (Conditions: 0.2 mM substrate, 20 mM conjugate, pH 7.5, 37 °C).[101] The methanephosphonate ODNs conjugate bearing an diimidazole or imidazole/amino cleaving agent in an intra-chain position in Fig. 4.18b showed to cleave less then 10 % of the RNA substrate at pH 7.2, 25 °C, in 5 days.[96a]

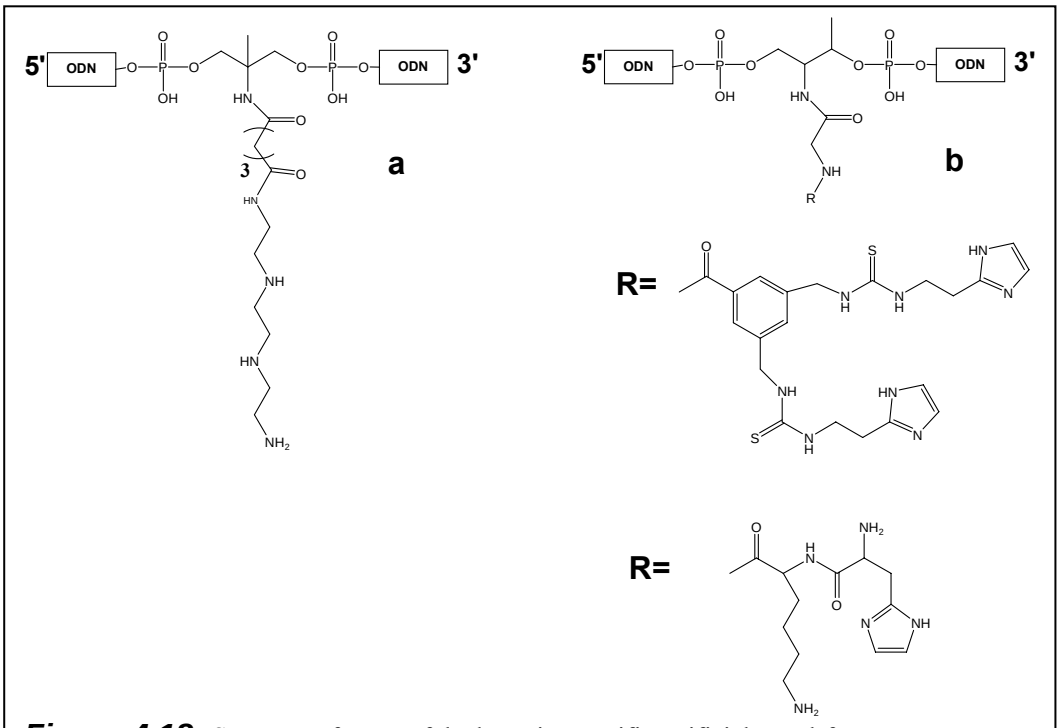

Figure 4.18: Structure of some of the best site specific artificial metal-free Rnases exhibiting turnover.

Table 4.6: Catalytic activity of various RNA-cleaving enzymes.[95]

Enzyme	k_{cat} h^{-1}
Ribonuclease A	
UpA substrate	50.4×10^5
Poly(C) substrate	18.6×10^5
Hairpin ribozyme	12.6×10^2
Hammerhead ribozyme	8.4×10^2
10-23 DNA enzyme[95]	20.4×10^2

To conclude this comparison the k_{cat}s of some natural enzymes and ribozymes are reported in Tab. 4.6.[95] Here the large difference still existing between the natural and the artificial systems becomes clear.

4.9 Conclusions

During this project site specific artificial RNases exhibiting turnover were obtained. Three different conjugates carrying the catalyst in an intra-chain position were synthesized. The most successful could exhibit a k_{cat} of 0.031 h^{-1}, probably the best site specific metal-free artificial ribonuclease showing turnover. Nevertheless, a quick comparison with natural ribozymes shows that this catalyst is still some thousand folds inferior.

It still remains to investigate the specificity and efficiency depending on the bulge-size, but this problem could be solved without big synthetic efforts by buying new substrates that can form bulges of the desired size.

Concerning the turnover project with 5' conjugates the first result are not extremely brilliant. Further studies must be undertaken to really understand the reasons governing bulge stability in these constructs.

5 Tris(2-aminobenzimidazole) in Affinity Cleavage

RNA can assume complicated structures that can be recognized specifically by binding proteins. Such interactions are important in numerous biological processes like splicing, polyadenylation, nuclear export, translation, mRNA localization and mRNA decay. To understand these processes several methodologies exist. During this work the possibility of applying the tris(2-aminobenzimidazole) in affinity cleavage was explored. At this purpose the tris(2-aminobenzimidazole) was conjugated to possible peptidic RNA ligands further in collaboration with the group of Professor Jean-Luc Décout (Université Joseph Fourier at Grenoble), a conjugate with neamine was achieved.

5.1 RNA Structure

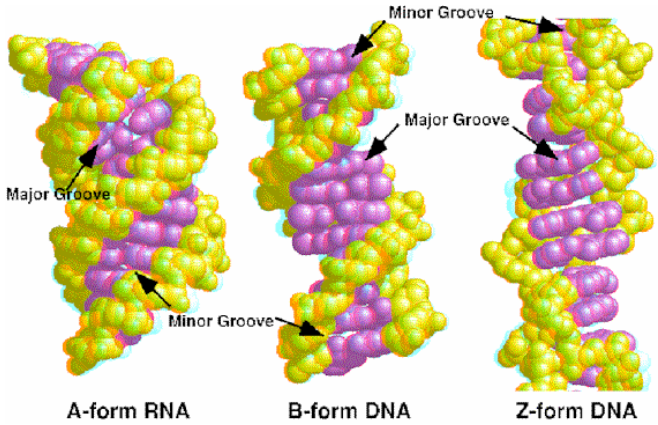

Figure 5.1: Double-helical molecular structure of nucleic acids

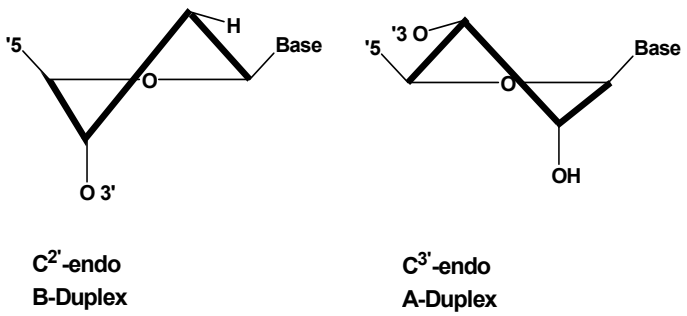

Figure 5.2: Conformation of deoxyribose and ribose in the B and A double helical form.

RNA chemically differs from DNA by the presence of uridine instead of thymidine and the 2'-OH. This extra hydroxyl group influences the reactivity against cleavage, but also the structure. The DNA helixes normally assume a B conformation and under particular conditions the Z form. RNA on the contrary assumes an A conformation (Fig. 5.1). The ribose in these different helices has also

Table 5.1: Parameters of the A and B helical form.

Parameters	A Form	B Form
Direction of helical rotation	Right	Right
Residues per turn of helix	11	10
Rotation of helix per residue (in degrees)	33	36
Base tilt relative to helix axis (in degrees)	20	6
Major groove	narrow and deep	wide and deep
Minor groove	wide and shallow	narrow and deep
Orientation of N-glycosidic Bond	Anti	Anti

different conformations as shown in Fig. 5.2, where for the B form the C 2' is in *endo*, while in the A form the C 3' is in *endo*. The differences of the two helixes are summarized in Tab. 5.1.

Another important difference between the two nucleic acids is that DNA usually forms regular double strand helices, while RNA is usually single stranded. This is an important difference because RNA single strand can remain without a particular structure (random coil) or when complementarities exist in the same sequence it can form short helices, letting other part of sequence unpaired. This leads to the formation of secondary structures, which are typical for RNA. A schematic view of such elements, bulges, loops, hairpin and pseudoknots is shown in Fig. 5.3.

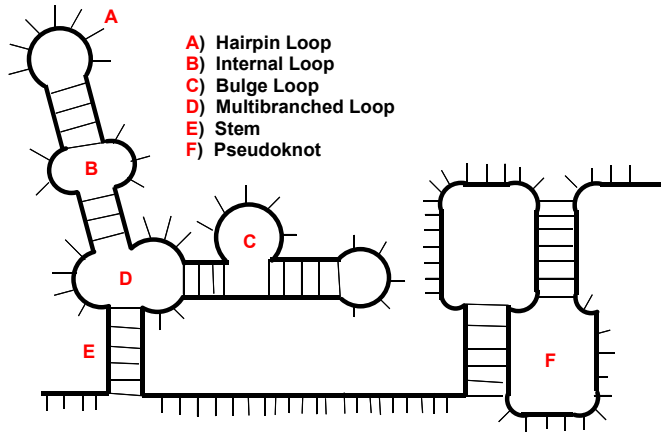

Figure 5.3: RNA secondary structures.

Furthermore, these secondary structures of RNA can fold into more complicated tertiary structures like in t-RNA. This allows RNA to adopt unique structures creating micro environments that can be specifically recognized by proteins, small molecules or generate catalytic functions. For these reasons this nucleic acid can have more complicated roles than being a simple carrier of genetic information,[102]

from here it develops the great interest for the interactions between RNA and its binding proteins or ligands.

5.2 Identification of RNA-Binding Proteins

The first step of studying RNA protein interactions is the identification and isolation of the proteins that could interact with a RNA target. To achieve this objective three methodologies exist: 1) North-western screening of a cDNA expression library, 2) Affinity chromatography, 3) Phage display.

5.2.1 North-Western Screening

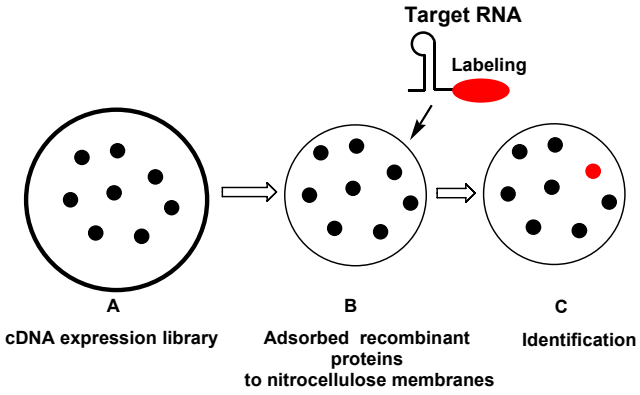

Figure 5.4: North-western screening.

In the **North-western screening** an expression library of cDNA is cloned into bacteriophage expression vector, displaying several different proteins (Fig. 5.4A). These proteins are then adsorbed by platting on a membrane of nitrocellulose that is a replica of the Petri dish. This membrane is then incubated with the labelled RNA target (Fig. 5.4B), after a rinsing step to reduce the false positive, it is possible to identify the clone expressing RNA binding proteins (Fig. 5.4C).[103]

5.2.2 Affinity chromatography

A second methodology is **affinity chromatography**.[104] Several variants of this technique are known, but the general principle can be explained in Fig. 5.5. The RNA target is fixed on a solid support, generally sepharose. A mixture of proteins is

eluted through the column, where the RNA binding proteins remain fixed. Using a different buffer, the fixed proteins then can be collected. A variant of this method makes use of columns with streptavidin fixed on the matrix. A biotinylated RNA target is used. In this way the protein-RNA interaction can occur in solution, and the RNA-protein complex is fixed in a second moment by the biotin streptavidin interaction. In both the cases the protein is isolated, sequenced and a clone expressing its gene can be identified.

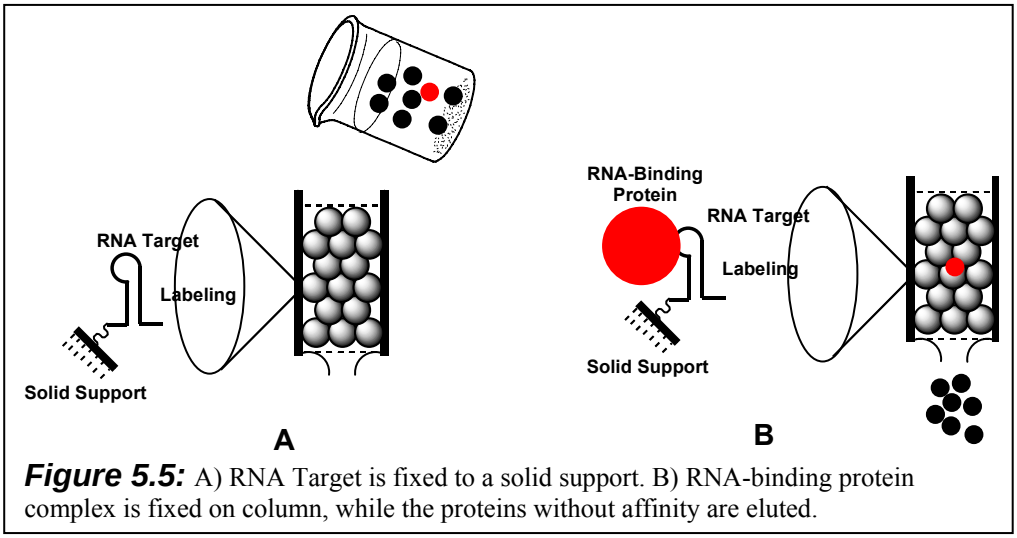

Figure 5.5: A) RNA Target is fixed to a solid support. B) RNA-binding protein complex is fixed on column, while the proteins without affinity are eluted.

5.2.3 Phage Display

Another system for identifying proteins with affinity for a certain target is **phage display**.[105] A modified version of this methodology can be used for *in vitro* selection of BP (binding protein) for a RNA target.[106] The system is summarized in Fig. 5.6 in the following steps: 1) Preparation of a combinatorial library of mutagenized cDNA encoding the RNA-binding domain, these fragments are then inserted in a phagemid vector in a way that the protein of interest is fused to the gene III coat protein of the phage. In this way the phage displays on its external face the protein of interest. This library is then transformed into an *E. coli* host. 2) Infecting the host with a helper phage, a pool of modified phages with coat proteins fused to RNA-BP variants is generated. 3) The phages are then released from the bacterium host into the external environment, so that they can be collected. In the next step the phages are incubated with the target RNA fixed on beads. Therefore, the phages expressing the RNA-BP's remain fixed to the target. 4) The bound viral particles are

washed, disconnected from the target and collected. These selected phages can be used for another cycle of infection, allowing amplification of the best clones and a better selection. At the end it is possible to have the best clones in useful amount to identify the new RNA binding protein.

This technology was used by Jörg Bäumler[106c] of the group of Dr. Manuel Grez at Georg Speyer Haus of Frankfurt, to select a peptide with affinity for mRNA of the Bcr-Abl fusion oncoprotein. (This peptide has been used also in this thesis. See 5.4.3).

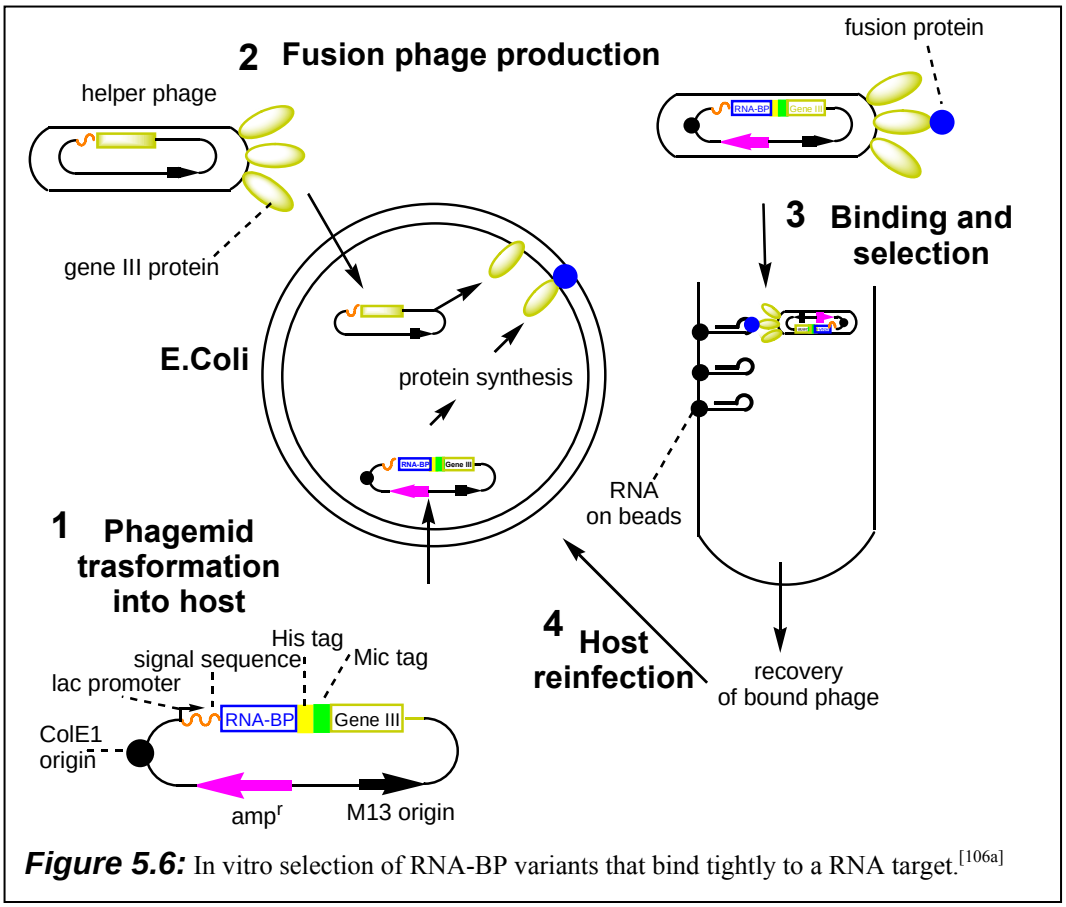

Figure 5.6: In vitro selection of RNA-BP variants that bind tightly to a RNA target.[106a]

5.3 Studying Ligand-Target Interactions by Affinity Cleavage

Once a binding protein for a RNA target is found, the problem arises of finding the specific binding site in a large RNA, and of studying the ligand-target interaction. For this purpose different systems exist, like X ray diffraction when it is possible to

isolate the crystal of the RNA-ligand complex or NMR when a high frequency spectrometer is available. In the absence of X ray or NMR data, there are different convenient systems like FRET assays,[107] and foot-printing.[108] Another system that allows to characterize the topology of RNA-protein complexes is affinity cleavage.[109] This method was introduced first by Dervan et al.[9a][9b] and was applied for investigating DNA-peptide interactions.[109][9c]

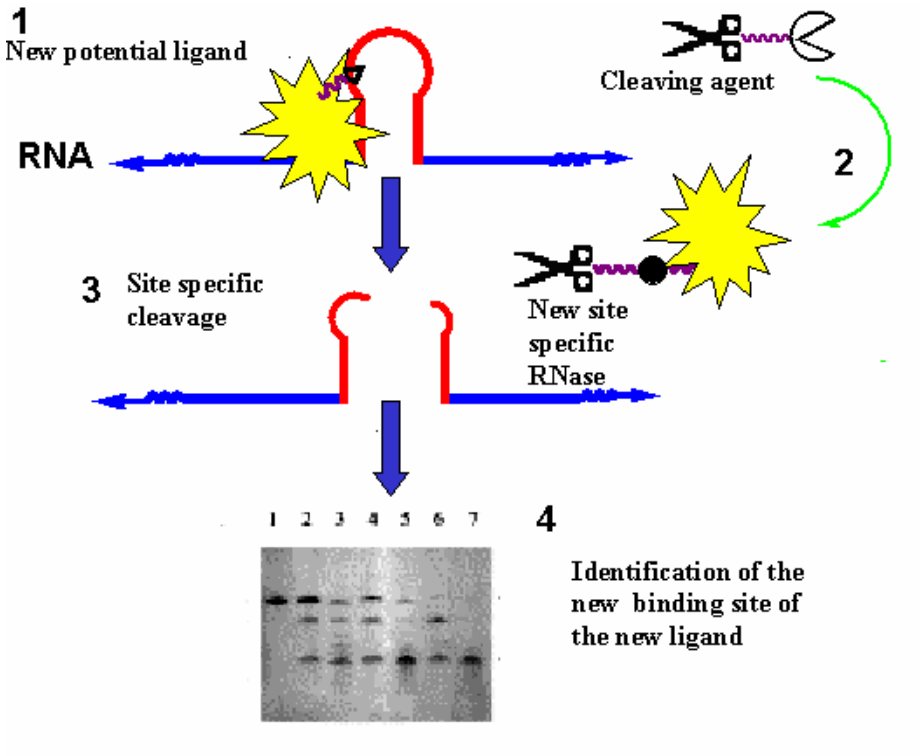

Figure 5.7: Schematic concept of affinity cleavage.

The concept of this technique is illustrated in Fig. 5.7. 1) Isolation of an RNA-binding protein. 2) The protein is conjugated to an unspecific cleaving agent forming a new specific nuclease. 3) The conjugate is incubated with the RNA substrate. Hence, we will have site-specific cleavage. 4) It is possible to identify the binding site, or to obtain even more precise information. For instance, changing the position of the amino acid for the conjugation it could reveal key topological features of the ligand-RNA complex.

The cleaving agents employed in this technique are usually metal complexes, able to cleave by oxidative mechanisms DNA and RNA equally well. Fig. 5.8 summarizes the cleaving agents most often used for this technique.[110] A well known agent is the

copper 1,10-*o*-phenanthroline (OP). This is a redox active complex, which is able to generate oxygen radicals that cleave the DNA or RNA backbone. Another family of catalysts are the derivatives of the Fe-EDTA complexes. The cleavage reaction is usually initiated by addition of a reducing agent such as DTT or sodium ascorbate in the presence of O_2. The scission of the nucleic acid backbone occurs by oxidation, through the formation of activated oxygen species, presumably hydroxyl radicals. The most successful of these EDTA derivatives is called BABE (S-1-[p-(bromoacetamido)benzyl]-EDTA).

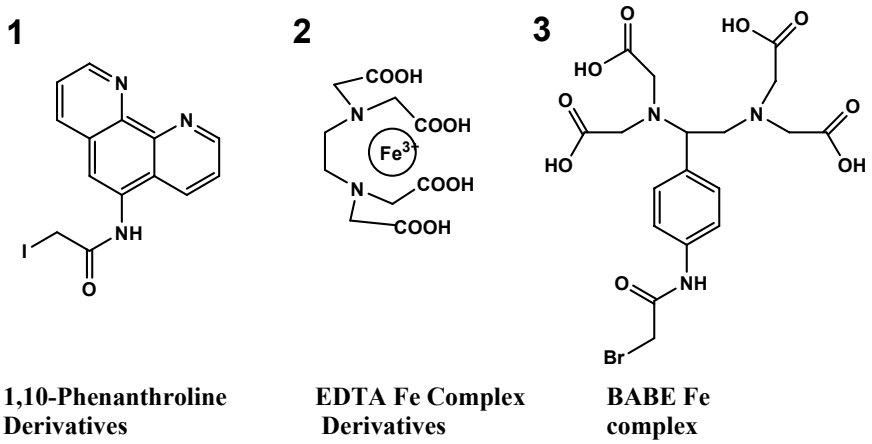

Figure 5.8: Cleaving agents employed in affinity cleavage.

However, these catalysts for affinity cleavage present the disadvantage to produce diffusible radicals and to generate pattern of cleavage, which are not always precise. Moreover, the EDTA derivatives cleave also peptidic bonds and therefore, can autocatalyticaly degrade their own binding protein. Once the activity of the tris(2-aminobenzimidazole) as RNase is confirmed a possible application of such molecules could be affinity cleavage. To explore such applications a set of 4 RNA binding peptides, and a small ligand for RNA were conjugated to the tris(2-aminobenzimidazole) and tested on the corresponding RNA substrates.

5.4 RNA Ligands

To set up a new methodology of affinity cleavage different RNA ligands were chosen for conjugation with our catalyst. A short description of these ligands is given below.

5.4.1 Tat Peptides

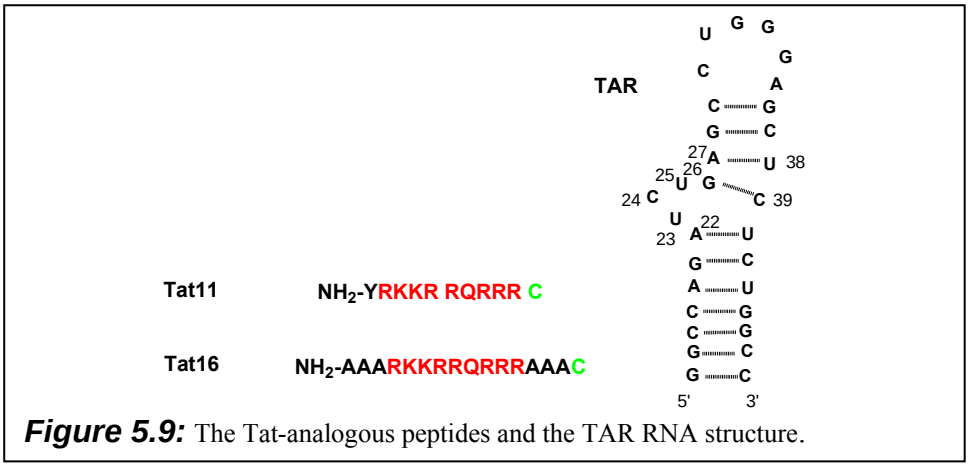

Figure 5.9: The Tat-analogous peptides and the TAR RNA structure.

The first two ligands (Fig. 5.9) are two peptides derived from Tat, the 86 amino acids long transactivator protein of HIV-1. Tat plays a crucial role in the viral life increasing the expression of the viral mRNA. For its function, the protein must bind the *trans*-activating response element TAR, a 59-bases hairpin-stem-bulge RNA structure positioned at the 5-end of all nascent HIV-1 transcripts.[111] The peptide sequence $Tat_{49\text{-}57}$ of this protein has been demonstrated to be essential for TAR RNA binding *in vivo* and sufficient for TAR recognition *in vitro*.[64a][112] In Fig. 5.9 the sequences of the two peptides used in this work are reported. In Tat11 the $Tat_{49\text{-}57}$ sequence is highlighted in red, in addition there are then an additional cysteine for the conjugation and a tyrosin for UV determination. Tat16, similar to Tat 11, has 3 additional alanines to evaluate the effect of an expanded peptidic spacer. [107]

5.4.2 Neamine

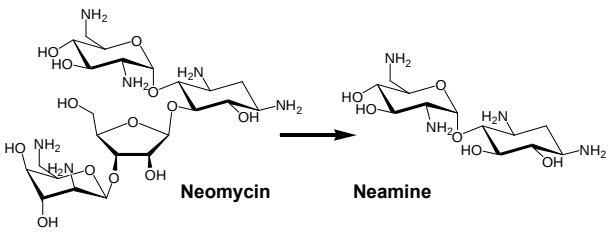

Figure 5.10: Neamine is a derivative of neomycin, less toxic, but still able to bind TAR.

Aminoglycosides constitute a large family of natural antibiotics that have as target rRNA. Neomycin B also binds to other RNA targets such as TAR, unfortunately this

molecule is highly toxic. Studies to improve its properties demonstrated that neamine is less toxic and it can serve as minimal structural motif still conserving affinity for RNA targets [17] (Fig. 5.10).

This small antibiotic with affinity for TAR was conjugated to **30** (Fig. 5.12) by Jérôme Désiré in the group of Jean-Luc Décout (Université Joseph Fourier at Grenoble).

5.4.3 Bcr-Abl Binding Peptide

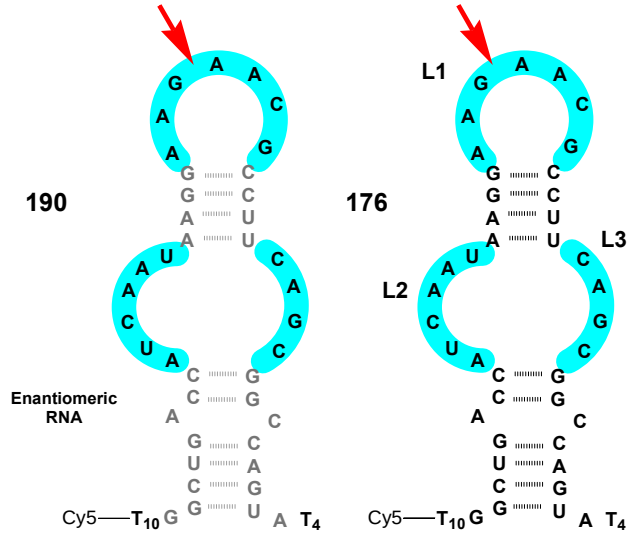

Figure 5.11: The two enantiomeric Bcr-Abl mRNA substrates. The arrow indicates the point of fusion of the two genes Bcr and Abl. Bottom: sequence of the binding peptides.

The sequence of the last ligands resulted from a collaboration with Jörg Bäumler who provided two peptides selected during his Ph.D. by phage display (Fig. 4.11).[106c] The target is a fragment of the mRNA of the Bcr-Abl oncoprotein, corresponding to the breakpoint sequence where the two fragments of the genes of BCR and ABL are fused to form the oncogene BCR-ABL (Fig 5.11).

The fatal effect of several oncogenes is based on aberrant exchange of genetic material, one of the most known is called Philadelphia chromosome. In this case a

translocation of DNA between the chromosome 9 and 22 with molecular juxtaposition of the gene BCR and ABL generates a fusion BCR-ABL oncogene. Both proteins are involved in the cell cycle. The onconcoprotein Bcr-Abl deregulates the cellular cycle and renders the leukaemia cells resistant against the programmed cell death (apoptosis). This BCR-ABL translocation is found in 90 % of the patients affected by chronic myelogenous leukaemia and in some with acute leukaemia.[113] The fusion of the two mRNAs creates a new RNA with peculiar characteristics that may be recognized by new ligands, such as the peptides selected by Jörg Bäumler. The two peptides were synthesised in both enantiomeric forms D and L, conjugated with the tris(2-aminobenzimidazole), and tested with the normal RNA substrate **176** and its enatiomeric form **190**.

5.5 Conjugation Strategies.

To obtain the conjugation of different ligands two approaches have been tried (Fig. 5.12). In the first approach two maleinimide tris(2-aminobenzimidazoles) derivatives were synthesized, with a long linker **37**, and in collaboration with Kathrin Beier with

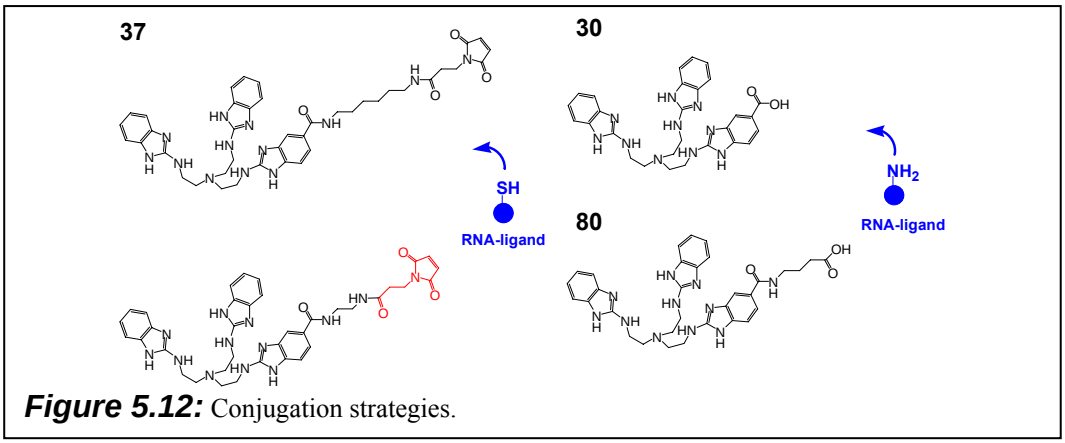

Figure 5.12: Conjugation strategies.

a shorter linker. These two molecules are suitable for the conjugation with mercapto groups present in RNA ligands. In the second approach, two carboxylic acid derivatives of the tris(2-aminobenzimidazole) were prepared, **30** without any linker and **80** with a GABA linker. These last two compounds are suitable for peptidic conjugation, when mercapto groups are not available in the binding domain of the ligand.

5.6 Synthesis of the Catalysts Suitable for Peptidic Conjugation

The synthesis of compound **37** and its analogue with the short linker are described below (Sch. 5.1). A diamine with 2 or 6 CH_2 was singly protected with BOC-ON. The mono protected amines **13** or **47** were then converted in the compounds **35** or **48** by amide coupling with **30,** using DIC and HOBT. The BOC protecting group of **35** was removed with a diluted solution of HCl, yielding **36**, which was coupled with the commercial N-succinimidyl 3-maleimidopropionate to give the desired compound **37**. The analogue of **37** with a short linker was prepared by Kathtrin Beier starting from the precursor **48**.

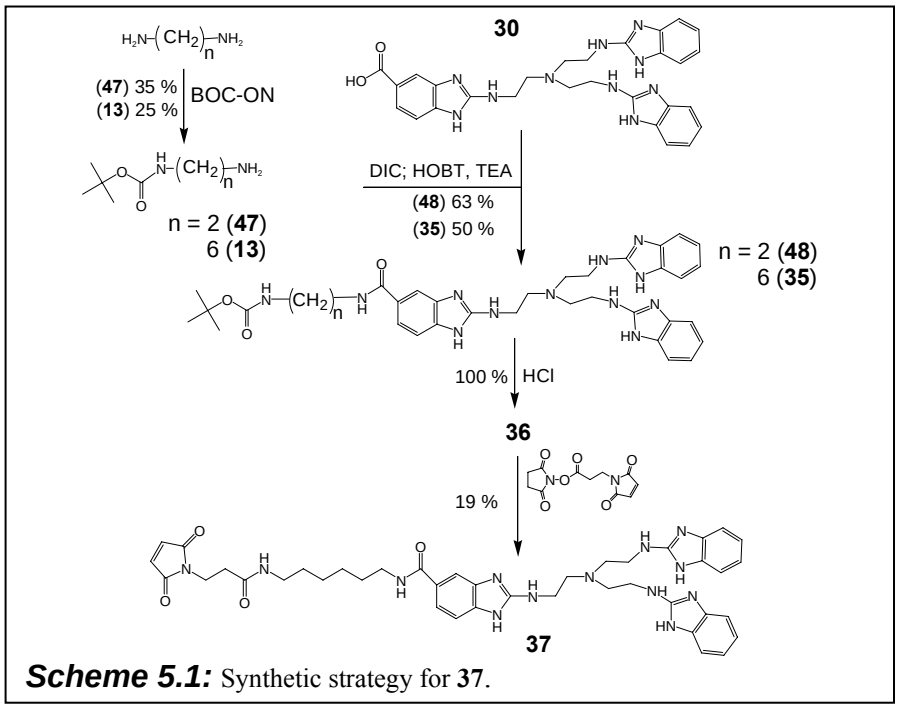

Scheme 5.1: Synthetic strategy for **37**.

For the conjugation by peptidic bonds the compound **30** is readily obtainable by acid induced hydrolysis of **29**. To introduce a short linker conserving a carboxylic acid, GABA was converted into **76** by protection of the amino group with a Z group using benzyl chloroformate. The subsequent esterification with *tert*-butanol and DCC gave **77**. Removal of the Z group with H_2/Pd produced **78**, which was coupled to **30** using DIC and HOBT to form **79**. The final compound **80** was obtained by hydrolysis of the *tert*-butyl ester of its precursor with diluted HCl (Sch. 5.2).

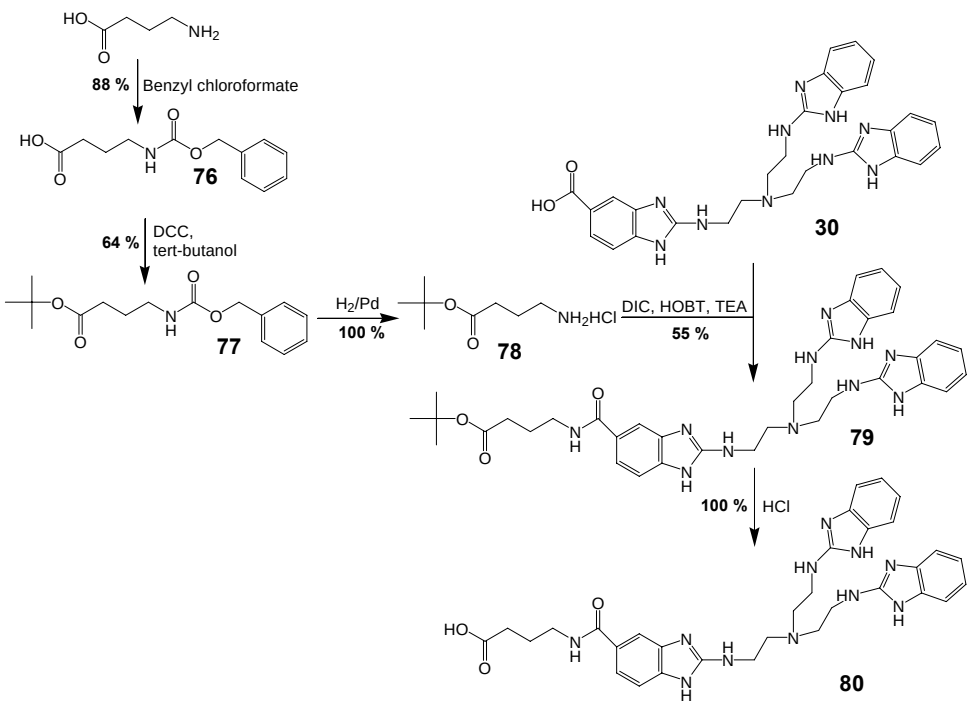

Scheme 5.2: Synthetic strategy for **80.**

5.7 Peptidic Conjugation

Starting form **37** and the peptides described above, 4 different conjugates were made via maleinimide chemistry (Sch. 5.3). In the protocol of this conjugation to a solution of 2 mg of peptides in water was added a solution of **37** (2 equivalents) in DMF. The reaction between the free thiol and the maleinimide occurred almost instantaneously and quantitatively (Sch. 5.3a). The purification was then performed by HPLC.

Jérôme Désiré made the fifth conjugate with neamine, using the compound **30** (Fig. 5.12) synthesized during my thesis.

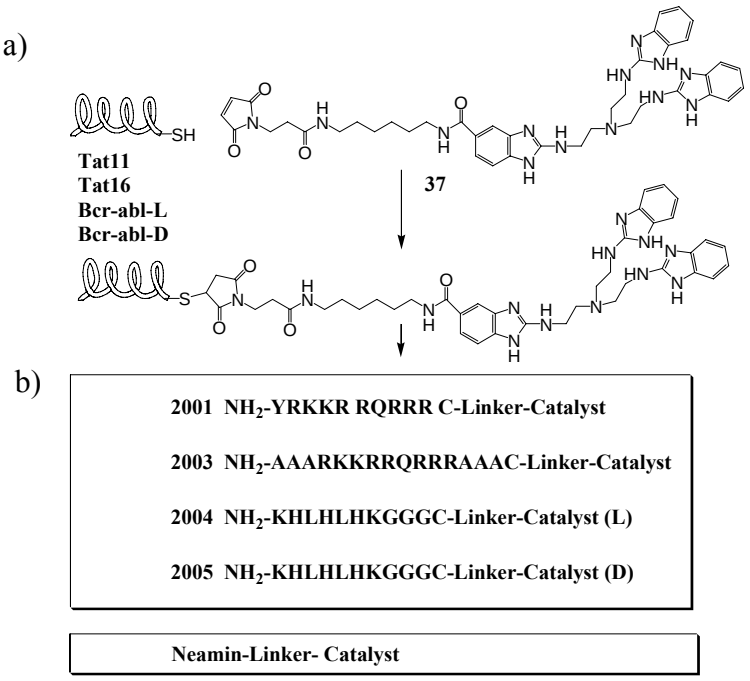

Scheme 5.3: Conjugation via thiol-maleinimide chemistry**.**

5.8 Test of Affinity Cleavage

Dr. Ute Scheffer performed the tests for affinity cleavage. The first test was made with the Tat11 conjugate named **2001** (Fig. 5.13C). The conjugate was incubated with TAR substrate **153** or its enantiomeric form **158** (Fig. 5.13B). In fact it is known that Tat11 made of (D)-amino acids conserves binding affinity for TAR.[114] Therefore, the (L) form is expected to bind the enantiomeric form of TAR. The use of the enantiomeric RNA substrate as shown above allows to exclude artefacts due to RNase contaminations (see 2.7.2). The concentration of the RNA substrate was kept constant (150 nM), while the pH was 6 or 7.5. The concentration of the conjugate was varied from 1.25 μM to 0.125 μM, the buffer used was 50 mM Tris-HCl, 20 mM KCl, 0.01 % Triton x-100, at 37 °C, for 20 h. The results of these preliminary studies are reported in Tab. 5.2. From these data a certain selectivity of the cleavage for the bulge and the hairpin loop emerged with a major selectivity for the last.

In Fig. 5.13A is shown the cleavage of the enantiomeric TAR **158** (150 nM) in presence of **2001** (0.31 μM), pH 7.5, 37 °C, 20 h. Here it is visible that the cleavage

occurred mostly in the hairpin loop. Probably the recognition occurred in the bulge, while the catalyst was addressed to the loop.

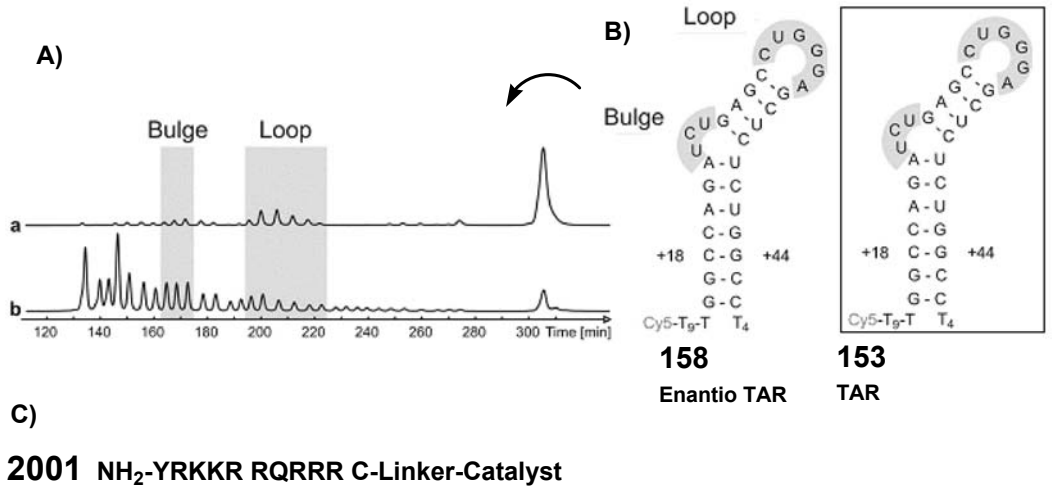

Figure 5.13: A) Cleavage of RNA **158** (150 nM) induced by conjugate **2001** at concentrations of 0.31 µM. Conditions: 50 mM Tris-HCl, 20 mM KCl, 0.01 % Triton x-100, pH 7.5, 37 °C, 20 h. Lane **b**: base ladder of substrate **158** (Na_2CO_3). B) RNA substrates **158** and **153**. C) Tat conjugate **2001**.

Table 5.2: Results of cleavage of **2001** when incubated with **153** and **158**. Conditions: 50 mM Tris-HCl, 20 mM KCl, 0.01 % Triton x-100, 37 °C, 20 h. ALF-file: 150_041.alx 150_041.fmv; RNA cleavage 150_041.xls

2001 conc., µM	TK buffer, pH 7.5 % degradation **153** (150 nM) **Total**	TK buffer, pH 6.0 % degradation **153** (150 nM) **Total**	TK buffer, pH 7.5 % degradation **158** (150 nM) **Total**	TK buffer, pH 6.0 % degradation **158** (150 nM) **Total**
1.25	27,37	25,51	12,89	26,41
0.63	35,14	36,84	11,44	27,47
0.31	contaminated	12,58	17,24	22,07
0.156	contaminated		14,11	27,67
2001 conc., µM	TK buffer, pH 7.5 % degradation **153** (150 nM) **Loop**	TK buffer, pH 6.0 % degradation **153** (150 nM) **Loop**	TK buffer, pH 7.5 % degradation **158** (150 nM) **Loop**	TK buffer, pH 6.0 % degradation **158** (150 nM) **Loop**
1.25	10,97	10,81	5,07	10,19
0.63	15,80	10,24	2,98	9,83
0.31	contaminated	8,03	7,41	7,72
0.156	contaminated	n.d.	6,95	10,02
2001 conc., µM	TK buffer, pH 7.5 % degradation **153** (150 nM) **Stem**	TK buffer, pH 6.0 % degradation **153** (150 nM) **Stem**	TK buffer, pH 7.5 % degradation **158** (150 nM) **Stem**	TK buffer, pH 6.0 % degradation **158** (150 nM) **Stem**
1.25	16,40	14,70	7,82	16,22
0.63	19,34	26,59	8,47	17,64
0.31	contaminated	4,55	9,84	14,34
0.156	contaminated	n.d.	7,16	17,65

After these preliminary studies also the Tat16 conjugate **2003** was tested (Fig. 5.13b). In this second series of experiments the conjugate was incubated with **158**, the proper substrate, but also with **190** and **202** (Fig. 2.32 and Fig. 5.11)**,** non-related RNA substrates, with the aim to characterize the selectivity of these peptides. The

buffer used was 50 mM Tris-HCl, 20 mM KCl, pH 7.5, at 37 °C for 20 h. The concentration of the RNA substrates was kept constant at 150 nM, while the concentration of **2003** was varied from 1000 nM to 63 nM. The influence of $MgCl_2$ was also tested to see if the Mg^{2+} could change the activity or the selectivity. In Fig. 5.14 is shown that a pattern similar to that of **2001** was produced when **2003** was incubated with **158.**

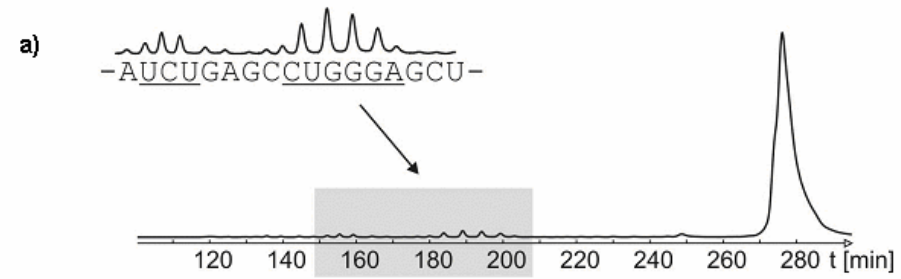

Figure 5.14: a) Cleavage pattern of **2003** (20 nM), with **TAR 158** (150 nM) Conditions: 50 mM Tris-HCl, 20 mM KCl, pH 7.5, at 37 °C, 20 h. b) Tat conjugate **2003**.

The summary of the results of these tests are reported in Tab. 5.3 where it is possible to see that the highest activity of **2003** is with **190** (mRNA of the Bcr-Abl, see 5.4.3), an RNA not related with TAR. Therefore it seems logical to conclude that the peptide used must have affinity for TAR but a low selectivity so that it can bind also non-related RNA. The action of Mg^{2+} seems not to be clear: in some cases it was possible to observe an increase of cleavage, in some other an inhibition.

Table 5.3: Cleavage of **2003** incubated with **158** ± Mg^{2+}, **190** ± Mg^{2+}, **202** ± Mg^{2+}. Conditions: 50 mM Tris-HCl, 20 mM KCl, ± 1 mM $MgCl_2$, pH 7.5, at 37 °C, 20 h. Substrate selectivity Tat conjugate **2003**. ALF-files: **158**: 286_041.alx 286_041.fmv, **190**: 287_041.alx 287_041.fmv, **202**: 285_041.alx 285_041.fmv; RNA cleavage285_041.xls

Tat-BnIm3 conc., µM	% degr. 158 -Mg^{2+}	% degr. 158 +Mg^{2+}	% degr. 190 -Mg^{2+}	% degr. 190 +Mg^{2+}	% degr. 202 -Mg^{2+}	% degr. 202 +Mg^{2+}
0 (Control 0h)	n.d.	n.d.	5,5	5,2	3,3	1,8
0 (Control 20h)	0,6	1,0	2,8	5,3	2,5	2,5
1	1,7	2,5	23,0	12,2	3,1	2,7
0.5	0,9	2,4	6,6	6,5	4,0	2,7
0.25	0,7	2,2	4,4	6,5	3,1	1,4
0.125	0,9	1,8	4,1	6,3	2,2	1,1
0.063	1,1	1,5	4,2	4,4	2,5	0,2

*n.d. = not detectable **n.a. = not analyzed

Within the series of the peptidic conjugates the last two were **2004** and its D enantiomer **2005**, selected to have affinity for the Bcr-Abl RNA substrate **176** and its enantiomeric form **190** (Fig. 5.11). Both conjugates were incubated with the corresponding RNA substrates: **2004** with **176** and **2005** with **190**, but also **2004** with the mirror image substrate **190**, and **2005** with **176**. The incubation was done in a buffer containing 50 mM Tris-HCl, 20 mM KCl, at pH 6, at 37 °C and for 20 h. As comparison the non-conjugate **29** (Fig. 2.22, Tab. 5.4) was also tested with both substrates **176** and **190**. The concentration of RNA substrates was kept constant (150 nM), while the concentration of the conjugates was varied from ~ 50 μM to ~ 2 μM. In Tab. 5.4 are reported the results of cleavage of these experiments. It is evident that no real specificity exists at least under these conditions. Moreover, the cleavage patterns for the conjugates are very similar with the pattern of the free catalyst **29**.

Table 5.4: Results of cleavage of **2004** (42, 10.5, 2.6 mM), **2005** (36, 9, 2.3 mM), and **29** (50, 12.5, 3.1 mM) with **176** (150 nM) and **190** (150 nM). Conditions: 50 mM Tris-HCl, 20 mM KCl, pH 6, 37 °C 20 h. ALF-file: 247_041; 247_041.fmv; RNA cleavage 247_041.xls

		L-bcrAbl **2004**			D-BcrAbl **2005**			BnIm3 **29**		
% degradation	bckg	42	10.5	2.6	36	9	2.3	50	12.5	3.1
BcrAbl **176**	18,20	90,57	95,74	93,15	98,30	94,74	85,56	92,30	22,08	31,49
L-BcrAbl **190**	14,36	92,47	78,07	54,26	60,44	38,43	42,21	68,96	21,85	22,82

2004 **NH_2-KHLHLHKGGGC-Linker-Catalyst (L)**

2005 **NH_2-KHLHLHKGGGC-Linker-Catalyst (D)**

29

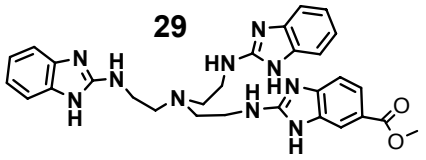

A different type of conjugate, but with relevance to these studies of affinity cleavage is the **29-neamine** conjugate, developed in collaboration with the group of Professor Jean-Luc Décout. This compound at concentrations of 630 nM and 320 nM**,** was incubated with **153** (150 nM) in a buffer containing 50 mM Tris-HCl, 20 mM KCl, at pH 7.4, at 37 °C and for 20 h.

The preliminary results of this compound are illustrated in Fig. 5.15. Two slightly different patterns were generated when the conjugate was at 630 nM (lane **a**) or 320 nM (lane **b**). The cleavage occurred in both cases mostly in the bulge of TAR where neamine presumably should bind. In this case a certain affinity cleavage was demonstrated.

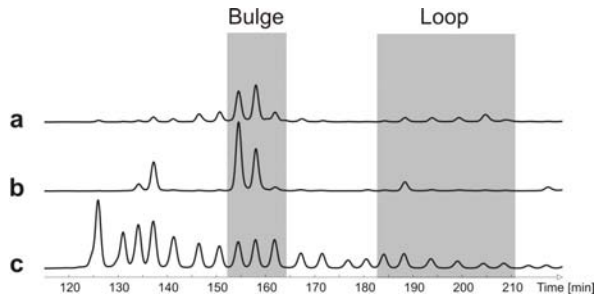

Figure 5.15: Cleavage pattern for the neamine conjugate. Lane a: **29-neamine** conjugate 630 nM. Lane b: **29-neamine** conjugate 320 nM. Lane c: base ladder of substrate **158** (Na_2CO_3). Conditions: 50 mM Tris-HCl, 20 mM KCl, pH 7.4, 37 °C, 20 h.

5.9 Conclusions

To conclude, tris(2-aminobenzimidazole) was converted in molecules that can be easily conjugated to ligands with primary mercaptans by maleinimide chemistry or to ligands with amino groups by peptidic linkage. In these preliminary studies of affinity cleavage, the RNase activity was always conserved, but due to low specificity of the ligands used, a consequent lack of specificity of the conjugates was evidenced. Therefore, applications in affinity cleavage for this catalyst should possible, but further validations with better ligands are still required.

6 Gold Nanoparticles Functionalised with 2-Aminobenzimidazoles

The development of the tris(2-aminobenzimidazole) as a catalyst started with the observation that monomeric 2-aminobenzimidazole could better catalyse RNA cleavage compared to simple guanidinium groups. When several of these groups were combined in the bis(2-aminobenzimidazole) and then in the tris(2-aminobenzimidazole), the activity increased progressively.[16] The reason of this increase of activity is still not clear, but 2-aminobenzimidazole was identified as a building block for construction of artificial RNases. From such observations the idea was developed to make gold nanoparticles functionalized with 2-aminobenzimidazoles that could act in cooperativity on the surface (Fig. 6.1). Using then the property of these materials,[18][19] by place-exchange it should be possible to achieve a further fuctionalisation with RNA ligands and to get substrate specificity.

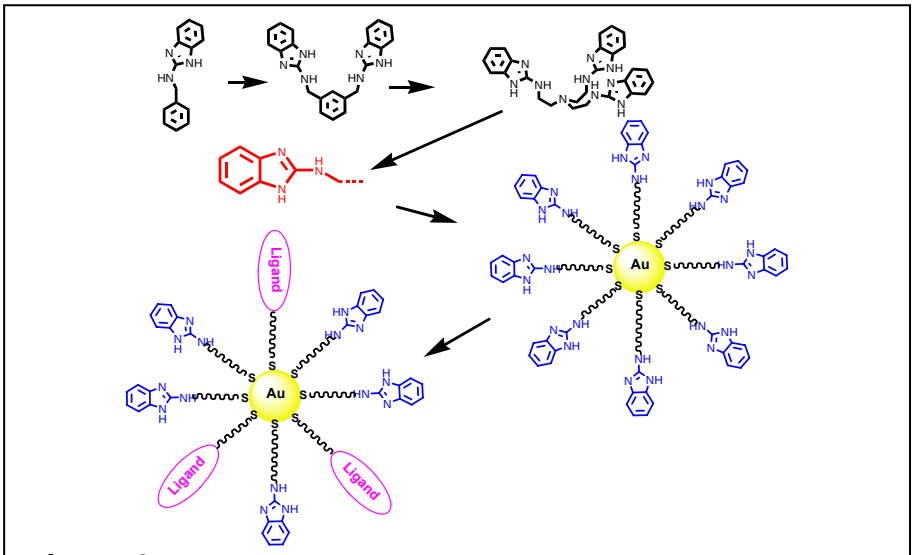

Figure 6.1: Conceptual development of gold nanoparticles functionalised with 2-aminobenzimidazoles.

6.1 Gold Nanoparticles in General

Aggregates of gold atoms with a size of several nm can be formed in solution under particular conditions.[115] These aggregates can be covered by a monolayer of thiols. The synthesis and characterization of these materials have reached good levels. They

have also found technological applications.[116] A summary of the reactivity and the possibility to modify these nanoparticles are reported in Fig. 6.2.

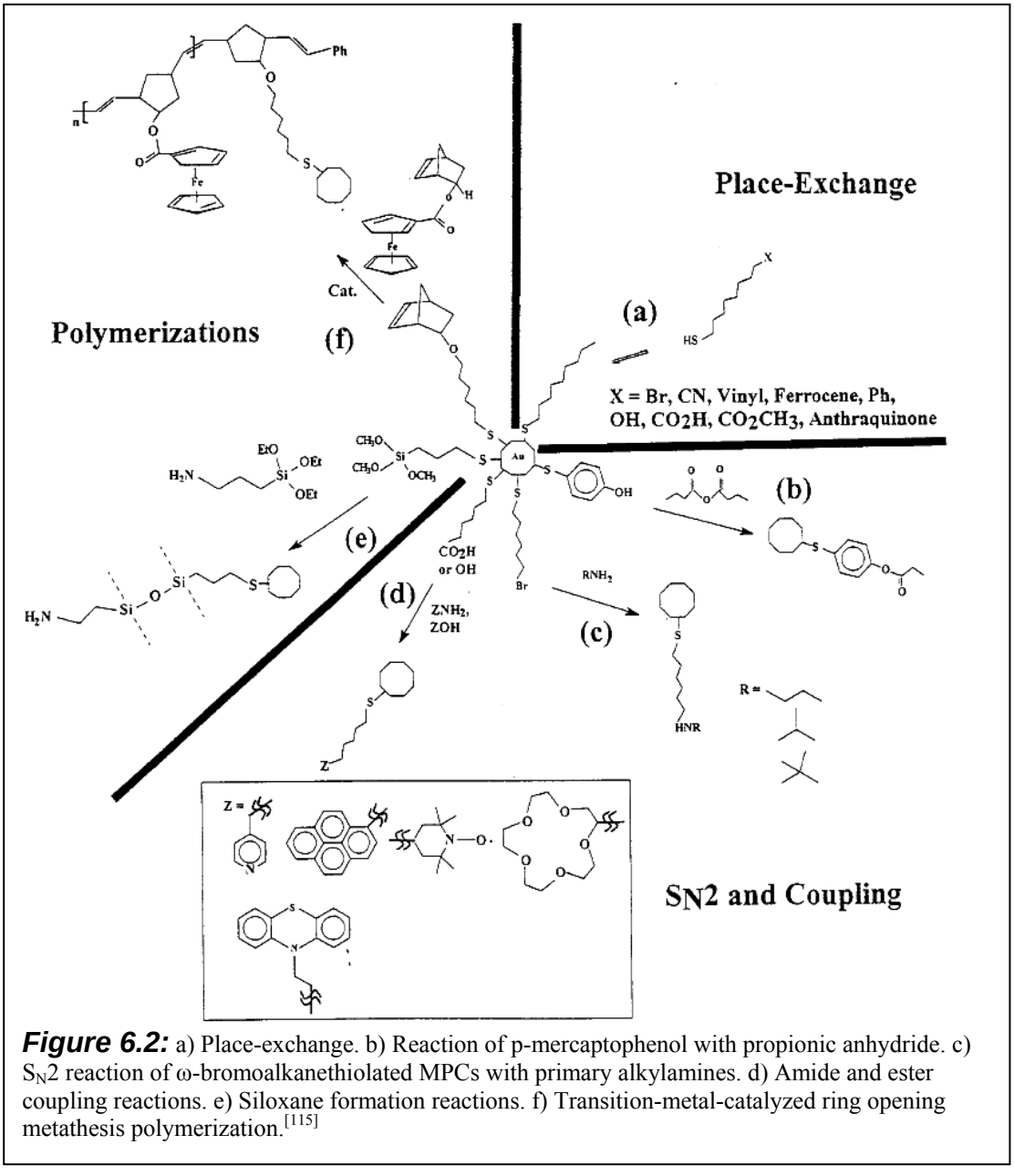

Figure 6.2: a) Place-exchange. b) Reaction of p-mercaptophenol with propionic anhydride. c) S_N2 reaction of ω-bromoalkanethiolated MPCs with primary alkylamines. d) Amide and ester coupling reactions. e) Siloxane formation reactions. f) Transition-metal-catalyzed ring opening metathesis polymerization.[115]

The organic layer that covers the surface of the gold aggregates, protects the surface of the metal, avoiding the association into bigger insoluble particles. The MPCs (monolayer protected clusters) are therefore stable and depending on the nature of the organic ligands that cover the metallic surface they are soluble in different solvents.

6.1.1 Synthesis of MPCs

The synthesis of MPCs became more easy and reproducible after the work of Brust and Schiffrin,[117] who demonstrated that in presence of an aliphatic thiol the reduction of $HAuCl_4$ to Au (0) by $NaBH_4$ led to the formation of gold aggregates protected with a monolayer of thiolates with a diameter of 1-3 nm (Sch. 6.1). The salts of Au^{3+} are not soluble in organic solvents. Therefore, they must be transferred in organic phase by a phase transfer reagent such as Oct_4NBr.

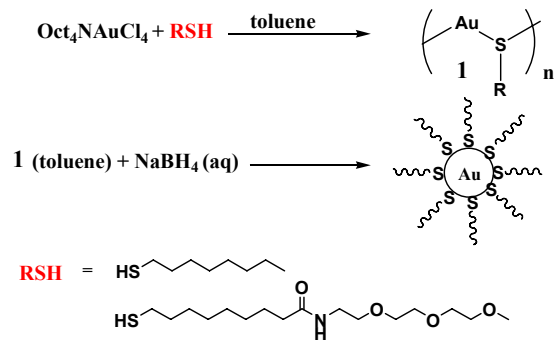

Scheme 6.1: Procedure of Schiffrin for the synthesis of gold MPC. $HAuCl_4$ is transferred in toluene by Oct_4NBr and then reduced in presence of thiols with $NaBH_4$.

The MPC obtained with this procedure are stable and soluble in common organic solvents, and they can be handled like normal organic compounds.

This procedure can be also started from thiols carrying some functional group. The result will be then gold nanoparticles with a functionalized surface.

When the thiolic ligand is soluble in water or in alcoholic solvents the synthesis can be done directly in this solvents without the use of the phase transfer catalyst.[118]

Another important point in this synthesis is that the size of the MPCs can be controlled in different ways. For example the ratio Au/RSH is proportional to the size, so with a ratio of 6/1 the inorganic core has a size of 6 nm, while using a large excess of mercaptan the core has a diameter of 1.5 nm.[119] Other parameters to control the diameter of the core are: the type of reductant, the time of reduction and the temperature.

6.1.2 Functionalization of MPCs

For rendering the gold nanoparticles able of some particular activity, the presence of functional groups on their surface are often required. This can be achieved with two methods:

a) Starting the synthesis from the beginning with a mercaptan carrying the required functional group (Fig. 6.3a).

b) By exchange. In fact a property of the thiols on the MPC surface is that they can exchange with other thiols in solution.[18][19] As consequence an unspecific MPC can be functionalized by a partial exchange with ligands carrying a functional group (Fig. 6.3b).

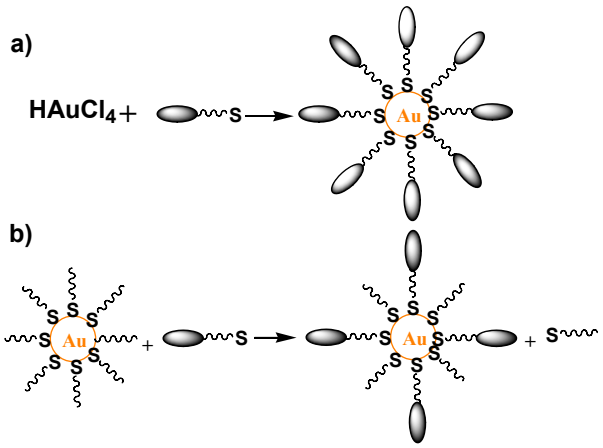

Figure 6.3: Functionalization of gold nanoparticles.

6.2 Gold Nanoparticles as Catalysts

By cooperativity of functional groups, nature is often able to increase the activity of single building blocks with poor catalytic activity.[120] This is well shown in RNase A, where two histidines work cooperatively. The viruses take also advantage of that. For example, the attachment of the influenza virus to a cell occurs through several interactions between hemagglutinin and sialic acid.[121] The gold nanoparticles are ideal to enhance the reactivity of weakly active functional groups because, by the self-assembly around the gold core, many identical groups are ordered and come into close contact. Pasquato and Scrimin have given two examples of this concept. In the first example a gold nanoparticle functionalised with N-

methylimidazole was able to catalyse in a methanol/water solution the cleavage of 2,4-dinitrophenyl acetate more than one order of magnitude faster compared to the momomeric acetyl-N-methylhistamine, and better then the comicellar analogue (Fig. 6.4).[122]

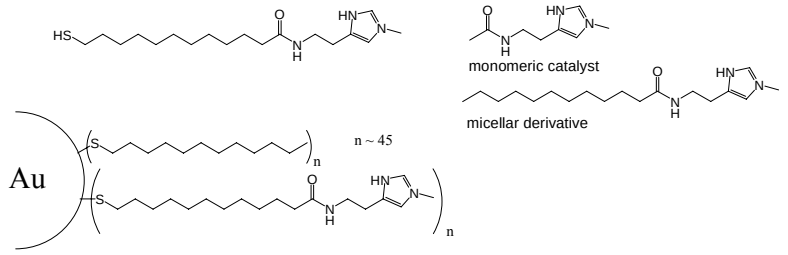

Figure 6.4: MPCs functionalized with N-methylimidazole.[122]

In a second example a gold nanoparticle protected by a monolayer of sulfanyloctane was prepared and subsequently subjected to place-exchange with an azacrown-functionalized thiol (Fig. 6.5).

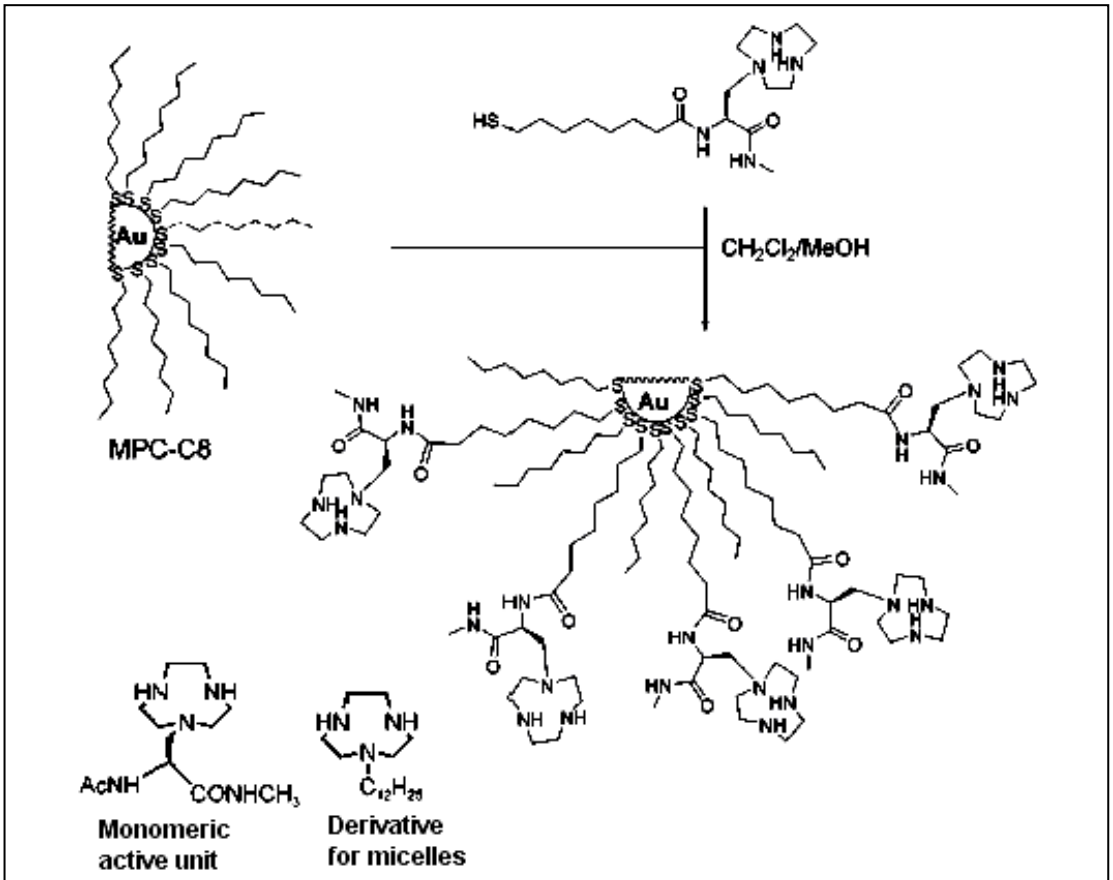

Figure 6.5: Gold MPCs functionalized with triazacyclononane.[123]

The triazacyclononane units are able to bind transition-metal ions such as Cu^{II} and Zn^{II}. This system was therefore supposed to operate as a metal enzyme mimic. In fact, the most active system was the one fully loaded with Zn^{II} ions. A kinetic analysis was done monitoring the cleavage of 2-hydroxypropyl *p*-nitrophenyl phosphate (HPNP). This study showed that the formal second-order rate constant for HPNP cleavage is of 4.4 $s^{-1}M^{-1}$, which is more than 600-times faster than the k_2 of a monomeric Zn^{II} "active unit" under the same conditions. Once again the micellar analogue showed a lower activity compared to the MPC.[123]

6.3 Synthesis of 45 as Ligand for Gold Nanoparticles

As already illustrated in Fig. 6.1, one aim of this work was to synthesize a MPC functionalised with 2-aminobenzimidazole units. To this purpose **45** was synthesized as a ligand suitable for the assembling and the functionalising of MPC. This molecule was then sent to the group of Professor Scrimin in Padova, for the assembling of the gold nanoparticles.

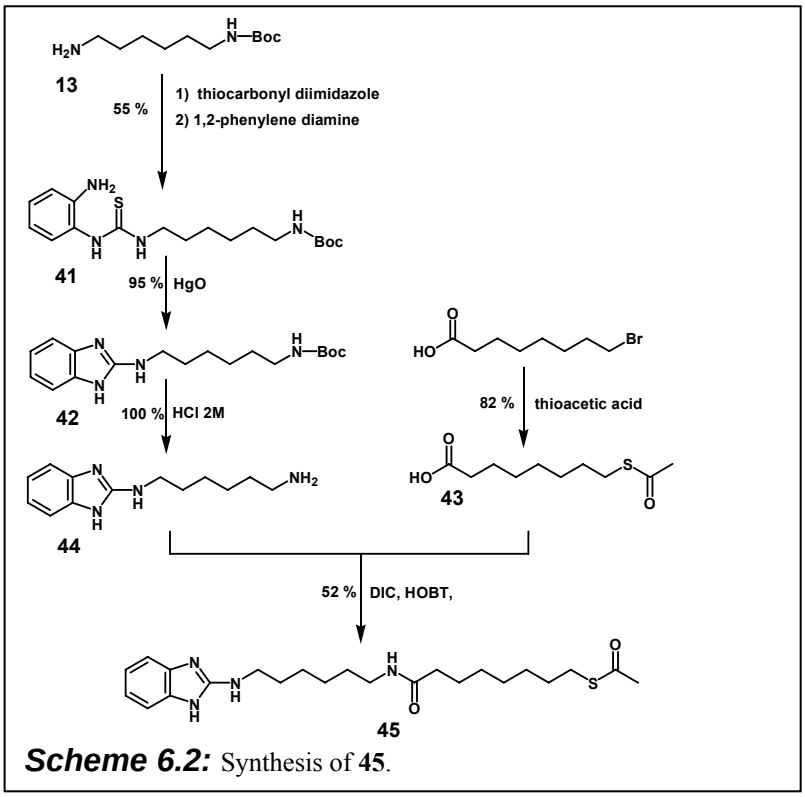

Scheme 6.2: Synthesis of **45**.

As it is illustrated in Sch. 6.2, the thiourea **41** was prepared with a yield of 55 %, by reaction of **13** with thiocarbonyl diimidazole, followed by a second substitution with 1,2-phenylene diamine. The 2-aminobenzimidazole derivative **42** was obtained with quantitative yield by closure of **41** in a solution of ethanol in presence of HgO, while the free primary amine **44** was got by hydrolysis of the Boc protecting group. In parallel the substitution of bromide with thioacetic acid in the 8-bromo-octanoic acid gave 8-acetylsulfanyl-octanoic acid **43**. Therefore, the hydrochloride amine **44** and the carboxylic acid **43** were coupled using DIC and HOBT as condensing agent, giving the final compound **45**.

6.4 Assembly of the Gold Nanoparticles

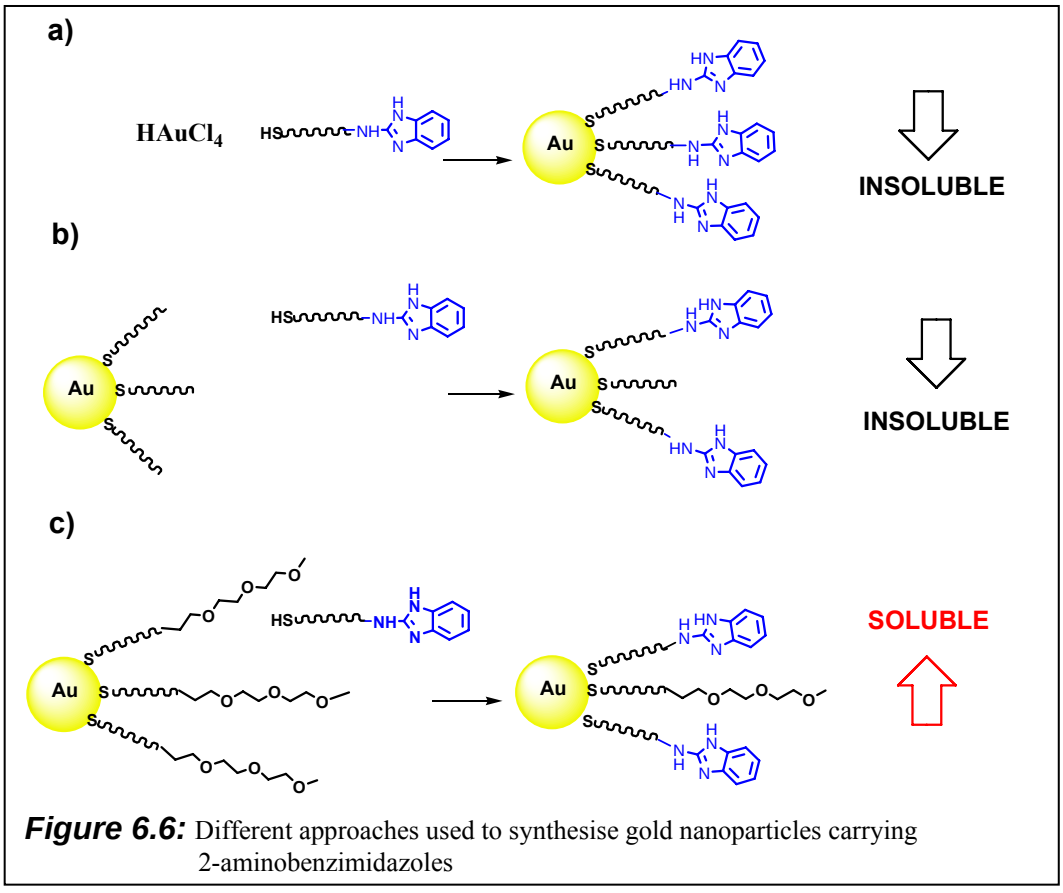

Figure 6.6: Different approaches used to synthesise gold nanoparticles carrying 2-aminobenzimidazoles

The ligand **45** was sent to Padova to the group of professor Scrimin, where Flavio Manea assembled the gold nanoparticles. Three different approaches were attempted to synthesize these gold nanoparticles. In the first attempt (Fig. 6.6a) the direct synthesis of the MPC from the 2-aminobenzimidazole ligand produced aggregates

that precipitated and resulted insoluble in most of the common solvents. The second attempt (Fig. 6.6b) was a functionalization by place exchange of hydrocarbon-protected MPCs, but also in this case an insoluble precipitated was formed. In the last approach water soluble MPCs were used for a place exchange with the 2-aminobenzimidazole ligand. The solubility of these MPCs in water is guaranteed by a monolayer of ligands with a hydrocarbon chain part anchored to the metal core and a water-soluble part of triethylene glycol on the external surface (Fig. 6.6c). This last place exchange produced gold nanoparticles soluble in DMF and in water with a percentage of the ligand **45** on the protecting ligand of 30 %. These last MPCs were finally tested by Kathrin Beier in our laboratory.

6.5 Assay for RNA Cleavage

Table 6.1: Results of cleavage test of the MPCs. Conditions: 50 mM Tris-HCl, 37 °C for 20 h.

pH	Conc. Catalyst	Conc. Substrate	% DMF	%Cleavage
6	35 µM	150 nM	20	12
6	17.5 µM	150 nM	10	1.7
6	8.7 µM	150 nM	5	15
6	4.4 µM	150 nM	2.5	9
7	35 µM	150 nM	20	2.4
7	17.5 µM	150 nM	10	12
7	8.7 µM	150 nM	5	13
7	4.4 µM	150 nM	2.5	1.5
8	35 µM	150 nM	20	25
8	17.5 µM	150 nM	10	5
8	8.7 µM	150 nM	5	3
8	4.4 µM	150 nM	2.5	1.7

The results of this test are reported in Tab. 6.1, where it is possible to see that under more basic conditions there was an increase of cleavage. A more careful analysis revealed that the cleavage occurred mostly between pyrimidine pyrimidine linkage. This kind of selectivity is typical for RNases contaminations. Therefore, these results

are not reliable and should be considered preliminary. Other tests could be done with enantiomeric RNA. However, the ratios of cleavage were not impressive. A reason could be that 30 % of the 2-aminobenzimidazole versus 70 % of triethylene glycol ligands, is insufficient to generate significant catalytic activity and to allow the 2-aminobenzimidazole to work cooperatively.

6.6 Conclusions

Future synthetic efforts to improve the system, should try to increase the percentage of catalytic units on the surface of MPC. This could be done for instance by reducing the size of the metal core to improve the solubility.

7 Non-Enzymatic Oligomerization of Ribonucleotides

7.1 Origin of Bioorganic Compounds

How life could have developed on our planet is still an open question that science has not been able to solve. Some points seem to be clear. For instance, that life started 3.8 billion years ago. It is obvious that life depends on the ability to self-replicate, to evolve and to self-adapt to different challenging situations. Mechanisms must exist to conserve the information acquired in the evolution and to transmit them to successive generations. In our days it is known that nature has chosen DNA for information storage. A widely accepted hypothesis assumes however, that in the early phases of life, RNA has adopted this role and also acted as catalyst.

From a chemical point of view the question is how these molecules could self-assemble within the prebiotic soup.

To explain the origin of life currently three hypotheses are taken in consideration:[124]

1. Synthesis in an reducing atmosphere
2. Input by meteorites
3. Synthesis on metal sulfides in deep-sea vents.

Some indications how organic compounds may be generated from inorganic material under conditions similar to those of the primitive atmosphere came from the classical experiment by Urey and Miller.[125] In their experiment they demonstrated how a mixture of CH_4, NH_3, H_2O and H_2 when subjected to electrical discharges can form amino acids. Much earlier it was demostrated that simple sugars can be formed readily from formaldehyde in the formose reaction.[126] However, this reaction is not selective, and biologically important sugars like ribose are formed only in trace amounts. In contrast, Eschenmoser has recently shown that glycoaldehyde phosphate aldomerizes in aqueous NaOH solution. In presence of 0.5 mol-equiv. of formaldehyde, sugar phosphates are produced with a yield of 45 %, with pentose

2,4-diphosphates predominating over hexose 2,4,6-triphosphates and with *rac*-ribose 2,4-diphosphates as major component (Fig. 7.1).[127]

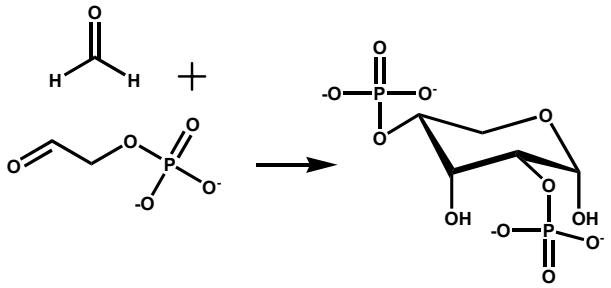

Figure 7.1: Aldomerization of glycoaldehyde phosphate.

Other key elements of life are the purines and pyrimidines. Evidence for a possible synthesis of adenine from aqueous solutions of ammonium cyanide at temperatures below 100 °C were given by Oro,[128] while Ferris, Sanchez and Orgel demonstrated the formation of pyrimidines from cyanoacetylene and cyanate.[129] Further cyanoacetylene in aqueous or anhydrous ammonia gives β-aminoacrylnitrile that leads to formation of imidazole by photolysis.[129]

In Fig. 7.2 are summarized some important reactions that could have contributed to the origin of life.

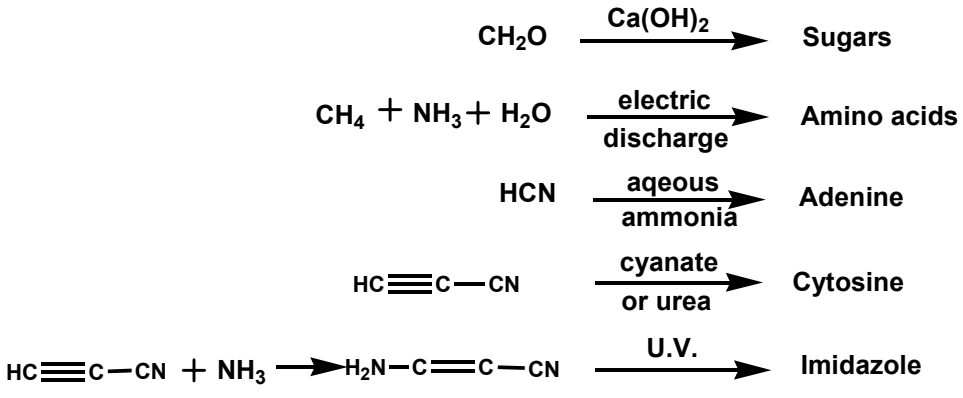

Figure 7.2: Reactions producing bioorganic compounds.[124][129]

7.2 The RNA World

In the past the biochemical dogma has been that chemical reactions are catalysed by proteins, while nucleic acids merely carry the genetic information. The recent discovery that also RNA itself possesses catalytic activity[20][21][22] has changed this

view, leading to the hypothesis that life may have been originated from an ‘‘*RNA world*’’, where RNA enzymes were able to catalyse all the necessary biochemical reactions. Some examples of living fossils of that world could be the ribosomes, nucleotidic cofactors and ribozymes as catalytic active RNA.

A recent review on the origin of RNA catalysis in ribozymes is given by Lilley.[130] RNA can generate catalysis by general acid-base catalysis, electrostatic effects, substrate orientation and proximity. The main players are the RNA nucleobases and bound metal ions. Experiments of *in vitro* selection have then shown that new ribozymes with unique abilities can be generated. One example, given by Unrau and Bartel[131] shows that isolated RNA molecules are able to catalyse the synthesis of pyrimidine nucleotides (Fig. 7.3).

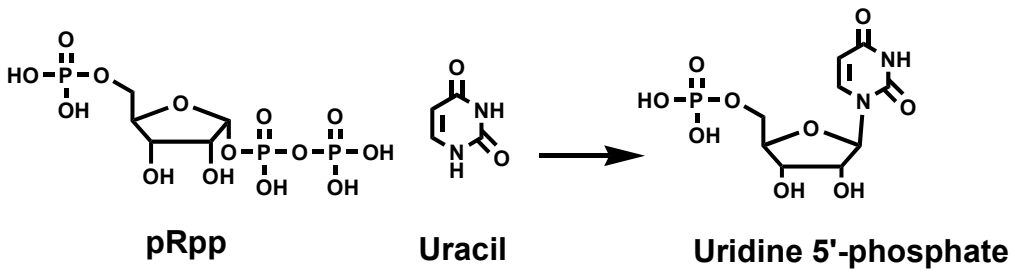

Figure 7.3: Ribozyme catalysed formation of uridine.

The ability to form amide-bonds should be necessary to pass from a RNA world to the contemporary protein dominated biology. Concerning this step Lohse and Szostak isolated ribozymes catalysing amino acid transfer reactions.[132]

7.2.1 Energetic Source of the RNA world

We know that most of the biological processes and syntheses need ATP or occasionally GTP as energetic source, but it seems unlikely that such sources of energy played a role in the evolution of biological compounds. Lohrmann and Orgel proposed that the primary chemical energy reserve was rather a mixture of inorganic and organic polyphosphates. In fact they demonstrated that by heating mixtures containing urea, ammonium phosphate, metal ions and nucleosides in various proportions at moderate temperature, phosphorylated nucleotide derivatives were formed. It was found that ATP or AppA react with imidazole to form ImpA (Fig.

7.4). Further studies of template-directed oligomerization showed that these phosphoroimidazolide nucleotides can condense on a poly U as template to form di- and short poly A oligonucleotides.[23][133] In this way it was demonstrated a possible spontaneous formation of short oligonucleotides.

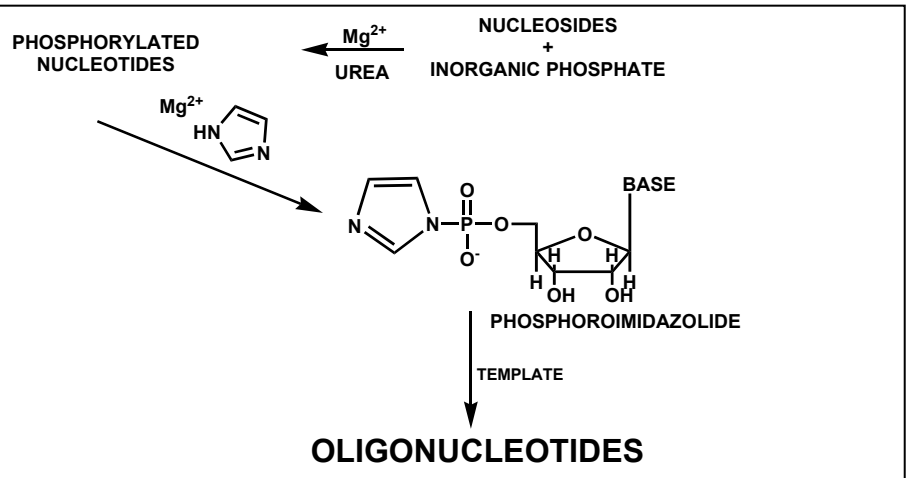

Figure 7.4: A scheme for the prebiotic activation of nucleotides.[23]

These first studies started to give some information of how biopolymers could have been formed. However, if there was an RNA world that evolved into the current biology, it needed as every evolving system to self replicate and to undergo selection, by which can originate new proprieties or more complex systems. Of course all this must have happened at least in the beginning, without the help of any enzyme or ribozyme. Assuming that the monomeric building blocks were available in sufficient amounts, the objective of this research became to find how polymers, possibly RNA, can self-replicate to undergo selection that led to the RNA world first, and then to the modern cellular biology.[134]

7.3 Non-Enzymatic Oligomerization

We have seen that to clarify the origin of life it is necessary to find a self replicating system. In this context we speak about *non-enzymatic oligomerization*, meaning a system where starting from activated building blocks a sequence-template drives the replication of new sequences without any enzyme. To evaluate how a template sequence is duplicated, we have to take into consideration[134]:

The efficiency, the amount of complementary copies of the template produced.

The fidelity, the percentage of wrong bases incorporated during the elongation.

The regiospecificity, the ratio of natural 3'-5' linkages to unnatural 2'-5'.

The non-enzymatic template-directed studies started using as activated building blocks phosphoroimidazolide nucleotides (Fig. 7.4). Later it was observed that phosphoroimidazolides with a methyl group in position 2 of imidazole gave a more efficient oligomerization.[135] As a consequence this compound became a model for non-enzymatic oligomerization (Fig. 7.5).[24]

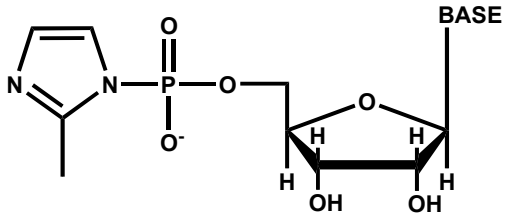

Figure 7.5: 5'-phosphoroimidazolide nucleotide.

After the first experiments of RNA oligomerization directed by a template, new problems and questions started to arise. The obstacles for an efficient RNA primer extension are:

1. Tendency of G-rich templates to form quadruplexes in presence of high concentration of Na^+. To bypass this problem a solution may be to work at low concentration of Na^+.[136]
2. Weakness of the A-U base pair is the cause for inefficient incorporation of U monomers on a polyA template. The oligomerization directed by random copolymer of A and C is also less efficient then that by a poly C or a copolymers of C and G. A solution of this problem can be the use of diaminopurine instead of A (Fig. 7.6).[137]

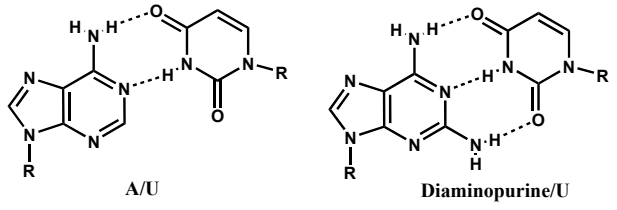

Figure 7.6: Alternative base pairing diaminopurine/U.

3. Inhibition by enantiomeric monomers.

4. Inhibition by purine-pyrimidine alternation.[137]

A solution at the latter problem would perhaps be to avoid the irregularities and the pyrimidines. An alternative could be therefore, the use of analogous Watson-Crick base pairing, but involving only purines. An example is given by the base pair G/isoG (Fig. 7.7).

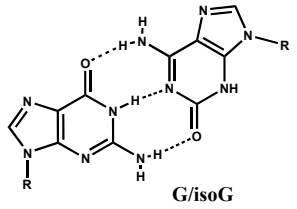

Figure 7.7: Base pairing G/isoG

5. Inhibition by single 2',5' connections.[138]
6. By-products due to hydrolysis or incorrect chain extension cause irreversible "poisoning".

In contrast to the natural RNA, where the connection is of 3',5'-bond type, studies of non-enzymatic oligomerization using the activated phosphoroimidazolides evidenced that the regioselectivity is much more in the direction of the 2',5'-bond, with a ratio of 6:1 and if the oligomerization is template directed the ratio became even 18:1.[138] Studies of the polymerisation of adenosine 2',3'-cyclic phosphate on a poly U template catalysed by aqueous ethylenediamine showed the formation of 97 % of 2',5'-linkage.[25]

Given this evidence, among the researchers of this field rose a new hypothesis, according to that before the RNA world could have existed another world. A new term was coined: "unnatural selection".[134] The idea is that a self-replicating system can evolve under selection also without being alive. Hence, not necessarily the natural RNA should be at the origin of life, but also something else that then evolved into the "RNA world" to arrive finally in the current biology. Consequently, the new aim was to find a more general self-replicating system, possibly related to RNA, but not necessarily.

7.4 Motivation to Synthesize an Oligonucleotide G/isoG

We have already seen that during a non-enzymatic polymerisation of RNA the most favoured connection results to be 2',5'. This could turn out to be advantageous. Actually during the enzymatic polymerisation there are mechanisms of correction to undo the mistakes of incorporation. These mechanisms are obviously not present in a non-enzymatic system. Nevertheless, knowing that the formation of 2',5' linkages are reversible while that of 3',5' bonds are not,[26] a sort of mechanism of correction can be introduced by the reversibility of the 2',5' linkage formation (Fig. 7.8).

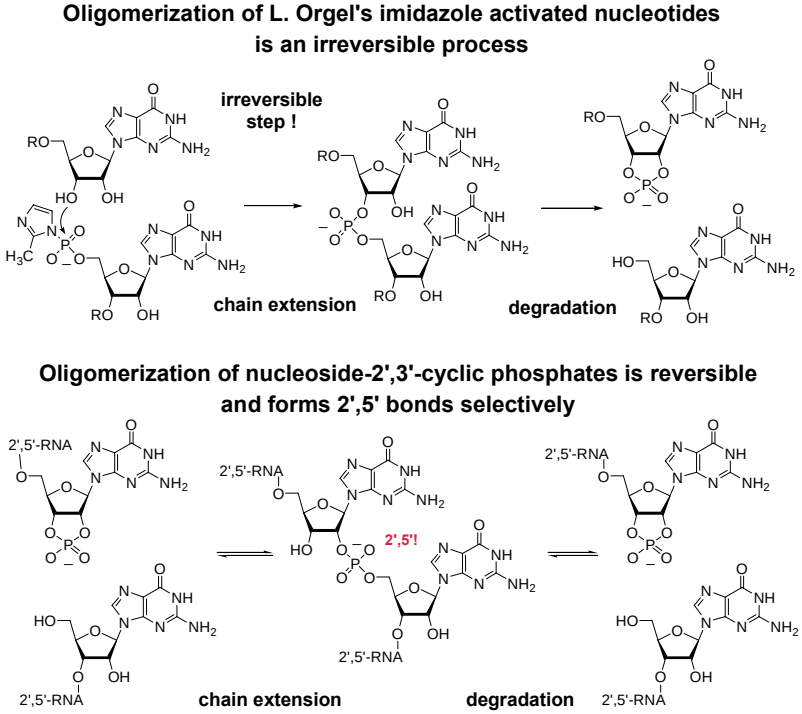

Figure 7.8: Advantages of a 2', 5' connection.

The reason of reversibility of the 2',5' linkages is illustrated in Fig. 7.9. The cleavage occurs by an in-line mechanism, for instance when the 3' OH and O in 5' are both in apical positions. In the linkage 3',5' the 2' OH does not adopt the proper position for an in-line cleavage (Fig. 7.9a). Therefore, this linkage results to be more resistant. On the contrary, in the 2',5' linkage (Fig. 7.9b), the 3' OH has the proper position for an in-line cleavage.[26]

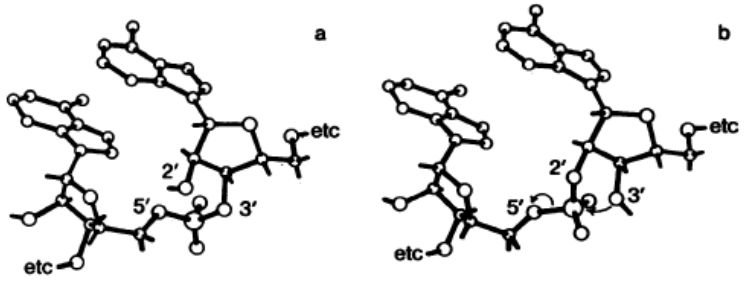

Figure 7.9: Structural basis of the reversibility of the 2'-5' connection.

We have seen that the 2'-5' connection should allow the correction of possible mistakes of incorporation. However, the formation of double stranded helixes is not favoured in nucleic acids connected by 2',5' linkages.[27][139] The reason lies in the electrostatic repulsion of the negative charges of the phosphates that get close in this kind of linkage. This poses a new problem for a self-replicating nucleic acid. To solve this problem, once again the solution could be to use an alternative base pairing involving only purines such as the base pair G/isoG. This should space out the negative charges of the phosphates (Fig. 7.10), allowing a formation of stable double stranded helixes.

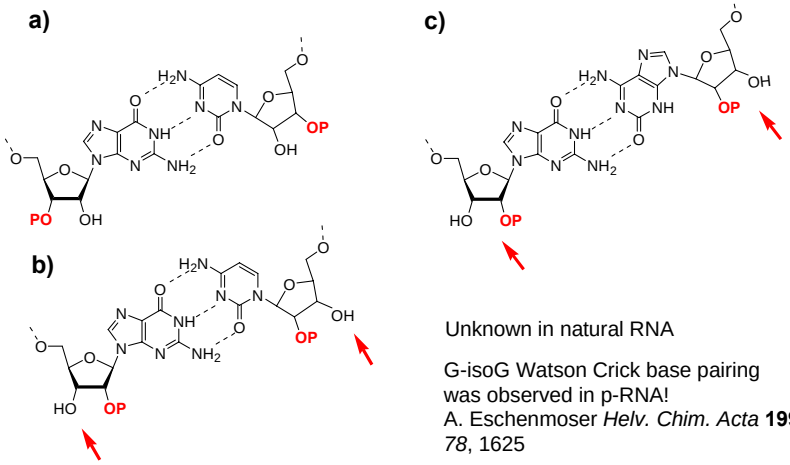

Figure 7.10: With G and IsoG the negative charge of the phosphate anions are spaced out

The stability of G/isoG pairing in a duplex was already observed in pyranosyl-RNA,[140] but not in RNA itself. Considering all these problems of oligomerization

with the natural bases, a solution may be to use a system consisting only of purines. A summary of the problems that could be solved using only purines for base pairing is reported in Fig. 7.11.

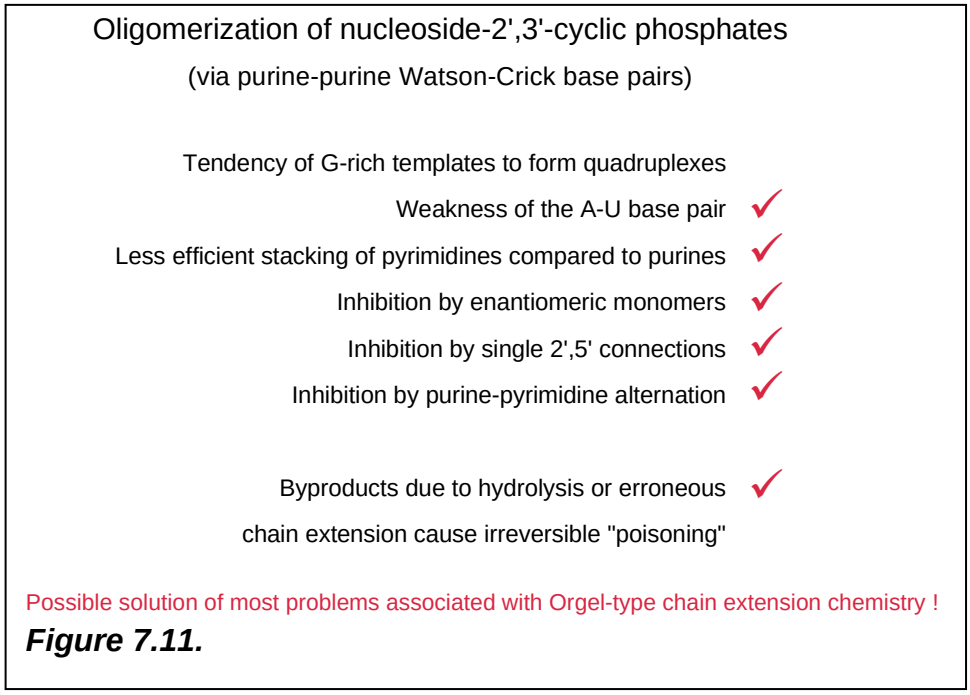

Figure 7.11.

A system capable to self-replicate should therefore fulfil the following requirement: 1) A reversible 2', 5' connection for having the possibility to correct the mistakes. 2) An efficient recognition of the template. For this reason three hydrogen bonds are better than two. 3) Formation of stable duplexes, this could be improved by stacking and spacing out the negative phosphate charges. All these motivations give the arguments to investigate the stability of an RNA duplex with purine/purine base pairing and with a 2', 5' connection.

Therefore, the synthesis of isoguanosine was started with the aim to investigate the palindromic sequences shown in Fig. 7.12c and Fig. 7.12d and to compare their duplex stability with the sequences in Fig. 7.12a and 7.12b. This would disclose important information about the stability of all-purine RNA duplexes connected by 2', 5' bonds. This could then form the basis for a new set of non-enzymatic oligomerization tests.

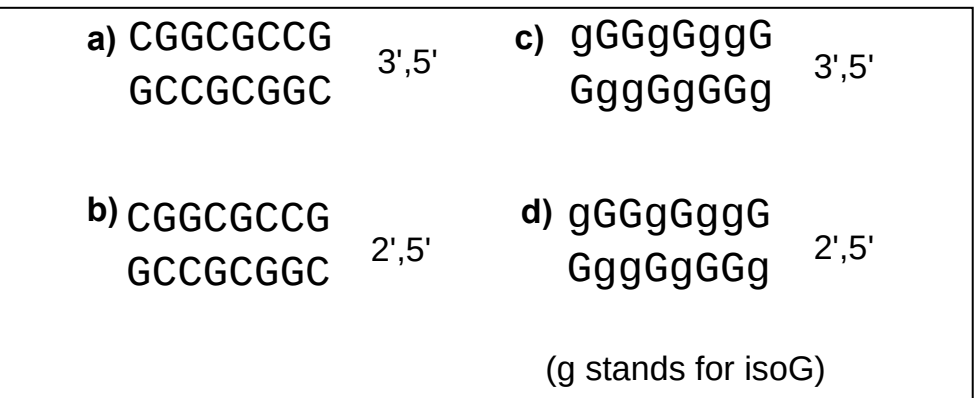

Figure 7.12: Objectives of this project.

7.4.1 Stability of Nucleic Acid Duplexes

The stability of a nucleic acid duplex is given by the so called melting point $\mathbf{T_m}$. Base stacking is accompanied by a reduction of UV absorption (hypochromicity). Therefore, a solution of polynucleotides has a lower extinction coefficient compared to a solution containing the same amount of mononucleotides. This phenomenon can be used as indicator of formation and breakdown of double helices. If the temperature of a solution containing a nucleic acid in duplex form is increased, at a certain temperature the absorption will increase suddenly. The midpoint of this transition is called the "melting temperature" or T_m. This parameter is characteristic of a certain nucleic acid sequence, and it shifts to higher temperature with an increase of the duplex stability. The factors that can increase the stability of the duplex are: stacking, length of the sequence, the ionic strength, the number of hydrogen bonds for base pairing, and the proximity of the phosphate anions. The increase of the extinction coefficient passing from ordered to disordered form is called hyperchromicity h_r and is defined in terms of absorbance:

$$\% \, h_r = \frac{\text{A(melted species) - A(double strand)}}{\text{A(double strand)}}$$

7.5 Synthesis of Isoguanosine

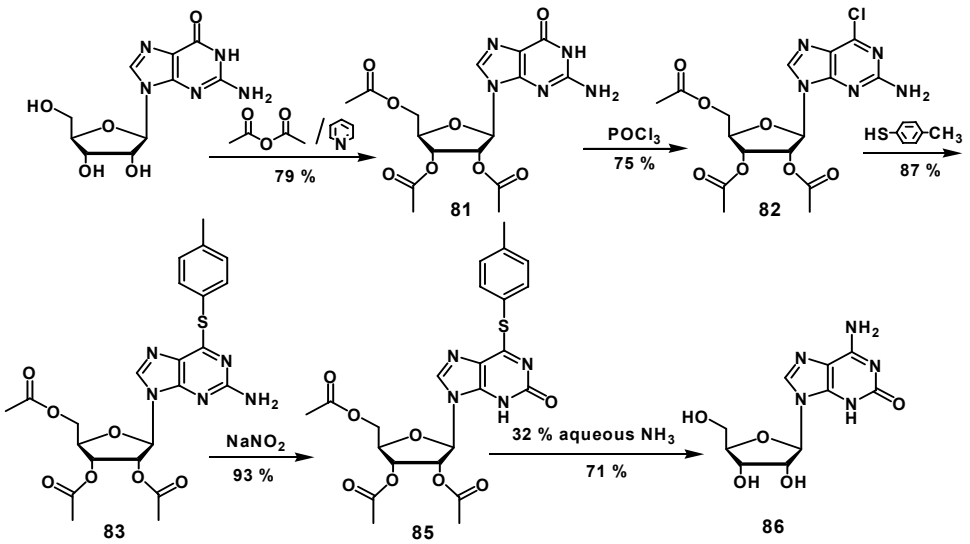

Scheme 7.1: Synthesis of isoguanosine.

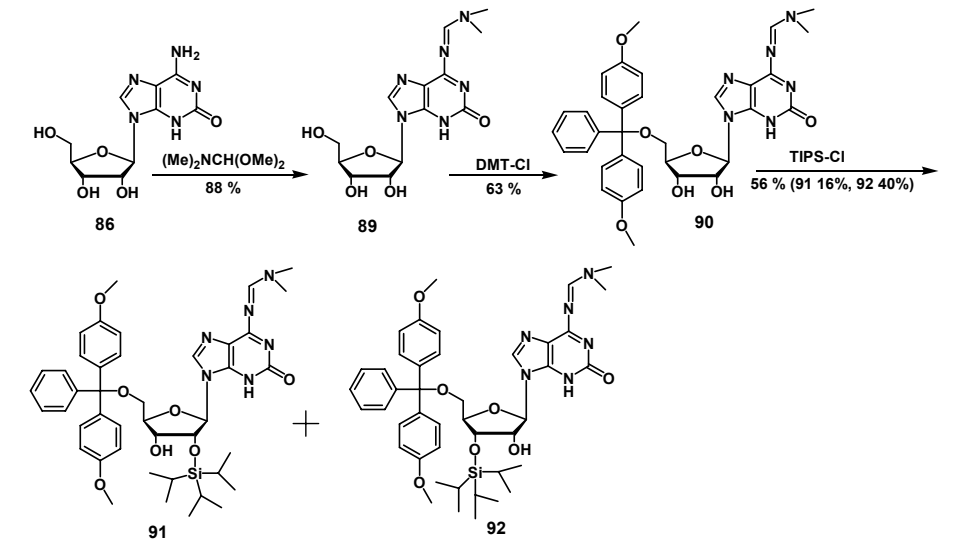

Scheme 7.2: Protection of isoguanosine.

Guanosine was converted into isoguanosine **86** following the procedure reported in literature (Sch. 7.1).[141] The first step was an esterification of the OH groups of the ribose using acetic anhydride in presence of pyridine. After a crystallization in propanol **81** was obtained in pure form. The base's carbonyl C-6 was chlorinated by $POCl_3$ giving **82**. Subsequently, compound **83** was synthesised heating a solution of **82** in DMF at 100 °C with toluene-4-thiol and triethylamine. Then, the treatment of **83** with $NaNO_2$ led to the compound **85**. The final isoguanosine **86** was achieved by

stirring a solution of **85** in concentrated aqueous NH_3 over night in an autoclave at **80** °C. The isoguanosine **86** was afterwards selectively protected following the scheme 7.2.[142] The amino group in position 6 was protected with N,N-dimethylformamide dimethyl acetal in DMF producing **89**. The primary 5' OH was protected with DMT-Cl in pyridine. The remaining OH groups in 2' and 3' of **90** were protected using $(i\text{-}Pr)_3Si\text{-}Cl$, furnishing a mixture of the two constitutional isomers that were separated by RP HPLC, with a yield of 16 % for **91** and of 40 % for **92**.

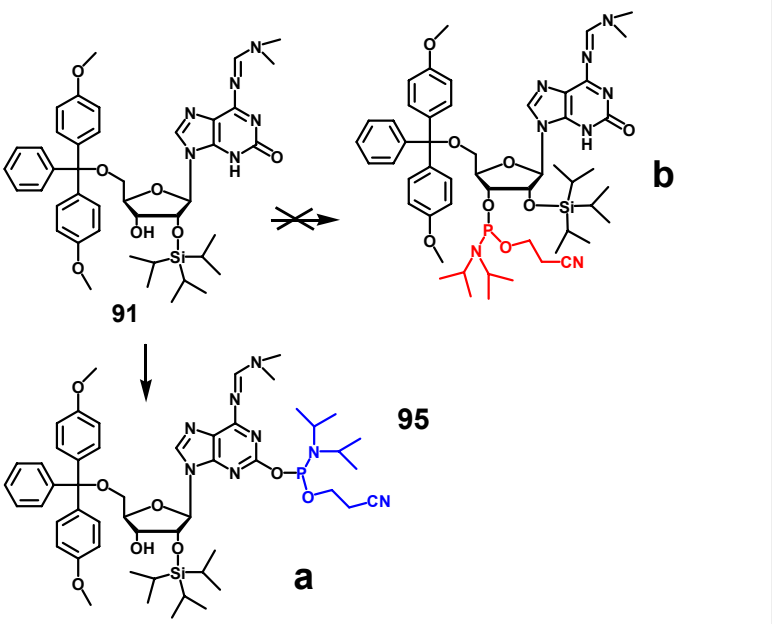

Figure 7.13: Phosphitylation of **91**.

The next step had to be the phosphitylation of the OH groups at 2' or 3' using the commercial 2-cyanoethoxy-*N*,*N*-diisopropylphosphoramidochloride. Surprisingly the phosphitylation did not occur at the expected position (Fig. 7.13b). Nevertheless, the isolated compound **95** had a proper ^{31}P NMR spectrum (Fig. 7.14). In a first comparison of the ^{1}H-NMR spectra of **91** and **95** (Fig. 7.15), it was clear that the signal of the N-H 3 of guanine had disappeared (arrow **a**). On the other side a shift of the H 8 signal occurred (arrow **b**) and the signal of the OH at 3' seemed to be still present (arrow **c**). A further COSY spectrum (see appendix), confirmed the presence of 3' OH and the formation of compound **95** as shown in Fig. 7.13a

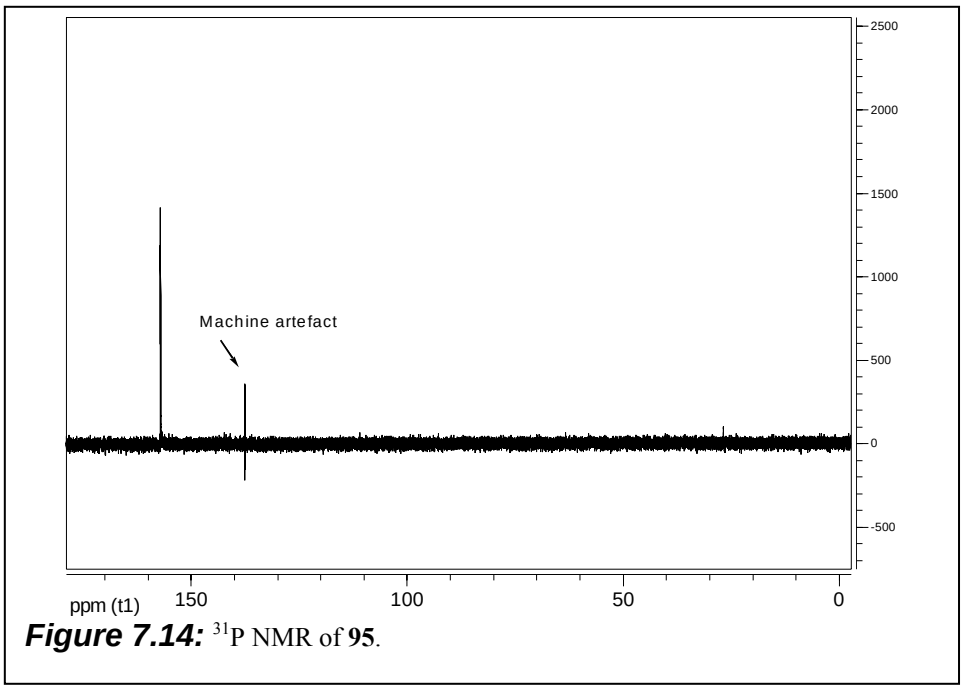

Figure 7.14: ^{31}P NMR of **95**.

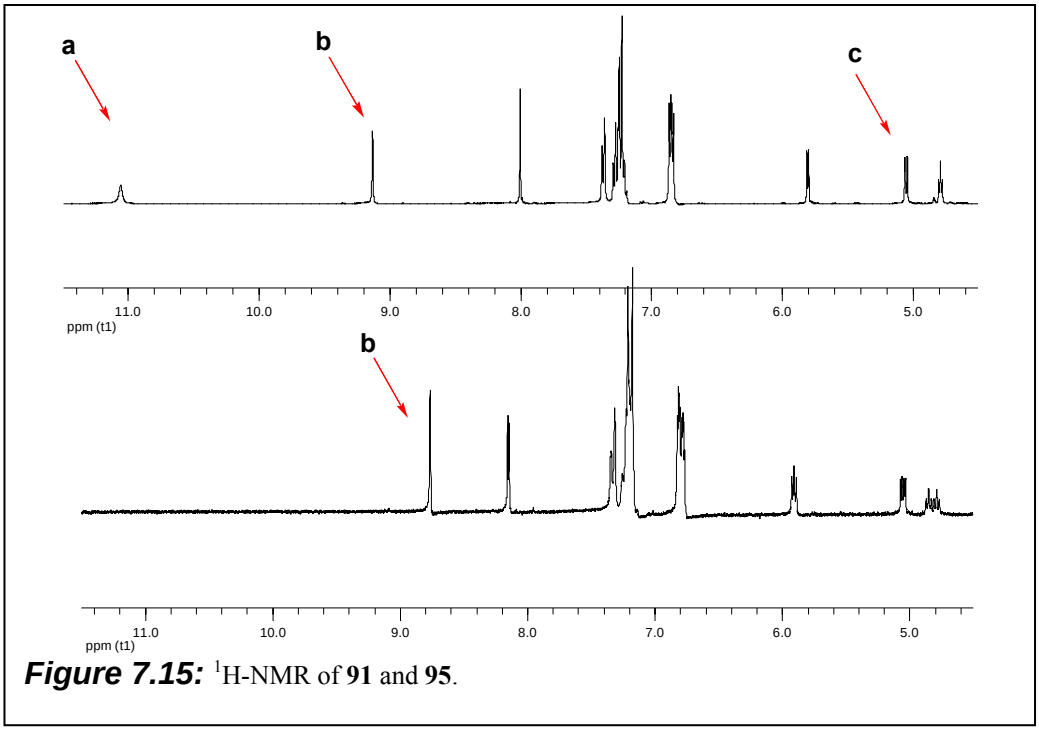

Figure 7.15: ^{1}H-NMR of **91** and **95**.

To avoid this side reaction, a protection of the carbonyl at position 2 was planned. According to the procedure published by Pfleiderer,[143] starting from a mixture of **91** and **92**, the *p*-nitrophenylethyl group (NPE) was introduced by the Mitsunobu reaction (Sch. 7.3). Consequently, a new mixture of the desired compounds **96**, **97**

plus the side products **98, 99**, and triphenylphosphine oxide was achieved. A HPLC separation was therefore required to isolate the single compounds.

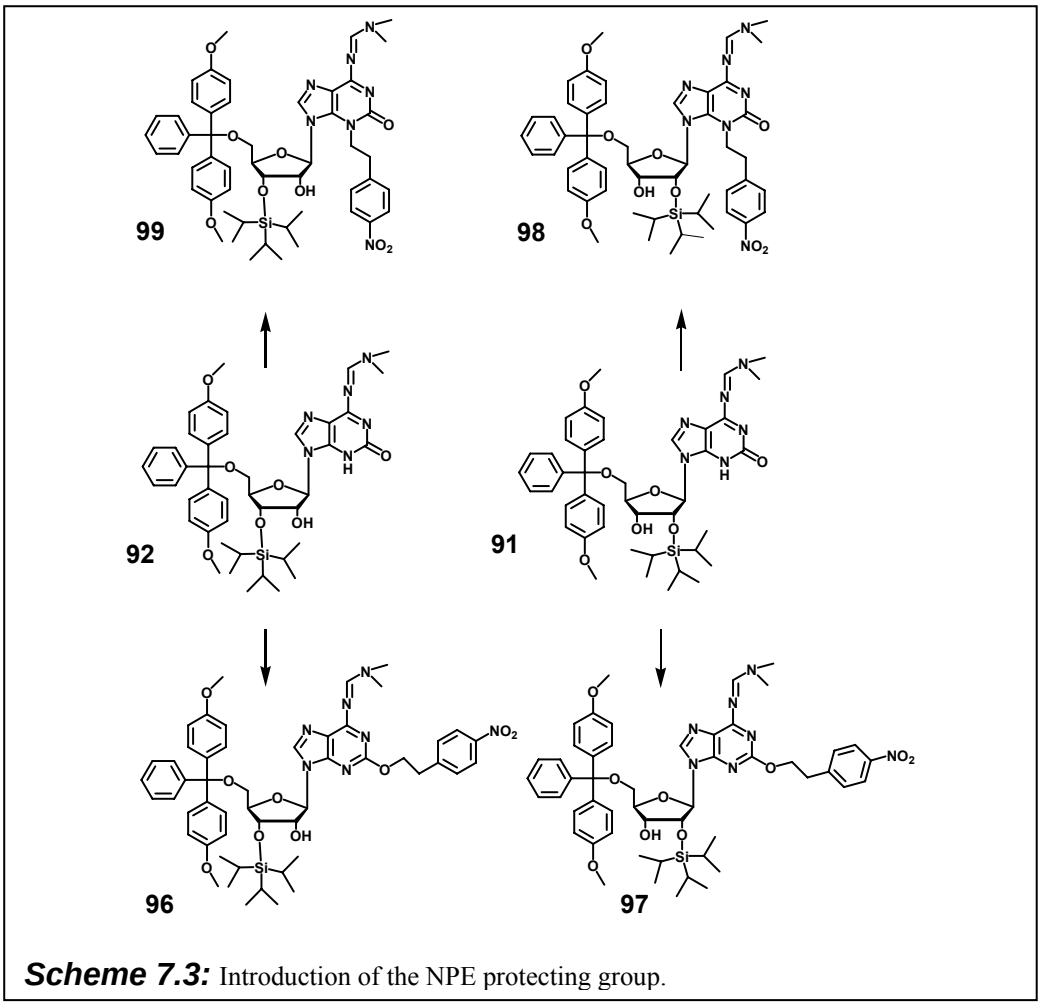

Scheme 7.3: Introduction of the NPE protecting group.

7.6 Conclusions

Although a synthetic route to the fully protected isoguanosine has been traced, an efficient synthesis of a phosphoramidite of isoguanosine would be improved by introducing a new set of protecting groups (Fig. 7.16).

The polarity of the molecule often complicated the purification during the normal silica gel flash chromatography, but also during HPLC purification, because neutral conditions were required to preserve all the protecting groups. To increase the lipophilicity, the NH_2 group in position 2 may be protected with N,N-dibutylformamide dimethyl acetal instead of N,N-dimethylformamide dimethyl

acetal. An alternative would be the 4-isopropyl phenoxy acetyl group. In addition the purine carbonyl group could be converted into a diphenylcarbamate,[144] in place of using the NPE as protecting group, which complicated the purification and led to the formation of side reactions.

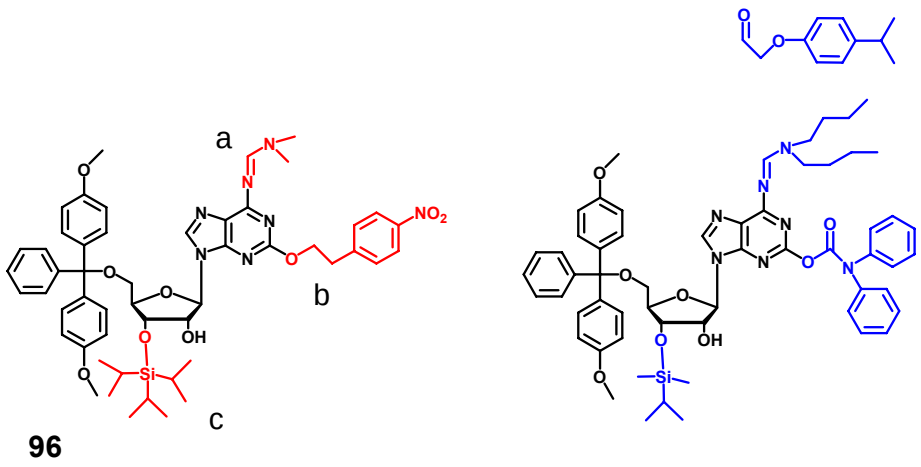

Figure 7.16: New set of protecting group for IsoG.

Concerning the OH groups at 2' and 3', they could be protected using *tert*-butyldimethylchlorosilyl instead of $(i\text{-}Pr)_3Si$-. This to reduce the steric hindrance and to make the phosphithylation of the remaining free OH group easier. For time reason the project was not finished, but a synthetic way to achieve the final product has been explored evidencing a set of synthetic problems, which can be solved as suggested.

8 Summary and Outlook

At the beginning of my thesis evidence from previous studies had shown that tris(2-aminobenzimidazoles) are excellent catalysts for RNA cleavage. However, due to the tendency of these molecules to aggregate, the activity of the monomeric non-aggregated catalyst was not exactly known. During my work 4 different 5' DNA conjugates were produced via disulfide linkage (Fig. 8.1: **1000**, **1001**, **1002**, **1006**). The cleavage tests of these conjugates proved without any doubt the activity of aminobenzimidazole catalysts. Furthermore, a pH activity relation was established, evidencing an optimum at pH 8. A high level of site-specific cleavage was obtained with these constructs by the use of helper oligonucleotides. A similar conjugate of PNA was also synthesised (Fig. 8.1 **1011**), but interestingly proved inactive. The reasons of this failure must still be investigated. Even if applications *in vivo* seem to be still difficult to achieve, *in vitro* these conjugates could be used as sequence specific artificial RNAses. Some questions about the mechanism of the catalyst are still open and important indications could come from a crystal of the catalyst-substrate complex. Moreover studies to clarify the action of these aminobenzimidazole catalysts will be fundamental to design new cleaving agents that could allow to reach promising results for applications *in vivo*.

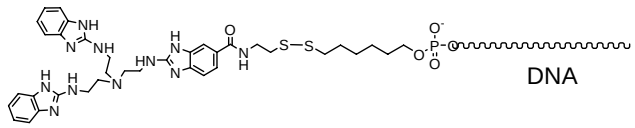

catalyst-linker-$^{5'}$TCGGCAGTCGGCTAG$^{3'}$ **1000**
catalyst-linker-$^{5'}$GATCGGCAGTCGGCTAG$^{3'}$ **1001**
catalyst-linker-$^{5'}$CGAGATCGGCAGTCGGCTAG$^{3'}$ **1002**
catalyst-linker-$^{5'}$CTCCTGACAAGGTAT$^{3'}$ **1006**

catalyst-linker-$^{5'}$tcggcagtcg$^{3'}$ **PNA-Oligo1011**

Figure 8.1: 5' Oligonucleotide conjugates.

These 5'-conjugates as expected did not show turnover. Consequently a new class of conjugates carrying the catalyst in the middle of the DNA strand was designed to allow multiple turnover (Fig. 8.2). Of these new conjugates two were based on serinol (**1007**, **1008**) and one on a modified nucleotide (**1004**). The conjugate **1007** based on serinol with a short linker resulted to be the most active. These molecules successfully achieved site-specific cleavage and, at the same time, multiple turnovers. For **1007** an approximated k_{cat} of 0.03 h^{-1} was obtained. Concerning this

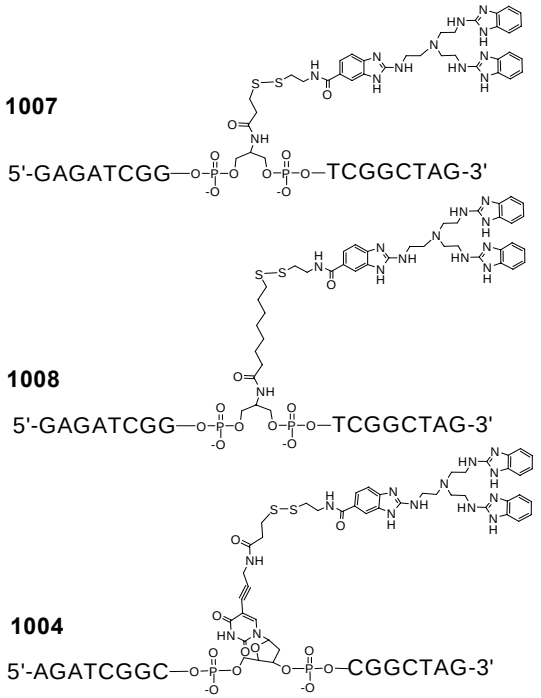

Figure 8.2: Oligonucleotide conjugates exhibiting turnover.

Figure 8.3: 5' Oligonucleotide conjugate producing turnover.

project it still remains to investigate the specificity and efficiency depending on the bulge-size. This problem could be solved without particular efforts by custom synthesis of new substrates that can form bulges of the desired size.

Based on a work of Häner,[54b][54c] an alternative strategy to allow turnover was applied by synthesizing **1012** (Fig. 8.3). This new DNA conjugate was prepared carrying the catalyst at the 5' end via amide bonds. In analogy to the work of Häner, conjugate **1012** was expected to form a bulge with substrate **210**. This bulge has been the principal cleavage site in the study of Häner (Fig. 8.3). Unfortunately in our case the formation of the bulge seems to be not energetically favoured, while an alternative bulge-less duplex structure seems to be more preferred. Therefore, the cleavage occurred exclusively in single strand region without exhibiting turnover. Hence, the key to solve this project will be to understand which factors are important in the stabilization of the bulge formation.

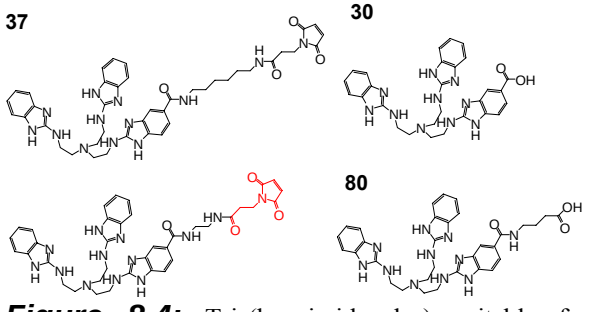

Figure 8.4: Tris(benzimidazoles) suitable for conjugation.

After these conjugation studies with DNA the tris(2-aminobenzimidazole) catalyst appeared suitable for practical applications such as affinity

cleavage. To test this application, different derivatives were prepared, suitable for conjugation via amide bonds and via maleimide chemistry (Fig. 8.4). Using **37,** four different peptide conjugates were synthesized (Fig. 8.5). **2001** and **2003** were based on the short sequence 49-57 of Tat, which is fundamental for the recognition of TAR. **2004** and **2005** were made from a peptide selected by Jörg Bäumler to have affinity for the mRNA of Bcr-Abl, and Again targeting TAR another conjugate with neamine was prepared in collaboration with the University of Grenoble (Professor Jean-Luc Décout). The tests of these 5 conjugates to validate our catalyst for affinity cleavage indicated that the cleaving activity was always conserved, but in some case the specificity for the target was lacking. Thereby, in this project an optimal system for conjugation via maleinimide and peptidic bonds was established, but to finally prove this method in affinity cleavage some more tests must be still done with more reliable specific RNA ligands.

2001 NH_2-YRKKR RQRRR C-Linker- Catalyst

2003 NH_2-AAARKKRRQRRRAAAC-Linker-Catalyst

2004 NH_2-KHLHLHKGGGC -Linker-Catalyst (L)

2005 NH_2-KHLHLHKGGGC -Linker-Catalyst (D)

Neamine-Linker- Catalyst

Figure 8.5: Peptide conjugates, neamine coniugate.

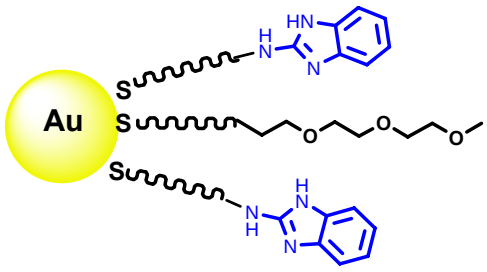

Figure 8.6: Gold nanoparticle functionalised with 2-aminobenzimidazoles.

In collaboration with Professor Paolo Scrimin and Flavio Manea, a gold nanoparticle functionalised with 2-aminobenzimidazole was prepared (Fig. 8.6). This project tried to answer the question if several copies of 2-aminobenzimidazole might cooperate in phosphoryl transfer catalysis when brought together in a geometrically less defined assembly. Due to reasons of poor solubility only the 30 % of the ligands on the metallic core carried the 2-aminobenzimidazole. The cleavage test could not show significant catalytic activity. Therefore, to achieve a positive result it seems necessary to increase the percentage of functional groups on the metallic surface. An alternative strategy to coordinate these functional groups could be the use of dendrimers.

A final project studied in this thesis, was the synthesis of a palindromic sequence of 2',5' guanosine/isoguanosine in order to verify the stability of this duplex expected to form Watson-Crick type purine-purine base pairs. This project had to be the basis for new experiments of non-enzymatic oligomerization of ribonucleotides. Consequently, the synthesis of a phosphoramidite of isoguanosine was started. However, due to a lack of time the project was not finished. Nevertheless, a synthetic path to this molecule was explored, recognizing series of synthetic problems that could be solved in the future with a new set of protecting groups, as illustrated in Fig. 8.7.

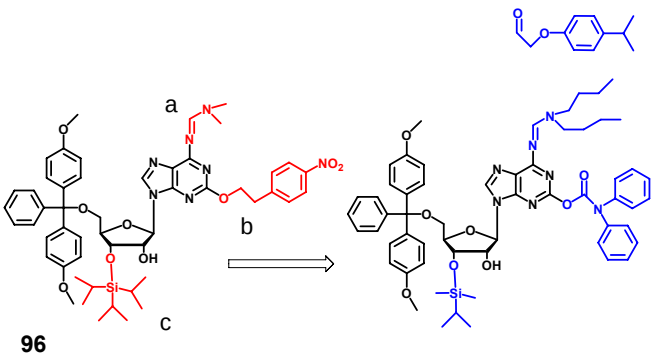

Figure 8.7: Isoguanosine protected for phosphoramidite chemistry and new possible set of protecting groups.

9 Experimental Section

9.1 Materials and Methods

General: All reagents were of the highest grades commercially available. Chemicals for polyacrylamide gel electrophoresis were purchased from Roth (Karlsruhe, Germany), blue dextran 2000 from Amersham Biosciences (Freiburg, Germany). The commercial chemical compounds were used without further purification, where not specified, and were provided by the following companies: Aldrich, Fluka, Merck, Lancaster, Biospring, Proligo, and Roth.

Solvents: The solvents for chromatography were distilled. Absolute solvents were used for reactions.

Thin Layer Chromatography (TLC): Aluminium sheets with silica gel 60 F_{254} (0.25 mm, Merck). The detection was done under UV lamp.

The oligonucleotides not synthesized in the own laboratory were obtained from Biospring (Frankfurt, Germany).

Inactivation of RNases: All experimental steps were performed under sterile conditions. Plasticware, tubes and most solutions were treated with diethylpyrocarbonate (DEPC). Solutions that are not compatible with DEPC treatment were prepared by mixing up molecular biology grade powdered reagents in DEPC-treated ultrapure water. All glassware was baked at 180 °C for six hours.

Purification of Cy-5-labelled oligonucleotides and conjugates: The oligonucleotides were purified by denaturing PAGE (16 % monomer, 7 M urea). The bands of interest were excised, the gel fragments transferred to a nuclease-free tube and submerged with elution buffer (500 mM NaOAc, 0.1 % SDS, 2 mM EDTA). We routinely incubated the gel fragments under vigorous shaking overnight at room temperature. Quantum Prep Freeze'N'Squeeze spin columns (BioRad, Munich, Germany) were used to remove the gel fragments. After ultrafiltration on Microcon YM3, the retentate was diluted to 1 mL with DEPC-treated H_2O and desalted on a NAP-10 column. The pooled fractions were lyophilized to dryness, and the pellet was dissolved in DEPC-treated H_2O to give a conc. of approximately 0.5 µg / µL.

Polyacrylamide gel electrophoresis: The oligonucleotide fragments were separated by denaturing PAGE (16 % monomer, 7 M urea) on a DNA sequencing device (ALFexpress, Amersham Biosciences). Prior to electrophoresis each sample was completed with one volume of loading buffer (5 mg / mL blue dextran in formamide) and 10 µL were loaded on the gel. Following running conditions were chosen: 1500 V (maximum), 60 mA (maximum), 30 W (constant), 55 °C, 2 s sampling interval and 350 minutes running time. For analysing the electropherograms the AlleleLinks 1.01 software package (Amersham Biosciences, Uppsala, Sweden) was used. The peak areas under the curves were added up, and the percentage of degraded RNA was calculated. Multiple cleavage reactions were disregarded in this system. All data were averaged over a minimum of two experiments.

RNA cleavage assay: 1.5 pmol Cy5-labelled RNA substrates were incubated in a final volume of 10 µL with the indicated conjugate concentration (0.15-1.5µM) in a 50 mM Tris- HCl buffer at pH 8.0 (if not indicated otherwise) containing 0 or 100 mM NaCl. All cleavage reactions were performed at 37 °C, time as indicated.

FCS Measurements: Aggregation studies were carried out with a ConfoCor 2 (Carl Zeiss, Jena, Germany). As additional equipment an Axiovert 200 M microscope containing a laser adapted Zeiss C-Apochromat 40x /1.2 W corr H_2O-immersion objective was used. Fluctuation measurements, which are calculated in real time to give an autocorrelation curve, and further analysis, like determination of the average number and the diffusion time (at 24 °C) of the fluorescent particles in the confocal volume, were performed with the Fluorescence Correlation Microscope ConfoCor 2 Software version 3.2 SP1. Free Cy5 dye was used for calibration of the instrument (excitation source: He/Ne laser at 633 nm) and cover slips (24 x 60 mm, Roth, Karlsruhe, Germany) served as sample carriers. For comparison reasons similar conditions as used for RNA-cleavage experiments were chosen. Conjugates **1000**, **1001**, **1002**, **1003**, and **1006** (1.5 µM) were either assayed with their cognate RNA (200nM) or with a mixture of an undegradable Cy5-labeled T20U probe **108** (25 nM) and an unlabeled DNA oligonucleotide **109** (175 nM) in 50 mM Tris-HCl buffer (pH 8.0). The incubation step (20 h, 37 °C) was omitted and the assay volume was increased to 30 µL. Each sample (30 µL droplet) was measured five times for 30 s.

Determination of oligonucleotide concentrations: To determine the concentration of an oligonucleotide an aliquot of 10 µL was diluted in 1 mL, the absorbance at 260

nm was measured corresponding to the OD^{260}. The molar extinction coefficient at 260 nm for the oligo is given by the following formula: a(16.000) + b(12.000) + c(7.000) + d(9.600)= ε, where a is the number of A's, b is the number of G's, c is the number of C's, d is the number of T's.

The molar concentration of the stock solution is given by:

(OD^{260} × dilution factor) / ε = concentration in μM.

9.2 Instrumentation

Melting point: Kofler hot plate microscope, uncorrected.

^{1}H-Nuclear Magnetic Resonance Spectroscopy (^{1}H-NMR): Bruker AM 250, Bruker Avance 400.

The chemical shifts (δ) in are indicated in ppm and the coupling constant (J) are expressed in Hertz (Hz).

The chemical shifts are given using the non-deuterated solvent as internal standard. The multiplicity of the signals are given according to the following indication: *s* = singlet, *d* = doublet, *t* = triplet and *m* = multiplet, br. = broad

^{31}P Nuclear Magnetic Resonance Spectroscopy (^{31}P-NMR): Bruker Avance 400 (162 MHz). phosphoric acid has been taken as external standard.

^{13}C Nuclear Magnetic Spectroscopy (^{13}C-NMR): Bruker AM 250 (63 MHz**)** Bruker AMX 400 (100 MHz). The signal of the solvent has been taken as internal standard.

Fourier-Transform-Infrared Spectroscopy (FT-IR): Perkin-Elmer 1600. In the infrared spectra the position of absorptions bands (ν) are given in cm^{-1}. The intensity is indicated with *s* = strong, *m* = medium and *w* = weak.

Ultraviolet Spectroscopy: Varian Cary 1E UV-Visible Spectrophotometer.

Mass Spectroscopy (MS): ESI: Fisons VG Platform II. MALDI: Fisons Instruments (VG Topspec / MALDI; N_2 – Laser 337 μm; Pulse frequency 4 nsec). MALDI-MATRIX: 2,5-Dihydroxy-benzoic acid.

Elementary Analysis: Hereaus CHN-Rapid.

Flash Chromatography: silica gel 60 (40-63 μm, 230-400 mesh) Merck.

Preparative High Performance Liquid Chromatography (HPLC): Merck sepTech, with Merck/Hitachi L4000A UV-Detector, column 700 x 50 mm und 250 x 50 mm internal diameter, packed with Macherey and Nagel Nucleoprep 20 μm.

Centrifuges: Eppendorf Centrifuge 5417R.

Lyophilisator: Christ Alpha 2-4.

Thermal Block: Biometra TB1 Thermoblock.

DNA-/RNA-Synthesizer: Applied Biosystems ABI 381A.

SpeedVac: vacuum pump Savant UVS400A, Savant SpeedVac Plus SC 110A.

9.3 Synthetic Methods

9.3.1 Methyl 3,4-diaminobenzoate (2)

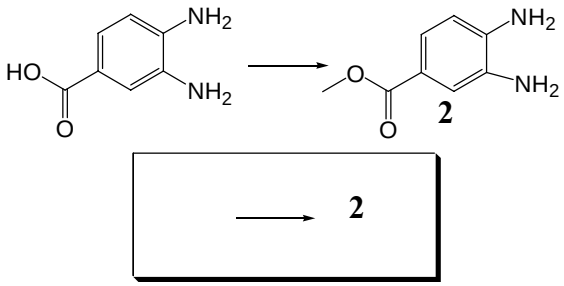

3,4-Diaminobenzoic acid (10.0 g, 65.7 mmol) was suspended in 200 mL of MeOH and cooled to 0 °C. Within 30 min 5 ml of $SOCl_2$ were added drop wise. The reaction was warmed up to room temperature, and then heated to reflux. After 15 h the reaction was complete. The solvent was evaporated ant the residue was adjusted to pH 9 adding a solution of saturated $NaHCO_3$. Ethyl acetate (300 mL) was added, the mixture was shaken in a separation funnel and the aqueous layer was further extracted with ethyl acetate (3×100 mL). The combined organic layers were washed with 5 % sodium bicarbonate (3×100 mL) and water (3×100 mL) and then dried over Na_2SO_4. The solvent was removed in *vacuo*. The crude material was purified by recrystallization from 30 mL chloroform adding 200 mL of hexane to provide 7.3 g (67 %) of the compound **2** as a pale yellow solid.

^{1}H-NMR (250 MHz, DMSO-d_6) δ: 3.71 (*s*, 3H, CH_3); 4.64 (*s*, 2H, NH_2); 5.26 (*s*, 2H, NH_2); 6.50 (*d*, *J*=8.3, 1H, Ar-H); 7.09 (*dd*, *J*=8.3, *J*=2.3, 1H, Ar-H); 7.15 (*d*, *J*=2.3, 1H, Ar-H).

IR (KBr): 3437*s*, 3365*s*, 3199*m*, 1692*s*, 1671*s*, 1630*m*, 1591*s*, 1514*m*, 1453*s*, 1428*m*, 1318*s*, 1296*m*, 1238*s*, 1189*w*, 1162*w*, 1112*w*, 1065*w*, 992*w*, 893*w*, 832*w*, 808*w*, 767*m*, 719*w*, 671*w*, 638w cm^{-1}.

MALDI-MS m/z: calcd for $C_8H_{11}N_2O_2^+$ ($M+H^+$) 167.1. Found 166.9 ($M+H^+$).

Analysis: $C_8H_{10}N_2O_2$ (166.18) calculated: C 57.82 H 6.07 N 16.86.
found: C 57.77 H 6.06 N 16.99.

M.p.: 103-105 °C. **Let:** 103-105 °C.

9.3.2 Bis-[2-(*tert*-butoxycarbonylamino)ethyl]-(2-aminoethyl)amine (5).

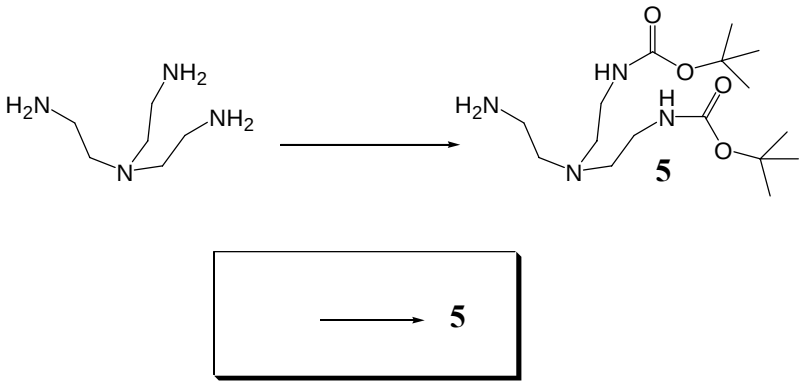

Tris(2-aminoethyl)amine **4** (1.49 mL, 9.50 mmol) was dissolved in 40 mL of dry THF and cooled to 0 °C. A solution of Boc-ON (4.95 g, 20.1 mmol) in 50 mL dry THF was added dropwise during 1 h. The mixture was stirred at room temperature for 48 h. After removal of the solvent under reduced pressure, the remaining yellow oil was dissolved in ethyl acetate and washed twice with 0.5 N NaOH. The aqueous phase was diluted with brine and reextracted with ethyl acetate. The combined organic phases were dried over $MgSO_4$ and the solvent was removed under reduced pressure. Chromatographic purification of the crude product (CH_2Cl_2/MeOH 45/4/1 % ammonia) yielded 2.07 g (63 %) of the compound **5** as a pale yellow oil.

^{1}H-NMR (DMSO-d_6) δ: 1.37 (*s*, 18H, CH_3); 2.38-2.44 (*m*, 6H, CH_2); 2.56 (*m*, 2H, CH_2); 2.95 (*m*, 4H, CH_2); 6.72 (br. *t*, 2H, NHC=O).

IR (KBr): 3356*m*, 2976*m*, 2818*m*, 1695*s*, 1521*s*, 1456*m*, 1391*m*, 1365*s*, 1276*s*, 1251*s*, 1172*s*, 1067*w*, 969*w*, 864*w*, 780*w*, 758*w* cm^{-1}.

ESI-MS m/z: calcd for $C_{16}H_{35}N_4O_4^+$ ($M+H^+$) 347.2. Found 347.1 ($M+H^+$).

9.3.3 4-Amino-3-(3-{2-[bis-(2-{*tert* butoxycarbonylamino} ethyl) amino]ethyl} thioureido) benzoic acid methyl ester (6).

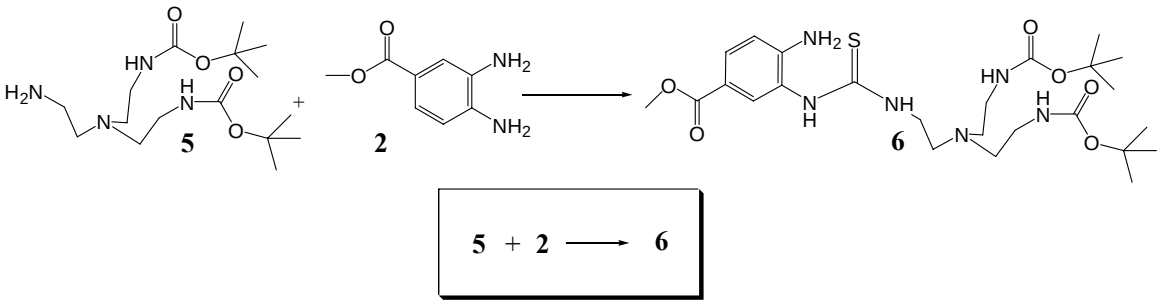

A solution of amine **5** (1.97 g, 5.68 mmol) in 20 mL acetonitrile was added dropwise at 0 °C to a mixture of thiocarbonyl diimidazole (1.52 g, 8.55 mmol) and imidazole (0.116 g, 1.71 mmol) in 30 mL acetonitrile. The reaction mixture was stirred at room temperature for 1 h. 3,4-diaminobenzoic acid methyl ester **2** (1.42 g, 8.55 mmol) was dissolved in 10 mL acetonitrile and added dropwise to the reaction mixture. The solution was stirred at 50 °C for 4 h and at room temperature over night. After the removal of the solvent the chromatographic purification (ethyl acetate/hexane 1/1 → ethyl acetate) yielded 2.80 g (88 %) of **6** as mixture with its constitutional isomer.

^{1}H-NMR (DMSO-d_6) δ: 1.38 (*s*, 18H, CH_3); 2.45-2.54 (*m*, 4H, CH_2, overlap with DMSO); 2.59 (*t*, *J*=5.6, 2H, CH_2); 2.94 (*m*, 4H, $CH_2NC{=}O$); 3.47 (*m*, 2H, $CH_2NC{=}S$); 3.76 (*s*, 3H, OCH_3); 5.68 (br. *s*, 2H, NH_2); 6.65 (*t*, *J*=5.2, 2H, NHC=O); 6.77 (*d*, *J*=9, 1H, Ar-H); 7.32 (br. *s*, 2H, NHC=S) 7.58-7.61 (*m*, 2H, Ar-H); 8.87 (*s*, 1H, NH-Ar).

IR (KBr): 3330*s*, 2977*s*, 2949*m*, 2839*w*, 1694*s*, 1625*s*, 1519*s*, 1438*m*, 1392*m*, 1366*s*, 1292*s*, 1251*s*, 1168*s*, 1103*m*, 1062*w*, 995*w*, 859*w*, 769*m* cm^{-1}.

ESI-MS m/z: calcd for $C_{25}H_{43}N_6O_6S^+$ ($M+H^+$) 555.3. Found 555.2 ($M+H^+$).

9.3.4 2-{2-[Bis-(2-{*tert*-butoxycarbonylamino}ethyl)amino]ethylamino}-1*H*-benzimidazole-5-carboxylic acid methyl ester (7).

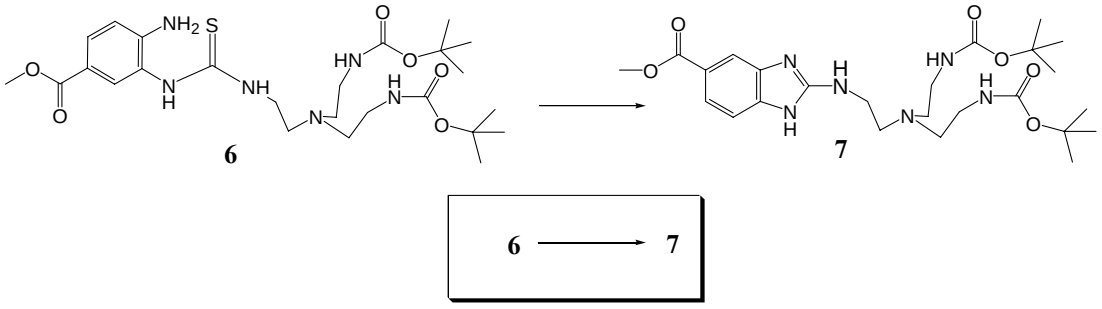

To a refluxing solution of thiourea **6** (1.50 g, 2.70 mmol) in 60 mL abs. EtOH containing a catalytic amount of sulfur, yellow HgO (2.34 g, 10.8 mmol) was added in several portions over 5 h. After filtration through celite®, the solvent was evaporated under reduced pressure. The residue was chromatographed (ethyl acetate/MeOH 5/1) yielding 1.36 g (97 %) of **7** as white solid.

^{1}H-NMR (DMSO-d_6) δ: 1.37 (*s*, 18H, CH_3); 2.49-2.54 (*m*, 4H, CH_2, overlap with DMSO); 2.67 (*t*, *J*=6.1, 2H, CH_2); 2.95-3.02 (*m*, 4H, $CH_2NC{=}O$); 3.33 (*m,* 2H, CH_2N-Ar, overlap wit H_2O); 3.82 (*s*, 3H, O-CH_3); 6.78 (*t*, *J*=4.6, 2H, NHC=O); 6.87 (br. *s*, 1H, NH-Ar); 7.18 (*d*, *J*=8.3, 1H, Ar-H); 7.59-7.62 (*m*, 1H, Ar-H); 7.74 (*d*, *J*=1.6, 1H, Ar-H) 10.96 (br. *s*, 1H, Ring-NH).

IR (KBr): 3358*s*, 2977*s*, 2826*m*, 1690*s*, 1636*s*, 1602*s*, 1578*s*, 1522*s*, 1458*m*, 1436*s*, 1392*m*, 1366*s*, 1290*s*, 1252*s*, 1170*s*, 1088*m*, 987*w*, 859*w*, 776*m*, 752*w* cm^{-1}.
ESI-MS m/z: calcd for $C_{25}H_{41}N_6O_6^+$ ($M+H^+$) 521.3. Found 521.4 ($M+H^+$).

9.3.5 2-[2-(Bis-{2-[3-(2-nitrophenyl)thioureido]ethyl}amino)ethylamino]-1*H*-benzimidazole-5-carboxylic acid methyl ester (24).

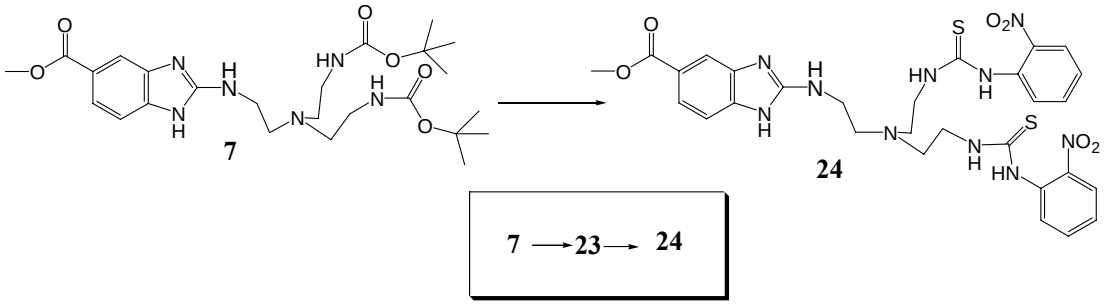

A solution of compound **7** (1.27 g, 2.44 mmol) in 30 mL abs. MeOH was cooled to 0 °C and $SOCl_2$ (1.77 mL, 24.4 mmol) was added dropwise. The mixture was stirred at room temperature for 3 h. The solvent was removed under reduced pressure yielding the hydrochloride of **23** quantitatively. NMR confirmed the removal of Boc and the crude product **23** was used in the next step without further purification.

^{1}H-NMR (250 MHz, DMSO-d_6) δ: 3.17 (br. *s*, 10H, CH_2); 3.87 (*m*, 5H, CH_2 CH_3); 7.51 (*d*, *J*=8.4, 1H, Ar-H); 7.87 (*dd*, *J*=1.5, *J*=8.4, 1H, Ar-H); 7.96 (*d*, *J*=1.5, 1H, Ar-H); 8.40 (br. *s*, 4H, NH); 9.64 (br. *t*, 1H, NH); 13.54 (br. *s*, 2H, NH).

A solution of 2-nitrophenylisothiocyanate (967 mg, 5.37 mmol) in 30 mL abs. EtOH was diluted with 10 mL TEA. The compound **23** was dissolved in 20 mL abs. EtOH with 10 mL TEA and added to the isothiocyanate solution at 0 °C. The mixture was stirred at room temperature over night. After removal of the solvent under reduced pressure, the crude product was chromatographed (ethyl acetate → ethyl acetate/MeOH 5/1) yielding 1.54 g (92 %) of **24** as a yellow solid:

^{1}H-NMR (250 MHz, DMSO-d_6) δ: 2.67-2.89 (*m*, 6H, CH_2); 3.40-3.53 (*m*, 2H CH_2); 3.54-3.71 (*m*, 4H, CH_2); 3.81 (*s*, 3H, CH_3); 6.86 (br. *t*, 1H, NH-Ar); 7.16 (*d*, *J*=8.3, 1H, Ar-H); 7.37 (*m*, 2H, Ar-H); 7.55-7.82 (*m*, 6H, Ar-H); 7.98 (*dd*, *J*= 8.2, *J*=1.3, 2H, Ar-H); 8.44 (br. *t*, 2H, NHC=S); 9.81 (*s*, 2H, C=S-NH-Ar); 11.0 (*s*, 1H, Ring-NH).

IR (KBr): 3300*m*, 3040*w*, 2947*m*, 2841*w*, 1701*m*, 1686*m*, 1635*m*, 1605*s*, 1578*m*, 1508*s*, 1458*m*, 1439*m*, 1341*s*, 1286*s*, 1206*m*, 1160*m*, 1088*m*, 1044*w*, 863*w*, 776*m*, 724*m* cm^{-1}.

MALDI-MS m/z: calcd. for $C_{29}H_{33}N_{10}O_6S_2^+$ ($M+H^+$) 681.2. Found 681.8 ($M+H^+$).

M.p.: 104 °C.

9.3.6 2-[2-(Bis-{2-[3-(2-aminophenyl) thioureido] ethyl}amino) ethylamino]-1*H*-benzimidazole-5-carboxylic acid methyl ester (25).

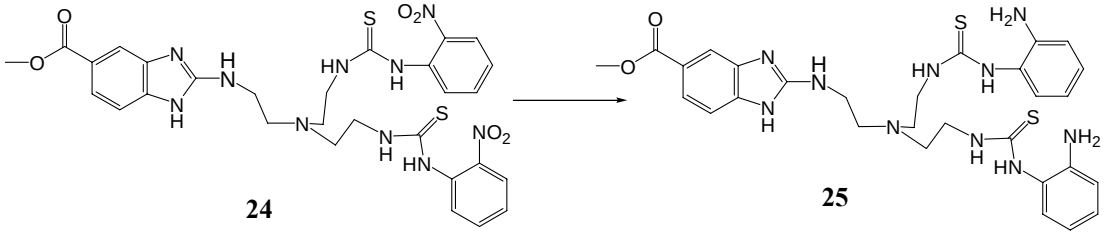

Nitro compound **24** (1.00 g, 1.47 mmol) was dissolved in MeOH (50 mL) saturated with ammonia. 20 % Pd on activated charcoal (200 mg) was added and the mixture was stirred in an autoclave (purged with Ar) at 50 bar hydrogen pressure and 60 °C for 5 h. The catalyst was removed by centrifugation at 6000 min^{-1} for 15 min and the clear solution was decanted from the charcoal. The solvent was evaporated under reduced pressure and the residue chromatographed (ethyl acetate/MeOH 9/1) to give 635 mg (70 %) of compound **25** as pale compound.

^{1}H-NMR (250 MHz, DMSO-d_6) δ: 2.59-2.76 (*m*, 6H, CH_2); 3.26-3.57 (*m*, 6H, CH_2); 3.82 (*s*, 3H, CH_3); 4.85 (*s*, 4H, NH_2); 6.52-6.51 (*dt*, *J*=7.5, 1.3, 2H, Ar-H); 6.75 (*dd*, *J*=8.3, *J*=1.3, 2H, Ar-H); 6.93-7.00 (*m*, 4H, Ar-H); 7.17 (*d*, *J*=8.3, 1H, Ar-

H); 7.58 (*dd*, *J*=8.40, J=1.2, 1H, Ar-H); 7.73 (*d*, *J*=1.3, 1H, Ar-H); 8.95 (*s*, 2H, NH-Ar); 10.97 (br. *s*, 1H, Ring-NH).

IR (KBr): 3364*s*, 3055*m*, 2948*m*, 1694*s*, 1634*s*, 1602*s*, 1575*s*, 1464*s*, 1404*w*, 1362*w*, 1290*s*, 1271*s*, 1237*m*, 1210*m*, 1163*w*, 1117*w*, 1089*w*, 1059*w*, 1013*w*, 742*m* cm^{-1}.

MALDI-MS m/z: calcd for $C_{29}H_{37}N_{10}O_2S_2^+$ ($M+H^+$) 621.3. Found 623.0 ($M+H^+$).

M.p.: 120 °C

9.3.7 2-(2-{Bis-[2-(1*H*-benzimidazol-2-ylamino)ethyl]amino}ethylamino)-1*H*-benzimidazole-5-carboxylic acid methyl ester (29)

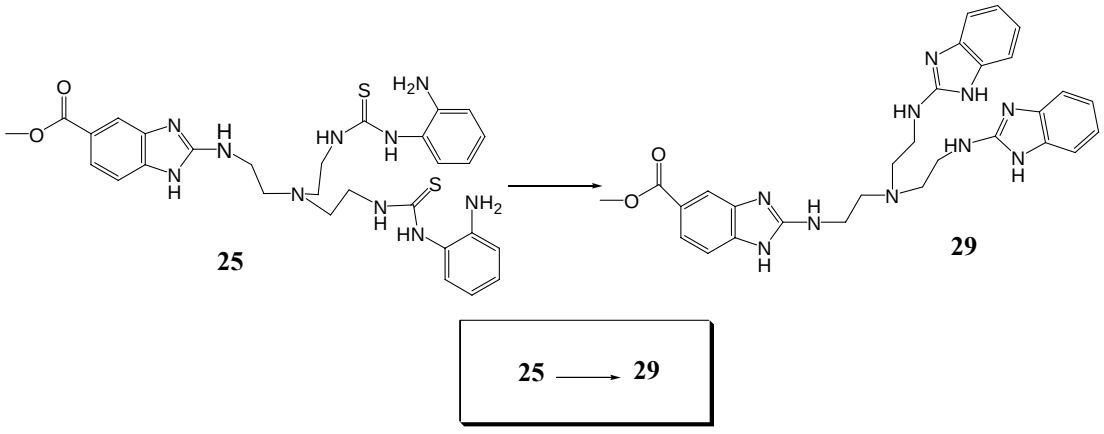

To a refluxing solution of thiourea **25** (582 mg, 0.94 mmol) in 50 mL abs. EtOH containing a catalytic amount of sulphur, yellow HgO (609 mg, 2.81 mmol) was added over 8 h in several portions. The mixture was filtered through celite® and the solvent removed at reduced pressure. Chromatography (CH_2Cl_2/MeOH 44/5/1 % NH_3) yielded 218 mg (58 %) of the trisbenzimidazole ester **29** as pink compound.

^{1}H-NMR (250 MHz, DMSO-d_6): δ 2.73-2.83 (*m*, 6H, CH_2); 3.34-3.51 (*m*, 6H, CH_2 overlap with water); 3.81 (*s*, 3H, CH_3); 6.52 (*s*, 2H, Ar-H); 6.87-6.92 (*m*, 4H, Ar-H);

7.00 (*s*, 1H, NH-Ar); 7.11-7.19 (*m*, 5H, Ar-H); 7.59 (*dd*, *J*=8.3, *J*=1.7, 1H, Ar-H); 7.72 (*d*, *J*=1.6, 3H, Ar-H); 9.62 (br.*s*, 3H, NHAr).

IR (KBr): 3312*s*, 2947*s*, 1686*s*, 1633*s*, 1603*s*, 1579*s*, 1464*s*, 1435*m*, 1401*m*, 1362*m*, 1289*s*, 1210*s*, 1162*m*, 1117*m*, 1089*m*, 1058*w*, 1013*w*, 896*w*, 742*s* cm^{-1}.

ESI-MS m/z: calcd for $C_{29}H_{33}N_{10}O_2^+$ ($M+H^+$) 553.3. Found 553.5 ($M+H^+$).

Analysis: $C_{29}H_{32}N_{10}O_2$ (552.64) calculated: C 63.03 H 5.84 N 25.35.
found: C 62.25 H 6.03 N 24.69.
0.4 H_2O (559.85) calculated: C 62.22 H 5.91 N 25.02.

M.p.: 155-158 °C.

9.3.8 (6-Amino-hexyl)-carbamic acid *tert*-butyl ester (13)

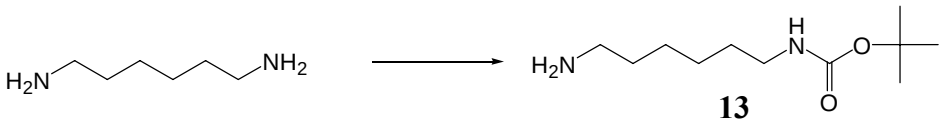

13

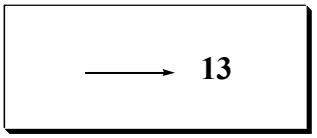

1,6-Diaminohexane (10.78 g, 92.8 mmol) was dissolved in 80 mL of dry THF and cooled to 0 °C. A solution of Boc-ON (5.71 g, 23.2 mmol) in 50 mL of dry THF was added dropwise during 1 h, the mixture was stirred for 48 h at room temperature. After filtration the solvent was removed under reduced pressure and the crude product was purified by silica gel chromatography (CH_2Cl_2/MeOH/aqueous NH_3 45/4/1) yielding 5.06 g (25 %) of **13** as colourless oil.

^{1}H-NMR (250 MHz, DMSO-d_6) δ: 1.25-1.56 (*m*, 17H, $4CH_2$, $3CH_3$); 2.51 (*m*, 2H, CH_2N overlap with DMSO); 2.89 (*m*, 2H, $CH_2NC{=}O$); 6.77 (*m*, 1H, NHC=O).

IR (KBr): 3369*s*, 2973*m*, 2935*s*, 2862*m*, 1686*s*, 1627*w*, 1522*s*, 1480*m*, 1465*m*, 1390*w*, 1365*m*, 1350*w*, 1278*m*, 1251*m*, 1173*s*, 1051*w*, 1016*w*, 995*w*, 869*w*, 821*w*, 782*w*, 730*w*, 606*w* cm^{-1}.

ESI-MS m/z: calcd for $C_{11}H_{25}N_2O_2^+$ ($M+H^+$) 217.2. Found 217.0 ($M+H^+$).

Analysis: $C_{11}H_{24}N_2O_2$ (216.3) calculated: C 61.07 H 11.18 N 12.95.
found: C 59.93 H 11.13 N 12.93.
0.2 H_2O (219.9) calculated: C 60.07 H 11.18 N 12.74.

9.3.9 (6-{[2-(2-{Bis-[2-(1*H*-benzoimidazol-2-ylamino)-ethyl]-amino}-ethylamino)-1*H*-benzoimidazole-5-carbonyl]-amino}-hexyl)-carbamic acid *tert*-butyl ester (35)

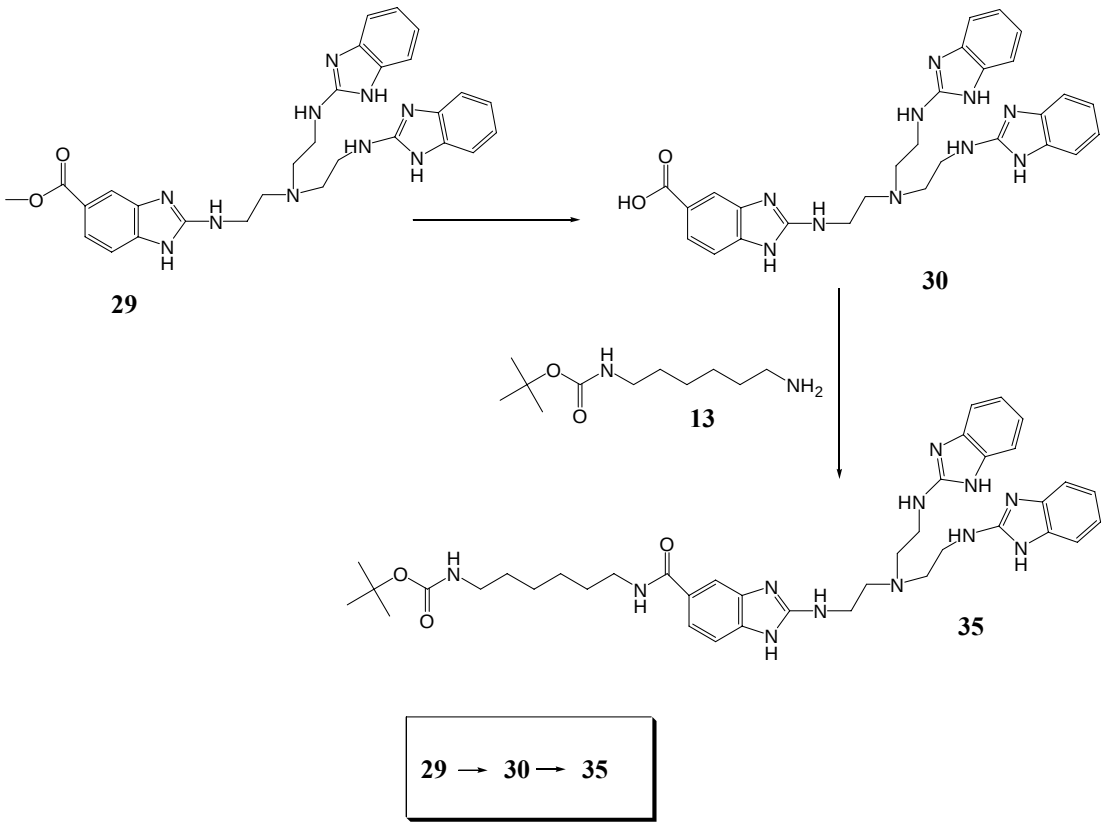

Methyl ester **29** (200 mg, 0.36 mmol) was refluxed in 25 mL of 6 M HCl for 2 h, the solvent was removed under reduced pressure. NMR and ESI spectrometry confirmed the ester hydrolysis. The crude product was used for the next step.

^{1}H-NMR (250 MHz, MeOD-*d*$_4$) δ: 3.90 (*m*, 6H, CH_2N); 4.19 (*m*, 6H, CH_2N); 7.28 (*m*, 4H, Ar-H); 7.38 (*m*, 4H, Ar-H); 7.44 (m, 1H, Ar-H); 7.97 (*m*, 1H, Ar-H); 7.99 (*m*, 1H, Ar-H).

ESI-MS m/z: calcd for $C_{28}H_{31}N_{10}O_2^+$ ($M+H^+$) 539.3. Found 539.2 ($M+H^+$).

To a solution of **30** (0.36 mmol) in anhydrous DMF (10 mL), Et_3N (500 μL), DIC (68 mg, 0.54 mmol), HOBt (73 mg, 0.54 mmol) and **13** (102 mg, 0.47 mmol) were added. The reaction was stirred at room temperature for 18 h. The solvent was evaporated by kugelrohr distillation, and the solid residue was purified by silica gel chromatography (CH_2Cl_2/MeOH/aqueous NH_3 55/4/1), giving 133 mg (50 %) of **35** as pink amorphous solid.

^{1}H-NMR (250 MHz, MeOD-*d*$_4$) δ: 1.35-1.68 (*m*, 17H, $4CH_2$, $3CH_3$); 2.88 (*t*, *J*=6.3, 6H, CH_2); 3.04 (*t*, *J*=6.8, 2H, CH_2); 3.37 (*t*, *J*=7.0, 2H, CH_2); 3.47 (*m*, 6H, CH_2); 6.96 (*m*, 4H, Ar-H); 7.12-7.19 (*m*, 5H, Ar-H); 7.47 (*dd*, *J*=8.3, *J*=1.7, 1H, Ar-H); 7.61 (*d*, *J*=1.7, 1H, Ar-H).

IR (KBr): 3299*m*, 3058*w*, 2974*w*, 2932*s*, 1684*s*, 1633*s*, 1602*s*, 1581*s*, 1523*m*, 1461*s*, 1398*w*, 1361*w*, 1267*s*, 1168*m*, 1105*w*, 1052*w*, 1010*w*, 738*s* cm^{-1}.

ESI-MS m/z: calcd for $C_{39}H_{53}N_{12}O_3^+$ ($M+H^+$) 737.4. Found 737.7 ($M+H^+$).

9.3.10 2-(2-{Bis-[2-(1*H*-benzoimidazol-2-ylamino)-ethyl]-amino}-ethylamino)-1*H*-benzoimidazole-5-carboxylic acid {6-[3-(2,5-dioxo-2,5-dihydro-pyrrol-1-yl)-propionylamino]-hexyl}-amide (37)

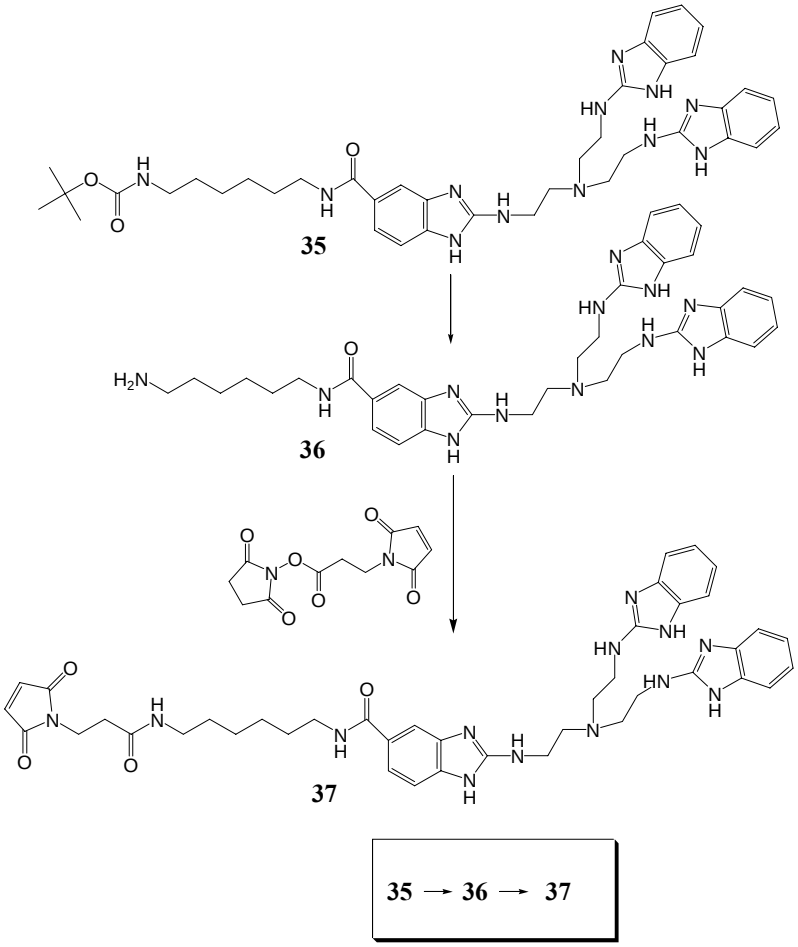

To **35** (200 mg, 0.27 mmol) in MeOH (20 ml) was added 2 mL of HCl (1 M), the reaction was stirred at room temperature for 2 h and the solvent was removed under reduced pressure. NMR and ESI spectrometry confirmed the Boc hydrolysis and the formation of **36**. The crude product was used for the next step.

^{1}H-NMR (250 MHz, MeOD-*d*$_4$) δ: 1.50 (*m*, 4H, CH_2); 1.71 (*m*, 4H, CH_2); 2.96 (*t*, *J* = 7.5, 2H, CH_2); 3.03 (*m*, 6H, CH_2); 3.44 (*t*, *J*=7.0, 2H, CH_2); 3.62 (*m*, 6H, CH_2); 7.21-7.35 (*m*, 9H, Ar-H); 7.71 (*dd*, *J*=8.3, *J*=1.7, 1H, Ar-H); 7.74 (*m*, 1H, Ar-H).

ESI-MS m/z: calcd for $C_{34}H_{45}N_{12}O^+$ ($M+H^+$) 637.4. Found 637.2 ($M+H^+$).

To **36** dissolved in DMF (8 mL), were added TEA (2 mL) and O-succinimidyl 3-maleimidopropionate (100 mg, 0.38 mmol). The reaction was followed by TLC (n-Butanol/AcOH/H_2O 5/2/3, rf 0.3). After 2 h at room temperature the solvent was removed, and the crude material was purified on RP HPLC performed on Maisch Reprosil-AQ column (250×20) using isocratic elution with 0.1 % TFA (*aq.*) 68 %, CH_3CN 32 %, flow: 7 ml/min, yielding 83.1 mg (19 %) of pure **37** compound in form of trifluoroacetate.

^{1}H-NMR (250 MHz, MeOD-d_4) δ: 1.28-1.69 (*m*, 8H, CH_2); 2.43 (*t*, *J*=6.8, 2H, CH_2C=O); 3.02 (*m*, 6H, CH_2N); 3.12 (*t*, *J*=6.0, 2H, CH_2NC=O); 3.39 (*t*, *J*=7.3, 2H, CH_2NC=O); 3.60 (*m*, 6H, CH_2N); 3.74 (*t*, *J*=6.8, 2H, $CH_2N(C=O)_2$); 6.79 (*s*, 2H, =CH); 7.17-7.30 (*m*, 9H, Ar-H); 7.65 (*m*, 1H, Ar-H); 7.70 (*m*, 1H, Ar-H).

MALDI-MS m/z: calcd for $C_{41}H_{50}N_{13}O_4^+$ ($M+H^+$) 788.4. Found 788.5 ($M+H^+$).

Analytical **HPLC** was performed on a Variant Polaris column (50×4.6) using 5 min. isocratic elution with 0.1 % TFA (*aq.*), then a linear gradient to the same buffer containing 70 % CH_3CN in 20 min.

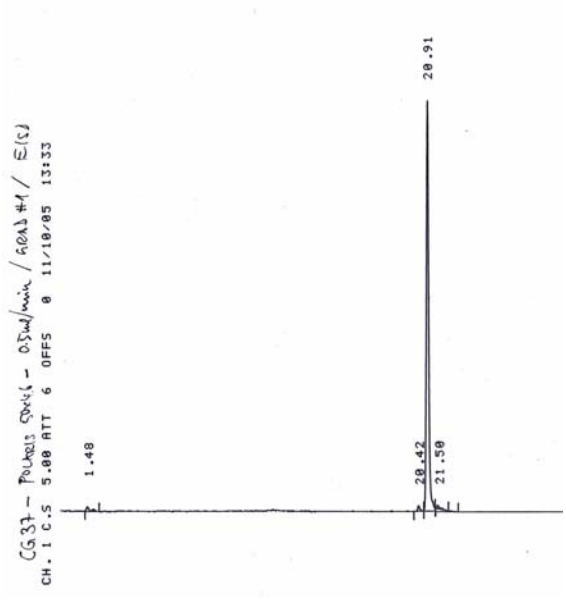

9.3.11 Peptide conjugates (2001, 2003, 2004, 2005).

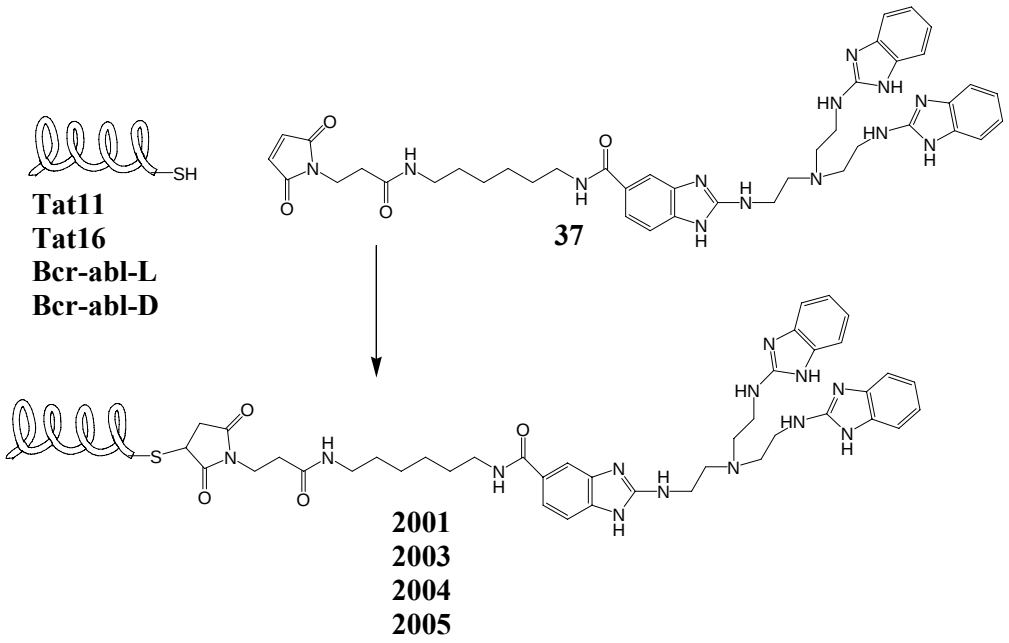

37 ⟶ **2001** **NH_2-YRKKR RQRRR C-Linker- Catalyst**

2003 **NH_2-AAARKKRRQRRRAAAC-Linker-Catalyst**

2004 **NH_2-KHLHLHKGGGC -Linker-Catalyst (L)**

2005 **NH_2-KHLHLHKGGGC -Linker-Catalyst (D)**

This general protocol was used for each of the 4 different peptides.

To a solution of peptide (2 mg) in 0.5 mL of 50 mM Tris-HCl pH 7 buffer, $NaBH_4$ (2.7 mg) was added, the disulfide reduction was followed by HPLC, and after 2 h, the reaction was quenched adding 100 µL of acetone, the pH adjusted to 7 and 4.6 mg of **37** trifluoroacetate in 200 µL of DMF were added. The reaction was followed by HPLC, was completed after 1 h. The reaction mixture was stored at –80 °C, and the crude material of **2001**, **2004**, **2005**, was purified on RP HPLC performed on Phenomex® Gemini column (250×10) using isocratic elution with 0.1 % TFA (*aq.*) 75 %, CH_3CN 25 %, flow: 2 mL/min. The crude material of **2003** was purified on RP HPLC performed on Nucleodur 100-7 C 18 ec (250×21) column using 30 min. isocratic elution with 0.1 % TFA (*aq.*), followed by a stepwise gradient 0.1 % TFA (*aq.*), 70 %, CH_3CN 30 %, flow 10 mL/min.

2001

MALDI-MS m/z: calcd for $C_{106}H_{171}N_{46}O_{175}$ **2001** ($M+H^+$) 2391.3. Found 2462.0, 2501.0

2003

MALDI-MS m/z: calcd for **2003** $C_{115}H_{192}N_{51}O_{21}S$ ($M+H^+$) 2655.2. Found 2696.6.

Analytical **HPLC** was performed on Variant Polaris column (50×4.6) using 5 min. isocratic elution with 0.1 % TFA (*aq.*), then a linear gradient to the same buffer containing 70 % CH_3CN in 20 min.

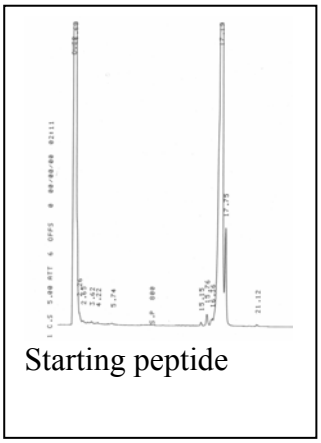
Starting peptide

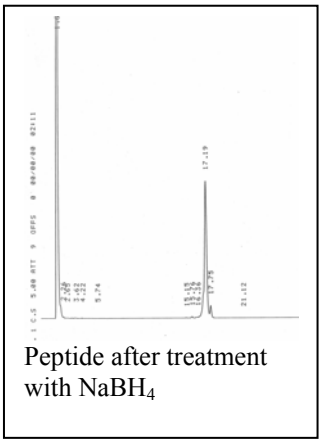
Peptide after treatment with $NaBH_4$

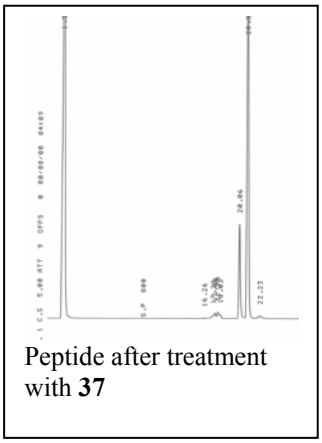
Peptide after treatment with **37**

Analytical **HPLC** was performed on Phenomex® Gemini column (150×4.6) using isocratic elution with 0.1 % TFA (*aq.*) 75 %, CH_3CN 25 %, flow: 0.8 mL/min.

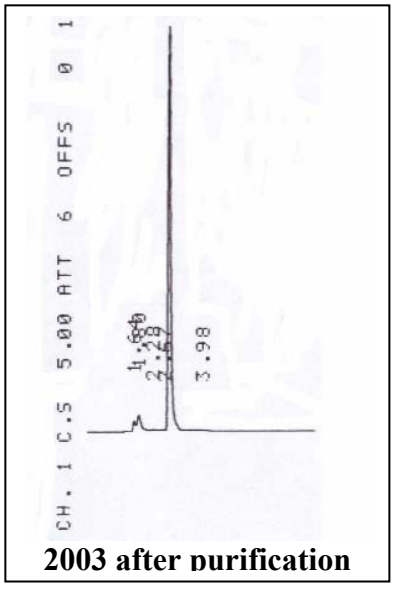

2003 after purification

2004

MALDI-MS m/z: calcd for $C_{92}H_{134}N_{33}O_{15}S$ **2004** ($M+H^+$) 1974.3.0. Found: 2059.7.

Analytical **HPLC** was performed on Variant Polaris column (50×4.6) using 5 min. isocratic elution with 0.1 % TFA (*aq.*), then a linear gradient to the same buffer containing 70 % CH_3CN in 20 min.

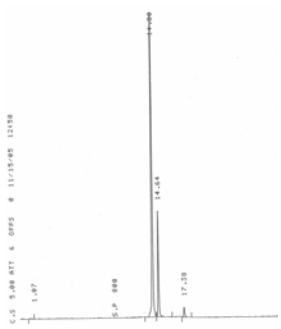

Starting peptide

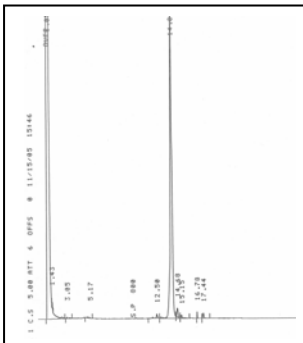

Peptide after treatment with $NaBH_4$

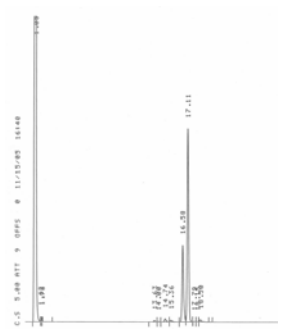

Peptide after treatment with **37**

Analytical **HPLC** was performed on Phenomex® Gemini column (150×4.6) using isocratic elution with 0.1 % TFA (*aq.*) 75 %, CH_3CN 25 %, flow: 0.8 mL/min.

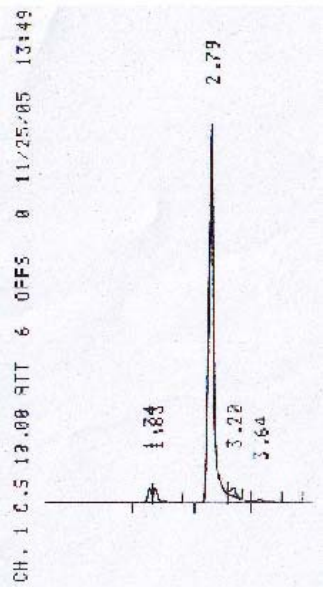

2004 after purification.

2005

MALDI-MS m/z: calcd for $C_{92}H_{134}N_{33}O_{15}S$ **2005** ($M+H^+$) 1974.3. Found 2057.4.

Analytical **HPLC** was performed on Variant Polaris column (50×4.6) using 5 min. isocratic elution with 0.1 % TFA (*aq.*), then a linear gradient to the same buffer containing 70 % CH_3CN in 20 min.

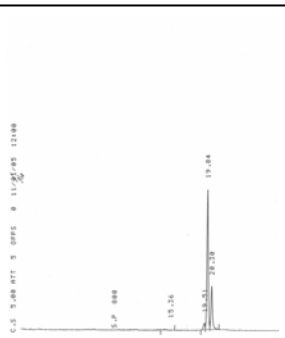

Starting peptide

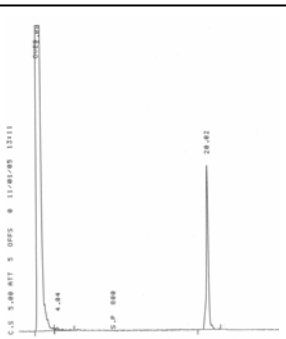

Peptide after treatment with $NaBH_4$

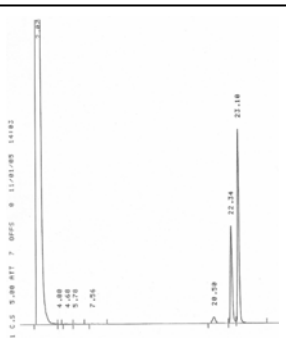

Peptide after treatment with 37

Analytical **HPLC** was performed on Phenomex® Gemini column (150×4.6) using isocratic elution with 0.1 % TFA (*aq.*) 75 %, CH_3CN 25 %, flow: 0.8 mL/min.

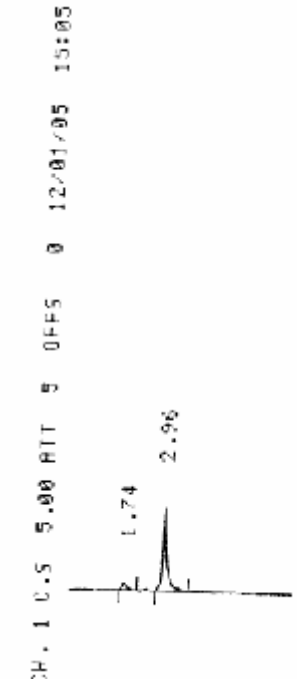

2005 after purification.

9.3.12 (2-Amino-ethyl)-carbamic acid *tert*-butyl ester (47)

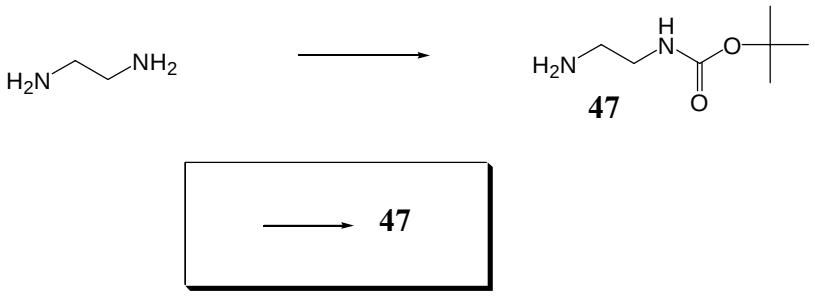

1,2-Diaminoethane (3 g, 49.9 mmol) was dissolved in 80 mL of dry THF and cooled to 0 °C. A solution of Boc-ON (6.15 g, 25.0 mmol) in dry THF (50 mL) was added dropwise during 1h, the mixture was stirred at room temperature 16 h. After filtration the solvent was removed under reduced pressure and the crude product was purified by silica gel chromatography (CH_2Cl_2/MeOH/aqueous NH_3 45/4/1 %) yielding 2.8 g (35 %) of **47** as colourless oil.

^{1}H-NMR (250 MHz, DMSO-d_6) δ: 1.38 (*s*, 9H, CH_3); 2.53 (*t*, *J*=6.5, 2H, CH_2N); 2.91 (*m*, 2H, $CH_2NC{=}O$); 6.76 (br. *t*, 1H, $NHC{=}O$).

ESI-MS m/z: calcd. for $C_7H_{17}N_2O_2^+$ ($M+H^+$) 161.1. Found 160.7 ($M+H^+$).

IR (KBr): 3364*s*, 2986*w*, 2937*w*, 1686*s*, 1639*w*, 1596*m*, 1534*s*, 1466*m*, 1390*w*, 1368*m*, 1278*s*, 1252*m*, 1223*w*, 1177*s*, 1039*w*, 974*w*, 870*w*, 818*w*, 792*w*, 767*w*, 632*m* cm^{-1}.

Analysis: $C_7H_{16}N_2O_2$ (160.7) calculated: C 52.48 H 10.07 N 17.48.
found: C 48.79 H 9.77 N 16.39.
0.65 H_2O (171.9) calculated: C 48.90 H 10.14 N 16.29.

9.3.13 (2- {[2 -(2 -{Bis-[2 -(1*H*-benzoimidazol-2-ylamino) -ethyl] amino} -ethylamino) -1*H*-benzoimidazole-5-carbonyl] -amino} -ethyl)-carbamic acid *tert*-butyl ester (48)

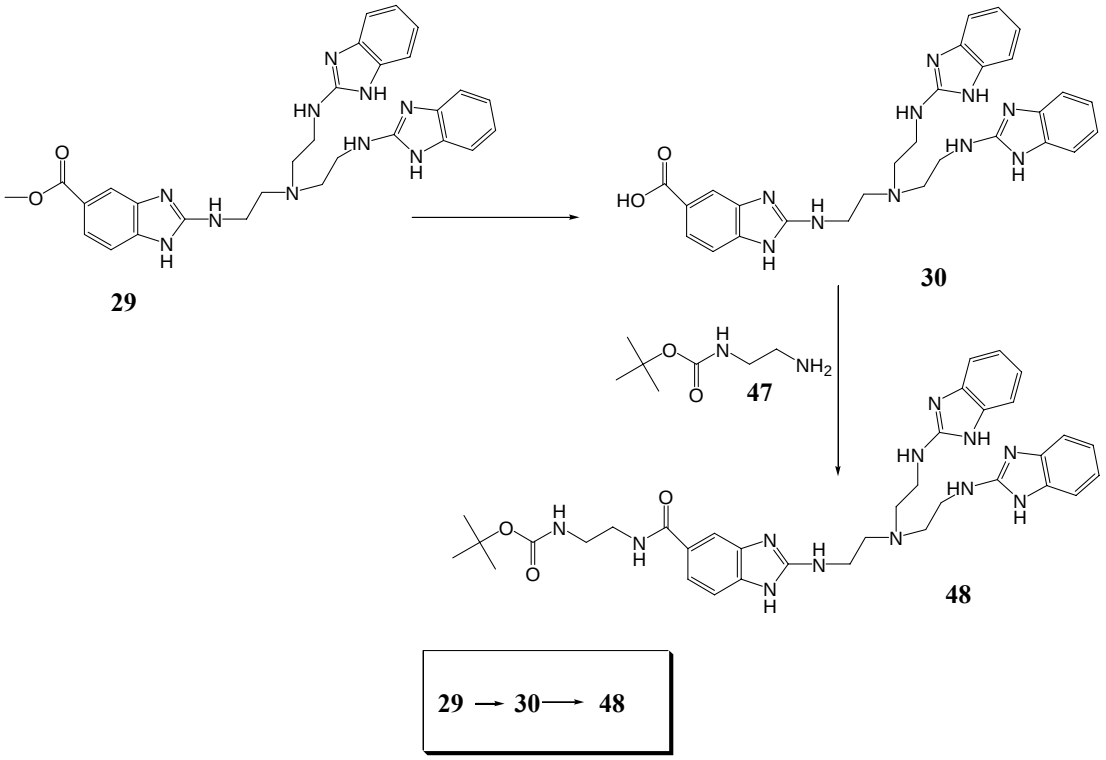

Methyl ester **29** (230 mg, 0.42 mmol) was refluxed in 25 ml of 6 M HCl for 2 h, the solvent was removed under reduced pressure. NMR and ESI spectrometry confirmed the complete formation of **30**. The crude was used for the next step.

^{1}H-NMR (250 MHz, MeOD-d_4) δ: 3.90 (*m*, 6H, CH_2N); 4.19 (*m*, 6H, CH_2N); 7.28 (*m*, 4H, Ar-H); 7.38 (*m*, 4H, Ar-H); 7.44 (m, 1H, Ar-H); 7.97 (*m*, 1H, Ar-H); 7.99 (*m*, 1H, Ar-H).

ESI-MS m/z: calcd for $C_{28}H_{31}N_{10}O_2$ ($M+H^+$) 538.3. Found 539.2 ($M+H^+$).

To a solution of the carboxylic acid **30** (0.42 mmol) in anhydrous DMF (10 mL), Et_3N (500 µl), DIC (80 mg, 0.63 mmol), HOBT (85 mg, 0.63 mmol) and **47** (101 mg, 0.63 mmol) were added. The reaction was stirred at room temperature for

18 h. The solvent was evaporated by distillation in the kugelrohr, and the solid residue was purified by silica gel column chromatography (CH_2Cl_2/MeOH/aqueous NH_3 55/4/1 %), giving 180 mg (63 %) of **48** as pink amorphous solid.

^{1}H-NMR (250 MHz, MeOD-d_4) δ: 1.46 (*s*, 9H, CH_3); 2.85 (*m*, 6H, CH_2); 3.22 (*t*, *J*=6.3, 2H, CH_2); 3.31 (*m*, 2H, CH_2); 3.46 (*m*, 6H, CH_2); 6.95 (*m*, 4H, Ar-H); 7.14 (*m*, 5H, Ar-H); 7.49 (*dd*, *J*=8.3, *J*=1.3, 1H, Ar-H); 7.63 (*m*, 1H, Ar-H).

IR (KBr): 3328*m*, 2975*w*, 1686*m*, 1636*s*, 1603*s*, 1578*s*, 1534*m*, 1465*s*, 1390*w*, 1365*m*, 1272*s*, 1165*m*, 1056*w*, 742*s*, cm^{-1}.

ESI-MS m/z: calcd for $C_{35}H_{45}N_{12}O_3$ ($M+H^+$) 681.4. Found 681.3 ($M+H^+$).

9.3.14 {6-[3-(2-Amino-phenyl)-thioureido]-hexyl}-carbamic acid *tert*-butyl ester (41)

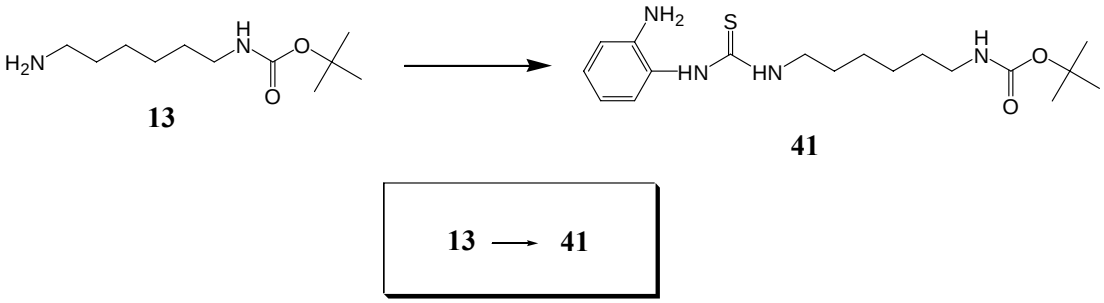

13 **41**

13 ⟶ **41**

A solution of amine **13** (3.00 g, 13.89 mmol) in 20 mL acetonitrile was added dropwise to a mixture of 1,1'-thiocarbonyldiimidazole (3.21 g, 18.1 mmol) and imidazole (0.200 g, 2.94 mmol) in acetonitrile (30 mL) at 0 °C. The reaction mixture was stirred at room temperature for 1 h. 1,2-Phenylenediamine (2.16 g, 20.0 mmol) was dissolved in 10 mL acetonitrile and was added dropwise to the reaction mixture. The reaction solution was stirred at 50 °C for 4 h and at room temperature over night. The solvent was removed and the crude material purified by silica gel chromatography (ethyl acetate/hexane 1/3) yielding 2.80 g (55 %) of **41** as pale amorphous solid.

^{1}H-NMR (250 MHz, DMSO-d_6) δ: 1.12−1.50 (*m*, 17H, 4CH_2, 3CH_3); 2.89 (*m*, 2H, CH_2NC=O); 3.40 (*m*, 2H, CH_2NC=S); 4.79 (*s*, 2H, NH_2); 6.56 (*dt*, *J*=7.5, *J*=1.4, 1H, Ar-H); 6.75 (*m*, 2H, NHC=O and Ar-H); 6.97 (*m*, 2H, Ar-H); 7.22 (*s*, 1H, NHC=S); 8.73 (*s*, 1H, Ar-NH).

IR (KBr): 3407*m*, 3283*s*, 3144*s*, 2974*m*, 2934*s*, 2855*w*, 1707*s*, 1690*s*, 1618*w*, 1540*s*, 1509*s*, 1495*s*, 1453*w*, 1390*w*, 1365*m*, 1302*w*, 1251*s*, 1170*s*, 1040*w*, 854*w*, 752*m*, 707*w*, 644*w*, 607*w* cm^{-1}.

ESI-MS m/z: calcd for $C_{18}H_{31}N_4O_2S$ ($M+H^+$) 367.2. Found 367.2 ($M+H^+$).

Anallysis: $C_{18}H_{30}N_4O_2S$ (366.5) calculated: C 58.98 H 8.25 N 15.29.
found: C 59.02 H 8.24 N 15.36.

M.p.: 115-116 °C.

9.3.15 [6-(1*H*-Benzoimidazol-2-ylamino)-hexyl]-carbamic acid *tert*-butyl ester (42)

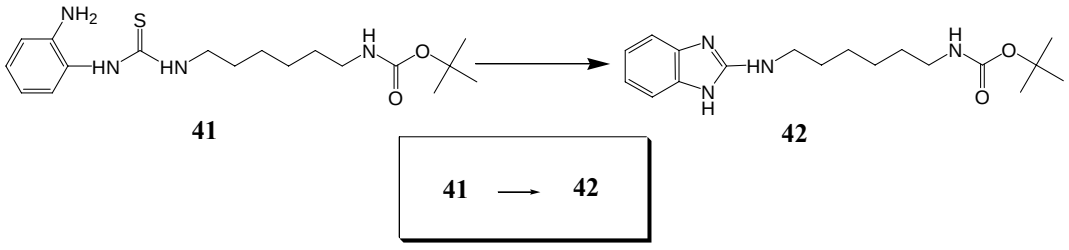

To a refluxing solution of thiourea **41** (2.00 g, 5.46 mmol) in abs. EtOH (50 mL) containing a catalytic amount of sulphur, yellow HgO (3 g, 13.9 mmol) was added over 1 h in several portions. The mixture was filtered through celite® and the solvent removed under reduced pressure. The crude material was purified by silica gel chromatography (Hexane/EtOAc/Et_3N 3/1/1 %) yielding 1.7 g (95 %) of **42** as white solid.

100 mg of product were crystallized from CH_2Cl_2 for full characterization.

^{1}H-NMR (250 MHz, DMSO-d_6) δ: 1.20–1.62 (*m*, 17H, 4CH_2, 3CH_3); 2.90 (*m*, 2H, CH2NC=O); 3.24 (*m*, 2H, CH_2N-Ar); 6.49 (*t*, *J*=5.7, 1H, NHC=O); 6.76 (br. *t*, 1H, NH-Ar); 6.84 (*m*, 2H, Ar-H); 7.09 (*m*, 2H, Ar-H); 10.64 (*s*, 1H, NHAr).

IR (KBr): 3438*w*, 3371*m*, 2929*m*, 2857*w*, 1685*s*, 1637*w*, 1626*w*, 1584*s*, 1519*s*, 1465*w*, 1365*w*, 1277*m*, 1256*w*, 1209*w*, 1179*w*, 969*w*, 916*w*, 850*w*, 760*w*, 750*w*, 670*w* cm^{-1}.

ESI-MS m/z: calcd for $C_{18}H_{29}N_4O_2$ ($M+H^+$) 333.2. Found 333.0 ($M+H^+$).

Analysis: $C_{18}H_{28}N_4O_2$ (332.4) calculated: C 65.03 H 8.49 N 16.85.
found: C 64.78 H 8.34 N 17.00.

M.p.: 159-160 °C.

9.3.16 8-Acetylsulfanyl-octanoic acid (43)

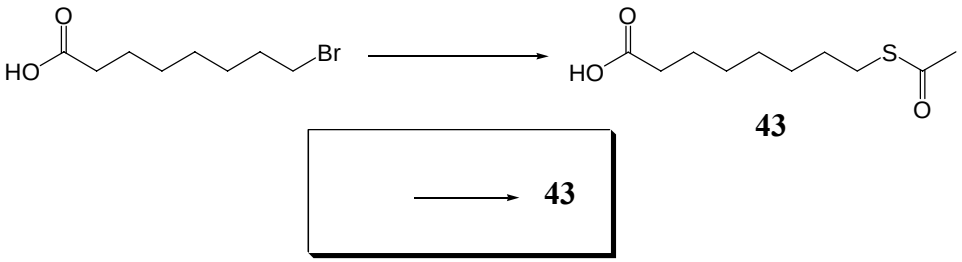

To 160 mL of MeOH 850 mg of Na (36.9 mmol) were added. After the development of H_2 had terminated, it was added in the follwing order: thioacetic acid (2.90 g, 38.1 mmol), 8-bromooctanoic acid (4.00 g, 17.9 mmol). The reaction was stirred under argon, at 80 °C for 15 h. The mixture was diluted with 15 g of ice, treated with HCl 6 M until pH 3 and extracted with CH_2Cl_2 (3×40 mL). The collected organic phases were washed with brine (3×40 mL) and a saturated solution of $NaHCO_3$ (3×40 mL). The organic layer was dried over Na_2SO_4, filtrated and evaporated. The oil obtained was purified on silica gel column chromatography (Hexane/EtOAc 1/1), giving 3.2 g (82 %) of **43** as yellow viscous product.

R*f* (Hexane/AcOEt 3/2) = 0.73.

^{1}H-NMR (250 MHz, $CDCl_3$) δ: 1.30 (*m*, 6H, $3CH_2$); 1.56 (*m*, 4H, $2CH_2$); 2.28 (*s*, 3H, CH_3); 2.30 (*t*, *J*=7.3, 2H, CH_2C=O); 2.82 (*t*, *J*=7.3, 2H, CH_2-S), 9.50 (br. *s*, 1H, COOH).

IR (KBr): 2932*m*, 2857*w*, 1707*s*, 1693*s*, 1413*w*, 1354*w*, 1280*w*, 1135*m*, 954*m*, 671*m*, 628*m* cm^{-1}.

ESI-MS m/z: calcd for $C_{10}H_{18}O_3S$ ($M+H^+$) 219.1. Found 218.7 ($M+H^+$).

Analysis: $C_{10}H_{18}O_3S$ (218.3) calculated: C 55.02 H 8.31.
found: C 54.83 H 8.29.

9.3.17 Thioacetic acid *S*-{7-[6-(1*H*-benzoimidazol-2-ylamino)-hexylcarbamoyl]-heptyl} ester (45)

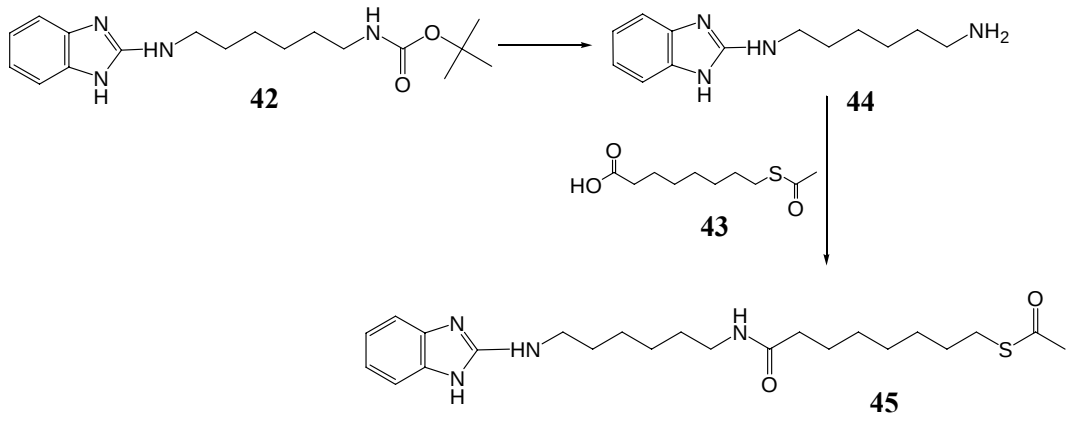

42 → **44** → **45**

To a solution of **42** (1.00 g, 3.01 mmol) in MeOH (20 mL) were added 2 mL of 1 M HCl, the reaction was stirred at room temperature for 2 h and the solvent was removed under reduced pressure. The Boc hydrolysis and the formation of **44** was

confirmed by NMR and ESI spectrometry, and the crude product was used for the next step.

^{1}H-NMR (250 MHz, DMSO-d_6) δ: 1.37 (*m*, 4H, $2CH_2$); 1.59 (*m*, 4H, $2CH_2$); 2.76 (*m*, 2H, CH_2 N); 3.43 (*m*, 2H, CH_2N-Ar); 7.20 (*m*, 2H, Ar-H); 7.39 (*m*, 2H, Ar-H) 8.00 (br. *s*, 3H, NH_3); 9.21 (*t*, *J*=5.7, 1H, NH-Ar); 12.90 (br. *s*, 2H, $1NHAr^+$).

ESI-MS m/z: calcd for $C_{13}H_{21}N_4^+$ ($M+H^+$) 233.2. Found: 232.9 ($M+H^+$).

To a solution of **43** (1 g, 4.58 mmol) in anhydrous DMF (10 mL), were added Et_3N (1 mL), DIC (578 mg, 4.58 mmol), HOBT (619 mg, 4.58 mmol) and the amine hydrochloride **44** (3.01 mmol). The reaction was stirred at room temperature for 18 h. The solvent was evaporated by kugelrohr distillation, and the solid residue was purified on silica gel column chromatography (CH_2Cl_2/MeOH/aqueous NH_3 45/4/0.15), giving 683 mg (52 %) of **45** as pale solid.

R*f* (CH_2Cl_2/MeOH/aqueous NH_3 45/4/0.15) = 0.62.

^{1}H-NMR (250 MHz, $CDCl_3$) δ: 1.17-1.69 (*m*, 18H, $9CH_2$); 2.19 (*t*, *J*=5.7, 2H, CH_2=O); 2.31 (*s*, 3H, CH_3); 2.84 (*t*, *J*=7.3, 2H, CH_2-S); 3.17 (*m*, 2H, CH_2NC=O); 3.39 (*t*, *J*=6.7, 2H, CH_2N); 5.42 (br. *s*, 1H, NH-Ar); 5.96 (br. *t*, *J*=5.9, 1H, NHC=O); 7.02 (*m*, 2H, Ar-H); 7.27 (*m*, 2H, Ar-H); 8.45 (br. *s*, 1H, NHAr).

IR (KBr): 3417*m*, 3299*m*, 3054*w*, 2933*s*, 2858*m*, 1692*s*, 1638*s*, 1601*s*, 1586*s*, 1542*s*, 1478*m*, 1462*s*, 1420*w*, 1353*w*, 1253*m*, 1207*w*, 1132*w*, 1051*w*, 1015*w*, 953*w*, 753*m*, 728*w*, 629*w* cm^{-1}.

ESI-MS m/z: calcd for $C_{23}H_{37}N_4O_2S$ ($M+H^+$) 433.3. Found 433.2 ($M+H^+$).

Analysis: $C_{23}H_{36}N_4O_2S$ (432.6) calculated: C 63.85 H 8.39 N 12.95.
found: C 63.59 H 8.36 N 13.05.

M.p.: 119-120 °C.

9.3.18 1-(2-Amino-phenyl)-3-(2-dimethylamino-ethyl)-thiourea (52).

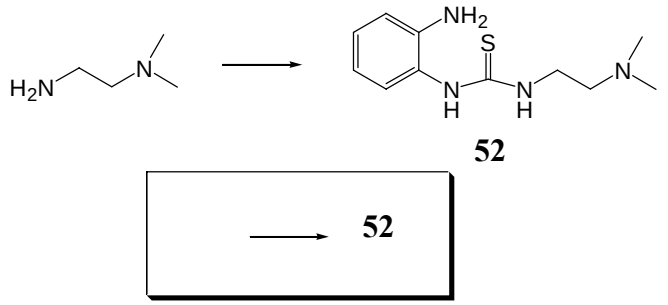

A solution of 2-dimethylaminoethylamine (1 g, 11.3 mmol) in 20 mL acetonitrile was added dropwise to a mixture of 1,1'-thiocarbonyldiimidazole (3.03 g, 17.0 mmol) and imidazole (0.200 g, 2.94 mmol) in acetonitrile (30 mL) at 0 °C. The reaction mixture was stirred at room temperature for 1 h. 1,2-P henylenediamine (1.84 g, 17.0 mmol) was dissolved in 10 mL acetonitrile and added dropwise to the reaction mixture. The solution was stirred at 50 °C for 4 h and at room temperature over night. After removal of the solvent the solid residue was purified on silica gel column chromatography (EtOAc/MeOH/Et_3N 84/16/1), giving 1.86 g (69 %) of **52** as pale solid.

R*f* (EtOAc/MeOH/Et_3N 84/16/1) = 0.2.

^{1}H-NMR (250 MHz, DMSO-d_6) δ: 2.18 (*s*, 6H, $2CH_3$); 2.42 (*t*, *J*=6.5, 2H, CH_2); 3.53 (*m*, 2H, CH_2NC=S); 4.83 (*s*, 2H, NH_2); 6.55 (*dt*, *J*=7.6, *J*=1.4, 1H, Ar-H); 6.74 (*dd*, *J*=7.8, *J*=1.0, 1H, Ar-H); 6.93-6.99 (*m*, 2H, Ar-H); 7.22 (*s*, 1H, NH); 9.00 (*s*, 1H, NH-Ar).

IR (KBr): 3403*m*, 3282*m*, 3250*m*, 3150*s*, 2931*m*, 2947*m*, 2823*w*, 2780*w*, 1618*m*, 1543*s*, 1508*s*, 1494*s*, 1456*m*, 1317*w*, 1299*w*, 1264*s*, 1236*s,* 1172*w*, 1158*m*, 1114*w*, 1063*m*, 1044*m*, 1022*s*, 868*w*, 857*w*, 790*w*, 749*s*, 707*w*, 646*m*, 613*m*, 572*w* cm^{-1}.

ESI-MS m/z: calcd for $C_{11}H_{19}N_4S$ ($M+H^+$) 239.13. Found 238.7 ($M+H^+$).

Analysis: $C_{11}H_{18}N_4S$ (238.4) calculated: C 55.43 H 7.61 N 23.51.
found: C 53.83 H 7.49 N 23.02.
0.4 H_2O (245.6) calculated: C 53.80 H 7.72 N 22.82.

9.3.19 *N'*-(1*H*-Benzoimidazol-2-yl)-*N,N*-dimethyl-ethane-1,2-diamine (54)

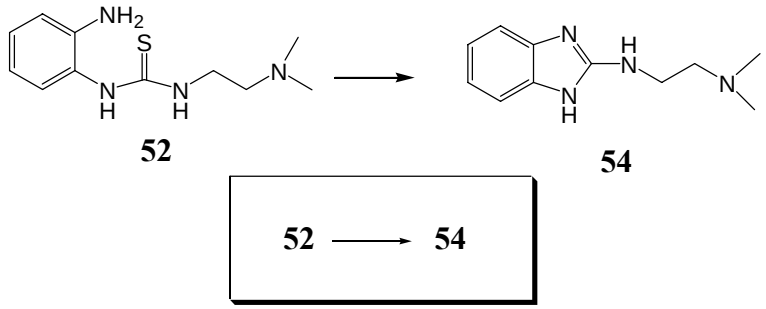

To a refluxing solution of thiourea **52** (1.8 g, 7.55 mmol) in abs. EtOH (50 mL) containing a catalytic amount of sulphur, yellow HgO (3.0 g, 13.9 mmol) was added over 1 h in several portions. The mixture was filtered through celite and the solvent removed at reduced pressure. The crude material was purified by silica gel chromatography (CH_2Cl_2/MeOH/aqueous NH_3 45/4/0.15). The compound was further crystallized from EtOAc yielding 1.4 g (91 %) of **54** as white solid.

R*f* (CH_2Cl_2/MeOH/ aqueous NH_3 45/4/1 %) = 0.39.

^{1}H-NMR (250 MHz, DMSO-*d*$_6$) δ: 2.18 (*s*, 6H, $2CH_3$); 2.45 (*t*, *J*=6.5, 2H, CH_2); 3.38 (*m*, 2H, CH_2); 6.34 (br. *t,* 1H, NH-Ar); 6.85 (*m*, 2H, Ar-H); 7.12 (*m*, 2H, Ar-H); 10.72 (*s*, 1H, HNAr).

^{13}C-NMR (75 MHz, $CDCl_3$) δ: 41.08, 45.19, 59.72, 112.19, 120.16, 138.51, 156.81.

IR (KBr): 3401*s*, 3191*m*, 2940*s*, 2819*s*, 1637*s*, 1602*s*, 1465*s*, 1465*s*, 1409*m*, 1362*m*, 1333*w*, 1309*w*, 1265*s*, 1186*m*, 1159*m*, 1118*m*, 1079*w*, 1059*m*, 1046*s*, 1013*s*, 997*w*, 959*w*, 914*w*, 858*m*, 788*w*, 760*m*, 745*s*, 723*m*, 668*w*, 616*w* cm^{-1}.

ESI-MS m/z: calcd for $C_{11}H_{17}N_4$ ($M+H^+$) 205.1. Found 204.9 ($M+H^+$).

M.p.: 147-149 °C.

9.3.20 S-(2-Pyridylthio) cysteamine Dihydrochloride (58)

Aldrithiol-2™ (2.21 g, 10.0 mmol) was dissolved in 20 ml of methanol and 0.8 mL of acetic acid. Into this mixture a solution of 2-amino-ethanethiol hydrochloride (570 mg, 5.0 mmol) in 10 ml of methanol was added over a period of 30 min. The reaction was stirred for 24 h at room temperature under argon. After the evaporation of the solvent, the oil obtained was washed twice with 20 ml of diethyl ether, the crude was dissolved in 5 mL of methanol, and the product precipitated twice, with 25 ml of diethyl ether each time, giving 868 mg (67 %) of **58** as white crystals.

^{1}H-NMR (250 MHz, MeOD-*d*$_6$) δ: 3.15 (*t*, *J*=6.5, 2H, CH_2); 3.30 (*m*, overlap with solvent signal, 2H, CH_2) 7.34 (*m*, 1H, Py-H); 7.68 (*m*, 1H, Py-H); 7.82 (*m*, 1H, Py-H); 8.56 (*m*, 1H, Py-H).

IR (KBr): 2953*s*, 2911*s*, 1608*m*, 1575*m*, 1558*m*, 1449*s*, 1417*m*, 1328*m*, 1245*w*, 1113*m*, 1040*m*, 948*w*, 870*m*, 811*m*, 765*s*, 713*w* cm^{-1}.

ESI-MS m/z: calcd for $C_7H_{11}N_2S_2^+$ ($M+H^+$) 187.0. Found 186.7 ($M+H^+$).

Analysis: $C_7H_{12}Cl_2N_2S_2$ (259.2) calculated: C 32.43 H 4.67 N 10.81.
found: C 31.35 H 4.76 N 10.47.
0.5 H_2O (268.2) calculated: C 31.35 H 4.89 N 10.44.

9.3.21 6-*S*-Trityl-6-mercapto-1-hexanol (61)

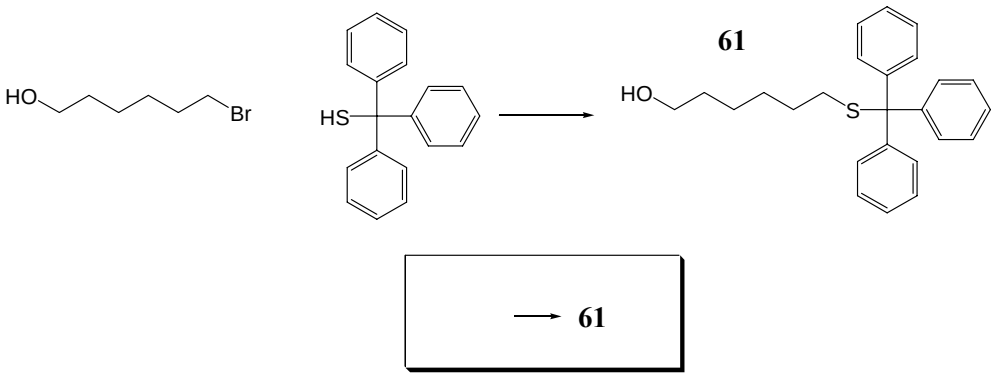

Triphenylmethyl mercaptan (2 g, 7.2 mmol) was added to a mixture of NaH (637 mg, 60 % in mineral oil 15.9 mmol) in DMF (40 mL) at 0 °C in 30 min. It was then added 6-bromo-1-hexanol (1.4 g, 7.7 mmol) and the reaction was stirred at room temperature for 16 h. To the mixture were added 50 mL of water, and 50 mL of $CHCl_3$; the extracted organic phase was washed with 3×50 mL of brine. The organic layer was evaporated, and the crude product purified by silica gel chromatography (hexane/ethyl acetate 5/1), affording 2.1 g (78 %) of **61** as colourless solid.

^{1}H-NMR (250 MHz, DMSO-*d*$_6$) δ: 1.09-1.37 (*m*, 8H, CH_2); 2.09 (*t*, *J*=7.1, 2H, CH_2-S); 3.32 (*m*, 2H, CH_2-O); 4.29 (*s*, 1H, OH); 7.21-7.38 (*m*, 15H, Ar-H).

IR (KBr): 3318*m*, 2931*s*, 2853*m*, 1593*w*, 1487*m*, 1440*s*, 1180*w*, 1051*w*, 1033*w*, 753*m*, 742*s*, 699*s*, 625*m*, 506*w* cm^{-1}.

Analysis: $C_{25}H_{28}OS$ (376.6) calculated: C 79.74 H, 7.49 O, 4.25 S, 8.52.
found: C 79.51 H, 7.69.

M.p.: 73-75 °C.

9.3.22 Diisopropyl-phosphoramidous acid 2-cyano-ethyl ester 6-tritylsulfanyl-hexyl ester (62)

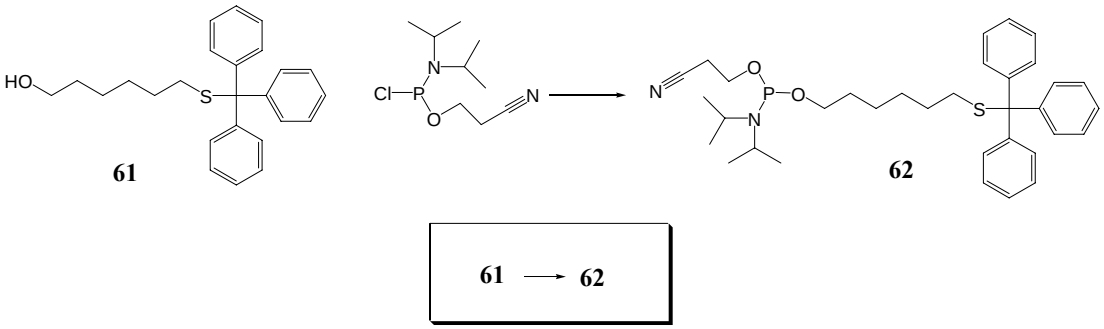

61 (1 g, 2.7 mmol) was dissolved in 10 mL of anhydrous CH_2Cl_2. To this solution were added in the following order: diisopropylethylamine (855 µL, 5 mmol) and 2-cyanoethoxy diisopropylchlorophosphoramidite (753 mg, 3.2 mmol). The reaction was stirred at room temperature under argon for 2 h. The crude material was poured onto 50 mL of ethyl acetate and the organic phase was washed twice with 40 mL of saturated $NaHCO_3$ solution. The extracted organic layer was dried with $MgSO_4$, the solvent removed under reduced pressure, and the phosphoramide was purified by silica gel chromatography (hexane/ethyl acetate/Et_3N 5/1/1 %), giving 1.3 g (83 %) of **62** as colourless oil.

^{1}H-NMR (400 MHz, CD_2Cl_2) δ: 1.19-1.36 (*m*, 16H, CH_2, CH3); 1.44 (*m*, 2H, CH_2βS); 1.57 (*m*, 2H, CH_2βO); 2.19 (*t*, *J*=7, 2H, CH_2S); 2.64 (*t*, *J*=6.5, 2H, CH_2CN); 3.51-3.74 (*m*, 4H, CH_2O, CH); 3.76-3.90 (*m*, 2H, CH_2βCN); 7.23-7.48 (*m*, 15H, Ar-H).

^{31}P NMR (161.98 MHz, DMSO-d_6) δ: 147.64.

IR (KBr): 2965*s*, 2253*m*, 1594*m*, 1444*s*, 1363*s*, 1183*s*, 975*s*, 892*m*, 699*s*, 621*m* cm^{-1}.

Analysis: $C_{34}H_{45}N_2O_2PS$ (576.8) calculated: C 70.80 H 7.86 N 4.86 O 5.55 P 5.37 S 5.56.
found: C 70.59 H 7.88 N 4.79.

ESI-MS m/z: calcd for $C_{34}H_{46}N_2O_2PS$ ($M+H^+$) 577.3. Found 577.4 ($M+H^+$), 599.3 ($M+Na^+$), 615.1 ($M+K^+$).

9.3.23 2-(2-{Bis-[2-(1*H*-benzoimidazol-2-ylamino)-ethyl]-amino}-ethylamino)-3*H*-benzoimidazole-5-carboxylic acid [2-(pyridin-2-yldisulfanyl)-ethyl]-amide (63)

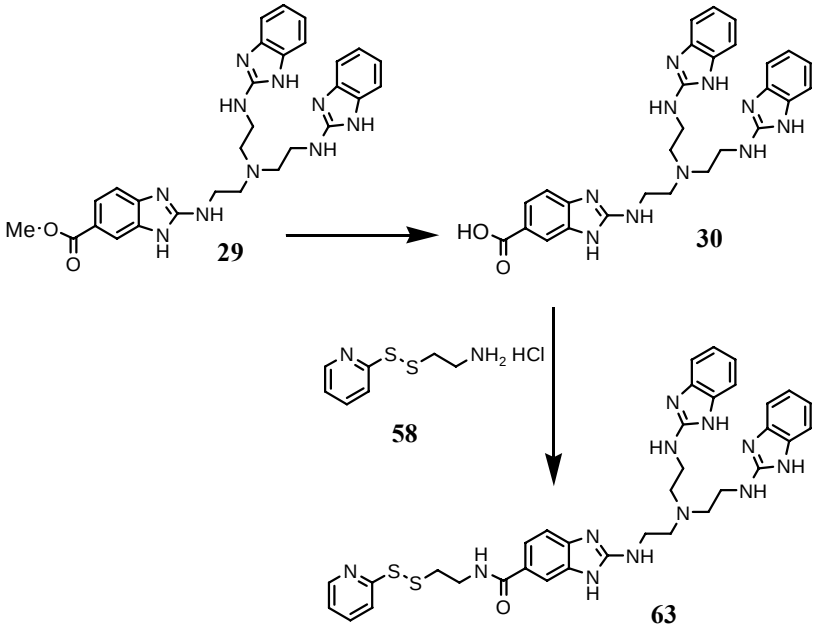

29 (200 mg, 0.36 mmol) was refluxed in 25 mL of HCl 6 M for 2 h, the solvent was removed under reduced pressure. The complete formation of **30** was confirmed by NMR and ESI spectrometry. The crude was used for the next step.

^{1}H-NMR (250 MHz, MeOD-d_4) δ: 3.90 (*m*, 6H, CH_2N); 4.19 (*m*, 6H, CH_2N); 7.28 (*m*, 4H, Ar-H); 7.38 (*m*, 4H, Ar-H); 7.44 (m, 1H, Ar-H); 7.97 (*m*, 1H, Ar-H); 7.99 (*m*, 1H, Ar-H).

ESI-MS m/z: calcd for $C_{28}H_{31}N_{10}O_2^+$ ($M+H^+$) 539.3. Found 539.2 ($M+H^+$).

To a solution of the carboxylic acid **30** (0.36 mmol) in anhydrous DMF (10 mL), were added Et_3N (500 µL), DIC (68 mg, 0.54 mmol), HOBT (73 mg, 0.54 mmol)

and **58** (104 mg, 0.47 mmol). The reaction was stirred at room temperature for 18 h. The solvent was evaporated by kugelrohr distillation, and the solid residue was purified on silica gel column chromatography (CH_2Cl_2/MeOH/aqueous NH_3 55/4/1 %), giving 80 mg (31 %) of **63** as pink amorphous solid.

^{1}H-NMR (250 MHz, MeOD-d_6) δ: 2.87 (*t*, *J*=6, 6H, CH_2N); 3.06 (*t*, *J*=6.5, 2H, CH_2S); 3.46 (*t*, *J*=6, 6H, CH_2N); 3.67 (*t*, *J*=6.5, 2H, CH_2N-C=O); 6.93-7.19 (*m*, 9H, Ar-H, 1H, Py-H); 7.47 (*m*, 1H, Py-H); 7.59-7.83 (*m*, 3H, Ar-H, 1H, Py-H); 8.36 (*m*, 1H, Py-H).

IR (KBr): 3280*s*, 2965*m*, 1633*s*, 1602*s*, 1578*s*, 1464*s*, 1417*w*, 1355*w*, 1270*m*, 1162*w*, 1115*w*, 1049*w*, 878*w*, 827*w*, 740*m* cm^{-1}.

ESI-MS m/z: calcd for $C_{35}H_{39}N_{12}OS_2^+$ ($M+H^+$) 707.3. Found 707.4 ($M+H^+$).

9.3.24 Synthesis of conjugates 1000, 1001, 1002 and 1006 via disulfide linkage linker chemistry

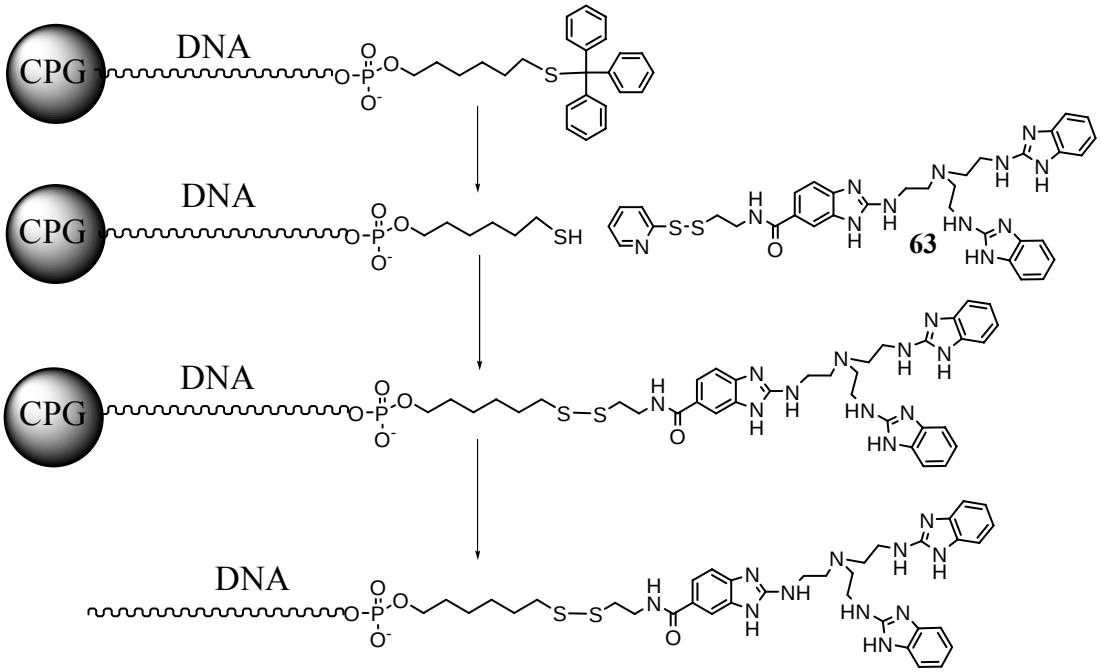

catalyst-linker-$^{5'}$TCGGCAGTCGGCTAG$^{3'}$ **Oligo1000**

catalyst-linker-$^{5'}$GATCGGCAGTCGGCTAG$^{3'}$ **Oligo1001**

catalyst-linker-$^{5'}$CGAGATCGGCAGTCGGCTAG$^{3'}$ **Oligo1002**

catalyst-linker-$^{5'}$CTCCTGACAAGGTAT$^{3'}$ **Oligo1006**

The oligonucleotides were assembled on an Applied Biosystems Model 381A DNA synthesizer with 2-cyanoethyl phosphoramidites (Proligo) and the thio linker building block **62** (1 μmol scale). All subsequent steps were done manually with the cartridge removed from the synthesizer. To detritylate the thio linker, the support carrying the fully protected DNA was treated for 10 min with 1 mL of 0.1 M aqueous $AgNO_3$ solution, followed by washing steps with 10 mL of H_2O and finally with 10 mL of CH_3CN. Disulfide bonds were then reduced by treatment with 1 mL of 0.1 M aqueous tris(2-carboxyethyl)phosphine (TCEP) over 10 min. Two washing steps with 10 mL of H_2O and with 10 mL of CH_3CN followed. The cartridge was now agitated for 12 h at room temperature with a solution of compound **63** (23.5 mg, 0.033 mmol in 300 μL DMF), followed by washing steps with 10 mL of DMF and 10 mL of CH_3CN. Afterwards the solid phase was collected in an Eppendorf tube,

treated with 1.5 mL 25 % aqueous ammonia and agitated at room temperature for 24 h. The solution obtained was filtrated through a syringe filter (rotilabo® PVDF 0.22 µm), and evaporated in a Speed Vac. The crude material was dissolved in 1 mL of H_2O, and the solution was desalted on a NAP^{TM}-10 column (Amersham Biosciences). The oligonucleotide conjugates were purified by denaturing PAGE and characterized by MALDI mass spectrometry.

Oligo 1000

MALDI-MS m/z: calcd. for **1000** ($M+H^+$) 5402. Found 5403 ($M+H^+$).

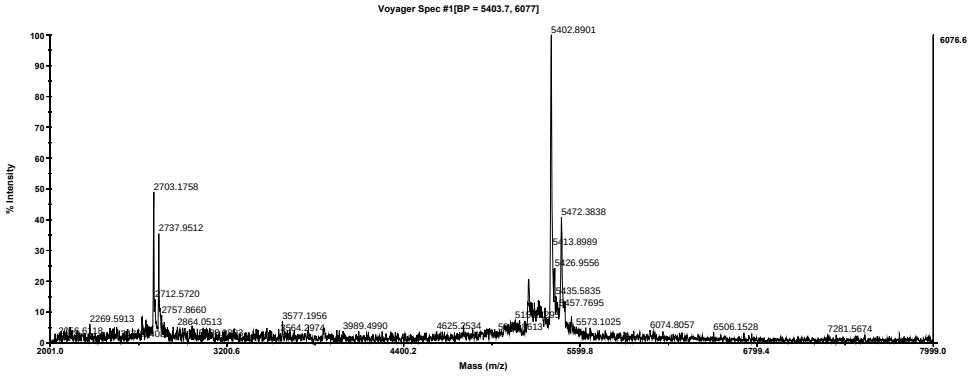

Oligo 1001

MALDI-MS m/z: calcd. for **1001** ($M+H^+$) 6044. Found 6042 ($M+H^+$).

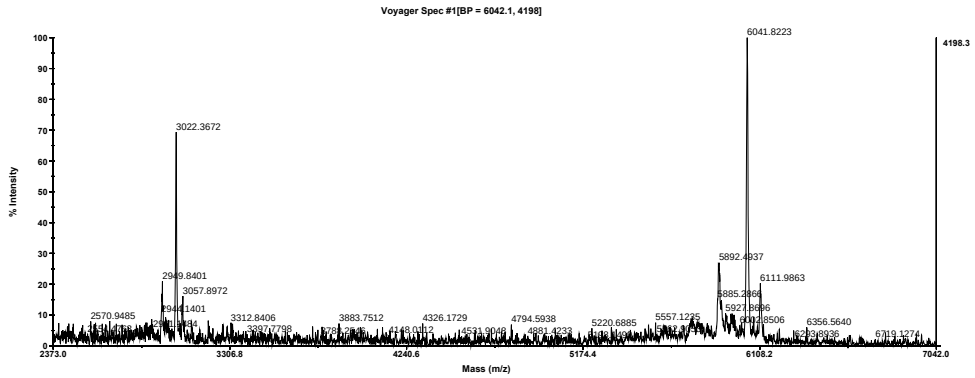

Oligo 1002

MALDI-MS m/z: calcd for **1002** ($M+H^+$) 6976. Found 6973.

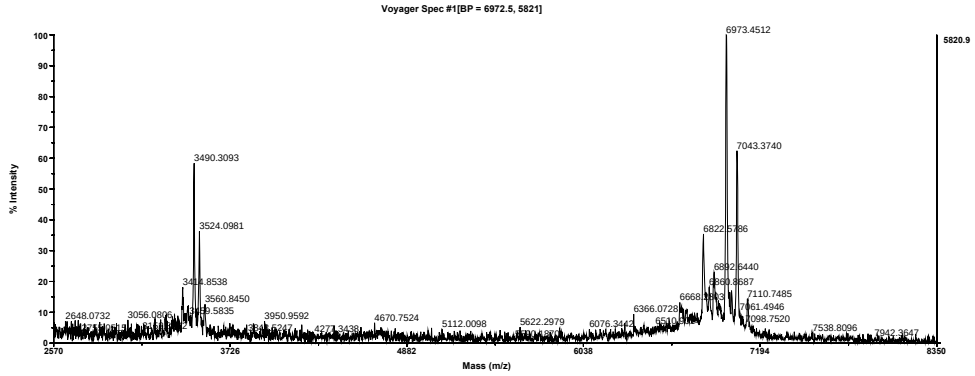

Oligo 1006

MALDI-MS m/z: calcd for **1006** ($M+H^+$) 5345. Found 5351.

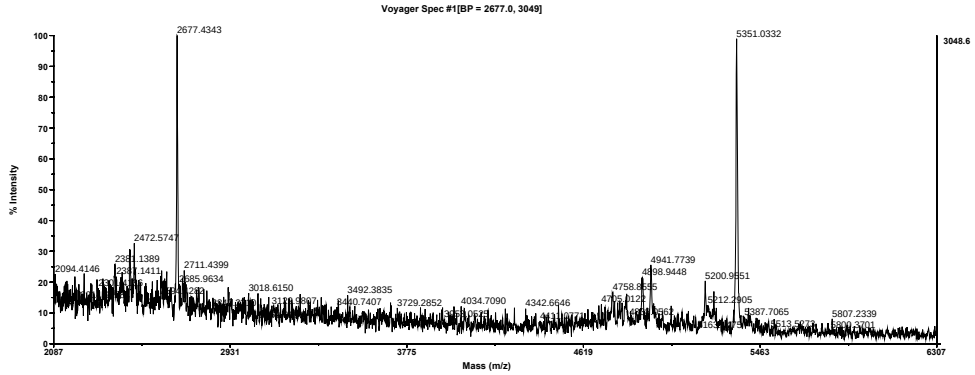

9.3.25 Synthesis of PNA conjugate 1011 via amino linker chemistry

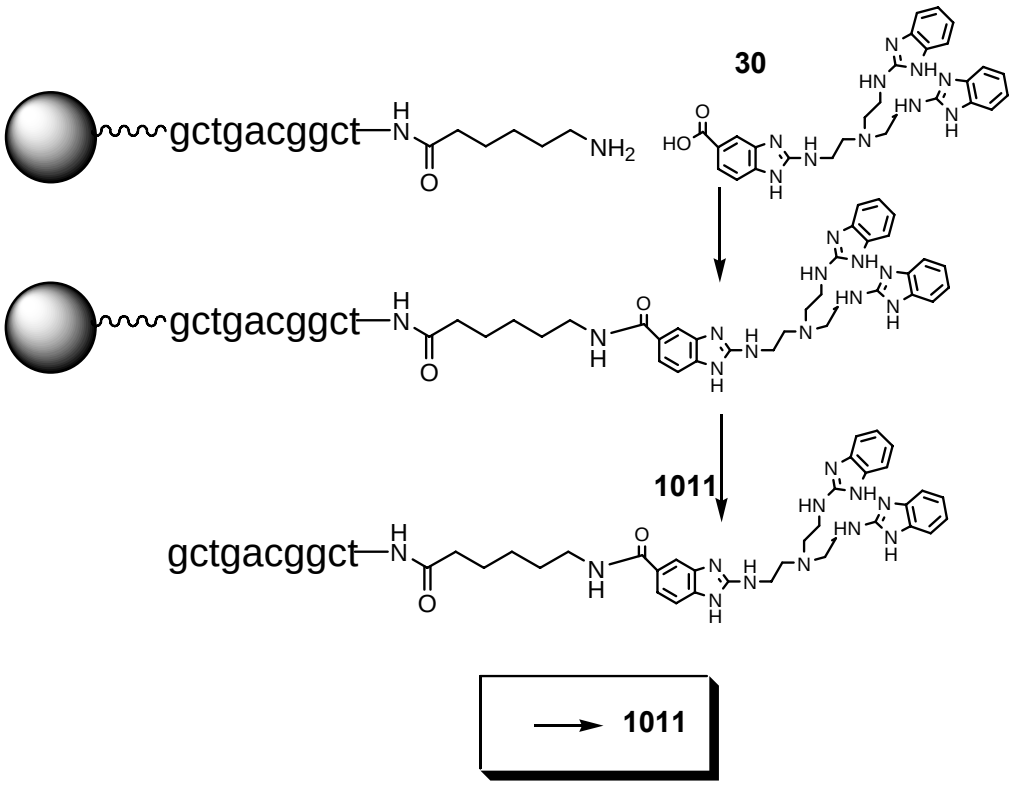

The PNA 10mer on solid phase was purchased in a 1 μmol scale by Eurogentec with the C_6 amino linker already deprotected. The trisbenzimidazole carboxylic acid **30** was obtained from methyl ester **29** (25 mg, 0.045 mmol) as already reported. Conjugate **1012** was prepared manually in the following way: All solutions were pumped through the cartridge by tightly fitting two 1 mL syringes (Luer fittings) to each side of the column and moving the pistons alternatingly. (45 μmol) of carboxylic acid **30**, 7.5 mg (49 μmol) *N*-hydroxybenztriazole mono hydrate and 6.2 mg (49 μmol) diisopropyl carbodiimide were dissolved in 1 mL DMF alkalized with three drops of NEt_3. The coupling solution was thoroughly agitated through the cartridge with the C_6-aminolinker-PNA over 5 h. The cartridge was then rinsed onece with DMF (10 mL) and once with CH_3CN (10 mL). The conjugate was cleaved from the solid support by agitating a mixture of 95%TFA/m-cresol 4:1 (200 μL, 90 min.) through the column.

To the mixture collected from the resin, was added diethyl ether (5 mL) and under vortexing the PNA precipitated. The precipitate was washed two more times with diethyl ether, and dried. The mass confirmed the successful conjugation.

MALDI-MS m/z: calcd for **1011** ($M+H^+$) 3375.41. Found 3374.65 ($M+H^+$).

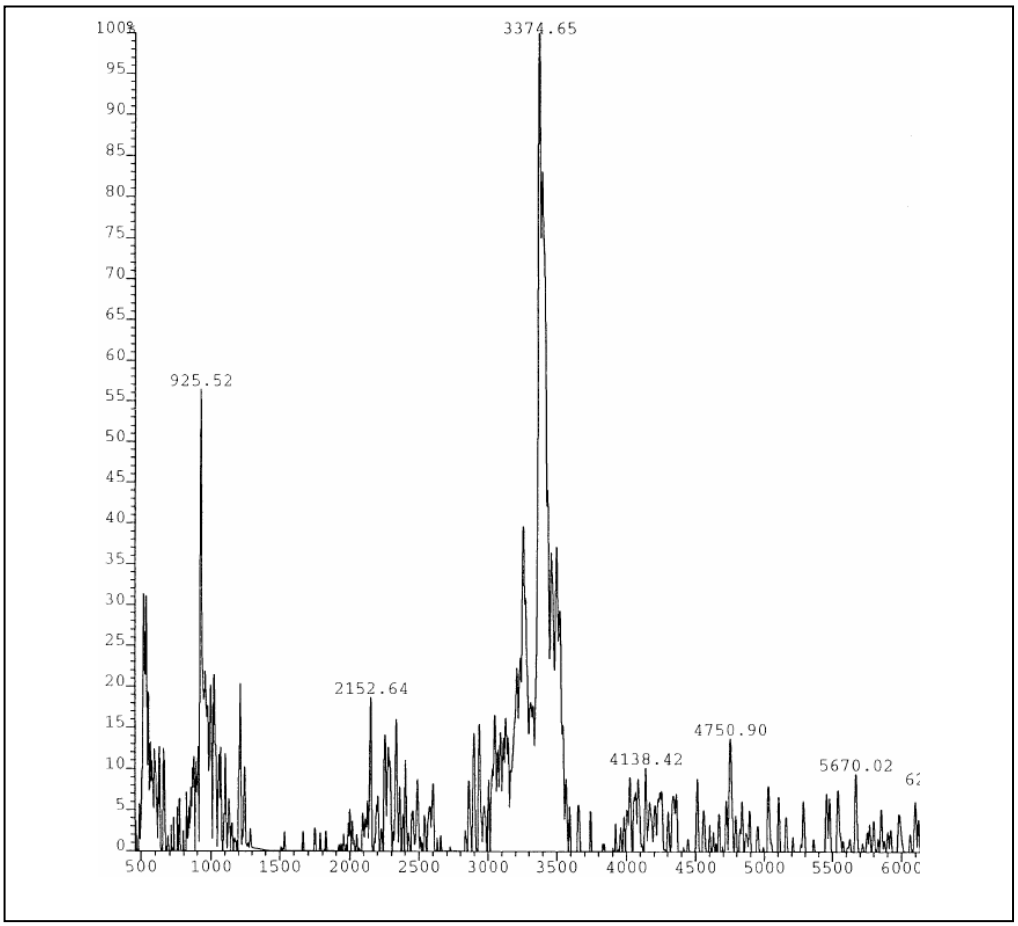

9.3.26 Synthesis of conjugate 1012 via amino linker chemistry

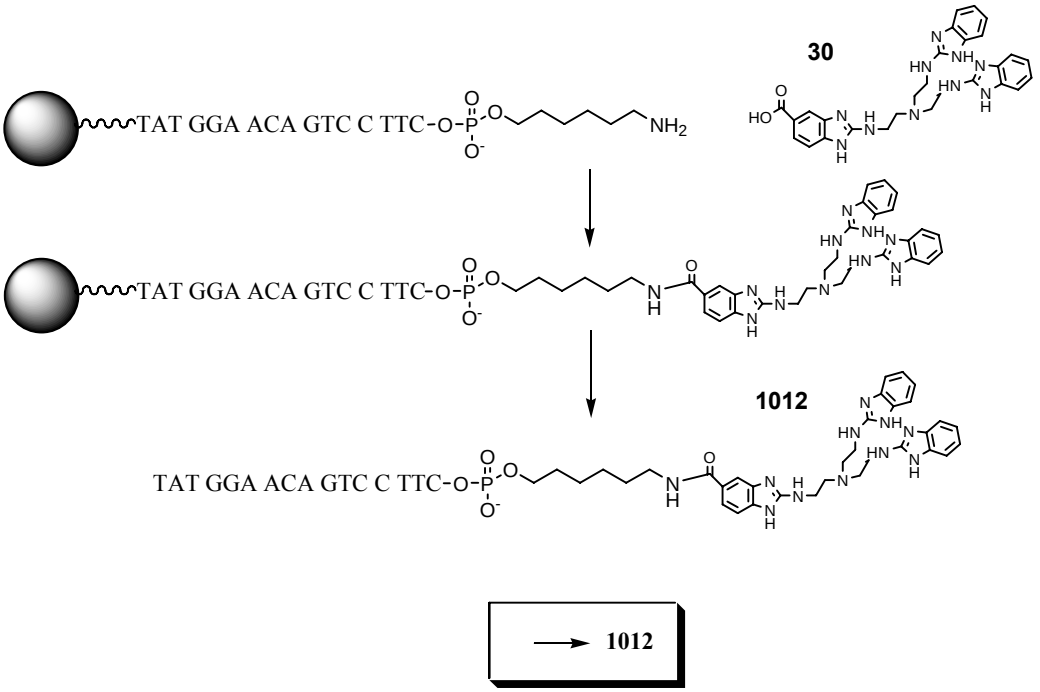

The oligonucleotide was assembled in a 1 µmol scale using an Applied Biosystems Model 381A DNA synthesizer with 2-cyanoethyl phosphoramidites (Proligo). The monomethoxytrityl protected C_6 amino linker (TriLink) was coupled to the 5' end of the DNA sequence and detritylated by the synthesizer. The trisbenzimidazole carboxylic acid **30** was obtained from methyl ester **29** (50 mg, 0.090 mmol) as already reported. Conjugate **1012** was prepared manually in the following way: All solutions were pumped through the CPG-cartridge by tightly fitting two 1 mL syringes (Luer fittings) to each side of the column and moving the pistons alternating. (90 µmol) of carboxylic acid **30**, 13 mg (96 µmol) *N*-hydroxybenztriazole and 12 mg (95 µmol) diisopropyl carbodiimide were dissolved in 1 mL DMF alkalized with three drops of NEt_3. The coupling solution was thoroughly agitated through the cartridge with the C_6-aminolinker-DNA over 5 h. The cartridge was then rinsed once with DMF (10 mL) and once with CH_3CN (10 mL). Afterwards the solid phase was collected in an Eppendorf tube, treated with 1.5 mL 25 % aqueous ammonia and agitated at room temperature for 24 h. The solution obtained was filtrated through a syringe filter (rotilabo® PVDF 0.22 µm), and evaporated in a Speed Vac. The crude material was dissolved in 1 mL of H_2O.

After evaporation the conjugate was desalted using a NAP-10 column. The conjugate **1012** was then purified by preparative PAGE.

MALDI-MS m/z: calcd for **1012** ($M+H^+$) 5556.9. Found 5558.87 ($M+H^+$).

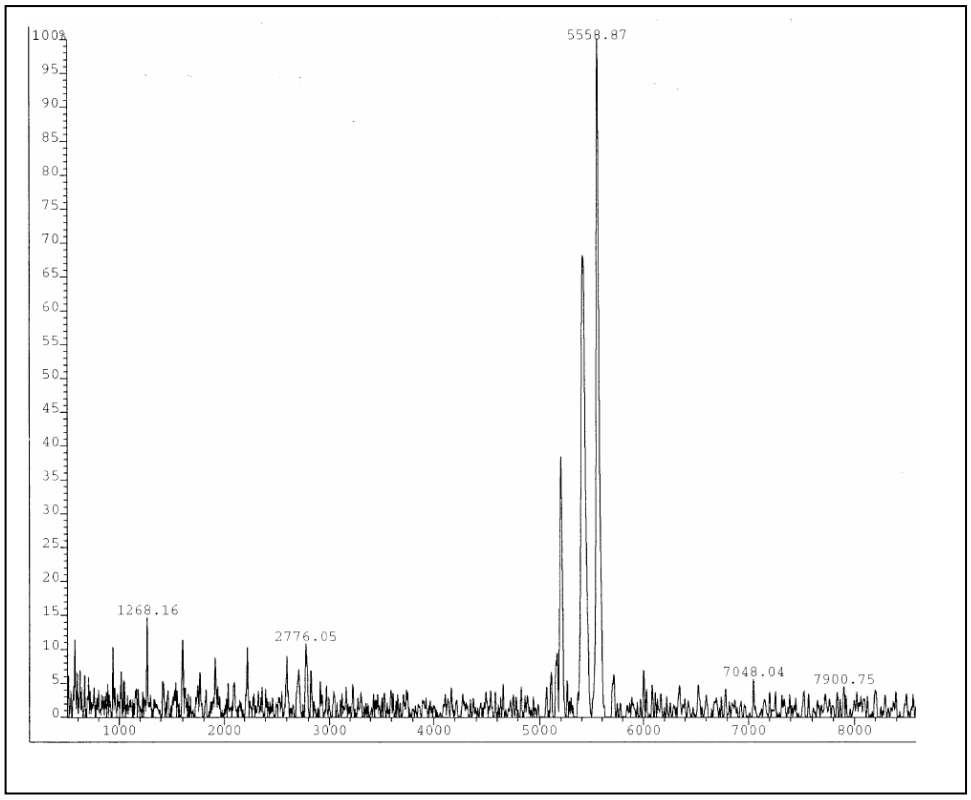

9.3.27 8-Tritylsulfanyl-octanoic acid (66)

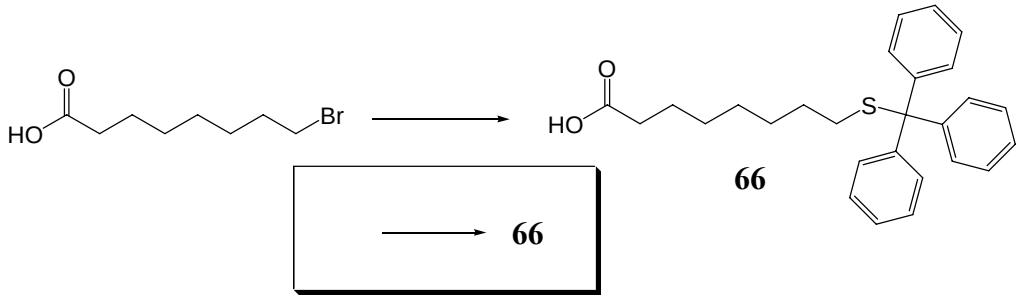

Triphenylmethyl mercaptan (1.24 g, 4.49 mmol) was added stepwise to a mixture of NaH (358 mg, 60% in mineral oil 8.95 mmol) in DMF (50 mL) at 0 °C. After 30 min. 8-bromo-octanoic acid (1.0 g, 4.48 mmol) was added. The reaction was stirred at room temperature for 16 h. To the mixture were added 50 mL of water and the pH was adjusted to 3 by treatment with HCl 6 M. 50 mL of $CHCl_3$ were added and the extracted organic phase was washed with 3×50 mL of HCl (pH 2). The organic layer was evaporated, and the crude product purified by silica gel chromatography (hexane/ethyl acetate 3/1), affording 1.37 g (73 %) of **66** as colourless oil.

R*f* (hexane/ethyl acetate 3/2) = 0.68.

^{1}H-NMR (250 MHz, DMSO-*d*$_6$) δ: 1.15-1.69 (*m*, 10H, $5CH_2$); 2.16 (*t*, *J*=7.2, 2H, CH_2); 2.34 (*t*, *J*=7.5, 2H, CH_2), 7.20-7.48 (*m*, 15H, Ar-H).

IR (KBr): 2929*m*, 1708*s*, 1595*w*, 1490*m*, 1444*m*, 1280*w*, 1082*w*, 1034*w*, 938*w*, 743*s*, 700*s*, 621*m* cm^{-1}.

ESI-MS m/z: calcd for $C_{27}H_{29}O_2S^-$ (M^-) 417.2. Found 417.2 (M^-).

Analysis: $C_{27}H_{30}O_2S$ (418.6) calculated: C 77.47 H 7.22.
found: C 75.70 H 7.26.
0.5 H_2O (427.6) calculated: C 75.84 H 7.31.

9.3.28 8-Tritylsulfanyl-octanoic acid (2-hydroxy-1-hydroxymethyl-ethyl)-amide (67)

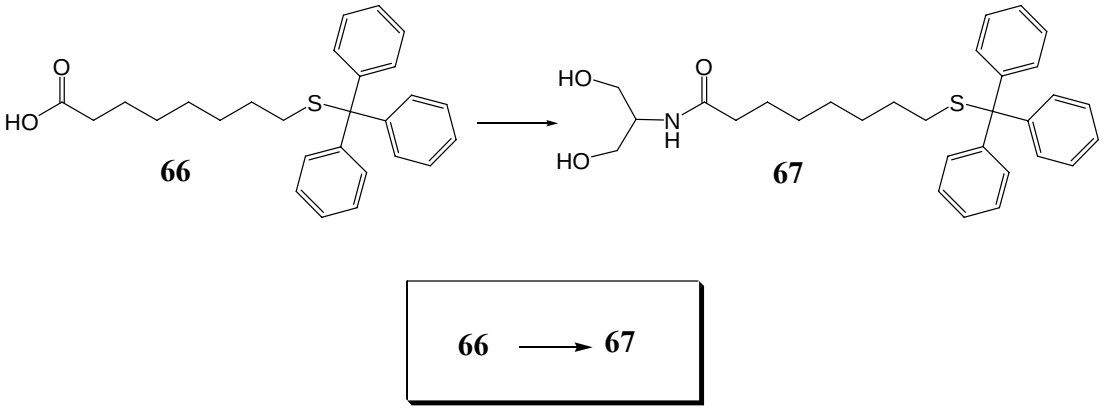

To a solution of **66** (2.9 g, 6.93 mmol) in anhydrous DMF (20 mL), Et_3N (2 mL), DIC (1.3 g, 10.30 mmol), HOBT (1.41 g, 10.41 mmol) and 2-amino-propane-1,3-diol (948 mg, 10.44 mmol) were added. The reaction was stirred at room temperature for 18 h. The solvent was removed by kugelrohr distillation, and the solid residue was purified on silica gel column chromatography, eluting with a gradient ethylacetate → ethylacetate / MeOH 95/5. To remove traces of DMF, the material was dissolved in CH_2Cl_2 (100 mL) and washed with brine (100 mL). The organic layer was dried over $MgSO_4$ and the solvent removed under reduced pressure yielding 2.05 g (60 %) of **67** as a white solid compound.

R*f* (AcOEt / MeOH 95/5) = 0.48.

^{1}H-NMR (400 MHz, CD_3CN) δ: 1.09-1.24 (*m*, 6H, $3CH_2$); 1.33 (*m*, 2H, CH_2); 1.49 (*m*, 2H, CH_2); 2.08-2.13 (*m*, 4H, CH_2-C=O, CH_2-S); 3.08 (br. *s*, 2H, OH); 3.53 (*m*, 4H, CH_2-O); 3.79 (*m*, 1H, CH); 6.34 (*d*, *J*=5.76, 1H, NH); 7.21-7.43 (*m*, 15H, Ar-H).

^{13}C-NMR (63 MHz, $CDCl_3$) δ: 25.97, 28.89, 29.25, 29.36, 32.23, 36.92, 62.93, 66.70, 126.89, 127.28, 128.17, 129.95, 130.48, 145.50, 174.64.

IR (KBr): 3405*s*, 3057*w*, 2927*m*, 2854*w*, 1638*s*, 1543*m*, 1490*m*, 1444*m*, 1364*w*, 1036*m*, 973*w*, 743*s*, 700*s*, 676*s*, 622*s* cm^{-1}.

ESI-MS m/z: calcd for $C_{30}H_{37}NO_3S\text{-}Na^+$ ($M+Na^+$) 514.2. Found 514.5 ($M+Na^+$).

Analysis: $C_{30}H_{37}NO_3S$ (491.68) calculated: C 73.28 H 7.58 O 2.85.
found: C 63.34 H 6.99 O 2.31.
1.2 CH_2Cl_2 (593.61) calculated: C 63.13 H 6.69 O 2.36.

9.3.29 (R,S)-8-Tritylsulfanyl-octanoic acid {1-[bis-(4-methoxy-phenyl)-phenyl methoxymethyl]-2-hydroxy-ethyl}-amide (*rac*-68)

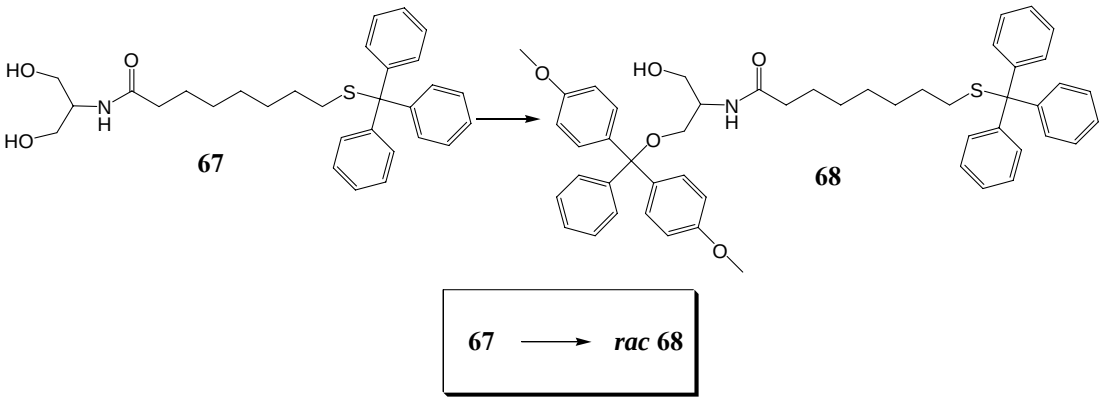

67 (1.38 g, 2.81 mmol) was dried by three co-evaporations with pyridine and dissolved in anhydrous pyridine (15 ml). Dimethoxytritylchloride (952 mg, 2.81 mmol) was added under argon atmosphere and stirred at room temperature for 2 h. The mixture was poured on water and extracted twice with dichloromethane, dried over $MgSO_4$ and evaporated. The crude material was purified by silica gel column chromatography (hexane/ethyl acetate 3/2), yielding 914 mg (41 %) of **rac-68** as a white solid compound.

R*f* (hexane/ethyl acetate, 1/1) = 0.36.

^{1}H-NMR (400 MHz, DMSO-d_6) δ: 1.02-1.16 (*m*, 6H, CH_2); 1.24 (*m*, 2H, CH_2); 1.42 (*m*, 2H, CH_2); 2.04 (*m*, 4H, CH_2-S, CH_2-C=O); 2.95 (*m*, 2H, CH_2OC); 3.43 (*m*, 2H, CH_2O); 3.71 (*s*, 6H, $2CH_3$); 3.99 (*m*, 1H, CH); 4.58 (*t*, *J*=5.4, 1H, OH); 6.83-6.86 (*m*, 4H, Ar-H); 7.07-7.38 (*m*, 24H, Ar-H); 7.56 (*d*, *J*=8.6, 1H, NH).

IR (KBr): 3422*m*, 3056*w*, 2928*m*, 2854*w*, 1654*s*, 1608*m*, 1508*s*, 1461*w*, 1444*m*, 1302*w*, 1250*s*, 1176*m*, 1155*w*, 1115*w*, 1082*w*, 1033*m*, 828*m*, 744*w*, 727*w*, 700*m*, 617*w*, 584*w* cm^{-1}.

Analysis: $C_{51}H_{55}NO_5S$ (794.1) calculated: C 77.14 H 6.98 N 1.76.
found: C 76.95 H 6.98 N 1.59.

M.p.: 44-45 °C.

9.3.30 Diisopropyl-phosphoramidous acid 3-[bis-(4-methoxy-phenyl)-phenyl-methoxy]-2-(8-tritylsulfanyl-octanoylamino)-propyl ester 2-cyano-ethyl ester (71) (mixture of stereoisomers)

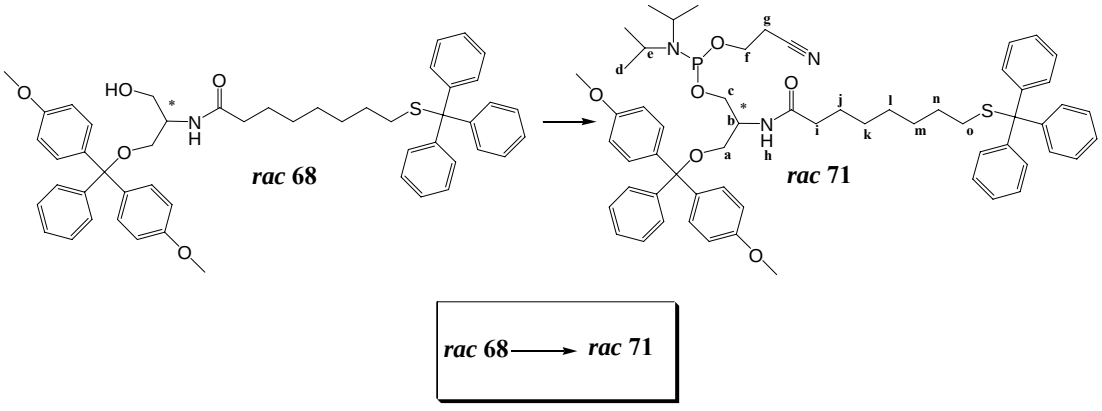

68 (914 mg, 1.15 mmol) was dried by three co-evaporations with pyridine and dissolved in 20 mL of anhydrous CH_3CN. To this solution were then added: diisopropylethylamine (600 µL, 3.47 mmol) and then 2-cyanoethoxy-*N*,*N*-diisopropylphosphoramidochloride (330 mg, 1.4 mmol). The reaction was stirred at

room temperature under argon for 2 h. The crude material was poured onto ethyl acetate and the organic phase was washed twice with saturated $NaHCO_3$ solution. The organic layer was dried over $MgSO_4$, the solvent removed at reduced pressure, and the phosphoramidite was purified by silica gel chromatography (hexane/ethyl acetate/Et_3N 3/1/1%), giving 537 mg (47 %) of **71** as a white solid.

R*f* (hexane/ethyl acetate/Et_3N 1/1/1%) = 0.83.

^{1}H-NMR (400 MHz, CD_3CN) δ: 1.06-1.20 (*m*, 18H, *d*CH_3, *k*CH_2, *l*CH_2, *m*CH_2,); 1.30 (*m*, 2H, *j*CH_2); 1.46 (*m*, 2H, 2-*n*CH_2); 2.04-2.10 (*m*, 4H, *i*CH_2, *o*CH_2); 2.54-2.58 (*m*, 2H, *g*CH_2); 3.07-3.16 (*m*, 2H, *a*CH_2); 3.48-3.60 (*m*, 2H, *e*CH); 3.63-3.73 (*m*, 4H, *c*CH_2, *f*CH_2); 3.75 (*s*, 6H, OCH_3); 4.12-4.24 (*m*, 1H, *b*CH); 6.23-6.29 (2*d*, *J*=8.8, 1H, *h*NH); 6.78-6.86 (*m*, 4H, Ar-H); 7.12-7.44 (*m*, 24H, Ar-H).

^{31}P NMR (162 MHz, DMSO-*d_6*) δ: 146.71, 147.04.

IR (KBr): 3422*m*, 3056*w*, 2928*s*, 2252*w*, 1654*s*, 1608*m*, 1578*w*, 1508*s*, 1459*w*, 1444*w*, 1364*w*, 1301*w*, 1250*s*, 1178*s*, 1126*w*, 1081*m*, 1033*s*, 976*m*, 899*w*, 828*m*, 790*w*, 743*m*, 700*s*, 616*w*, 583*w* cm^{-1}.

Analysis: $C_{60}H_{72}N_3O_6PS$ (994.3) calculated: C 72.48 H 7.30 N 4.23.
found: C 72.31 H 7.48 N 3.96.

9.3.31 3-Tritylsulfanyl-propionic acid (69)

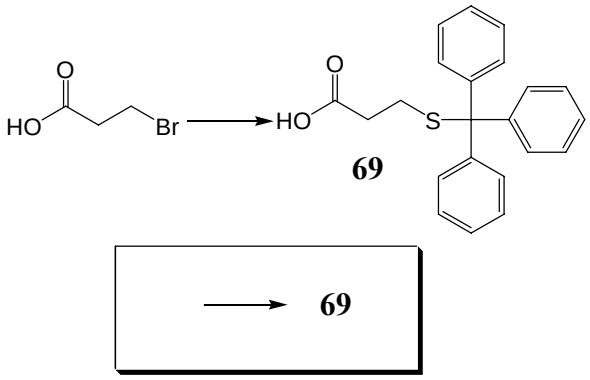

69

→ **69**

Triphenylmethyl mercaptan (3.63 g, 13.1 mmol) was added stepwise to a mixture of NaH (1.21 g, 60% in mineral oil, 30.3 mmol) in DMF (50 mL) at 0 °C. After 30 min 3-bromo-propionic acid (2 g, 13.1 mmol) was added and the reaction was stirred at room temperature for 16 h. To the mixture were added 50 mL of water and the pH was adjusted to pH 3 with 6 M HCl. 50 mL of $CHCl_3$ were added and the extracted organic phase was washed with 3×50 mL of HCl (pH 2). The organic layer was evaporated, the crude product dissolved in 150 mL of $CHCl_3$ and 200 mL of hexane were added. The precipitate formed was collected by filtration yielding 3.86 g (85 %) of **69** as a white powder.

R*f* (ethyl acetate) = 0.65.

^{1}H-NMR (250 MHz, DMSO-d_6) δ: 2.13-2.32 (*m*, 4H, $CH_2C{=}O$, CH_2S); 7.02-7.66 (*m*, 15H, Ar-H); 12.23 (br. *s*, 1H COOH).

IR (KBr): 3031*w*, 2912*w*, 1705*s*, 1592*w*, 1488*m*, 1448*m*, 1431*m*, 1408*w*, 1342*w*, 1253*s*, 1032*w*, 958*m*, 747*s*, 702*s*, 620*w* cm^{-1}.

ESI-MS m/z: calcd for $C_{22}H_{19}O_2S^-$ (M^-) 347.1. Found 347.1 (M^-).

Analysis: $C_{22}H_{20}O_2S$ (348.5) calculated: C 75.83 H 5.79.
found: C 75.63 H 5.82.

M.p.: 203-204 C.

9.3.32 *N*-(2-Hydroxy-1-hydroxymethyl-ethyl)-3-tritylsulfanyl-propionamide (73)

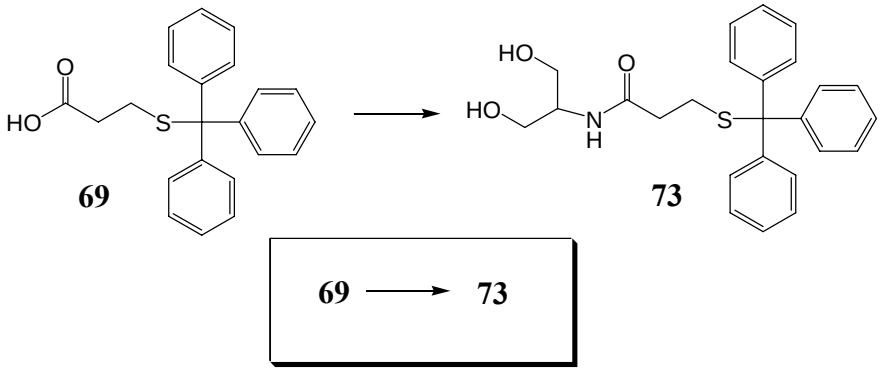

To a solution of **69** (2 g, 5.7 mmol) in anhydrous DMF (20 mL), Et_3N (2 mL), DIC (869 mg, 6.9 mmol), HOBT×H_2O (1.06 mg, 6.9 mmol) and 2-amino-propane-1,3-diol (628 mg, 6.9 mmol) were added. The mixture was stirred at room temperature for 18 h. The solvent was removed by kugelrohr distillation, and the solid residue was purified on silica gel column chromatography (gradient ethylacetate → ethylacetate / MeOH 95/5), yielding 1.53 g (63 %) of **73** as a white solid compound.

R*f* (ethyl acetate/MeOH 95/5) = 0.53.

^{1}H-NMR (250 MHz, DMSO-*d*$_6$) δ: 2.20 (*m*, 4H, CH_2S, CH_2C=O); 3.35 (*m*, 4H, CH_2O); 3.59-3.71 (*m*, 1H, CH); 4.57 (*t*, *J*=5.5, 2H, OH); 7.21-7.38 (*m*, 15H, Ar-H); 7.52 (*d*, *J*=8.1,1H, NH).

^{13}C-NMR (63 MHz, DMSO-*d*$_6$) δ: 169.90, 144.44, 129.04, 127.99, 126.67, 65.88, 60.04, 52.85, 33.86, 27.43.

IR (KBr): 3382*s*, 3310*s*, 3064*w*, 2937*w*, 1654*s*, 1560*m*, 1490*w*, 1441*w*, 1279*m*, 1069*w*, 1030*w*, 1001*w*, 754*m*, 744*m*, 701*s*, 676*w*, 625*m* cm^{-1}.

MALDI-MS m/z: calcd for $C_{25}H_{27}NNaO_3S^+$ ($M+Na^+$) 444.2. Found 445.9 ($M+Na^+$).

Analysis: $C_{25}H_{27}NO_3S$ (421.55) calculated: C 71.23 H 6.46 N 3.32.
found: C 68.87 H 6.48 N 3.02.
0.8 H_2O (435.97) calculated: C 68.87 H 6.61 N 3.21.

9.3.33 (R,S)-*N*-{1-[Bis -(4-methoxy-phenyl) -phenyl-methoxymethyl] 2-hydroxy-ethyl} -3-tritylsulfanyl-propionamide (*rac*-74)

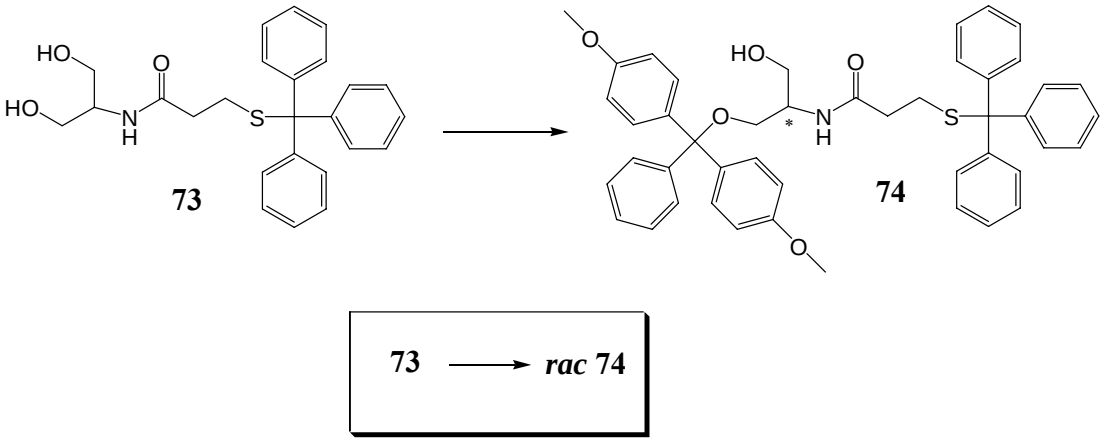

73 (1 g, 2.37 mmol) was dried by three co-evaporations with pyridine and dissolved in anhydrous pyridine (15 mL). Dimethoxytritylchloride (883 mg, 2.61 mmol) was added under argon atmosphere and stirred at room temperature for 2 h. The mixture was poured on water and the organic phase was extracted twice with dichloromethane, dried over $MgSO_4$ and concentrated. The crude material was purified by silica gel column chromatography (hexane/ethyl acetate 3/2), yielding 739 mg (43 %) of **74** as white solid compound.

R*f* (hexane/ethyl acetate 3/2) = 0.46.

^{1}H-NMR (400 MHz, $CDCl_3$) δ: 1.96 (*t*, *J*=7.3, 2H, CH_2C=O); 2.51 (*t*, *J*=7.3, 2H, CH_2S); 2.70 (*m*, 1H, OH); 3.28 (*m*, 2H, CH_2OC); 3.59-3.81 (*m*, 2H, CH_2O); 3.77 (*s*, 6H, OCH_3); 4.02 (*m*, 1H, CH); 5.83 (*d*, *J*=7.6, 1H, NH); 6.80-6.83 (*m*, 4H, Ar-H); 7.17-7.44 (*m*, 24H, Ar-H).

^{13}C-NMR (63 MHz, DMSO-d_6) δ: 27.44, 34.02, 50.92, 54.96, 60.69, 62.49, 65.90, 85.06, 113.03, 126.48, 126.64, 127.68, 127.96, 129.04, 129.67, 135.35, 135.80, 144.44, 145.07, 157.94, 169.80.

IR (KBr): 3406*m*, 3056*w*, 2931*w*, 2834*w*, 1654*s*, 1607*m*, 1508*s*, 1444*m*, 1301*w*, 1250*s*, 1176*s*, 1081*m*, 1033*s*, 829*s*, 744*m*, 701*s*, 617*w*, 584*w* cm^{-1}.

ESI-MS m/z: calcd for $C_{46}H_{45}NNaO_5S^+$ ($M+Na^+$) 746.3. Found 746.2 ($M+Na^+$).

Analysis: $C_{46}H_{45}NO_5S$ (723.9) calculated: C 76.32 H 6.27 N 1.93.
found: C 76.04 H 6.34 N 1.75.

9.3.34 Diisopropyl-phosphoramidous acid 3-[bis-(4-methoxy-phenyl)-phenyl-methoxy]-2-(3-tritylsulfanyl-propionylamino)-propyl ester 2-cyano-ethyl ester (75) (mixture of stereoisomers)

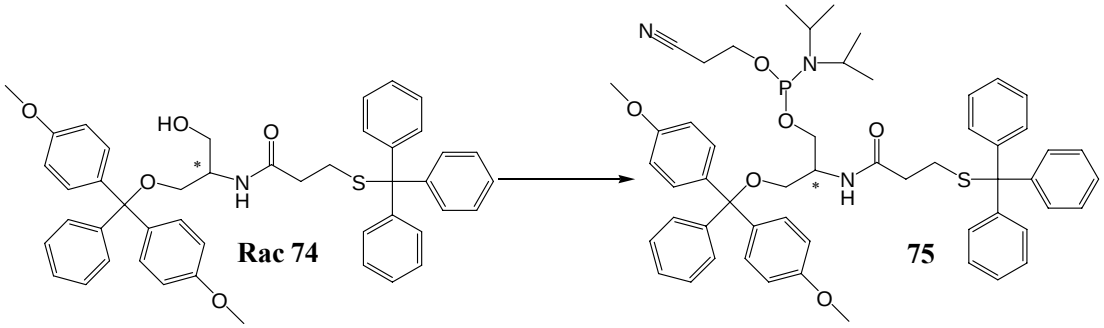

74 (700 mg, 0.97 mmol) was dried by three co-evaporations with pydidine and dissolved in 20 mL of anhydrous CH_3CN. To this solution were added: diisopropylethylamine (600 µL, 3.47 mmol) and then 2-cyanoethoxy-*N*,*N*-diisopropylphosphoramidochloride (274 mg, 1.16 mmol). The reaction was stirred at room temperature under argon for 2 h. The crude material was poured onto ethyl acetate and the organic phase was washed twice with saturated $NaHCO_3$ solution. The organic layer was dried over $MgSO_4$, the solvent removed by reduced pressure. The purification by silica gel chromatography (hexane/ethyl acetate/Et_3N 2/1/1 %), yielded 537 mg (60 %) of **75** as white solid.

R*f* (hexane/ethyl acetate/Et_3N 2/1/1%) = 0.55.

^{1}H-NMR (400 MHz, DMSO-*d*$_6$) δ: 1.00-1.16 (*m*, 12H, CH_3); 2.16-2.28 (*m*, 4H, CH_2S, $CH_2C{=}O$); 2.60-2.68 (*m*, 2H, CH_2CN); 2.92-3.03 (*m*, 2H, CH_2OC); 3.42-3.55 (*m*, 2H, CH-Isoprop); 3.60 (*m*, 2H, $CH_2\beta CN$); 3.71 (*s*, 6H, OCH_3); 4.03-4.14 (*m*, 1H, CH-NC=O); 6.80-6.88 (*m*, 4H, Ar-H); 7.17-7.37 (*m*, 24H, Ar-H); 7.78-7.82 (*2d*, *J*=5.2, 1H, NH).

^{31}P NMR (162 MHz, DMSO-*d*$_6$) δ: 149.30, 149.52.

IR (KBr): 3423*m*, 3057*w*, 2965*s*, 2252*w*, 1676*m*, 1654*m*, 1608*m*, 1560*w*, 1508*s*, 1459*w*, 1444*m*, 1364*w*, 1301*m*, 1301*m*, 1250*s*, 1178*s*, 1155*w*, 1126*w*, 1081*m*, 1033*s*, 977*m*, 878*w*, 829*m*, 790*w*, 744*m*, 701*s*, 617*w*, 583*w* cm^{-1}.

ESI-MS m/z: calcd for $C_{55}H_{63}N_3O_6PS^+$ ($M+H^+$) 924.4, $C_{55}H_{62}N_3NaO_6PS^+$ ($M+Na^+$) 946.4. Found 924.2 ($M+H^+$), 946.4 ($M+Na^+$).

Analysis: $C_{55}H_{62}N_3O_6PS$ (924.14) calculated: C 71.48 H 6.76 N 4.55.
found: C 71.20 H 6.85 N 4.32.

9.3.35 *N*-[3-(1-{5-[Bis-(4-methoxy-phenyl)-phenyl-methoxymethyl]-4-hydroxy-tetrahydro-furan-2-yl}-2,4-dioxo-1,2,3,4-tetrahydro-pyrimidin-5-yl)-prop-2-ynyl]-3-tritylsulfanyl-propionamide (70)

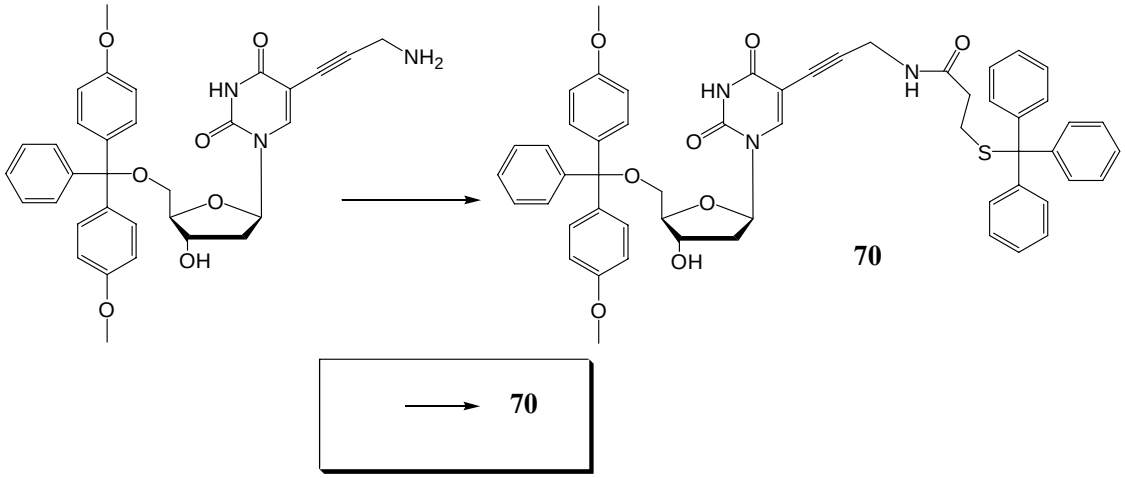

To a solution of **69** (522 mg, 1.50 mmol) in anhydrous DMF (20 mL), Et_3N (0.5 mL), (DIC 189.3 mg, 1.5 mmol), HOBT (202.7 mg, 1.50 mmol) and amino derivative (800 mg, 1.37 mmol) were added. The reaction was stirred at room temperature for 18 h. The solvent was removed by kugelrohr distillation, and the solid residue was purified by silica gel column chromatography (ethyl acetate), yielding 639 mg (51 %) of **70** as white foam.

R*f* (CH_2Cl_2/MeOH 9/1) = 0.27.

^{1}H-NMR (400 MHz, CD_3CN) δ: 2.01 (*t*, *J*=7.3, 2H, CH_2-C-S); 2.25-2.34 (*m*, 4H, CH_2S, 2'-H); 3.16-3.34 (*m*, 2H, 5'-H); 3.48 (*d*, *J*=4.3, 1H, OH); 3.74 (*s*, 3H, OCH_3); 3.75 (*s*, 3H, OCH_3); 3.78 (*dd*, *J*=5.3, *J*=2.4, 2H, $CH_2C{\equiv}C$); 3.98 (*m*, 1H, 4'-H); 4.46-4.52 (*m*, 1H, 3'-H); 6.11 (*m*, 1H, 1'-H); 6.20 (br. *t*, 1H, NHC=O); 6.85-6.89 (*m*, 4H, Ar-H); 7.19-7.46 (*m*, 24H, Ar-H); 7.94 (*s*,1H, 6-H); 9.25 (*s*, 1H, 3-NH).

IR (KBr): 3412*m*, 3058*w*, 2932*w*, 1686*s*, 1608*m*, 1560*w*, 1508*s*, 1458*m*, 1444*m*, 1281*m*, 1250*s*, 1177*m*, 1090*w*, 1033*m*, 829*w*, 744*w*, 701*s*, 618*w*, 585*w* cm^{-1}.

ESI-MS m/z: calcd. for $C_{55}H_{50}N_3O_8S^-$ (M^-) 912.3, $C_{55}H_{55}N_4O_8S^+$ ($M+NH_4^+$) 931.4, $C_{55}H_{51}N_3NaO_8S^+$ ($M+Na^+$) 936.3. Found 912.4 (M^-), 931.4 ($M+NH_4^+$), 936.3 ($M+Na^+$).

Analysis: $C_{55}H_{51}N_3O_8$ (914.07) calculated: C 72.27 H 5.62 N 4.60.
found: C 71.19 H 5.78 N 4.18.
0.7 ethyl acetate (975.77) calculated: C 71.15 H 5.85 N 4.31.

9.3.36 Diisopropyl-phosphoramidous acid 2-[bis-(4-methoxy-phenyl)-phenyl-methoxymethyl]-5-{2,4-dioxo-5-[3-(3-tritylsulfanyl-propionylamino)-prop-1-ynyl]-3,4-dihydro-2H-pyrimidin-1-yl}-tetrahydro-furan-3-yl ester 2-cyano-ethyl ester (72) (Mixture of diastereoisomers)

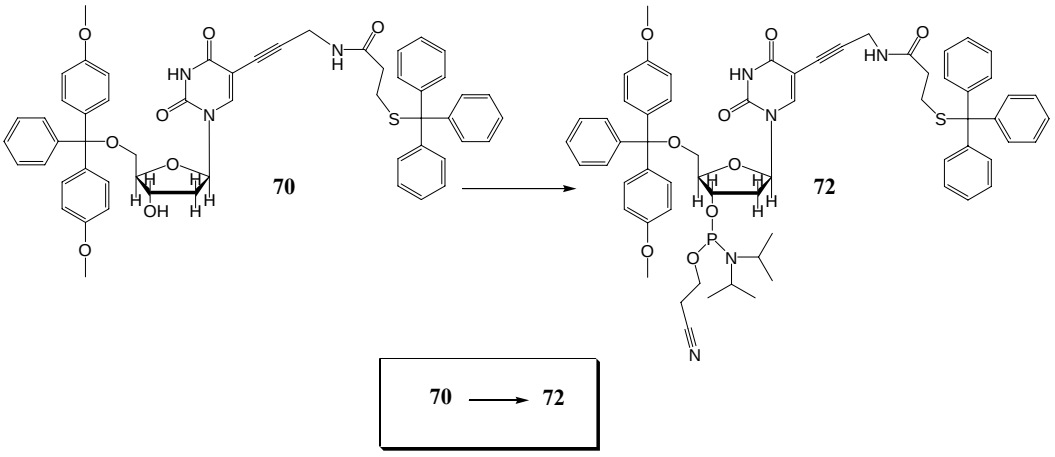

70 (447 mg, 0.49 mmol) was dissolved in 10 mL of anhydrous CH_2Cl_2. To this solution were then added: diisopropylethylamine (500 µL, 2.9 mmol) and then 2-cyano-*N*,*N*-diisopropylphosphoramidochloride (174 mg, 0.74 mmol). The reaction was stirred at room temperature under argon for 2 h. The crude material was poured onto ethyl acetate (150 mL) and the organic phase was washed twice with saturated $NaHCO_3$ solution and the organic layer was dried over $MgSO_4$. The solvent was removed under reduced pressure, and the phosphoramidite was purified by silica gel chromatography (hexane/ethyl acetate 4/1), giving 323 mg (59 %) of **72** as white foam.

^{1}H-NMR (400 MHz,CD_3CN) δ: 1.05-1.18 (m, 12H, $CH_3{}^i$prop); 1.99 (*m*, 2H, CH_2-C-S); 2.29 (*m*, 2H, CH_2S); 2.33-2.51 (*m*, 2H, 2'-H); 2.59 (*m*, 2H, CH_2CN); 3.23-3.37 (*m*, 2H, 5'-H); 3.52-3.79 (*m*, 12H, 2CH ^{i}prop, CH_2OP, $2OCH_3$, $CH_2C{\equiv}C$); 4.10-4.15 (*m*, 1H, 4'-H); 4.58-4.67 (*m*, 1H, 3'-H); 6.07 (br. *m*, 1H, NHC=O); 6.09-6.15 (*m*, 1H,

1'-H); 6.85-6.89 (*m*, 4H, Ar-H); 7.10-7.46 (*m*, 24H, Ar-H); 7.95 (2*s*, 1H, 6-H); 9.00 (br. *s*, 1H, 3-NH).

^{31}P-NMR (161.98 MHz, CD_3CN) δ: 148.176, 149.184.

9.3.37 Synthesis of conjugates 1004, 1007 and 1008 via thio linker chemistry

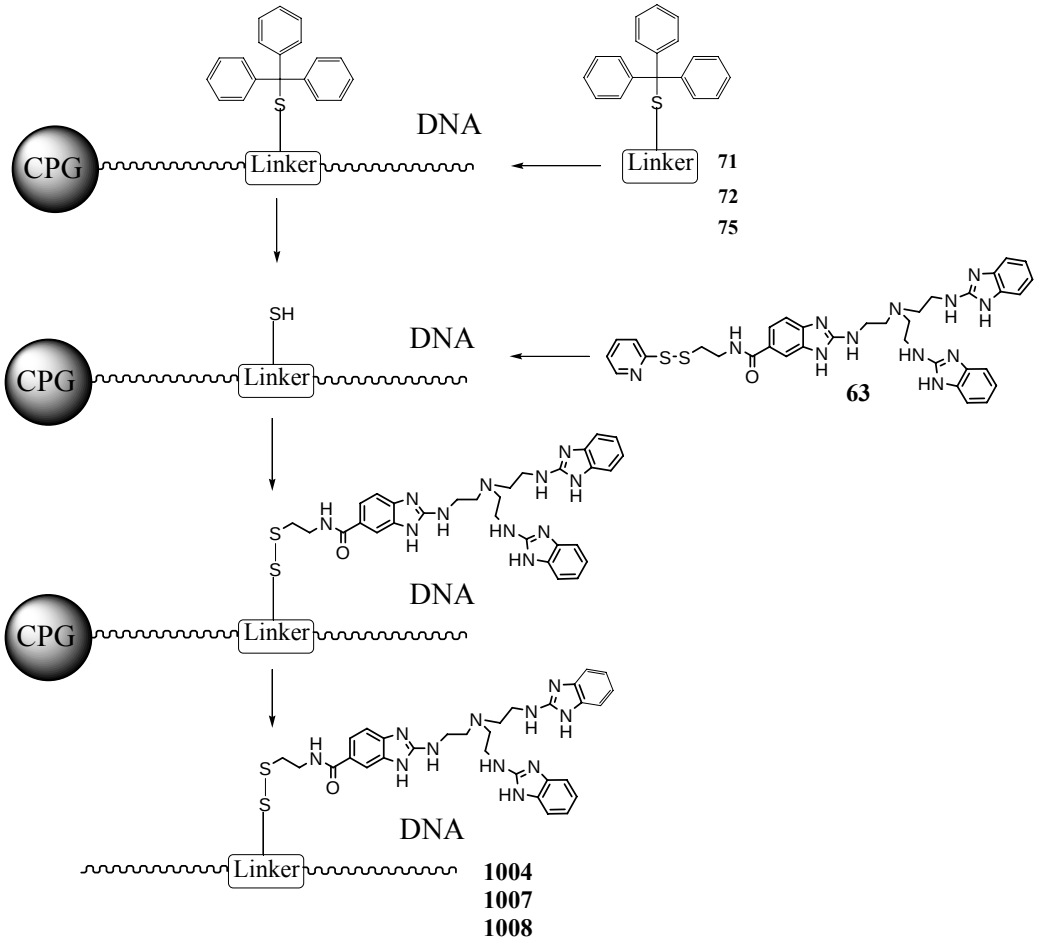

71	**1008**	**$^{5'}$GAGATCGG-Linker-Catalyst-TCGGCTAG$^{3'}$**
72	**1004**	**$^{5'}$AGATCGGC-Linker-Catalyst-CGGCTAG$^{3'}$**
75	**1007**	**$^{5'}$GAGATCGG-Linker-Catalyst-TCGGCTAG$^{3'}$**

The oligonucleotides were assembled on an Applied Biosystems Model 381A DNA synthesizer with 2-cyanoethyl phosphoramidites (Proligo) and the thio linker

building blocks **71**, **72** or **75** (1 μmol scale). All subsequent steps were done manually with the cartridge removed from the synthesizer. To detritylate the thio linker, the support carrying the fully protected DNA was treated for 10 min. with 1 mL of 0.1 M aqueous $AgNO_3$ solution, followed by washing steps, first with 10 mL of H_2O and then with 10 mL of CH_3CN. Disulfide bonds were then reduced by treatment with 1 mL of 0.1 M aqueous tris(2-carboxyethyl)phosphine (TCEP) over 10 min. Two washing steps, first with 10 mL of H_2O and then with 10 mL of CH_3CN followed. The cartridge was now agitated for 12 h at room temperature with a solution of compound **63** (23.5 mg, 0.033 mmol, in 300 μL DMF), followed by washing steps with 10 mL of DMF and 10 mL of CH_3CN. Afterwards the solid phase was collected in an Eppendorf tube, treated with 1.5 mL 25 % aqueous ammonia and agitated at room temperature for 24 h. The solution obtained was filtrated through a syringe filter (rotilabo® PVDF 0.22 μm), and evaporated in a Speed Vac. The crude material was dissolved in 1 mL of H_2O, and the solution was desalted on a NAP^{TM}-10 column (Amersham Biosciences). The oligonucleotide conjugates were purified by denaturing PAGE and characterized by MALDI mass spectrometry**.**

MALDI-MS m/z: calcd for **oligo 1004** ($M+H^+$) 5646. Found 5645.22 ($M+H^+$).

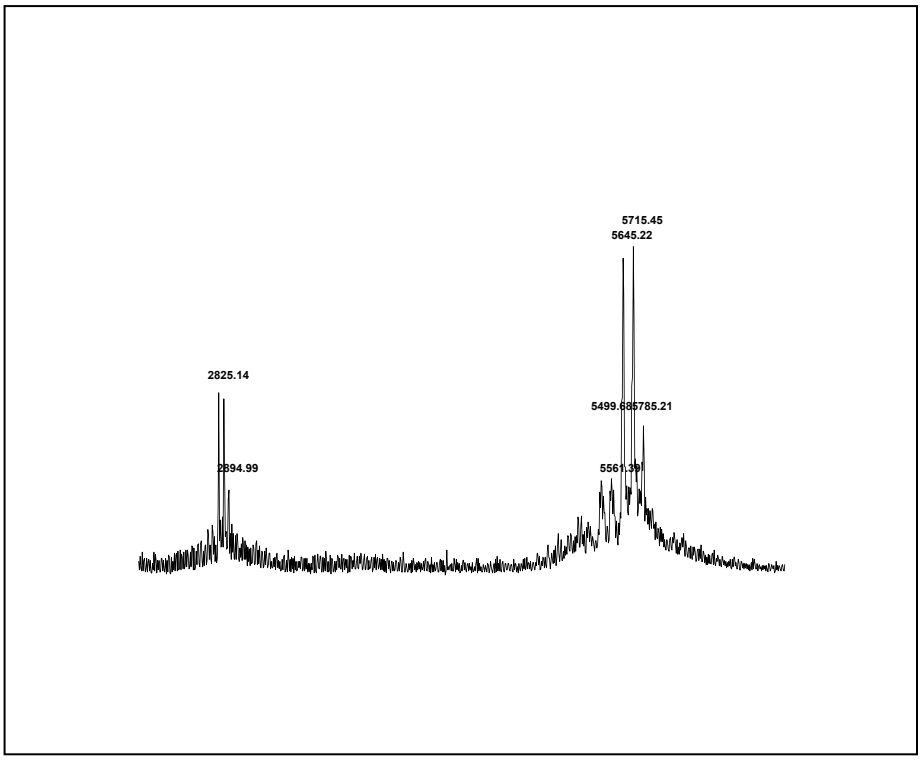

MALDI-MS m/z: calcd for **oligo 1007** ($M+H^+$) 5784.1. Found 5782.6 ($M+H^+$).

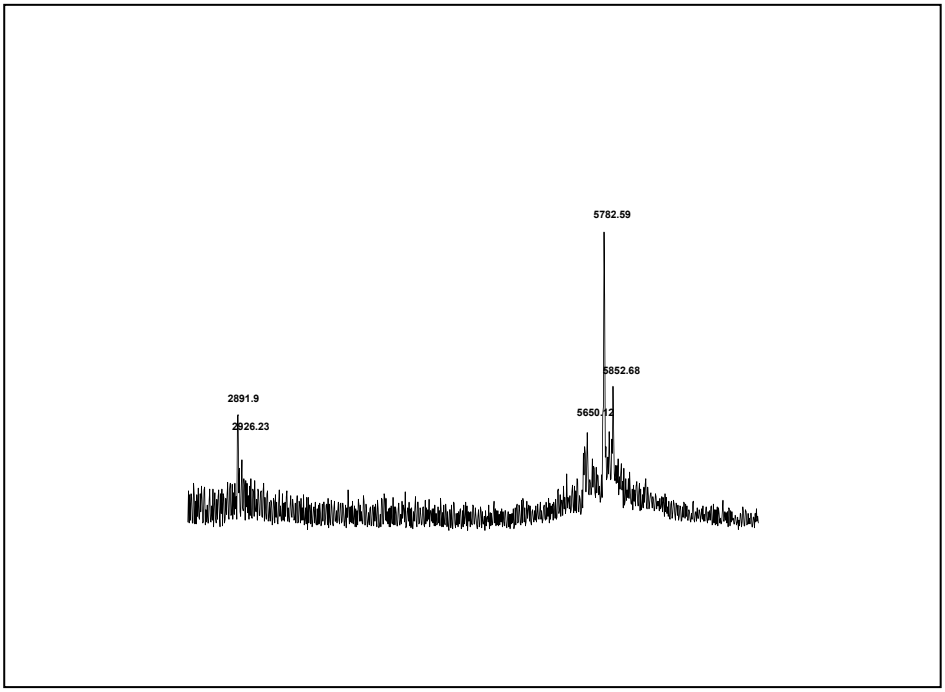

MALDI-MS m/z: calcd for **oligo 1008** ($M+H^+$) 5854.3. Found 5866.7.

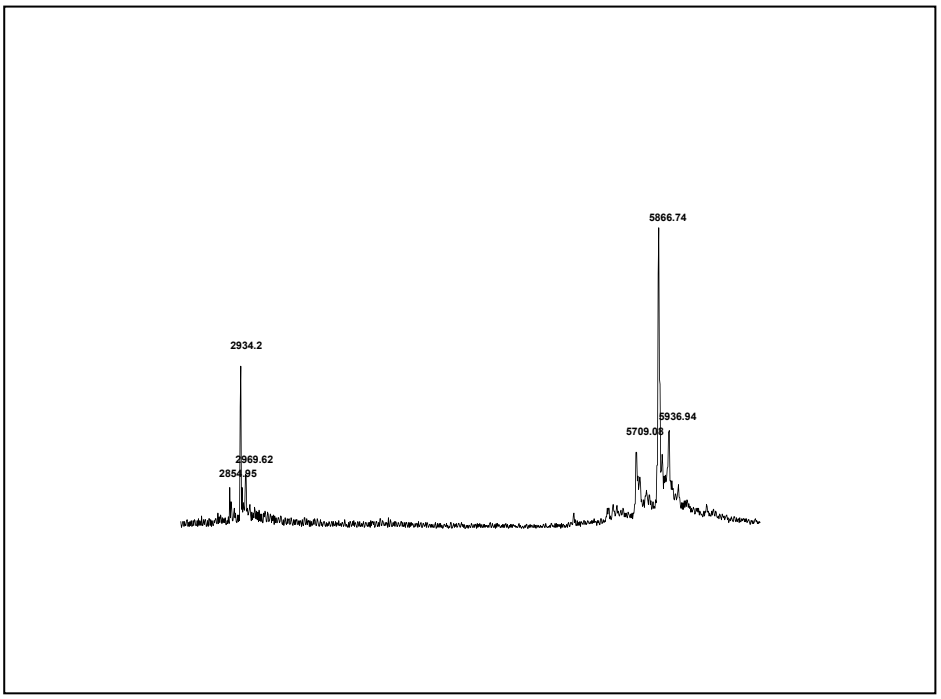

9.3.38 4-Benzyloxycarbonylamino-butyric acid (76)

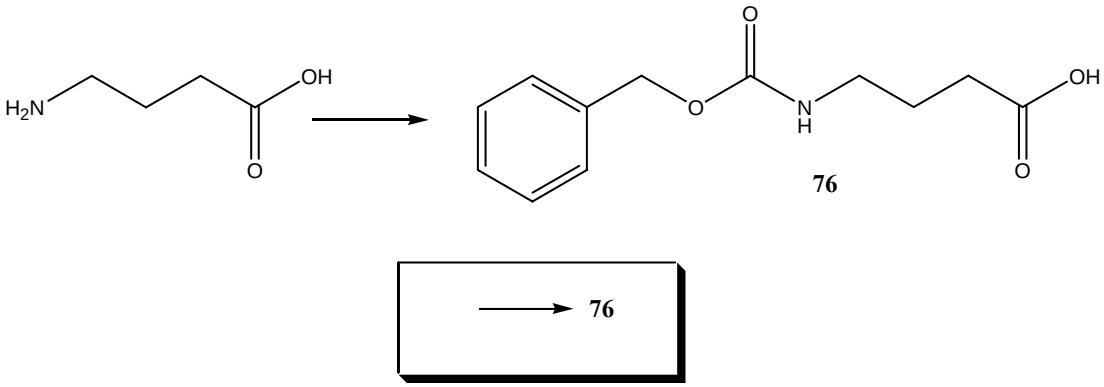

To a solution of 4-amino-butyric acid (2 g, 19.4 mmol) dissolved in 40 mL of 3 N NaOH at 0 °C, 2.73 mL (19.4 mmol) of benzyl chloroformate were added. The reaction mixture was stirred at room temperature for 2 h, then neutralized by adding 6 M aqueous HCl solution until pH 2. The protected amino acid was extracted with a 1:1 mixture of ether and ethyl acetate. The organic layer was dried over $MgSO_4$, filtered and evaporated to give 4.05 g (88 %) of **76** as a white solid product.

R*f* (ethyl acetate) = 0.68.

^{1}H-NMR (250 MHz, DMSO-*d*$_6$) δ: 1.63 (*m*, 2H, $CH_2\beta$); 2.22 (*t*, *J*=7.4, 2H, $CH_2\alpha$); 3.01 (*m*, 2H, $CH_2\gamma$); 5.01 (*s*, 2H, OCH_2); 7.26-7.38 (*m*, 6H, NH, Ar-H); 12.05 (*s*, 1H, COOH).

IR (KBr): 3332*m*, 3061*w*, 2922*w*, 1689*s*, 1547*s*, 1499*w*, 1453*m*, 1427*w*, 1414*w*, 1364*w*, 1316*w*, 1272*s*, 1211*m*, 1185*w*, 1144*w*, 1103*w*, 1077*w*, 1019*m*, 908*w*, 868*w*, 780*w*, 749*m*, 722*m*, 698*m*, 620*w*, 574*w* cm^{-1}.

MALDI-MS m/z: calcd for $C_{12}H_{15}NNaO_4^+$ ($M+Na^+$) 260.09. Found 260.04 ($M+Na^+$).

Analysis: $C_{12}H_{15}NO_4$ (237.25) calculated: C 60.75 H 6.37 N 5.90.
found: C 60.86 H 6.61 N 6.09.

M.p.: 58-59 °C.

9.3.39 4-Benzyloxycarbonylamino-butyric acid *tert*-butyl ester (77)

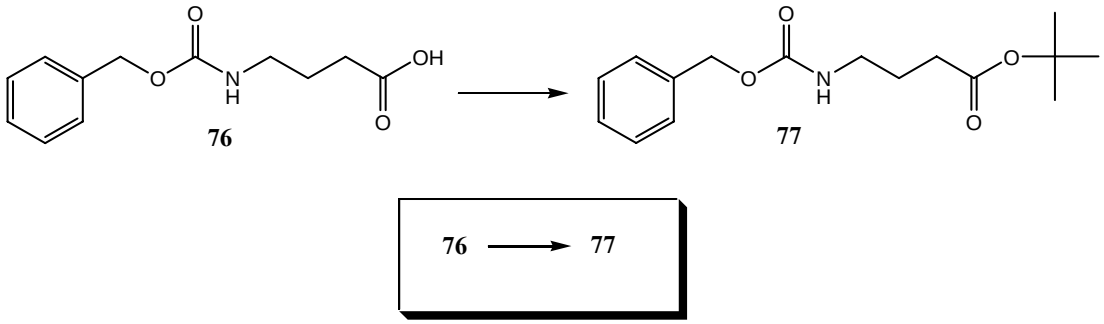

To a solution of **76** (1 g, 4.22 mmol) in DCM (50 mL), were added in the following order: *t*-butanol (938 mg, 12.7 mmol), DMAP (51 mg, 0.42 mmol) and DCC (1 g, 4.85 mmol). The reaction was stirred at room temperature for 18 h. The mixture was filtrated and the solution washed with 2×50 mL of H_2O, 2×50 mL of 1N HCl, 2×50 mL of 5 % $NaHCO_3$ solution. The organic phase was dried over Na_2SO_4, the solvent was evaporated *in vacuo,* and the residue product was purified by silica gel chromatography (hexane/ethyl acetate 4/1), giving 800 mg (65 %) of **77** as colourless oil.

R*f* (hexane/ethyl acetate 5/1) = 0.30.

^{1}H-NMR (250 MHz, DMSO-*d*$_6$) δ: 1.39 (*s*, 9H, CH_3); 1.63 (*m*, 2H, $CH_2\beta$); 2.20 (*t*, *J*=7.4, 2H, $CH_2\alpha$); 3.01 (*m*, 2H, $CH_2\gamma$); 5.02 (*s*, 2H, OCH_2); 7.27 (br. *t*, 1H, NH); 7.29-7.38 (*m*, 5H, Ar-H).

^{13}C-NMR (63 MHz, $CDCl_3$) δ: 25.19, 28.36, 32.78, 40.47, 66.56, 80.45, 128.04, 128.28, 128.47, 136.61, 156.45, 172.58.

IR (film): 3345*m*, 2977*m*, 2935*m*, 1726*s*, 1702*s*, 1534*m*, 1456*m*, 1367*m*, 1253*s*, 1154*s*, 1090*w*, 1025*w*, 845*w*, 777*w*, 752*w*, 697*m* cm^{-1}.

Analysis: $C_{16}H_{23}NO_4$ (293.36) calculated: C 65.51 H 7.90 N 4.77.
found: C 65.32 H 7.77 N 4.64.

9.3.40 4-Amino-butyric acid *tert*-butyl ester (78)[145]

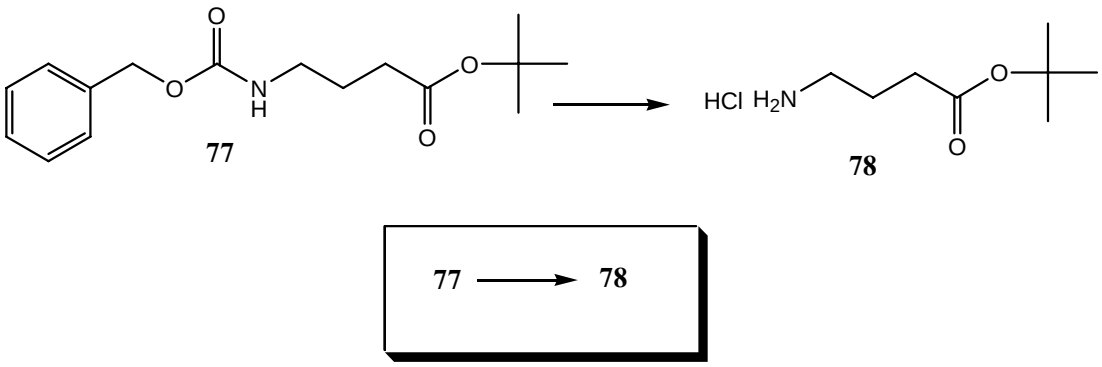

To a solution of **77** (543.6 mg, 1.85 mmol) in 10 mL of MeOH and 1 mL of CH_3COOH, 15% w/w of Pd/C (150 mg) was added. The reaction mixture was hydrogenated at normal pressure for 4 h at room temperature. The catalyst was removed by filtration, and the clear solution was evaporated. 50 mL of 0.5 M HCl were added to the residue and the solution washed with a mixture of hexan:ether 1:1 (2×50 mL). The pH was then adjusted to 10 with aqueous ammonia. The product was then extracted with a mixture of 2-propanol:chloroform 1:3 (3×50 mL), the organic layer was dried over Na_2SO_4, and evaporated. The crude product was used for the further step.

^{1}H-NMR (250 MHz, MeOD) δ: 1.42 (*s*, 9H, CH_3); 1.86 (*m*, $CH_2\beta$); 2.34 (*t*, *J*=7.2, 2H, $CH_2\alpha$); 2.91 (*m*, 2H, $CH_2\gamma$).

MALDI-MS m/z: calcd for $C_8H_{18}NO_2^+$ ($M+H^+$) 160.1. Found 159.8 ($M+H^+$).

9.3.41 4-{[2-(2-{Bis-[2-(1H-benzoimidazol-2-ylamino)-ethyl]-amino}-ethylamino)-1*H*-benzoimidazole-5-carbonyl]-amino}-butyric acid tert-butyl ester (79)

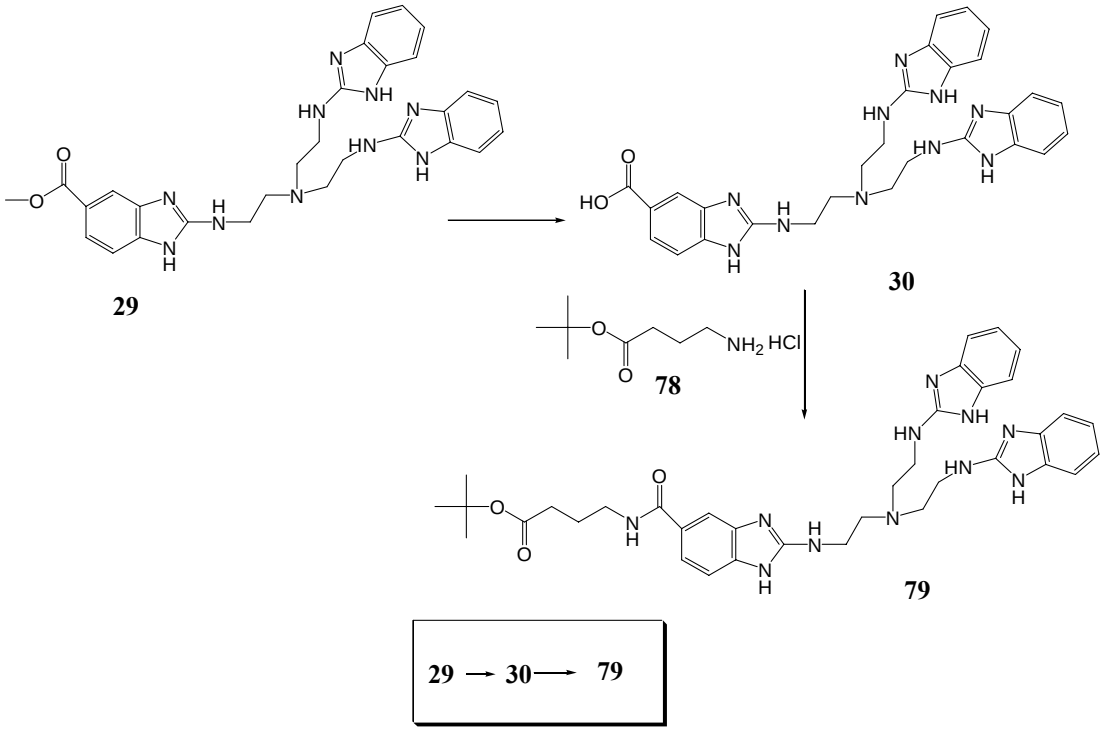

Methyl ester **29** (270 mg, 0.49 mmol) was refluxed in 25 mL of HCl 6 M for 2 h, the solvent was removed under reduced pressure. The ester hydrolysis was confirmed by NMR and ESI spectrometry, and the crude product was used for the next step.

^{1}H-NMR (250 MHz, MeOD-*d*$_4$) δ: 3.90 (*m*, 6H, CH_2N); 4.19 (*m*, 6H, CH_2N); 7.28 (*m*, 4H, Ar-H); 7.38 (*m*, 4H, Ar-H); 7.44 (m, 1H, Ar-H); 7.97 (*m*, 1H, Ar-H); 7.99 (*m*, 1H, Ar-H).

ESI-MS m/z: calcd for $C_{28}H_{31}N_{10}O_2^+$ ($M+H^+$) 539.3. Found 539.2 ($M+H^+$).

To a solution of **30** (0.49 mmol) in anhydrous DMF (10 mL), were added Et_3N (500 µL), DIC (125 mg, 0.99 mmol), HOBT×H_2O (150 mg, 0.98 mmol) and **78** (194 mg, 0.99 mmol). The reaction was stirred at room temperature for 18 h. The solvent was evaporated by kugelrohr distillation, and the solid residue was purified on silica

gel column chromatography (CH_2Cl_2/MeOH/aqueous NH_3 55/4/1), giving 183 mg (55 %) of **79** as a pink amorphous solid.

R*f* (CH_2Cl_2/MeOH/NH_3 55/4/1%) = 0.23.

^{1}H-NMR (250 MHz, MeOD-*d*$_4$) δ: 1.43 (*s*, 9H, CH_3); 1.87 (*m*, 2H, $CH_2\beta$); 2.32 (*t*, *J*=7.3, 2H, $CH_2\alpha$); 2.86 (*m*, 6H, CH_2-N-Ar); 3.39 (*m*, 2H, $CH_2\gamma$); 3.45 (*m*, 6H, CH_2-C-N-Ar); 6.91 (*m*, 4H, Ar-H); 7.10 (*m*, 5H, Ar-H); 7.43 (*dd*, *J*=8.3, *J*=1.4, 1H, Ar-H); 7.58 (*d*, *J*=1.4, 1H, Ar-H).

IR (KBr): 3384*m*, 3058*w*, 2974*w*, 2922*w*, 1636*s*, 1628*s*, 1603*s*, 1578*s*, 1465*m*, 1364*w*, 1271*m*, 1157*m*, 741*m* cm^{-1}.

ESI-MS m/z: calcd for $C_{36}H_{46}N_{11}O_3^+$ ($M+H^+$) 680.4. Found 680.4 ($M+H^+$).

9.3.42 4-{[2-(2-{Bis-[2-(1*H*-benzoimidazol-2-ylamino)-ethyl]-amino}-ethylamino)-1*H*-benzoimidazole-5-carbonyl]-amino}-butyric acid (80)

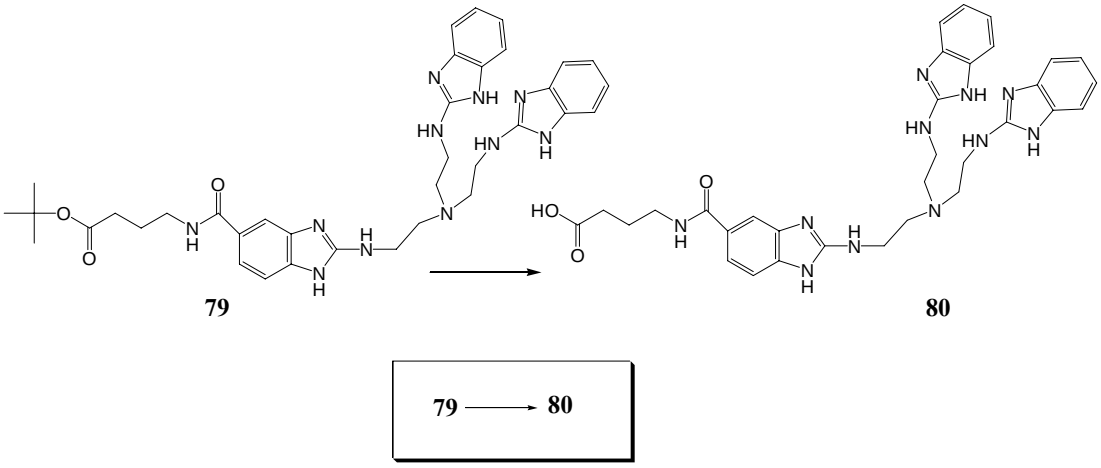

To a solution of **79** (100 mg, 0.147 mmol) in THF (4 mL) was added 0.5 M HCl (20 mL). The mixture was stirred at 70 °C for 3 h. The solvent was removed under reduced pressure to give the desired product in form of thydrochloride. NMR and

ESI spectrometry confirmed the ester hydrolysis and the crude product was used for the next step (expected to be done by a cooperation partner).

^{1}H-NMR (250 MHz, MeOD-*d*$_4$) δ: 1.90 (*m*, 2H, $CH_2\beta$); 2.40 (*t*, *J*=7.5, 2H, $CH_2\alpha$); 3.40 (*t*, *J*=6.4, 2H, $CH_2\gamma$); 3.80 (br. *m*, 6H, CH_2-N-Ar); 4.11 (br. *m*, 6H, CH_2-C-N-Ar); 7.21-7.34 (*m*, 8H, Ar-H); 7.37 (br. *d*, *J*=8.2, 1H, Ar-H); 7.71 (br. *dd*, *J*=8.2, *J*=1.4, 1H, Ar-H); 7.79 (br. *d*, 1H, Ar-H).

ESI-MS m/z: calcd. for $C_{32}H_{38}N_{11}O_3^+$ ($M+H^+$) 624.3. Found 624.3 ($M+H^+$).

9.3.43 9-(2',3',5'-tri-*O*-acetyl- β-D-ribofuranosil)-2-amino-6-oxopurine (81)

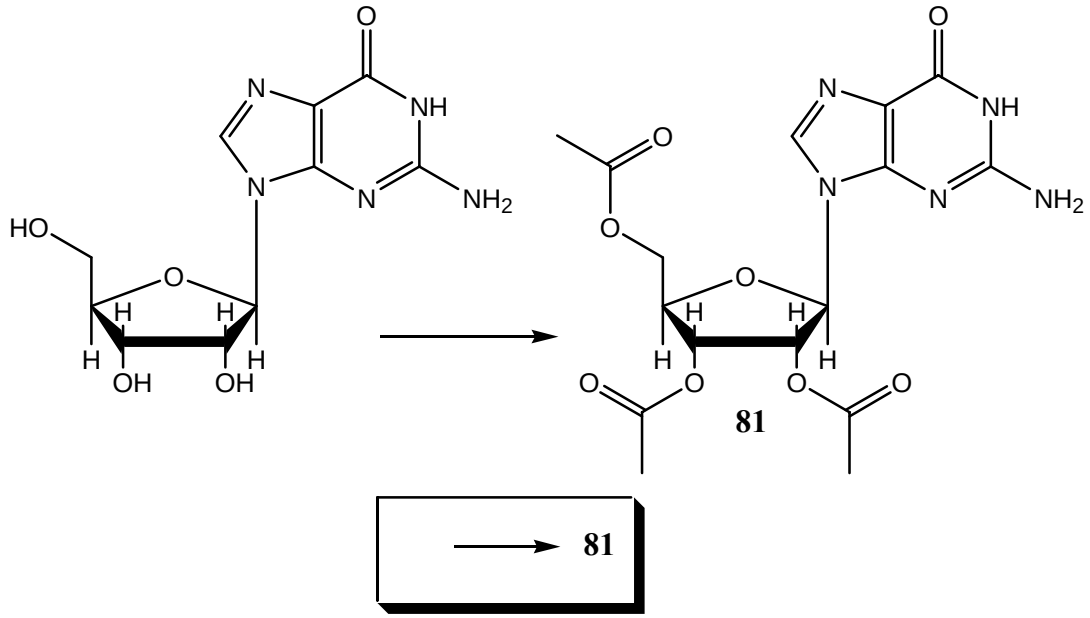

To a mixture of pyridine (37 mL) and acetic anhydride (47 mL, 497.7 mmol), in abs. DMF (60 mL), guanosine (20 g, 70.6 mmol) was added under an atmosphere of argon. The mixture was stirred for 5 h at 75 °C. The solvent was evaporated under reduced pressure, and the solid residue was purified by crystallization from 200 mL of isopropanol, giving 22.9 g (79 %) of **81** as a white solid.

R*f* **(**CH_2Cl_2/MeOH 9/1) = 0.25.

^{1}H-NMR (250 MHz, DMSO-d_6) δ: 2.03 (*s*, 3H, CH_3); 2.04 (*s*, 3H, CH_3); 2.11 (*s*, 3H, CH_3); 4.22-4.40 (*m*, 3H, 4'-H, 5'-H); 5.49 (*m*, 1H, 3'-H); 5.79 (*t*, *J*=6.1, 1H, 2'-H); 5.98 (*d*, *J*=6.0, 1H, 1'-H); 6.53 (br. *s*, 2H, NH_2); 7.93 (*s*, 1H, 8-H); 10.72 (*s*, 1H, N-H).

IR (KBr): 3464*m*, 3312*m*, 3196*s*, 3033*w*, 2936*m*, 2852*w*, 2734*m*, 2288*w*, 1747*s*, 1700*s*, 1633*s*, 1597*m*, 1538*m*, 1485*s*, 1418*m*, 1373*s*, 1227*s*, 1171*m*, 1092*w*, 1050*m*, 10189*w*, 958*w*, 910*m*, 859*w*, 809*w*, 783*m*, 736*w*, 678*m*, 638*w*, 603*w* cm^{-1}.

ESI-MS m/z: calcd for $C_{16}H_{20}N_5O_8^+$ ($M+H^+$) 410.1. Found 409.9 ($M+H^+$).

Analysis: $C_{16}H_{19}N_5O_8$ (409.35) calculated: C 46.95 H 4.68 N 17.11.
found: C 46.87 H 4.77 N 16.99.

M.p.: 229-230 °C. Lit. [146]: 230-233 °C.

9.3.44 9-(2',3',5'-tri-*O*-acetyl-β-D-ribofuranosil)-2-amino-6-chloropurine (82)

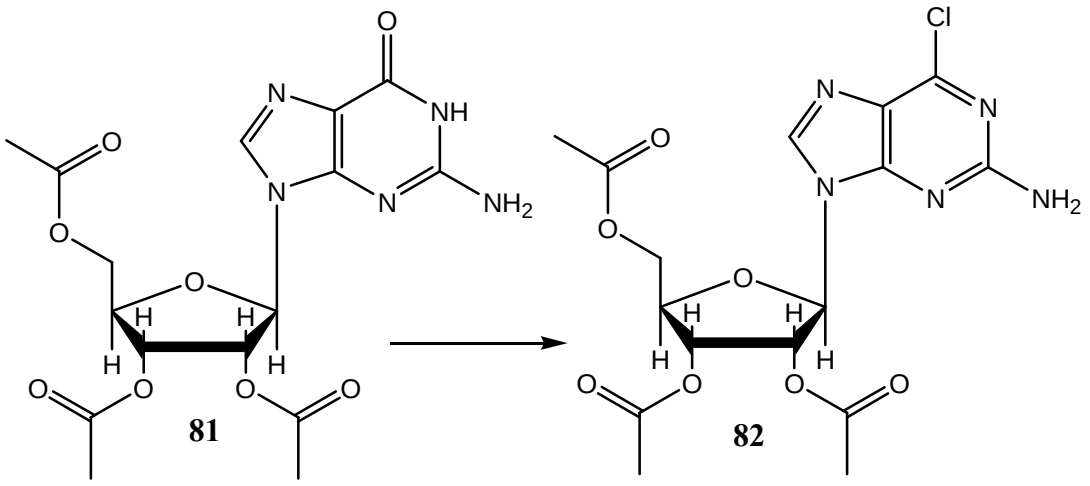

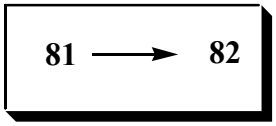

To a suspension of **81** (14.9 g, 36.4 mmol) in dry CH_3CN (200 mL), were added in the following order: anhydrous Et_4NCl (12.1 g, 73.0 mmol), *N,N*-Dimethylaniline (4.41 g, 36.4 mmol) and $POCl_3$ (16.5 g, 107.6 mmol). The mixture was stirred at 100 °C (at reflux) for 20 minutes. The solvent was evaporated under reduced pressure. The solid residue was dissolved in 200 mL of CH_2Cl_2, poured on water and the organic phase was extracted with dichloromethane (2×50 mL). The collected organic phases were washed with a saturated solution of $NaHCO_3$ (3×100 mL), dried over $MgSO_4$ and evaporated. The solid residue was purified by crystallization from 200 mL of i-PrOH, giving 11.7 g (75 %) of **82** as a white solid.

R*f* **(**CH_2Cl_2/MeOH 9/1) = 0.50.

^{1}H-NMR (250 MHz, DMSO-d_6) δ: 2.04-2.05 (2*s*, 6H, 2'+3' CH_3); 2.12 (*s*, 3H, 5' CH_3); 4.26–4.43 (*m*, 3H, 4'-H, 5'-H); 5.53 (*m*, 1H, 3'-H); 5.87 (*t*, *J*=5.9, 1H, 2'-H); 6.10 (*d*, *J*=5.9, 1H, 1'-H); 7.06 (*s*, 2H, NH_2); 8.36 (*s*, 1H, 8-H).

IR (KBr): 3444*s*, 3312*s*, 3209*s*, 2922*w*, 1732*s*, 1635*s*, 1613*s*, 1557*s*, 1521*m*, 1484*s*, 1409s, 1377*s*, 1323*m*, 1249*s*, 1215*s*, 1144*m*, 1103*w*, 1047*s*, 997*m*, 939*w*, 907*s*, 805*s*, 784*s*, 740*s*, 729*m*, 643*m*, 597*m*, 572*w* cm^{-1}.

ESI-MS m/z: calcd for $C_{16}H_{19}ClN_5O_7^+$ ($M+H^+$) 428.1. Found 427.9 ($M+H^+$).

Analysis: $C_{16}H_{18}ClN_5O_7$ (427.80) calculated: C 44.92 H 4.24 N 16.37.
found: C 44.88 H 4.37 N 16.23.

M.p.: 152-153 °C. Lit. [146]: 152-153 °C.

9.3.45 2-Amino-6-[(4-methylphenyl)thio]-9-(2,3,5-tri-*O*-acetyl-β-D-ribofuranosyl)purine (83)

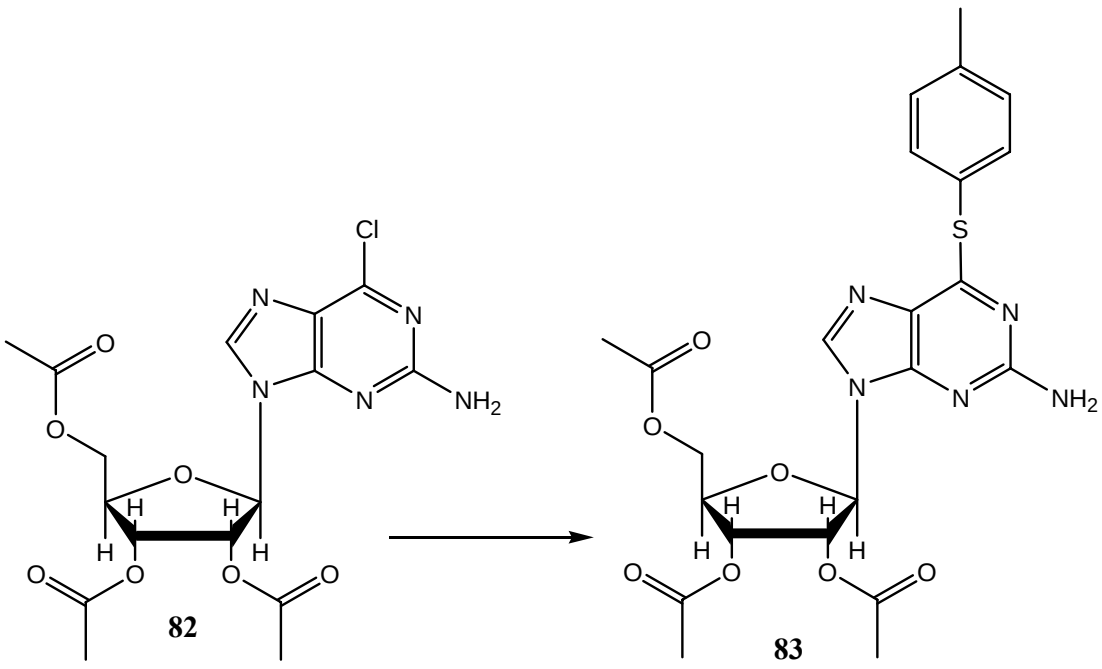

To a solution of **82** (3 g, 6.98 mmol) in DMF (30 mL) were added toluene-4-thiol (1.75 g, 14.1 mmol) and Et_3N (2.1 mL, 15 mmol). The mixture was heated at 100 °C and stirred for 1 h. The solvent was evaporated under reduced pressure, and the solid residue was purified by crystallization from 30 mL of EtOH giving 3.15 g (88 %) of the compound **83** as white crystals.

R*f* **(**CH_2Cl_2/MeOH 9/1) = 0.80.

^{1}H-NMR (250 MHz, DMSO-*d*$_6$) δ: 2.03 (*s*, 6H, 2 CH_3); 2.12 (*s*, 3H, CH_3); 2.35 (*s*, 3H, Ar-CH_3); 4.25-4.45 (*m*, 3H, 4'-H, 5'-CH_2); 5.55 (*dd*, *J*=3.7, *J*=5.8, 1H, 3'H); 5.87 (*t*, *J*=5.9, 1H, 2'-H); 6.09 (*d*, *J*=6.0, 1H, 1'-H); 6.45 (*s*, 2H, NH_2); 7.27 (*d*, *J*=8.3, 2H, o-Phenyl-H); 7.48 (*d*, *J*=8.1, 2H, m-Phenyl-H); 8.22 (*s*, 1H, 8-H).

IR (KBr): 3451*s*, 3325*s*, 3206*s*, 2885*m*, 1910*w*, 1753*s*, 1619*s*, 1592*s*, 1556*s*, 1506*s*, 1466*s*, 1402*s*, 1370*s*, 1318*m*, 1259*s*, 1025*s*, 990*s*, 910*m*, 799*m* cm^{-1}.

ESI-MS m/z: calcd for $C_{23}H_{26}N_5O_7S^+$ ($M+H^+$) 516.2. Found 515.9 ($M+H^+$).

Analysis: $C_{23}H_{25}N_5O_7S$ (515.54) calculated: C 53.58 H 4.89 N 13.58.
found: C 53.23 H 4.91 N 13.75.

M.p.: 176 °C. Lit. [141]: 175-176 °C.

9.3.46 6-[(4-Methylphenyl)-thio]-2-oxo-9(2',3',5'-tri-*O*-acetyl-β-D-ribofuranosyl)-purine (85)

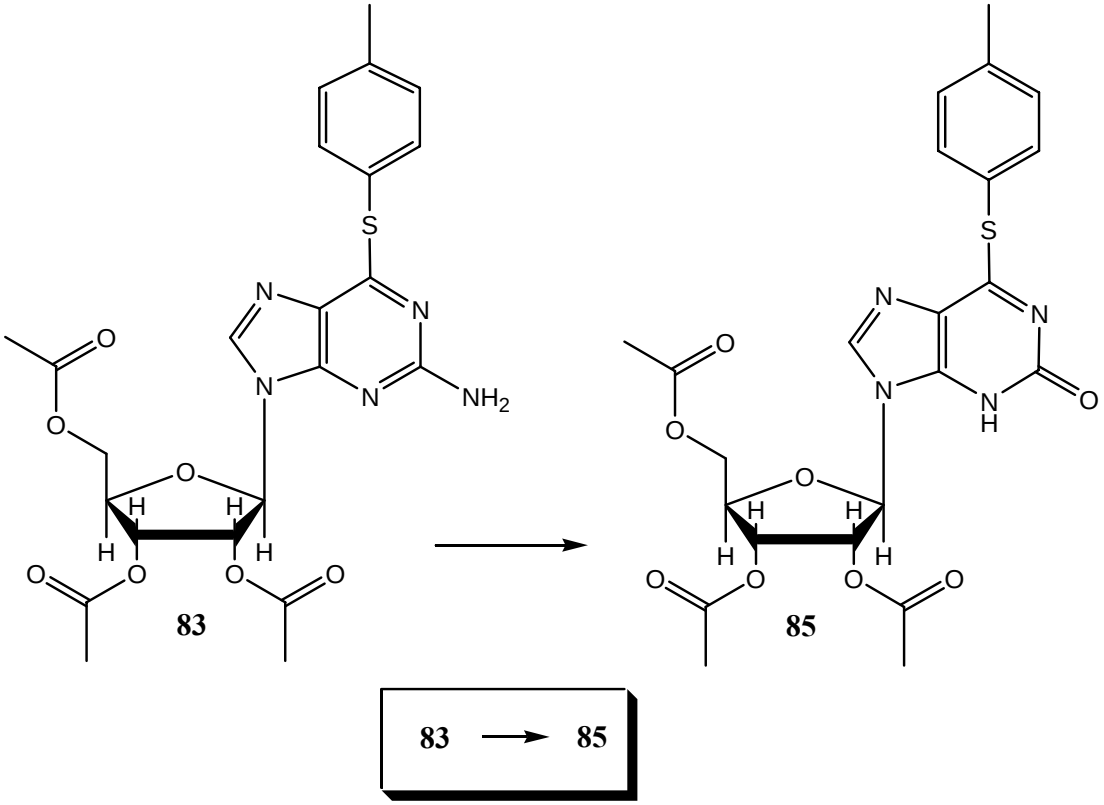

To a mixture of **83** (18 g, 34.9 mmol) in 180 mL of CH_3COOH/H_2O (1:1 v/v) at 50 °C, $NaNO_2$ (6.9 g, 100 mmol) was added in 1 h. The reaction was followed by TLC and after 2 h the deamination process was completed. The products were concentrated under reduced pressure, the solid residue dissolved in DCM (150 mL) and the resulting solution was washed with satured $NaHCO_3$ solution (2×150 mL), dried over $MgSO_4$ and evaporated. The solid residue was purified by silica gel chromatography (ethyl acetate/hexane 3/1), giving the 16.7 g (93 %) of the compound **84** as a white solid compound.

R*f* **(**CH_2Cl_2/MeOH 9/1) = 0.75.

^{1}H-NMR (250 MHz, DMSO-*d*$_6$) δ: 2.04 (*s*, 6H, $2CH_3$); 2.12 (*s*, 3H, CH_3); 2.37 (*s*, 3H, Ar-CH_3); 4.25-4.45 (*m*, 3H, 4'-H, 5'-CH_2); 5.56 (*m*, 1H, 3'H); 5.91 (*t*, *J*=5.9, 1H, 2'-H); 6.15 (*d*, 1H, *J*=5.7, 1'-H); 7.29 (*d*, 2H, *J*=7.7, o-Phenyl); 7.50 (*d*, *J*=8.0, 2H, m-Phenyl); 8.41 (*s*, 1H, 8-H); 11.74 (*s*, 1H, N-H).

IR (KBr): 3470*w*, 3108*w*, 2954*m*, 1751*s*, 1623*m*, 1563*s*, 1507*m*, 1445*m*, 1375*s*, 1318*w*, 1231*s*, 1135*w*, 1094*m*, 1047*m*, 1006*w*, 908*m*, 808*m*, 790*w*, 737*w* cm^{-1}.

ESI-MS m/z: calcd for $C_{23}H_{25}N_4O_8S^+$ ($M+H^+$) 517.1. Found 516.9 ($M+H^+$).

Analysis: $C_{23}H_{24}N_4O_8S$ (516.52) calculated: C 53.48 H 4.68 N 10.85.
found: C 53.34 H 4.90 N 10.67.

M.p.: 109 °C.

9.3.47 Isoguanosine (86)

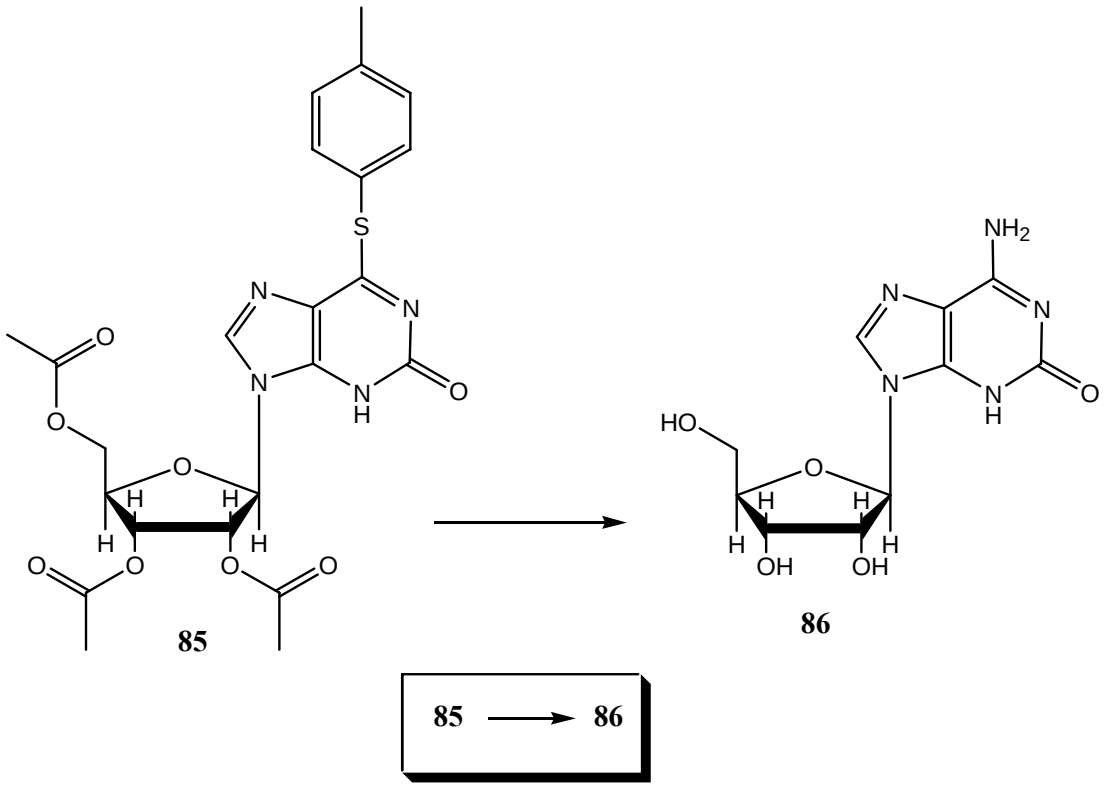

To a mixture of **85** (3 g, 5.81 mmol) in EtOH (15 mL) stirred in the glass inset of a steel autoclave, was added aqueous ammonia (32 %, 45 mL). The autoclave was closed and the mixture stirred at 80 °C for 18 h. The resulting mixture was evaporated and the solid residue was purified by crystallization from absolute ethanol (15 mL), giving 1.17 g (71 %) of the compound **86** a white powder.

R*f* (Butanol/HOAc/H_2O 5/2/3 = 0.6

^{1}H-NMR (250 MHz, DMSO-d_6/D_2O) δ: 3.53 (*dd*, *J*=2.6, *J*=12.3, 1H, 5'-CH_2); 3.61 (*dd*, *J*=2.6, *J*=12.3, 1H, 5'H); 3.93 (*m*, 1H, 4'H); 4.08 (*m*, 1H, 3'H); 4.53 (*m*, 1H, 2'H); 5.64 (*d*, *J*=6.5, 1H, 1'H); 7.95 (*s*, 1H, 8-H).

IR (KBr): 3246*s*, 3108*s*, 2931*s*, 1672*s*, 1614*s*, 1529*m*, 1400*s*, 1319*m*, 1216*m*, 1122*m*, 1083*m*, 1053*m*, 902*w*, 865*w*, 803*w*, 770*m*, 694*m*, 672*w*, 629*m* cm^{-1}.

ESI-MS m/z: calcd for $C_{10}H_{12}N_5O_5^-$ (M^-) 282.1. Found 281.9 (M^-).

Analysis: $C_{10}H_{13}N_5O_5$ (283.24) calculated: C 42.40 H 4.63 N 24.73.
Found: C 39.75 H 4.90 N 22.53
1 H_2O (301.26) calculated: C 39.87 H 5.02 N 23.25

9.3.48 6-*N*-[(Dimethylamino)methylene]-isoguanosine (89).

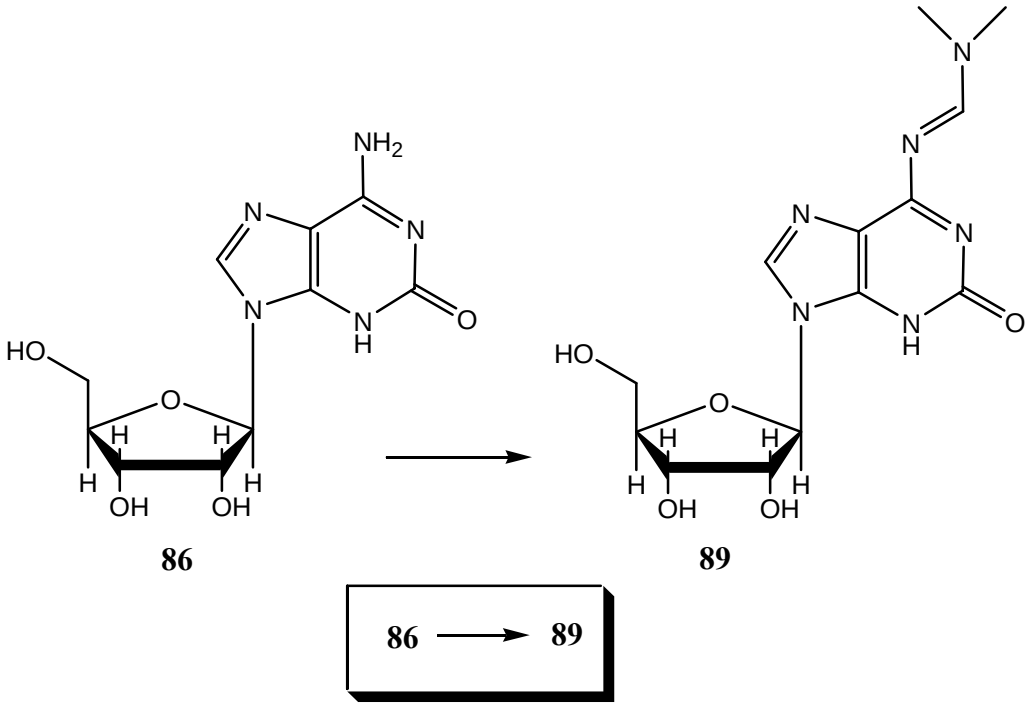

86 **89**

86 → 89

To a mixture of **86** (2 g, 7.06 mmol) in abs. DMF (30 mL), was added *N,N*-dimethylformamide dimethyl acetal (3 g, 25.2 mmol). The mixture was stirred at

room temperature for 24 h. The solvent was removed under reduced pressure and the crude material crystallized from MeOH (15 mL), giving 2.1 g (88 %) of the compound **89** as a white powder.

^{1}H-NMR (250 MHz, DMSO-*d*$_6$) δ: 3.10 (br. *d*, 3H, CH_3); 3.21 (*s*, 3H, CH_3); 3.47-3.67 (*m*, 2H, 5'H); 3.92 (*m*, 1H, 4'H); 4.09 (br. *m*, 1H, 3'H); 4.55 (br. *m*, 1H, 2'H); 5.12 (br. *s*, 1H, 3'OH); 5.40 (br. *s*, 1H, 2'OH); 5.60 (br. *s*, 1H, 5'OH); 5.66 (*d*, *J*=6.3, 1H, 1'H); 8.06 (*s*, 1H, 8-H); 9.18 (*s*, 1H, N=CH-N); 11.11 (br. *s*, 1H, NH).

IR (KBr): 3385*m*, 2926*w*, 1654*m*, 1604*s*, 1560*s*, 1425*m*, 1370*s*, 1314*w*, 1124*m*, 1086*w*, 1044*w*, 981*w*, 874*w*, 827*w*, 781*w*, 713*w*, 630*w* cm^{-1}.

ESI-MS m/z: calcd for $C_{13}H_{19}N_6O_5^+$ ($M+H^+$) 339.1. Found 338.9 ($M+H^+$).

Analysis: $C_{13}H_{18}N_6O_5$ (338.32) calculated: C 46.15 H 5.36 N 24.84.
found: C 44.44 H 5.55 N 24.83.
0.6 H_2O (349.13) calculated: C 44.72 H 5.54 N 24.07.

9.3.49 5'-*O*-(4,4'-Dimethoxytrityl)-6-*N*-[(dimethylamino)methylene]-isoguanosine (90)

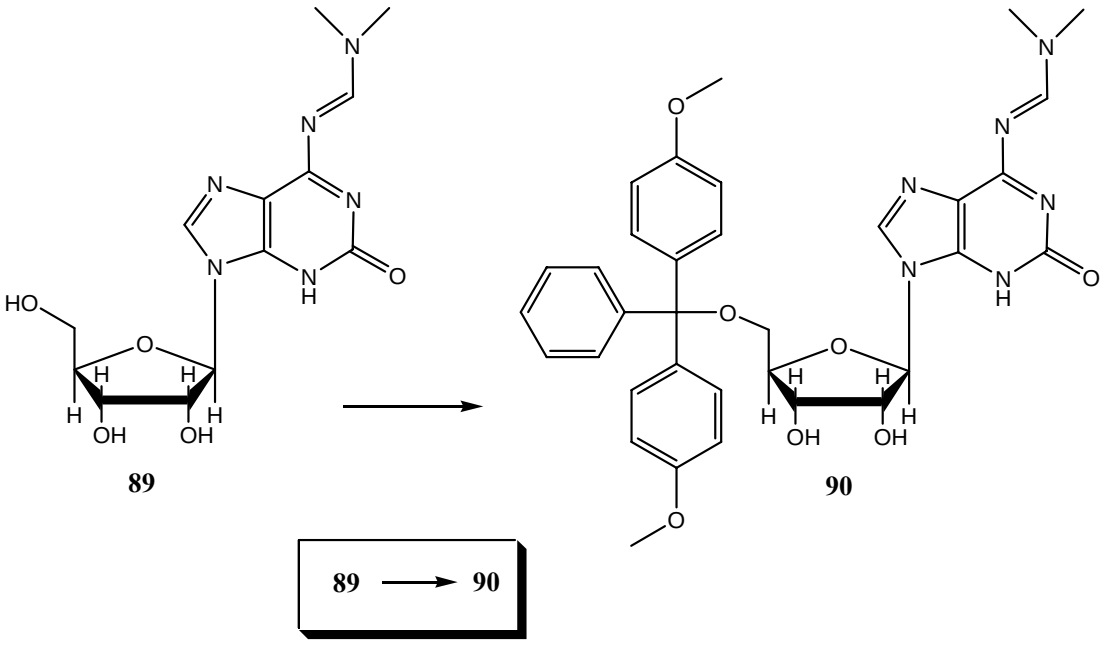

Compound **89** (5 g, 14.8 mmol) was co-evaporated three times with anhydrous pyridine, and dissolved in anhydrous pyridine (200 mL). Dimethoxytritylchloride (10 g, 29.5 mmol) was added under argon atmosphere at 60 °C in 6 h (this uncommon temperature was required due to the low solubility of the starting material **89** in all solvents tested). After the mixture was stirred over night at room temperature the mixture was treated with 5% aq. $NaHCO_3$ solution (90 mL) and extracted with DCM (2×150 mL). The combined organic layers were dried over $MgSO_4$ and evaporated. The crude material was purified by silica gel column chromatography (DCM/MeOH 9/1) yielding 5.97 g (63 %) of **90** as a white solid compound.

R*f* **(**CH_2Cl_2/MeOH 9/1) = 0.51.

^{1}H-NMR (250 MHz, DMSO-*d*$_6$) δ: 3.10 (*s*, 3H, N-CH_3); 3.15-3.23 (*m*, 5H, N-CH_3, 5'H); 3.73 (*s*, 6H, O-CH_3); 4.00 (*m*, 1H, 4'H); 4.20 (*m*, 1H, 3'H); 4.49 (*m*, 1H, 2'H); 5.15 (*d*, *J*=6.1, 1H, 3'OH); 5.55 (*d*, *J*=5.4, 1H, 2'OH); 5.74 (*d*, *J*=4.2, 1H, 1'H); 6.82-6.87 (*m*, 4H, Ar-H); 7.17-7.38 (*m*, 9H, Ar-H); 7.97 (*s*, 1H, 8-H); 9.15 (*s*, 1H, N=CH-N); 10.90 (*s*, 1H, NH).

IR (KBr): 3126*w*, 2931*m*, 2835*w*, 1608*s*, 1558*s*, 1508*s*, 1423*m*, 1368*s*, 1302*w*, 1250*m*, 1177*m*, 1120*m*, 1063*w*, 1032*m*, 903*w*, 828*m*, 780*w*, 756*w*, 728*w*, 704*w*, 662*w*, 635*w*, 585*w* cm^{-1}.

ESI-MS m/z: calcd for $C_{34}H_{37}N_6O_7^+$ ($M+H^+$) 641.27, $C_{34}H_{35}N_6O_7^-$ (M^-) 639.26. Found 641.2 ($M+H^+$), 639.5 (M^-).

9.3.50 5'-*O*-(4,4'-Dimethoxytrity)-6-*N*-[(dimethylamino)methylene]-2'-*O*-(triisopropisilyl)isoguanosine (91) and 5'-*O*-(4,4'-Dimethoxytrity)-6-*N*-[(dimethylamino)methylene]-3'-*O*-(triisopropisilyl)isoguanosine (92)

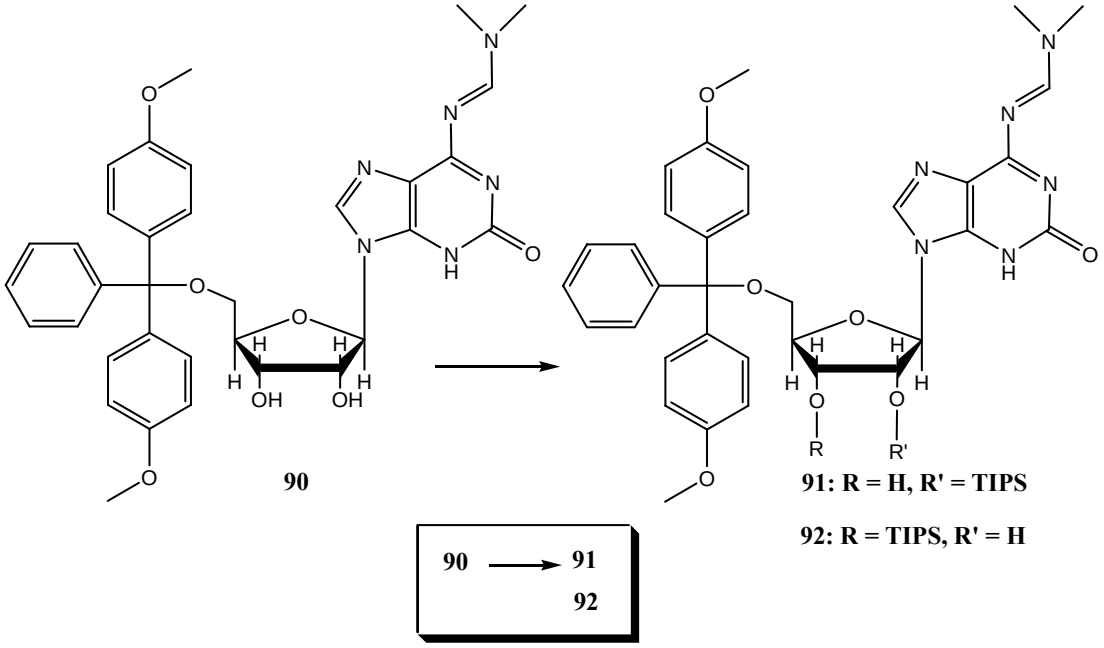

Compound **90** (5.6 g, 8.74 mmol) was co-evaporated three times with anhydrous pyridine, dryed *in vacuo* over night and dissolved in anhydrous DMF (50 mL). To this solution under argon, were added imidazole (1.53 g, 22.5 mmol) and dropwise in 10 minutes triisopropylsilyl chloride (3.54 g, 18.4 mmol). The mixture was stirred at room temperature for 24 h. The reaction was quenched with 5% aqueous $NaHCO_3$ (20 mL) and concentrated *in vacuo.* The solid residue was redissolved in CH_2Cl_2 (150 mL), washed with satured $NaHCO_3$ solution (2×150 mL), dried over $MgSO_4$ and concentrated. The solid residue was purified by silica gel column chromatography (DCM/MeOH 9/0.1) yielding 3.9 g (56%) of a mixture of **91** and **92** as a white solid compound, the mixture of the two stereoisomers was purified by HPLC performed on Macherey-Nagel Nucleoprep (250×50 mm, 20 μm) column, using isocratic elution with dioxane, flow: 1 ml/min, giving the coumpond **91** (1.09 g, 16 %) and **92** (2.81 g, 40 %).

R*f* **(**DCM/MeOH 9/0.1) = 0.34

91:

^{1}H-NMR (250 MHz, DMSO-d_6) δ: 0.87-1.00 (*m,* 21H, 3CH, 6CH_3, ^{i}Prop); 3.10 (*s*, 3H, CH_3) 3.15-3.27 (*m*, 2H, 5'H); 3.20 (*s*, 3H, CH_3); 3.72 (*s*, 6H, CH_3O); 4.03 (*m*, 1H, 4'H); 4.21 (*m*, 1H, 3'H); 4.79 (*m*, 1H, 2'H); 5.05 (*d*, *J*=6.7, 1H, 3'OH); 5.81 (*d*, *J*=4.90, 1H, 1'H); 6.83-6.87 (*m*, 4H, Ar-H); 7.19-7.38 (*m*, 9H, Ar-H); 8.01 (*s*, 1H, 8-H); 9.13 (*s*, 1H, N=CH-N); 11.06 (*s*, 1H, NH).

IR (KBr): 3404*w*, 2942*m*, 2865*m*, 1654*m*, 1610*s*, 1553*s*, 1508*m*, 1458*w*, 1423*w*, 1367*m*, 1301*w*, 1251*m*, 1176*m*, 1177*m*, 1120*m*, 1032*m*, 874*w*, 830*w*, 782*w*, 704*w*, 687*w* cm^{-1}.

ESI-MS m/z: calcd for $C_{43}H_{57}N_6O_7Si^+$ ($M+H^+$) 797.4. Found 797.5 ($M+H^+$).

92:

^{1}H-NMR (250 MHz, DMSO-d_6) δ: 0.94-1.01 (*m,* 21H, 3CH, 6CH_3, ^{i}Prop); 3.10 (*s*, 3H, CH_3); 3.11-3.15 (*m*, 2H, 5'H); 3.19 (*s*, 3H, CH_3); 3.71 (*s*, 6H, CH_3O); 4.01 (*m*, 1H, 4'H); 4.36 (*m*, 1H, 3'H); 4.62 (*m*, 1H, 2'H); 5.45 (*d*, *J*=6.3, 1H, 2'OH); 5.73 (*d*, *J*=5.7, 1H, 1'H); 6.83-6.86 (*m*, 4H, Ar-H); 7.18-7.36 (*m*, 9H, Ar-H); 7.98 (*s*, 1H, 8-H); 9.15 (*s*, 1H, N=CH-N); 11.06 (*s*, 1H, NH).

IR (KBr): 3230*w*, 2940*m*, 2865*m*, 1654*m*, 1609*s*, 1560*s*, 1508*m*, 1459*w*, 1424*w*, 1368*s*, 1301*w*, 1251*s*, 1177*w*, 1120*w*, 1068*w*, 1032*w*, 996*w*, 915*w*, 880*w*, 829*m*, 781*w*, 755*w*, 727*w*, 684*w* cm^{-1}.

ESI-MS m/z: calcd for $C_{43}H_{57}N_6O_7Si^+$ ($M+H^+$) 797.4. Found 797.6 ($M+H^+$).

9.3.51 5'-*O*-(4,4'-Dimethoxytrityl)-6-*N*-[(dimethylamino)methylene]-2'-*O* (triisopropylsilyl) isoguanosine 2-*N*,*N'*-Diisopropyl(cyanoethoxy)phosphoramidite (95).

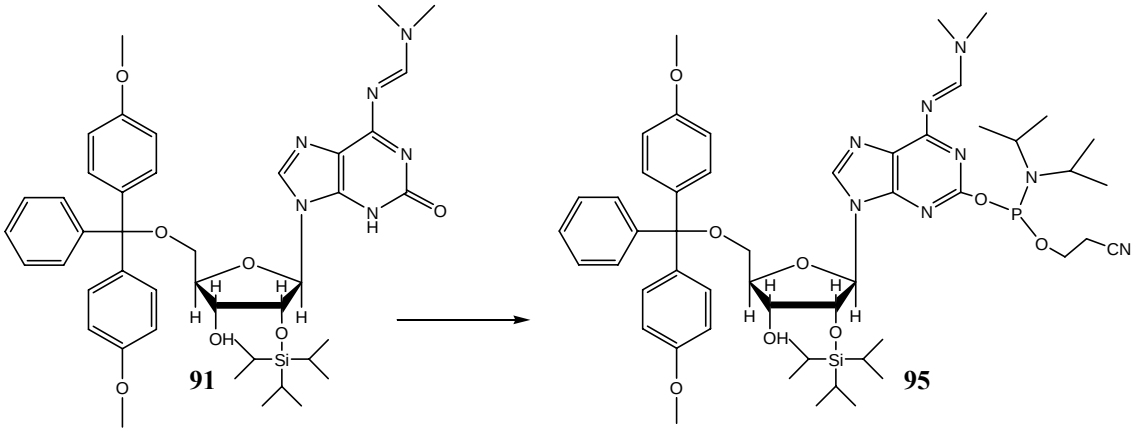

91 (600 mg, 0.753 mmol) was dried by three co-evaporations with anhydrous THF and dissolved in 20 mL of anhydrous THF. To this solution were added: diisopropylethylamine (600 µL, 3.51 mmol) and then 2-cyanoethoxy-*N*,*N*-diisopropylphosphoramidochloride (213.8 mg, 0.903 mmol). The reaction was stirred at room temperature under argon for 2 h. The crude material was poured onto ethyl acetate, the organic phase was washed twice with saturated $NaHCO_3$ solution and the organic layer was let over Na_2SO_4 for 20 min. After filtration the solvent was removed by reduced pressure, and the crude material purified by silica gel chromatography (CH_2Cl_2/ethyl acetate/Et_3N 1/1/1 %), giving 340 mg (45 %) of **95**.

^{1}H-NMR (250 MHz, DMSO-d_6) δ: 0.86-1.00 (*m,* 21H, 3CH, 6CH_3, ^{i}Prop); 1.12-1.20 (*m*, 12H, $CH_3{}^i$Prop); 2.76 (*t*, *J*=5.82, 2H, CH_2CN) 3.10-3.27 (*m*, 8H, 2CH_3, 5'H); 3.66-3.76 (*m*, 8H, CH^iProp, CH_3O); 3.92 (*m*, 2H, $CH_2\beta CN$); 4.08 (*m*, 1H, 4'H); 4.21 (*m*, 1H, 3'H); 4.83 and 4.89 (2*t*, *J*=4.9, 1H, 2'H); 5.10 (2*d*, *J*=2.9, 1H, 3'OH); 5.95 (2*d*, *J*=3.9 1H, 1'H); 6.82-6.87 (*m*, 4H, Ar-H); 7.20-7.38 (*m*, 9H, Ar-H); 8.19-8.20 (2*s*, 1H, 8-H); 8.81 (*s*, 1H, N=CH-N).

^{31}P-NMR (161.98 MHz, C_6D_6) δ: 157.06, 157.08.

9.3.52 Synthesis of 96-99

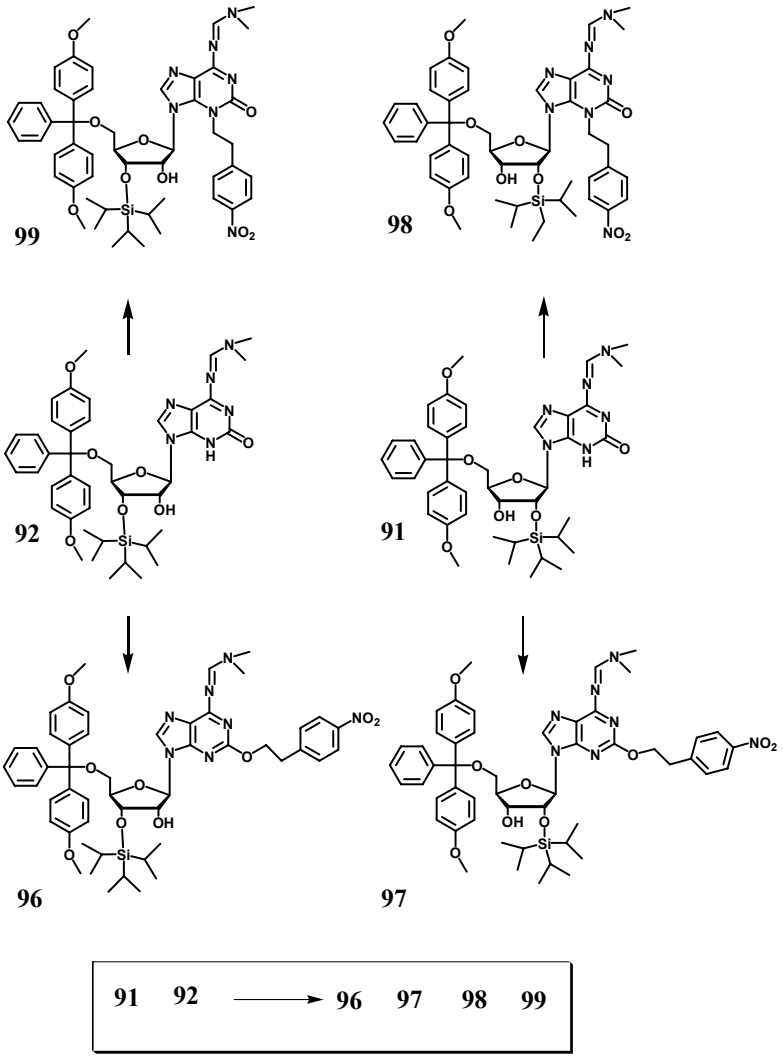

To the mixture of **91** and **92** (3.65 g, 4.58 mmol) in 200 mL of abs. dioxan, were added triphenylphosphine (1.44 g, 5.50 mmol), diethyl azodicarboxylate (958 mg, 5.50) and *p*-nitrophenylethanol (919 mg, 5.50 mmol). The reaction was stirred for 24 h at room temperature. After evaporation to a smaller volume and dilution in 500 mL of $CHCl_3$, the solution was washed with water (2 × 100 mL). The organic layer was separated, dried over Na_2SO_4 and evaporated. After a prepurification by silica gel column chromatography (EtOAc), a mixture of **96-99** plus triphenylphosphineoxide

was obtained. A part of the mixture was purified by HPLC performed on a Macherey-Nagel Nucleoprep (250×50 mm, 20 µm) column, using isocratic elution with ethyl acetate 90 %, dioxane 10 %, flow: 2 ml/min. 4 different fractions were isolated and analysed.

R*f* (Ethyl acetate) = 0.16, 0.28, 0.38, 0.48.

96:

^{1}H-NMR (250 MHz, DMSO-*d*$_6$) δ: 0.97-1.02 (*m,* 21H, 3CH, 6CH_3, ^{i}Prop); 3.04 (*t*, *J*=7.2, 2H, CH_2-Ar); 3.10 (*s*, 3H, CH_3); 3.12-3.37 (*m*, 2H, 5'H); 3.16 (*s*, 3H, CH_3); 3.72 (2*s*, 6H, CH_3O); 4.03 (*m*, 1H, 4'H); 4.39-4.44 (*m*, 3H, CH_2-O, 3'H); 4.66 (*m*, 1H, 2'H); 5.43 (*d*, *J*=6.3, 1H, 2'OH); 5.74 (*d*, *J*=5.5, 1H, 1'H); 6.82-6.87 (*m*, 4H, Ar-H); 7.14-7.36 (*m*, 9H, Ar-H); 7.41 (*m*, 2H, Ar-NO_2); 7.99 (*s*, 1H, 8-H); 8.10 (*m*, 2H, Ar-NO_2); 8.87 (*s*, 1H, N=CH-N).

ESI-MS m/z: calcd for $C_{51}H_{64}N_7O_9Si^+$ ($M+H^+$) 946.5. Found 946.9 ($M+H^+$).

97:

^{1}H-NMR (250 MHz, DMSO-*d*$_6$) δ: 0.90-0.98 (*m,* 21H, 3CH, 6CH_3, ^{i}Prop); 3.05 (*t*, *J*=7.1, 2H, CH_2-Ar); 3.09 (*s*, 3H, CH_3); 3.16 (*s*, 3H, CH_3); 3.17-3.28 (*m*, 2H, 5'H); 3.72 (2*s*, 6H, CH_3O); 4.04 (*m*, 1H, 4'H); 4.21 (*m*, 1H, 3'H); 4.43 (*m*, 2H, CH_2-O); 4.80 (*m*, 1H, 2'H); 5.06 (*d*, *J*=6.7, 1H, 3'OH); 5.80 (*d*, *J*=4.9, 1H, 1'H); 6.83-6.87 (*m*, 4H, Ar-H); 7.16-7.38 (*m*, 11H, Ar-H); 8.08 (*m*, 2H, Ar-NO_2); 8.00 (*s*, 1H, 8-H); 8.83 (*s*, 1H, N=CH-N).

ESI-MS m/z: calcd for $C_{51}H_{64}N_7O_9Si^+$ ($M+H^+$) 946.5. Found 946.6 ($M+H^+$).

98:

^{1}H-NMR (250 MHz, DMSO-*d*$_6$) δ: 0.82-0.93 (*m*, 21H, 3CH, 6CH_3, ^{i}Prop); 3.08 (*t*, *J*=7.1, 2H, CH_2-Ar); 3.11 (*s*, 3H, CH_3); 3.19 (*s*, 3H, CH_3); 3.24 (*m*, 2H, 5'H); 3.71 (2*s*, 6H, CH_3O); 4.08 (*m*, 1H, 4'H); 4.29 (*m*, 1H, 3'H); 4.33-4.48 (*m*, 2H, CH_2-O); 4.97 (*m*, 1H, 2'H); 5.16 (*d*, *J*=6.2, 1H, 3'OH); 5.94 (*d*, *J*=5.2, 1H, 1'H); 6.78-6.83

(*m*, 4H, Ar-H); 7.18-7.38 (*m*, 9H, Ar-H); 7.50 (*m*, 2H, Ar-NO_2); 8.14 (*m*, 2H, Ar-NO_2); 8.19 (*s*, 1H, 8-H); 8.82 (*s*, 1H, N=CH-N).

ESI-MS m/z: calcd for $C_{51}H_{64}N_7O_9Si^+$ ($M+H^+$) 946.5. Found 946.5 ($M+H^+$).

99:

^{1}H-NMR (250 MHz, DMSO-*d*$_6$) δ: 0.94-1.00 (*m,* 21H, 3CH, $6CH_3$, ^{i}Prop); 3.09-3.40, (*m*+2*s*, 10H, CH_2-Ar, $2CH_3$, 5'H); 3.70 (2*s*, 6H, CH_3O); 4.03 (*m*, 1H, 4'H); 4.39-4.50 (*m*, 3H, CH_2-O, 3'H); 4.82 (*m*, 1H, 2'H); 5.40 (*d*, *J*=6.4, 1H, 2'OH); 5.88 (*d*, *J*=5.4, 1H, 1'H); 6.75-6.81 (*m*, 4H, Ar-H); 7.16-7.34 (*m*, 9H, Ar-H); 7.52 (*m*, 2H, Ar-NO_2); 8.15 (*m*, 2H, Ar-NO_2); 8.20 (*s*, 1H, 8-H); 8.84 (*s*, 1H, N=CH-N).

ESI-MS m/z: calcd for $C_{51}H_{64}N_7O_9Si^+$ ($M+H^+$) 946.5. Found 946.8 ($M+H^+$).

10 Appendix

10.1 References

[1] Griffith, F. *J. Hygiene* **1928**, *27*, 113-159.

[2] Avery, O. T.; MacLeod, C. M.; McCarty, M. *J. Exp. Med.* **1944**, *79*, 137-158.

[3] Herschey, A. D.; Chase, M. *J. Gen. Physiol*. **1952**, *36*, 39-56.

[4] Watson, J. D.; Crick, F. H. C. *Nature* **1953**, *171*, 737-738.

[5] Hoagland, M. B.; Stephenson, M. L.; Scott, J. F.; Hecht L. I.; Zamecnik P. C. *J. Biol. Chem.* **1958**, *231*, 241-257.

[6] a) Jacob, F.; Perrin, D.; Sánchez, C.; Monod, J. *C. R. Acad. Sci. Paris* **1960**, *250*, 1727-1729. b) Jacob F. *C. R. Biologies* **2005**, *328*, 514-520.

[7] Brenner, S.; Jacob, F.; Meselson, M. *Nature* **1961**, *190*, 576-581.

[8] a) Fire, A.; Xu S.; Montgomery M. K.; Kostas, S. A.; Driver, S. E.; Mello, C. C. *Nuture* **1998**, *391*, 806-811.
b) http://nobelprize.org/nobel_prizes/medicine/laureates/2006

[9] a) Hertzberg, R. P.; Dervan, P. B. *J. Am. Chem. Soc*. **1982**, *104*, 313-315. b) Hertzberg, R. P.; Dervan, P. B. *Biochemistry* **1984**, *23*, 3934-3945. c) Sluka, J. P.; Horvath, S. J.; Glasgow, A. C.; Simon, M. I.; Dervan, P. B. *Biochemistry* **1990**, *29*, 6551-6561.

[10] Gnaccarini, C.; Peter, S.; Scheffer, U.; Vonhoff, S.; Klussmann, S.; Göbel M. W. *J. Am. Chem. Soc.* **2006**, *128*, 8063-8067.

[11] a) Scherer, L.; Rossi, J. *Nat. Biotechnol*. **2003**, *21*, 1457-1465. b) De Mesmaeker, A.; Häner, R.; Martin, P.; Moser, H. E. *Acc. Chem. Res.* **1995**, *28*, 366-374.

[12] a) Crouch, R. J.; Dirksen, M.-L. In *Nucleases*; Linn, S. M.; Lloyd, R. S.; Roberts, R. J. Eds.; Cold Spring Harbor Laboratory Press: Cold Spring Harbor: NY, **1982**; pp. 211-241. b) Nakamura H.; Oda Y.; Iwai S.; Inoue H.; Ohtsuka E.; Kanaya S.; Kimura S.; Katsuda C.; Katayanagi K.; Morikawa, K.; Miyashiro H.; Ikehara M. *Proc. Natl. Acad. Sci. U. S. A.* **1991**, *88*, 11535-11539.

[13] a) Nielsen P. E.; Egholm, M.; Berg, R. H.; Buchardt, O. *Science* **1991**, *254*, 1497-1500. b) Hyrup, B.; Nielsen, P. E. *Biorg. Med. Chem.* **1996**, *4*, 5-23.

[14] Imbach, J. L.; Rayner, B.; Morvan, F. *Nucleosides Nucleotides* **1989**, *8*, 627-648. b) Monia, B. P.; Lesnik, E. A.; Gonzalez, C.; Lima, W. F.; McGee D.; Guinosso, C. J.; Kawasaki, A. M.; Cook, P. D.; Freier, S. M. *J. Biol. Chem.* **1993**, *268*, 14514-1452. c) Davies, J.; Hostomka, Z.; Hostomsky, Z.; Jordan, S.; Matthews, D. *Science* **1991**, *252*, 88-95. d) Hostomsky, Z.; Hostomska, Z.; Matthews, D. A. In *Nucleases*; Linn, S. M.; Lloyd, R. S.; Roberts, R. J. Eds.; Cold Spring Harbor Laboratory Press: Cold Spring Harbor: NY, **1993**. e) Crooke, S. T.; Lemonidis, K. M.; Neilson, L.; Griffey, R.; Lesnik, E. A.; Monia, B. P. *Biochem. J.* **1995**, *312*, 599-608.

[15] Trawick, B. N.; Daniher, A. T.; Bashkin, J. K. *Chem. Rev.* **1998**, *98*, 939-960.

[16] Scheffer, U.; Strick, A.; Ludwig, V.; Peter, S.; Kalden, E.; Göbel M. W. *J. Am. Chem. Soc.* **2005**, *127*, 2211-2217.

[17] a) Mei, H. Y.; Galan, A. A.; Halim, N. S.; Mack, D. P.; Moreland, D. W.; Sanders, K. B.; Truong, H. N.; Czarnik, A. W. *Bioorg. Med. Chem. Lett.* **1995**, *5*, 2755-2760. b) Riguet, E.; Désiré, J.; Bailly, C.; Décout J.-L. *Tethrahedron* **2004,** *60*, 8053-8064.

[18] Hostetler, M. J.; Green, S. J.; Stokes J. J.; Murray, R. W. *J. Am. Chem. Soc.* **1996**, *118*, 4212-4213.

[19] Hostetler, M. J.; Templeton, A. C.; Murray, R. W. *Langmuir* **1999**, *15*, 3782-3789.

[20] Guerrier-Takada, C.; Gardiner, K.; Marsh, T.; Pace, N.; Altman, S. *Cell* **1983**, *35*, 849-57.

[21] Kruger, K.; Gabrowski, P. J.; Zaug, A. J.; Sands, J.; Gottschling, D. E.; Cech, T. R. *Cell* **1982**, *31*, 147-157.

[22] Cech, T. R.; Zaug, A. J.; Grabowski, P. J. *Cell* **1981**, *27*, 487-496.

[23] Lohrmann, R.; Orgel, L. E. *Nature* **1973**, 244, 418-420

[24] Inoue, T.; Orgel, L. E. *Science* **1983**, *219*, 859-862.

[25] a) Renz, M.; Lohrmann, R.; Orgel, L. E. *Biochim. Biophys. Acta* **1971**, *240*, 463-471. b) Usher, D. A.; McHale, A. H. *Science* **1976**, *192*, 5345, 53-54.

[26] Usher, D. A.; McHale, A. H. *Proc. Nat. Acad. Sci. U.S.A*. **1976**, *73*, 1149-1153.

[27] Kierzek, R.; He, L.; Turner, D. H. *Nucleic Acids Res.* **1992**. *20*, 1685-1690.

[28] a) Oivanen, M.; Kuusela, S.; Lönnberg, H. *Chem. Rev.* **1998**, *98*, 961-990. b) Zhou, D.-M.; Taira, K. *Chem. Rev.* **1998**, *98*, 991-1026. c) Perreault, D. M.; Anslyn, E. V. *Angew Chem. Int. Ed. Engl.* **1997**, *36*, 432-450.

[29] Kirby, A. J.; Younas M. *J. Chem. Soc.(B)* **1970**, 510-513.

[30] a) Kirby, A. J. *Adv. Phys* Org. C*hem.* **1980**, *17*, 183-278. b) Oakenfull, D. G.; Richardson, D. I. Jr.; Usher, D. A. *J. Am. Chem. Soc.* **1967**, *36*, 5491-5492.

[31] Usher D. A.; Richardson, D. I. Jr.; Oakenfull D. G. *J. Am. Chem. Soc*. **1970**, *92*. 4699-4712.

[32] Niittymäki, T.; Lönnberg H. *Org. Biomol. Chem*. **2006**, *4*, 15-25.

[33] Westheimer, F. H. *Acc. Chem. Res.* **1968**, *1*, 70-78.

[34] a) Kaukinen, U.; Venäläinen, T.; Lönnberg, H.; Peräkylä, M. *Org. Biomol. Chem.* **2003**, *1*, 2439-2447. b) Kaukinen, U.; Lyytikäinen, S.; Mikkola, S.; Lönnberg, H. *Nucleic Acids Res*. **2002**, *30*, 468-474.

[35] a) Kunitz, M. *Science* **1939**, *90*, 112-113. b) Kunitz, M. *J. Gen. Physiol.* **1940**, *24*, 15-32.

[36] Fankuchen, I. *J. Gen. Physiol.* **1941**, *24*, 315-316.

[37] Findlay, D.; Herries, D. G.; Mathias, A. P.; Rabin, B. R.; Ross, C. A. *Nature* **1961**, *190*, 781-784.

[38] Raines R. T. *Chem. Rev.* **1998**, *98*, 1045-1065.

[39] Roberts, G. C. K.; Dennis, E. A.; Meadows, D. H.; Cohen, J. S.; Jardetzky, O. *Proc. Natl. Acad. Sci. U.S.A.* **1969**, *62*, 1151-1158.

[40] Flogel, M.; Albert, A.; Biltonen, R. *Biochemistry* **1975**, *14*, 2616-2621.

[41] Gerlt, J. A.; Gassman, P. G. *Biochemistry* **1993**, *32*, 11943-11952.

[42] Cotton, A. F.; Hazen, E. E. Jr.; Legg, M. J. *Proc. Natl. Acad. Sci. U.S.A*. **1979**, *76*, 6, 2551-2555.

[43] Serpersu E. H.; Shortle, D.; Mildvan, A. S. *Biochemistry* **1987**, *26*, 1289-1300.

[44] Morrow, J. R.; Iranzo, O. *Curr. Opin. Chem. Biol.* **2004**, *8*, 192-200.

[45] Kimura, E. *Curr. Opin. Chem. Biol.* **2000**, *4*, 207-213.

[46] Emilsson, G. M.; Nakamura, S.; Roth, A.; Breaker, R. R. *RNA* **2003**, *9*, 907-918.

[47] Iranzo, O.; Kovalevsky, A. Y.; Morrow, J. R.; Richard, J. P. *J. Am. Chem. Soc.* **2003**, *125*, 1988-1993.

[48] Butzow, J. J.; Eichhorn, G. L. *Biopolymers* **1965**, *3*, 95-107.

[49] Eichhorn, G. L.; Tarien, E.; Butzow, J. J.; *Biochemistry* **1971**, *10*, 2014-2019.

[50] Nakano, S.-I.; Uotani, Y.; Uenishi, K.; Fujii, M.; Sugimoto, N. *J. Am. Chem. Soc.* **2005**, *127*, 518-519.

[51] Bamann, E. *Angewandte Chemie* **1939**, *52*, 186-189.

[52] Morrow, J. R.; Buttrey, L. A.; Shelton, V. M.; Berback, K. A. *J. Am. Chem. Soc.* **1992**, *114*, 1903-1905.

[53] Matsumura, K.; Endo, M.; Komiyama, M. *Chem. Commun.* **1994**, 2019-2020.

[54] a) Hall J.; Hüsken, D.; Pieles, U.; Moser, H. E.; Häner, R. *Chem. Biol.* **1994**, *1*, 185-190. b) Hall J.; Hüsken, D.; Häner R. *Nucleic. Acids. Res.* **1996**, *24*, 3522-3526. c) Häner, R.; Hall, J.; Pfützer, A.; Hüsken, D. *Pure Appl. Chem.* **1998**, *70,* 111-116. d) Canaple, L.; Hüsken, D.; Hall, J.; Häner, R. *Bioconjugate Chem.* **2002**, *13*, 945-951.

[55] a) Magda, D.; Miller, R. A.; Sessler, J. L.; Iverson, B. L. *J. Am. Chem. Soc.* **1994**, *116*, 7439-7440. b) Magda, D.; Crofts, S.; Lin, A.; Miles, D.; Wright, M.; Sessler, J. L. *J. Am. Chem. Soc.* **1997**, *119*, 2293-2294. c) Magda, D.; Wright, M.; Crofts, S.; Lin, A.; Sessler, J. L. *J. Am. Chem. Soc.* **1997**, *119*, 6947-6948.

[56] Bashkin, J. K.; Frolova, E. I.; Sampath, U. *J. Am. Chem. Soc.* 1994, **116**, 5981-5982.

[57] Scarso, A.; Scheffer, U.; Göbel, M.; Broxterman, Q. B.; Kaptein, B.; Formaggio, F.; Toniolo, C.; Scrimin, P. *Proc. Natl. Acad. Sci. U.S.A.* **2002**, *99*, 5144-5149.

[58] Labelle, M.; Breslow, R. *J. Am. Chem. Soc.* **1986**, *108*, 2655-2659.

[59] Breslow, R. *Acc. Chem. Res.* **1991**, *24*, 317-324.

[60] Breslow, R.; Dong, S. D.; Webb, Y.; Xu, R. *J. Am. Chem. Soc.* **1996**, *118,* 6588-6600.

[61] Fersht, A. In *Structure and Machanism in Protein Science: a guide to Enzyme catalysis and protein Folding*; W. H. Freeman and Company: New York, **1999**; chap. 1.

[62] Perreault, D. M.; Cabell, L. A.; Anslyn, E. V. *Bioorg. Med. Chem.* **1997**, *5*, 1209-1220.

[63] Cotton, F. A.; Day, V. W.; Hazen, E. E. Jr.; Larsen, S.; Wong, S. T. K. *J. Am. Chem. Soc.* **1974**, *96*, 4471-4477.

[64] a) Calnan, B. J.; Tidor, B.; Biancalana, S.; Hudson, D.; Frankel, A. D. *Science* **1991**, *252*, 1167-1171. b) Curtis, R. M.; Pasternak, R. A. *Acta Crystallogr.* **1955**, *A8*, 675-681. c) Adams, J. M.; Small, R. W. H. *Acta Crystallogr.* **1976**, *B32*, 832-835.

[65] a) Thompson, J. E.; Raines, R. T. *J. Am. Chem. Soc.* **1994**, *116*, 5467-5468. b) Ballinger, P.; Long, F. A. *J. Am. Chem. Soc.* **1960**, *82,* 795-798.

[66] a) Weber, D. J.; Serpersu, E. H.; Shortle, D.; Mildvan, A. S. *Biochemistry* **1990**, *29*, 8632-8642. b) Piatek, A. M.; Gray, M.; Anslyn E. V. **2004**, *126*, 9878-9879.

[67] Yoshinari, K.; Yamazaki, K.; Komiyama, M. *J. Am. Chem. Soc.* **1991**, *113*, 5899-5901.

[68] Komiyama, M.; Yoshinari, K. *J. Org. Chem.* **1997**, *62*, 2155-2160.

[69] Shinozuka, K.; Shimizu, K.; Nakashima, Y.; Sawai, H. *Bioorg. Med. Chem. Lett.* **1994**, *4*, 1979-1982.

[70] Podyminogin, M. A.; Vlassov, V. V.; Giege, R. *Nucleic Acids Res.* **1993**, *21*, 5950-5956.

[71] Kato, T.; Takeuchi, T.; Karube, I. *J. Chem. Soc., Chem. Commun.* **1996**, 953-954.

[72] Smith, J.; Ariga, K.; Anslyn, E. V. *J. Am. Chem. Soc*. **1993**, *115*, 362-365.

[73] Gross, R.; Dürner, G.; Göbel M. W. *Liebigs Ann. Chem.* **1994**, 49-58.

[74] Muche, M.-S.; Göbel M. W. *Angew. Chem. Int. Ed. Engl.* **1996**, *35*, 2126-2128.

[75] Brown, D. M.; Uscher, D. A. *J. Chem. Soc.* **1965**, 6558-6564.

[76] Davis, A. M.; Hall, A. D.; Williams, A. *J. Am. Chem. Soc.* **1988**, *110*, 5105-5108.

[77] Scheffer, U.; Göbel, M. W. In *Oligonucleotide Synthesis: Methods and applications,* of *Methods in Molecular Biology* Series; P. Herdewijn Ed.; Humana Press: Totowa, **2005**; chap. 16.

[78] Schmidt, C.; Welz, R.; Müller, S. M. *Nucleic Acids Res.* **2000**, *28*, 886-894.

[79] Pitsch, S.; Scheffer, U.; Hey, M.; Strick, A.; Göbel, M. W. *Helv. Chim. Acta* **2003**, *86*, 3740-3752.

[80] http://www.chemistryexplained.com/Ne-Nu/Nucleic-Acids

[81] a) Matteucci, M. D.; Caruthers, M. H. *Thetrahedron Lett.* **1980**, *21*, 719-722. b) Beaucage, S. L.; Caruthers, M. H. *Thetrahedron Lett.* **1981**, *22*, 1859-1862. c) Matteucci, M. D.; Caruthers, M. H.;. *J. Am. Chem. Soc.* **1981**, *103*, 3185-3191. d) Itakura, K.; Rossi, J. J.; Wallace, R. B. *Ann. Rev. Biochem.* **1984**, *53*, 323-356.

[82] a) Zuckermann, R.; Corey, D.; Schultz, P. *Nucleic Acids Res.* **1987**, *15*, 5305-5321. b) Ebright, Y. W.; Chen, Y.; Pendergrast, P. S.; Ebright, R. H. *Biochemistry* **1992**, *31*, 10664–10670. c) Hayward, M. M.; Adrian, J. C. Jr.; Schepartz, A. *J. Org. Chem.* **1995**, *60*, 3924-3927. d) Connolly, B. A.; Rider, P. *Nucleic Acids Res.* **1985**, *13*, 4485–4502. e) Gazal, S.; Gelerman, G.; Ziv, O.; Karpov, O.; Litman, P.; Bracha, M.; Afargan, M.; Gilon, C. *J. Med. Chem.* **2002**, *45*, 1665-1671.

[83] Niittymäki, T.; Kaukinen, U.; Virta, P.; Mikkula, S.; Lönnberg, H. *Bioconjugate Chem.* **2004**, *15*, 174-184.

[84] a) Burns, J. A.; Butler J. C.; Moran, J.; Whitesites G. M. *J. Org. Chem.* **1991**, *56*, 2648-2650. b) Burmeister Getz, E.; Xiao, M.; Chakrabarty, T.; Cooke, R.; Selvin, P. R. *Anal. Biochem*. **1999**, *273*, 73-80.

[85] Hutchings, M. G.; Grossel, M. C.; Merckel, D. A. S.; Chippendale, A. M.; Kenworthy, M.; McGeorge, G. *Cryst. Growth Des.* **2001**, *1*, 339-342.

[86] Peter S. *Ph.D. thesis*, University of Frarkfurt, **2007**.

[87] Kuzuya, A.; Mizoguchi, R.; Morisawa, F.; Machida, K.; and Komiyama M. *J. Am. Chem. Soc.* **2002**, *124*, 6887-6894.

[88] a) Inoue, H.; Furukawa, T.; Shimizu, M.; Tamura, T.; Matsui, M.; Ohtsuka E. *Chem. Commun.* **1999**, 45-46. b) Sakamoto, S.; Tamura, T.; Furukawa, T.; Komatsu, Y.; Ohtsuka, E.; Kitamura, M.; Inoue H. *Nucleic Acids Res.* **2003**, *31*, 1416-1425.

[89] Verheijen, J. C.; Deiman, B. A. L. M.; Yeheskiely, E.; Van der Marel, G. A.; Van Boom, J. H. *Angew. Chem. Int. Ed.* **2000**, *39*, 369-372.

[90] Beloglazova, N. G.; Fabani, M. M.; Zenkova, M. A.; Bichenkova, E. V.; Polushin, N. N.; Silnikov, V. V.; Douglas, K. T.; Vlassov, V. V. *Nucleic Acids Res.* **2004**, *32*, 3887-3897.

[91] Kolasa, K. A.; Morrow, J. R.; Sharma, A. P. *Inorg. Chem.* **1993**, *32*, 3983-3984.

[92] Hüsken, D.; Goodall, G.; Blommers, M. J. J.; Jahnke, W.; Hall, J.; Häner, R.; Moser, H. E. *Biochemistry* **1996**, *35*, 16591-16600.

[93] a) Åström, H.; Williams, N. H.; Strömberg R. *Org. Biomol. Chem.* **2003**, *1*, 1461-1465. b) Åström H.; Strömberg R. *Org. Biomol. Chem.* **2004**, *2*, 1901-1907.

[94] a) Hertel, K. J.; Herschlag, D.; Uhlenbeck, O. C. *EMBO J.* **1996**, *15*, 3751-3757. b) Hegg, L. A.; Fedor, M. J. *Biochemistry* **1995**, *34*, 15813-15828.

[95] Santoro, S. W.; Joyce, G. F. *Proc. Natl. Acad. Sci. USA* **1997**, *94*, 4262-4266.

[96] a) Reynolds, M. A.; Beck, T. A.; Say, P. B.; Schwartz, D. A.; Dwyer, B. P.; Daily, W. J.; Vaghefi, M. M.; Metzler, M. D.; Klem, R. E.; Arnold L. J. Jr. *Nucleic Acids Res.* **1996**, *24*, 760-765. b) Daniher, A. T.; Bashkin, J. K. *Chem. Commun.* **1998**, 1077-1078.

[97] Copeland, R. A. In *Enymes: A Practical Introduction to Structure, Mechanism, and Data Analysis*; Wiley-VCH, inc.: **2000**; chap 4.

[98] Lima, W. F.; Crooke, S. T. *Proc. Natl. Acad. Sci. USA* **1999**, *96*, 10010-10015.

[99] a) Eadie, G. S. *J. Biol. Chem.* **1942**, *146,* 85-93. b) Hofstee, B. H. J. *J. Biol. Chem.* **1952**, *199*, 357-364.

[100] Trawick, B. N.; Osiek, T. A.; Bashkin, J. K. *Bioconjugate Chem.* **2001**, *12*, 900-905.

[101] Endo, M.; Azuma, Y.; Saga, Y.; Kuzuya, A.; Kawai, G.; Komiyama, M. *J. Org. Chem.* **1997**, *62*, 846-852.

[102] a) Burd, C. G.; Dreyfuss, G. *Science* **1994**, *265*, 615-621. b) Soukup, G. A.; Breaker, R. R. *Curr. Opin. Struct. Biol.* **2000**, *10*, 318-325. c) He, L.; Hannon, G. J. *Nat. Rev. Genet*. **2004**, *5*, 522-531.

[103] a) Qian, Z.; Wilusz, J. *Anal. Biochem*. **1993**, *212*, 547-554. b) Prombona, A.; Tabler, M.; Providaki, M.; Tsagris, M. *Plant Mol. Biol*. **1995**, *27*, 1109-1118. c) Werner, R.; Mühlbach, H.-P.; Guitton, M.-C. *BioTechniques* **1995**, *19*, 218-221. d) Sägesser, R.; Martinez E.; Tsagris M.; Tabler, M. *Nucleic Acids Res.* **1997**, *25*, 3816-3822. e) Wilusz, J. In *RNA: Protein Interactions, a*

practical approach; Smith, C. W. J. ed.: Oxford University press.: **1998**; chap. 7.

[104] Kaminski, A.; Ostareck, D. H.; Standart, N. M.; Jackson, R. J. In *RNA: Protein Interactions, a practical approach*; Smith, C. W. J ed.; Oxford University press.: **1998**, chap. 5.

[105] a) Smith, G. P. *Science* **1985**, *228*, 1315-1316. b) Hoess, R. H. *Chem. Rev.* **2001**, *101*, 3205-3218.

[106] a) Laird-Offringa, I. A.; Belasco, J. G. *Methods Enzymol.* **1996**, *267*, 149-168. b) Laird-Offringa, I. A.; Belasco, J. G. *Proc. Natl. Acad. Sci. USA* **1995**, *92*, 11859-11863. c) Bäumler J. *Ph.D. thesis*, University of Frarkfurt, **2005**.

[107] Matsumoto, C.; Hamasaki, K.; Mihara, H.; Ueno, A. *Bioorg. Med. Chem. Lett.* **2000**, *10*, 1857-1861.

[108] Hochschild, A. *Methods Enzymol.* **1991**, *208*, 343-361.

[109] Dervan, P. B. *Methods Enzymol.* **1991**, *208*, 497-515.

[110] Qi, D.; Tann, C.-M.; Haring, D.; Distefano, M. *Chem. Rev*. **2001**, *101*, 3081-3111.

[111] a) Madore, S. J.; Cullen, B. R. *J. Virol*. **1993**, *67*, 3703-3711. b) Jones, K. A.; Peterlin, B. M. *Annu. Rev. Biochem*. **1994**, *63*, 717-743. c) Frankel, A. D.; Young, J. A. *Annu. Rev. Biochem*. **1998**, *67*, 1-25. d) Tan, R.; Brodsky, A.; Williamson, J. R.; Frankel, A. D. *Seminars in Virology* **1997**, *8*, 186-193.

[112] a) Hauber, J.; Malim, M. H.; Cullen, B. R. *J. Virol* **1989**, *63*, 1181-1187. b) Weeks, K. M.; Ampe, C.; Schultz, S. C.; Steitz, T. A.; Crothers, D. M. *Science* **1990**, *249*, 1281-1284.

[113] Kurzrock, R.; Kantarjian, H. M.; Druker, B. J.; Talpaz, M. *Ann. Intern. Med.* **2003**, *138*, 819-830.

[114] Huq, I.; Ping, Y.-H.; Tamilarasu, N.; Rana, T. M. *Biochemistry* **1999**, *38,* 5172 –5177.

[115] Templeton, A. C.; Wuelfing, W. P.; Murray, R. W. *Acc. Chem. Res.* **2000**, *33*, 27-36.

[116] a) Ulman A.; *Chem. Rev.* **1996**, *96*, 1533-1554. b) Daniel, M.-C.; Astruc, D.; *Chem. Rev.* **2004**, *104*, 293-346.

[117] Brust, M.; Walker M.; Berthell, D.; Schiffrin, D. J.; Whyman, R. *J. Chem. Soc. Chem. Commun.* **1994**, 801-802.

[118] Weisbecker, C. S.; Merritt, M. V.; Whitesides, G. M. *Langmuir* **1996**, *12*, 3763-3772.

[119] Hostetler, M. J.; Wingate, J. E.; Zhong, C.-J.; Harris, J. E.; Vachet, R. W.; Clark, M. R.; Londono, J. D.; Green, S. J.; Stokes, J. J.; Wignall, G. D.; Glish, G. L.; Porter, M. D.; Evans, N. D.; Murray, R. W. *Langmuir* **1998**, *14*, 17-30.

[120] Menger, F. M. *Angew.Chem.* **1991**, *103*, 1104-1118; *Angew. Chem. Int. Ed. Engl.* **1991**, *30*, 1086-1099.

[121] Mammen M.; Choi, S.-K.; Whitesides, G. M. *Angew. Chem.* **1998**, *110*, 2908–2953; *Angew. Chem. Int. Ed.* **1998**, *37*, 2754-2794.

[122] Pasquato L.; Cancan, F.; Scrimin, P.; Mancin, F.; Frigeri, C. *Chem. Commun.* **2000**, 2253-2254.

[123] Manea. F.; Bodar Houillon, F.; Pasquato, L.; Scrimin, P. *Angew. Chem. Int. Ed.* **2004**, *43*, 6165-6169.

[124] Orgel, L. E. *Trends in Biochem. Sci.* **1998**, *23*, 491-495.

[125] Miller, S. L. *Science* **1953**, *117*, 528-529.

[126] Butlerow, A. *Liebigs Annalen der Chemie* **1861**, *120*, 295-298.

[127] Müller, D.; Pitsch, S.; Kittaka, A.; Wagner, E.; Eschenmoser, A. *Helv. Chim. Acta* **1990**, *73*, 1410-1427.

[128] Oro, J. *Biochim. Biophys. Res. Comm.* **1960**, *2*, 407-412.

[129] Ferris, J.; Sanchez, A.; Orgel, L. *J. Mol. Biol.* **1968**, *33*, 693-704.

[130] Lilley, D. M. J. *Trends in Biochem. Sci.* **2003**, *28*, 495-501.

[131] Unrau, J. P.; Bartel, D. P. *Nature* **1998**, *395*, 260-263.

[132] Lohse, P. A.; Szostak J. W. *Nature* **1996**, *381*, 442-444.

[133] a) Österberg, R.; Orgel, L. E.; Lohrmann, R. *J. molec. Evolution* **1973**, *2*, 231-234. b) Österberg, R.; Orgel, L. E. *J. molec. Evolution* **1972**, *1*, 241-248. c) Handschuh G. J.; Lohrmann, R.; Orgel, L. E. *J. molec. Evolution* **1973**, *2*, 251-262.

[134] Orgel, L. E. *Acc. Chem. Res.* **1995**, *28*, 109-118.

[135] Inoue, T.; Orgel, L. E. *J. Am. Chem. Soc.* **1981**, *103*, 7666-7667.

[136] Kurz, M.; Göbel, K.; Hartel, C.; Göbel, W. M. *Angew. Chem. Int. Ed.* **1997**, *36*, 842-845.

[137] Joyce, G. F.; Orgel, L. E. *J. Mol. Biol*. **1988**, *202*, 677-681.

[138] Lohrmann, R.; Orgel, L. E. *Tetrahedron* **1978**, *34*, 853-855.

[139] Jung, K.-E.; Switzer, C. *J. Am. Chem. Soc.* **1994**, *116*, 6059-6061.

[140] Pitsch, S.; Krishnamurthy, R.; Bolli, M.; Wendeborn, S.; Holzner, A.; Minton, M.; Lesueur, C.; Schlönvogt, I.; Jaun, B.; Eschenmoser, A. *Helv. Chim. Acta* **1995**, *78*, 1621-1635.

[141] Divakar, K. J.; Mottahedeh M.; Reese, C. B.; Sanghvi, Y. S.; Swift, K. A. D. *J. Chem. Soc. Perkin Trans.* **1991**, *1*, 771-774.

[142] Seela, F.; Fröhlich, T. *Helv. Chim. Acta* **1994**, 77, 399-408.

[143] Himmelsbach, F.; Schulz, B. S.; Trichtinger, T.; Charubala, R.; Pfleiderer, W. *Tetrahedron* **1984**, *40*, 59-72.

[144] Roberts, C.; Bandaru, R.; Switzer, C. *Tetrahedron Lett.* **1995**, *36*, 3601-3604.

[145] Muller, D.; Zeltser, I.; Bitan, G.; Gilon, C. *J. Org. Chem.* **1997**, *62*, 411-416.

[146] Hey, M. Dissertation Frankfurt **2004**.

10.2 List of Abbreviations

Abs. : Absolute
AppA : Diadenosine 5',5'-pyrophosphate
ApA : Adenosyl(3'-5')adenosine
ApUp : Adenosyl(3'-5')-uridine phosphate
Ar : Aromatic ring
Arg : Arginine
ATP : Adenosine 5'-triphosphate
B : Base
BABE : (S)-1-[p-(bromoacetamido)benzyl]-EDTA
Boc : T*ert*-butyloxycarbonyl
Boc-ON : [2-(Boc-oxyimino)-2-phenylaceonitrile, 2-(tert-Butoxycarbonyloxyimino)-2-phenyl-acetonitrile
BP : Binding Protein
cDNA : Complementary DNA
$CNCH_3$: Acetonitrile
COSY : COrrelated SpectroscopY
CPG : Controlled Pore Glass
Cy5 : Cyanine 5
DCC : N,N'-Dicyclohexyl-Carbodiimide
DCM : Dichloromethane
Degr. : Degradation
DIEA : Diisopropylethylamine
DEPC : Diethylpyrocarbonate
DIC : Diisopropylcarbodiimide
DMAP : 4-Dimethylaminopyridine
DMF : N,N'-Dimethylformamide
DMSO : Dimethyl sulfoxide
DMT : Dimethoxy trityl
DMTCl : Dimethoxytrityl chloride

DNA : Desoxyribonucleic Acid
DTT : Dithiothreitol
E : Enzyme
EtOH : Ethanol
Equiv : Equivalent
EDTA : EthyleneDiAmineTetraAcetic acid
ESI-MS : ElectroSpray Ionization Mass Spectrometry
EtOAc : Ethyl Acetate
FCS : Fluorescence Correlation Spectroscopy
FRET : Fluorescence Resonance Energy Transfer
FT-IR : Fourier Transform Infrared spectroscopy
GABA : 4-Amino-butyric acid
Glu : Glutamic Acid
GTP : Guanosine-5'-Triphosphate
H : Hours
Hex : Hexane
His : Histidine
HIV : Human Immunodeficiency Virus
HOBT : Hydroxybenzotriazole
HPLC : High performance liquid chromatography
HPNP : 2-Hydroxypropyl *p*-nitrophenyl phosphate
HpPNP : 2-Hydroxylpropyl-*p*-nitrophenyl phosphate (2-hydroxylpropyl-4-nitrophenyl phosphate)
ImpA : 5'-Phosphorimidazolide of adenosine
IR : Infrared
Lys : Lysine
MALDI : Matrix-Assisted Laser Desorption/ionization
Me : Methyl
MeOH : Methanol
M.p. : Melting point
MPC : Monolayer Protected Clusters
mRNA : Messenger RNA
NPE : *p*-NitroPhenylEthyl

NMR : Nuclear Magnetic Resonance
ODN : OligoDeoxyriboNucleotides
OP : 1,10-*o*-Phenanthroline
P : Product
PAGE : PolyAcrylamide Gel Electrophoresis;
Phe : Phenylalanine
pRpp : Phospho-Ribosyl-pyrophosphat
PNA : Peptide Nucleic Acid
Py : Pyridine
RNA : RiboNucleic Acid
RNase : Ribonuclease
RP : Reverse Phase
rRNA : Ribosomal RNA
S : Substrat
SDS : Sodium Dodecyl Sulfate
SiRNAs : Small interfiring RNAs
TAR : *Tran*s-Activation Responsive
tRNA : Transporter RNA
Tat : Transactivator
TCA : Trichloroacetic acid
TCEP : Tris(2-carboxyethyl)phosphine hydrochloride
TEA : Triethylamine
TFA : Trifluoroacetic acid.
THF : Tetrahydrofuran
TIPS-Cl : Tri-(Iso-Propyl)Silyl Chloride
TLC : Thin layer Chromatography
T_m : Melting Temperature
TREN : Tris(2-aminoethyl)amine
Tris : Trishydroxymethylaminomethane
Triton : Octyl phenol ethoxylate
UpNP : Uridine 3'-*p*-nitrophenyl phosphate (uridine 3'-4-nitrophenyl phosphate
UV-vis : Ultraviolet-visible spectroscopy

Vmax : Maximal Velocity

Z : Benzyloxycarbonyl

10.3 Supplementary NMR – COSY Spectra

10.3.1 NMR – COSY (62)

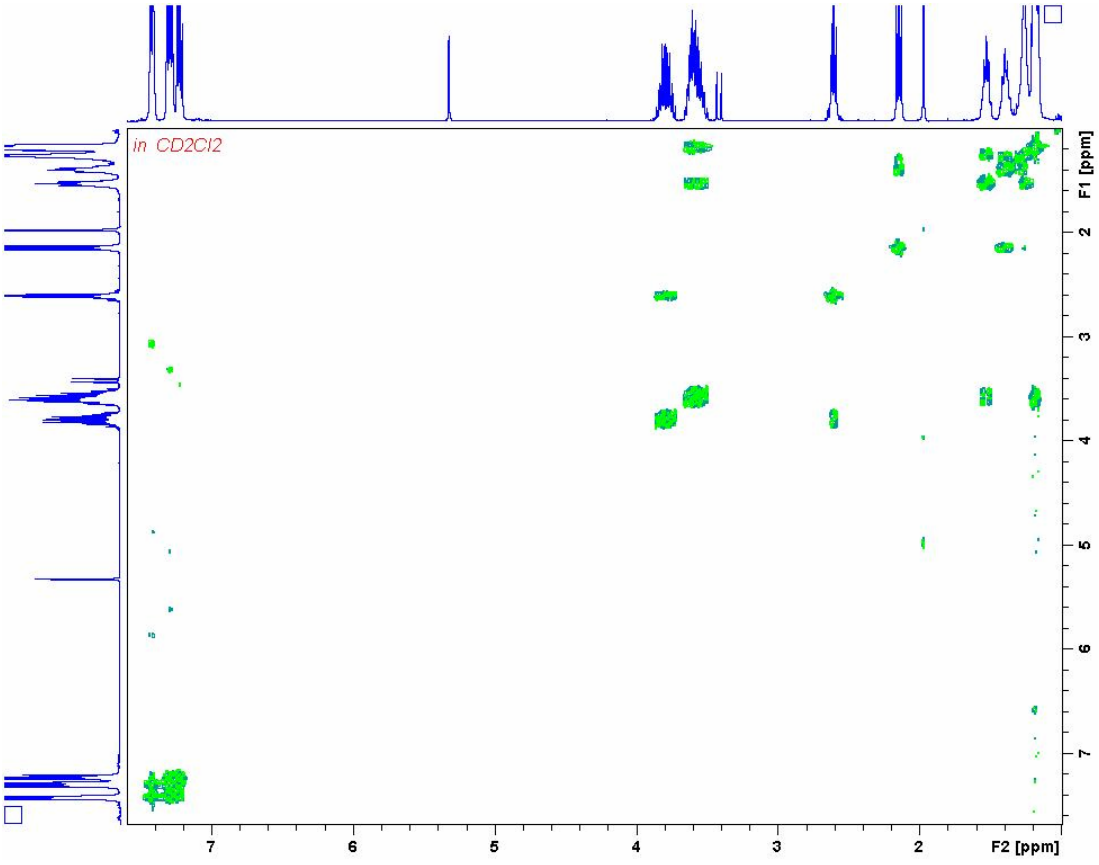

10.3.2 NMR – COSY (71)

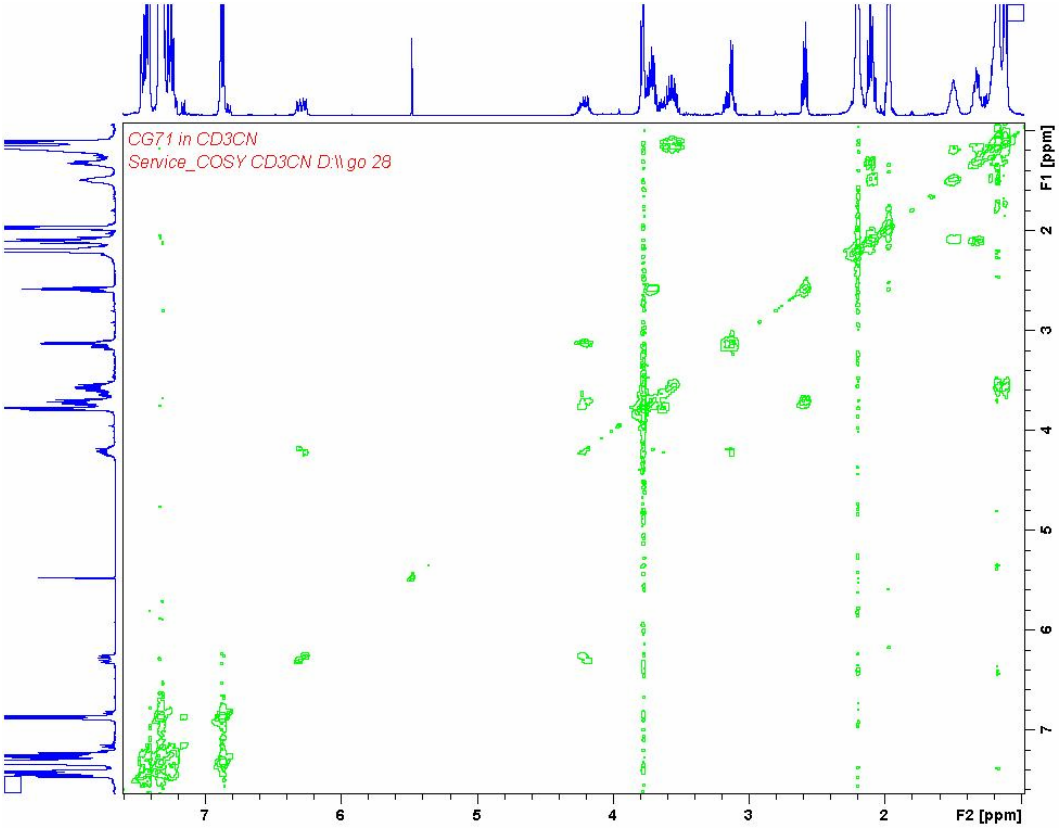

10.3.3 NMR – COSY (75)

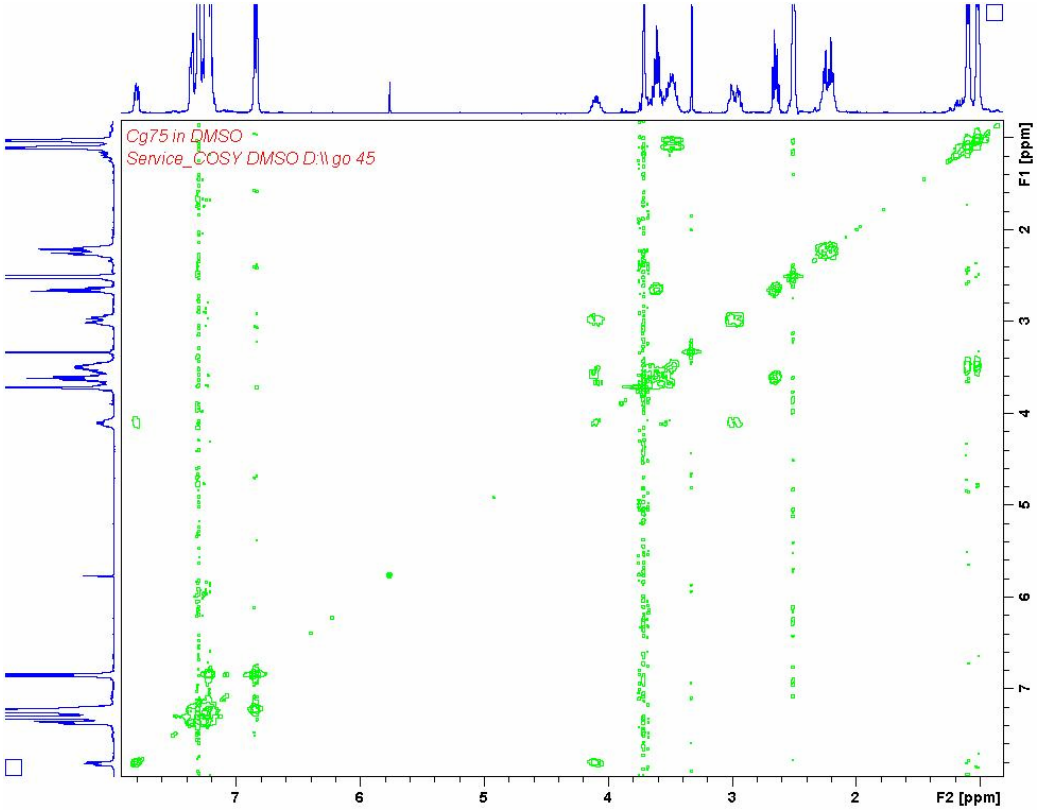

10.3.4 NMR – COSY (72)

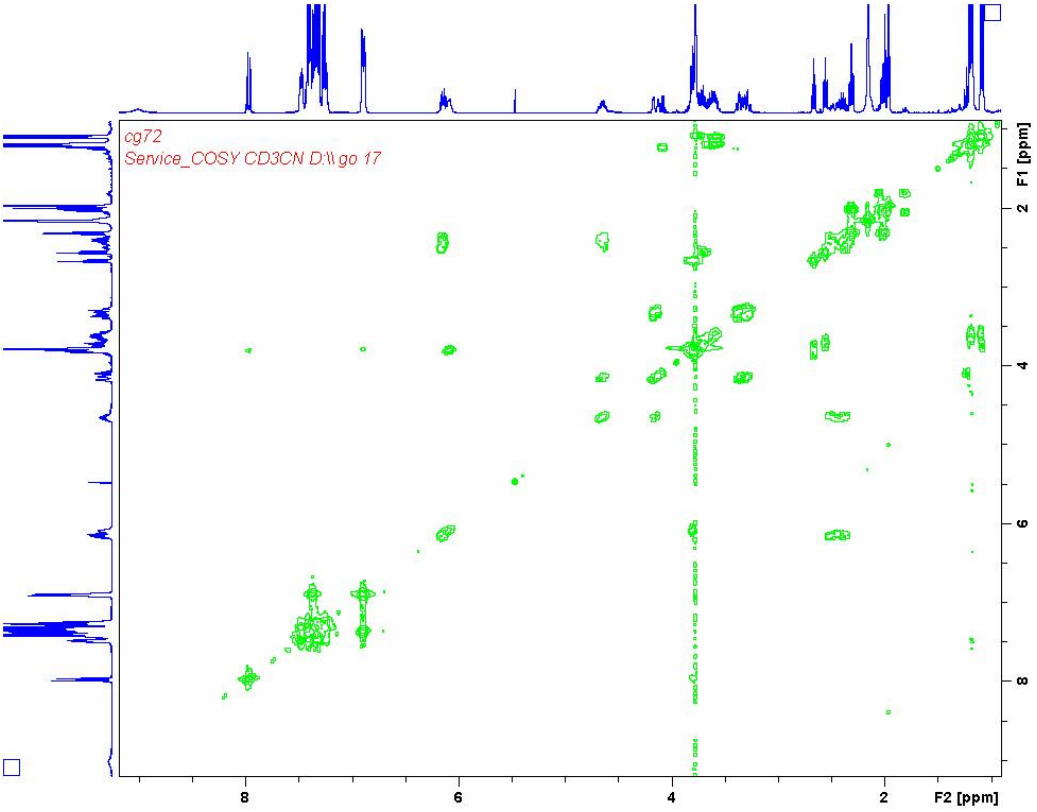

10.3.5 NMR – COSY (91)

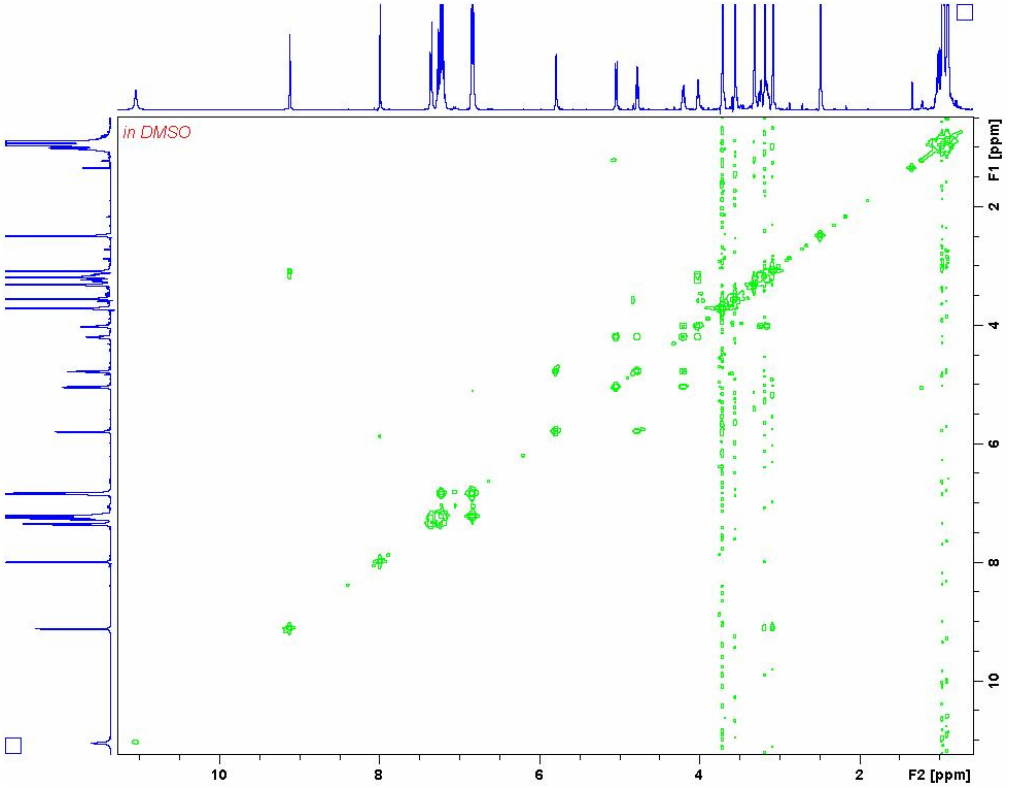

10.3.6 NMR – COSY (92)

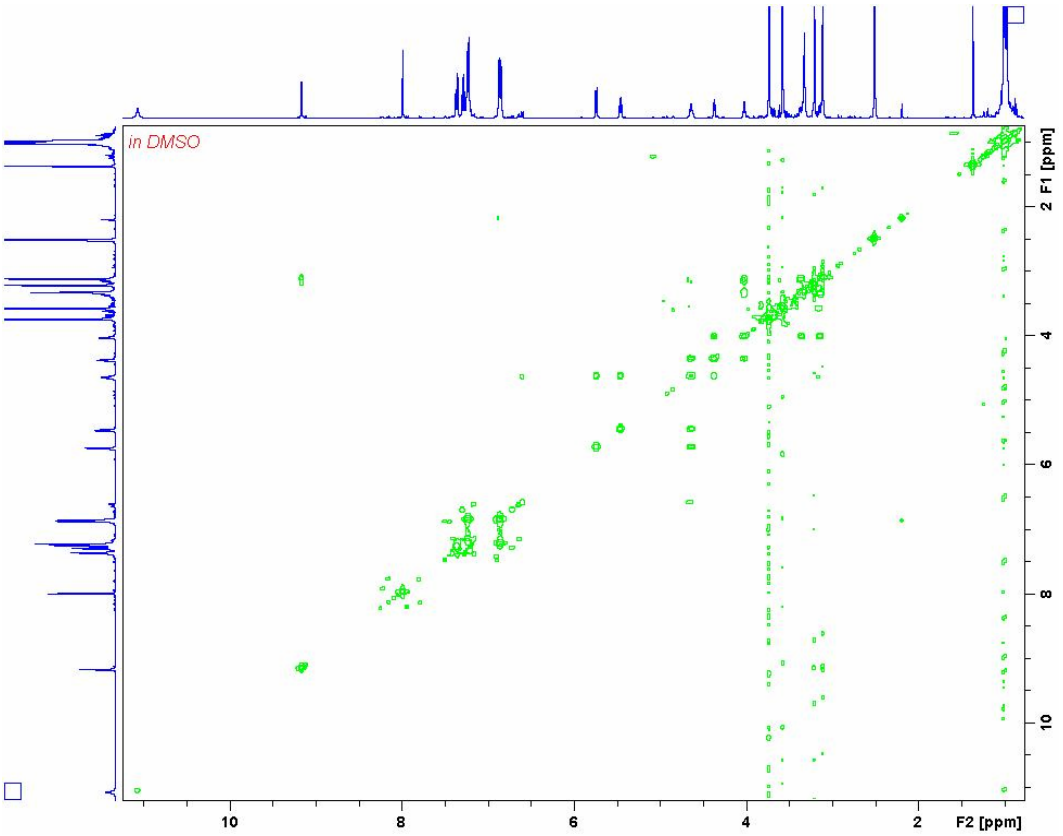

10.3.7 NMR – COSY (95)

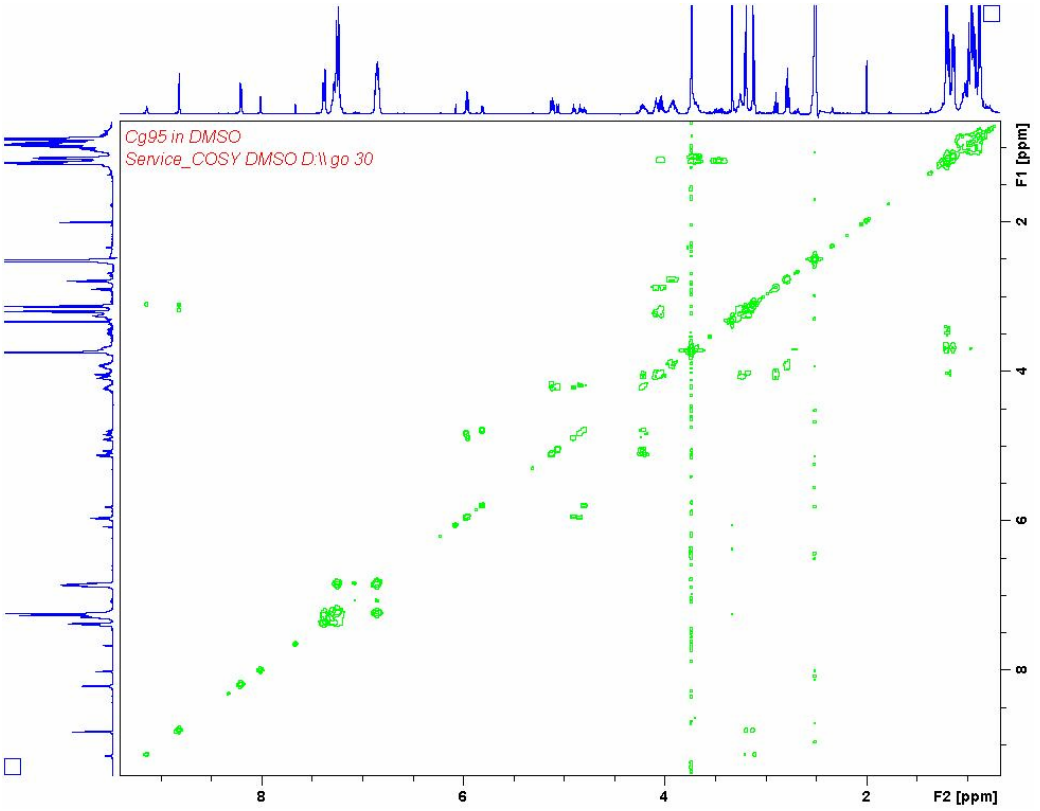

10.3.8 NMR – COSY (96)

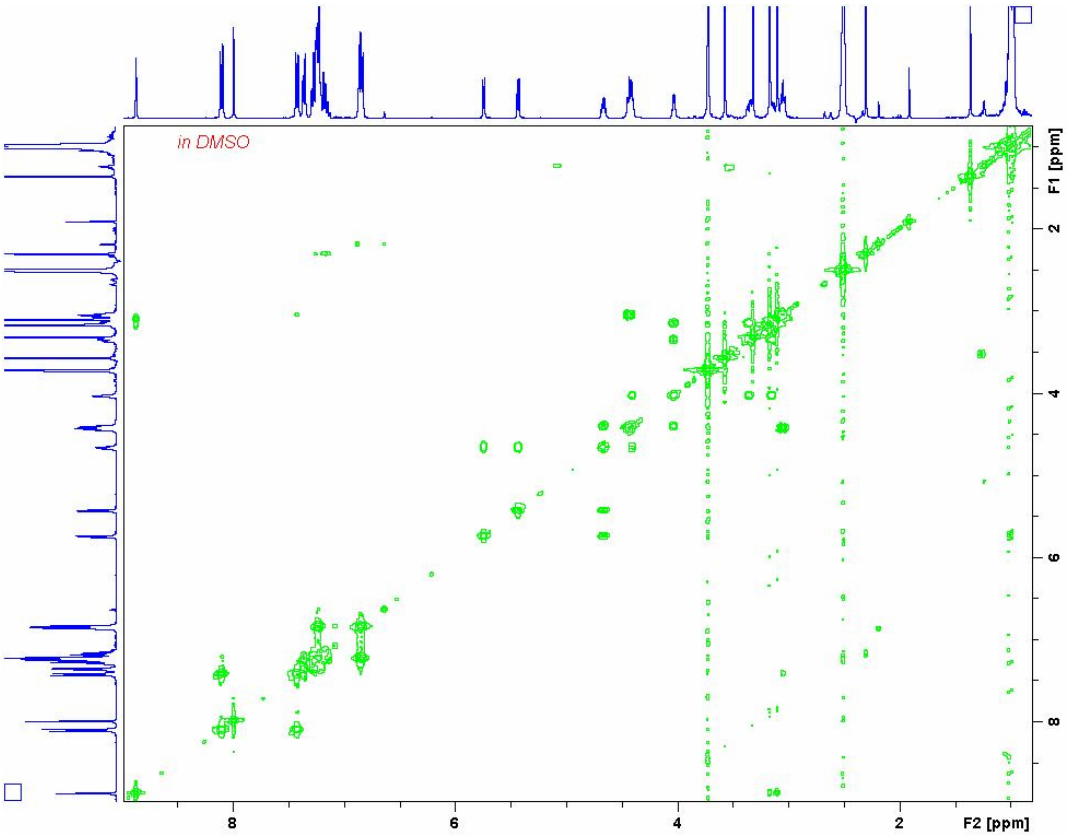

10.3.9 NMR – COSY (97)

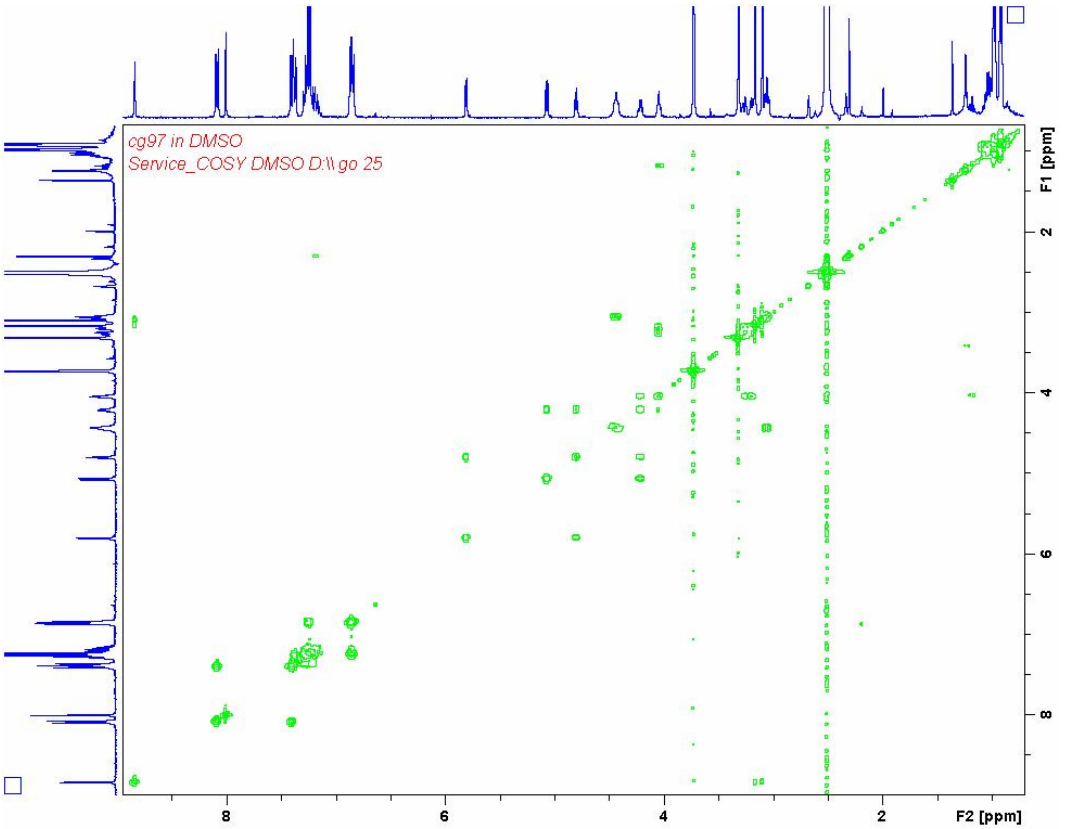

10.3.10 NMR – COSY (98)

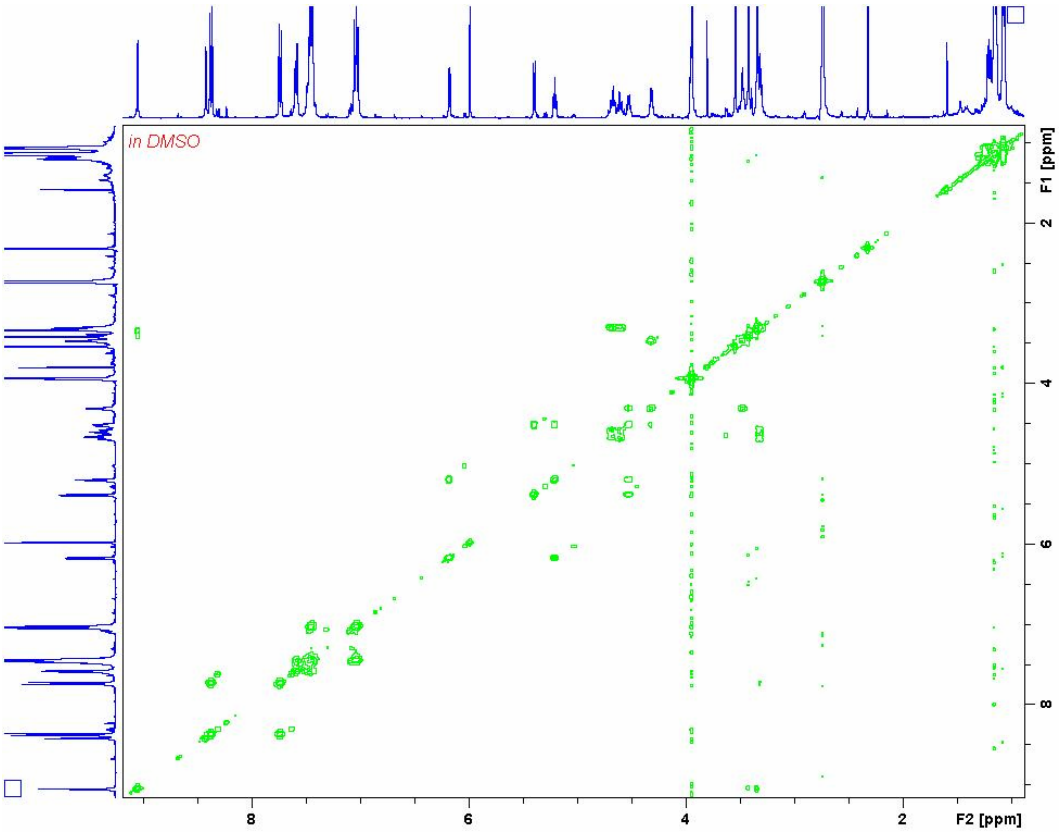

10.3.11 NMR – COSY (99)

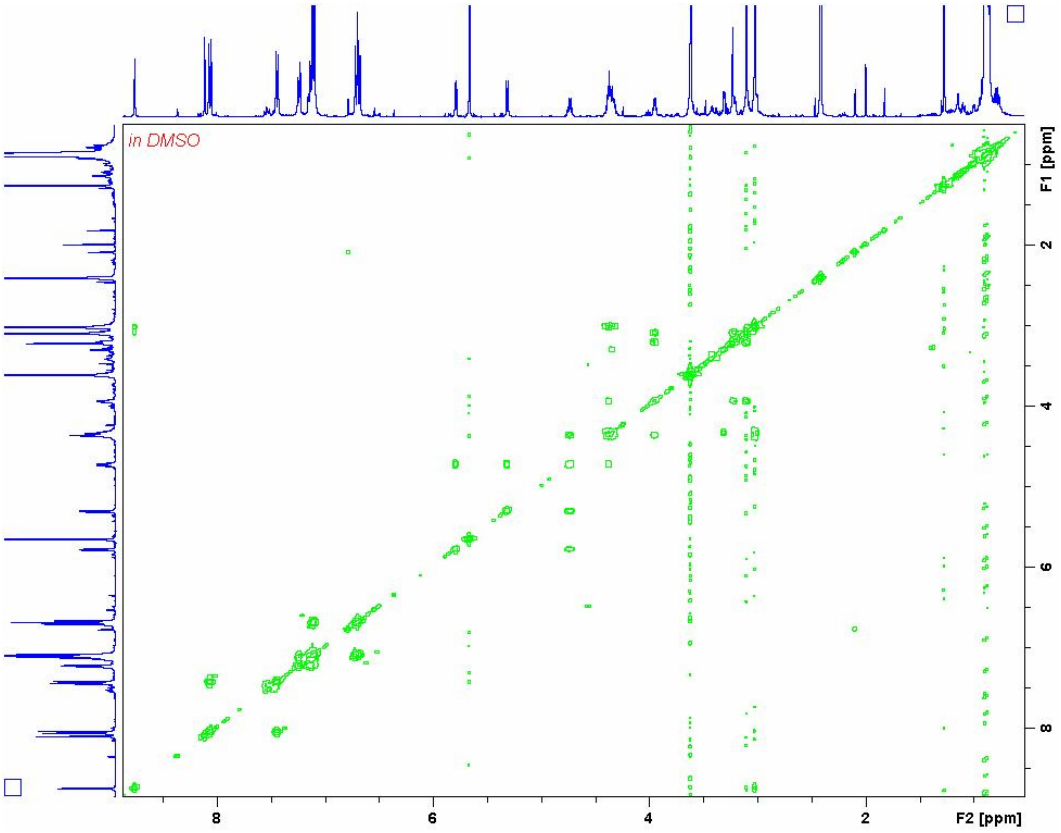

10.4 Curriculum Vitae

Claudio Gnaccarini

Date of Birth: **February 14, 1977**

Place of Birth: Negrar (Verona), Italy

10.4.1 Education:

Primary school (Scuole Elementari): **1983-1988**

First 3 years of secondary school (Scuole Medie): **1988-1991**

Technical college for surveyors (Instituto Tecnico per Geometri)
"Cangrande della Scala" Verona: (**56/60**) **1991-1996**

Degree in Chemistry and Pharmaceutical Technologies,
specialising in Biotechnologies.
University of Padova (Italy): (**Summa Cum Laude**) **1996-2002**

Laurea (Master) thesis at University of Padova, Prof. Paolo Scrimin Department of Chemical Sciences.
''*Synthesis and characterization of gold nanoparticles functionalised with fullerene derivatives*'': **March 2001-March 2002**

Apprenticeship of 4 months, at University of Padova, Prof. Giorgio Palù, Dr. Cristiano Salata, Department of Histology, Micro-Biology, and Medical Biotechnology: **April 2002-July 2002**

Doctor's degree at University of Frankfurt, Prof. Dr. Michael Göbel Institute for Organic Chemistry and Chemical Biology.''*Synthesis of Site-Specific Artificial Ribonucleases ''*: **Beginning: March 2003**

10.5 Publications

1) Gnaccarini, C., Peter, S., Scheffer, U., Vonhoff, S., Klussmann, S., Göbel, M. W.: **Site Specific Cleavage of RNA by a Metal Free Artificial Nuclease Attached to Antisense Oligonucleotides**. *J. Am. Chem. Soc.* **2006**, *128*, 8063-8067.

2) Gnaccarini, C., Göbel, M. W., et alt.: **Peptidic RNA Ligands conjugated with the Cleaving Agent Tris-2-aminobenzimidazole: Applications in Affinity Cleavage**. *In preparation*.

3) Gnaccarini, C., Göbel, M. W., et alt.: **RNA Cleavage in Bulges Induced by DNA Conjugates with Tris-2-aminobenzimidazole**. *In preparation*.

4) Gnaccarini, C., Göbel, M. W., et alt.: **RNA Cleavage by Conjugates of Tris-2-aminobenzimidazole with Antisense DNA, Improved Methods Leading to Turnover and High Site Specificity**. *In preparation*.

10.6 Eidesstattliche Erklärung

Hiermit erkläre ich an Eides statt, dass ich die vorgelegte Dissertation über *„Synthesis of site-specific artificial ribonucleases“* selbständig angefertigt habe, und dass Entlehnungen aus Schriften, soweit sie in der Dissertation nicht ausdrücklich als solche mit Angabe der betreffenden Schrift bezeichnet sind, nicht stattgefunden haben.

Frankfurt am Main:

Claudio Gnaccarini